

Originaldokument gespeichert auf dem Dokumentenserver der Universität Basel
edoc.unibas.ch



Dieses Werk ist unter dem Vertrag „Creative Commons Namensnennung-Keine kommerzielle Nutzung-Keine Bearbeitung 2.5 Schweiz“ lizenziert. Die vollständige Lizenz kann unter **creativecommons.org/licences/by-nc-nd/2.5/ch** eingesehen werden.

Benzylthioether Stabilized Gold Nanoparticles: Towards Novel Hybrid Superstructures

Inaugural Dissertation

zur

Erlangung der Würde eines Doktors der Philosophie

vorgelegt der

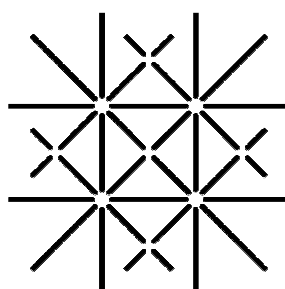
Philosophisch-Naturwissenschaftlichen Fakultät
der Universität Basel

von

Torsten Peterle

aus Friedrichsdorf/Taunus (Deutschland)

Basel 2009



**UNI
BASEL**

Genehmigt von der Philosophisch-Naturwissenschaftlichen Fakultät der Universität Basel
auf Antrag von

Prof. Dr. Marcel Mayor

Prof. Dr. Andreas Pfaltz

Basel, den 26. Mai 2009

Prof. Dr. Eberhard Parlow
Dekan

Acknowledgments

I want to thank my supervisor Prof. Dr. Marcel Mayor for the opportunity to work on this fascinating topic and for the cooperative working atmosphere that was governed by scientific curiosity, confidence and optimism. Also, I would like to express my gratitude to Prof. Dr. Andreas Pfaltz and Prof. Dr. Günter Schmid for co-refereeing this thesis.

I would like to thank Prof. Dr. Ulrich Simon for giving me the chance to spend time in his group and to learn about the synthesis of gold nanoparticles. Annika Leifert, Jan Timper, Monika Fischler, Birgit Hahn and Fei Wen: Thank you for introducing me to the different techniques in nanoparticle preparation and characterization, for your ideas and also for the great time in Aachen. I am grateful to Alla Sologubenko for performing HRSTEM.

My thanks go to Dr. Philippe Ringler for the measurement of the TEM micrographs and to Prof. Dr. Andreas Engel for providing me access to his microscopes. I would also like to express my gratitude to Michael Zharnikov and his team for the NEXAFS and XPS investigations.

I am grateful to Dr. Daniel Häussinger for his helping hand and also the helpful discussions concerning the NMR investigations. I am also thankful to Dr. Heinz Nadig, who recorded the EI and FAB mass spectra, Werner Kirsch, who performed the elemental analyses, the complete 'Werkstatt' and 'Materialausgabe' team and the secretaries of the department. These are the people who keep the Department of Chemistry running.

My thanks go to all members of the Mayor group for their support and for sharing their knowledge and opinions, as well as for everything that goes far beyond chemistry or work. I am especially grateful to Sandro Gabutti, Sergio Grunder, Marcel Müri, Federica Reinders and Jens Tüxen for having an open ear, for making lab work fun, for their help and support and also for the great time here in Basel.

For their support and for being there for me in good and in bad times, I would like to deeply thank my family.

To Tina:

You know how much I owe to you, your love and your ability to bring me back to real life. Thank you.

Table of Contents

| | | |
|-------|--|-----|
| 1 | Introduction | 1 |
| 1.1 | Gold Nanoparticles..... | 1 |
| 1.2 | Applications of Gold Nanoparticles | 2 |
| 1.3 | Clusters and Nanoparticles: Structure and Synthesis..... | 4 |
| 1.4 | Arrangement and Assembly of Gold Nanoparticles | 7 |
| 1.5 | Defined Functionalization of Nanoparticles | 12 |
| 2 | Research Project and Concept..... | 17 |
| 3 | Thioether Coated Gold Nanoparticles..... | 21 |
| 3.1 | Linear Thioether Ligands for the Inclusion of Gold Clusters | 21 |
| 3.1.1 | Ligand Synthesis | 24 |
| 3.1.2 | Au ₉ Ligand Exchange Experiments | 34 |
| 3.1.3 | Thioether Coated Gold Nanoparticles by Ligand Exchange..... | 41 |
| 3.1.4 | Summary and Conclusions..... | 43 |
| 3.2 | Direct Synthesis of Thioether Stabilized Gold Nanoparticles | 45 |
| 3.2.1 | Initial Studies..... | 49 |
| 3.2.2 | Thioether Oligomers for the Stabilization of Gold Nanoparticles | 51 |
| 3.2.3 | Summary and Conclusions..... | 62 |
| 3.3 | Functionalized Gold Nanoparticles | 63 |
| 3.3.1 | Monofunctionalized Thioether Ligands | 65 |
| 3.3.2 | Towards Functionalized Building Blocks for Electronic Applications | 84 |
| 3.3.3 | Preparation of Acetylene Functionalized Gold Nanoparticles | 96 |
| 3.3.4 | Diacetylene Interlinked Nanoparticle Superstructures..... | 104 |
| 3.3.5 | Summary and Conclusions..... | 115 |
| 3.4 | Dendritic Thioether Ligands | 117 |
| 3.4.1 | Synthetic Strategy and Synthesis | 118 |
| 3.4.2 | Gold Nanoparticle Formation Experiments | 125 |
| 3.4.3 | Further Development of the Thioether Dendrimers | 127 |
| 3.4.4 | Dendrimer Stabilized Gold Nanoparticles | 136 |
| 3.4.5 | Formation of Gold Nanoparticle Superstructures | 140 |
| 3.4.6 | Summary and Conclusions..... | 145 |
| 4 | Mixed Thiol-Thioether Monolayers on Gold Surfaces | 147 |
| 4.1 | Film Preparation and Investigation | 148 |
| 5 | Summary and Outlook | 153 |

| | | |
|-------|--|-----|
| 6 | Experimental Part..... | 159 |
| 6.1 | Materials and Methods..... | 159 |
| 6.2 | Synthetic Procedures..... | 163 |
| 6.2.1 | Unfunctionalized Thioether Ligands..... | 163 |
| 6.2.2 | Linear Monothiol Building Blocks..... | 182 |
| 6.2.3 | Acetylene Functionalized Thioether Ligands..... | 191 |
| 6.2.4 | Azide Functionalized Thioether Ligands..... | 217 |
| 6.2.5 | Pyridine Functionalized Thioether Ligands..... | 222 |
| 6.2.6 | Towards Thiophenol Building Blocks..... | 235 |
| 6.2.7 | Dendritic Thioether Ligands..... | 245 |
| 6.3 | Gold Nanoparticle Experiments..... | 273 |
| 6.3.1 | Gold Cluster Ligand Exchange Experiments..... | 273 |
| 6.3.2 | Gold Nanoparticle Formation and Purification, General Procedure..... | 275 |
| 6.3.3 | Gold Nanoparticle Superstructures..... | 275 |
| 7 | Appendix: TEM Micrographs..... | 277 |
| 7.1 | OPE Functionalized Linear Thioether Ligands..... | 277 |
| 7.2 | Dendritic Thioether Ligands..... | 282 |
| 8 | Abbreviations..... | 285 |
| 9 | Literature..... | 287 |

1 Introduction

1.1 Gold Nanoparticles

Scientific research on gold nanoparticles (or colloids) and gold cluster compounds already dates back to the 19th century. In 1857, Michael Faraday presented his work on the interaction between ‘diffused’ gold and light.^[1] Amongst other things, the preparation of ruby red gold nanoparticle dispersions by reduction of an aqueous solution of the gold(III) precursor tetrachloroaurate with white phosphorus was reported in this ‘landmark paper’.^[2] It was found nearly a century later by transmission electron microscopy (TEM) that these preparative routes lead to gold particles with a size distribution between 3 and 30 nm with an average diameter of 6 ± 2 nm,^[3] which was in good accordance with Faraday’s assumptions. The term ‘colloid’ was then coined shortly after Faraday’s report by Graham in 1861.^[4] This term is still in use but has been mostly substituted by the terms ‘nanoparticle’, ‘nanocrystal’ and ‘cluster’.^[5] Within this work, ‘nanoparticle’ will be used for gold particles on the nanoscale (diameters between 1 and 50 nm) that are not uniform in size and structure, while gold ‘clusters’ are species which are stoichiometrically defined and of uniform structure, even when the boundary is not clearly assignable in some cases.^[6] The term ‘nanocrystal’ will not be used throughout this thesis.

Long before the exact scientific engagement with gold nanoparticles, such structures were used as colorants for glass and ceramics. A famous example is the dichroic Lycurgus cup from the 4th century AD, which appears ruby red in transmitted light and green in reflected light due to the presence of colloidal gold.^[7] In the Middle Ages, sols of gold nanoparticles had also the reputation of having curative powers for various diseases.^[8]

The color that made gold nanoparticles so interesting results from the collective oscillation of surface electrons induced by the electric field of the entering light and is therefore directly attributed to the small size of the particles. These so called surface plasmons occur in conducting materials at a broad range of frequencies. The plasma frequency of gold and the other coinage metals is however pushed to the visible part of the spectrum due to d-d transitions, which leads to the size-dependent absorption of visible light in the range between 500 and 600 nm and hence the color of spherical gold nanoparticles (Figure 1).^[9,10]

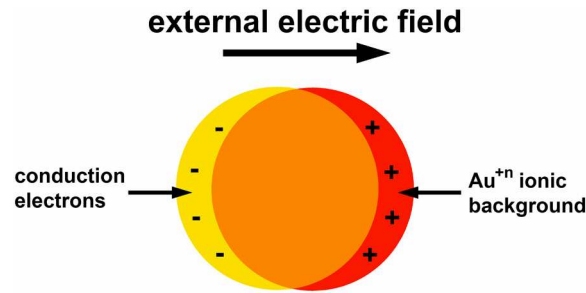


Figure 1. Schematic representation of the plasmon oscillation of a gold nanoparticle.

1.2 Applications of Gold Nanoparticles

Nanoparticles exhibit an electronic structure that lies in between the band structure of a bulk material and the discrete electronic levels of atoms or molecules (Figure 2).^[11-14] In bulk metal, the overlap of valence and conduction band leads to a quasi-delocalized electronic state that provides conductivity (Figure 2a). On the way from bulk metal to nanoparticles, the density of states in the valence and conduction bands decreases and the energy bands split eventually to quantized levels due to the confinement of the electrons on the nanoscale object (Figure 2b). With decreasing size of the nanoparticle, metal clusters are reached, which are characterized by localized bonds between a few atoms and have defined molecular orbitals (Figure 2c). As the splitting of the energy levels is directly dependent on the size of the nanoparticle, also the physical properties depend on the size of the nanoscale object.

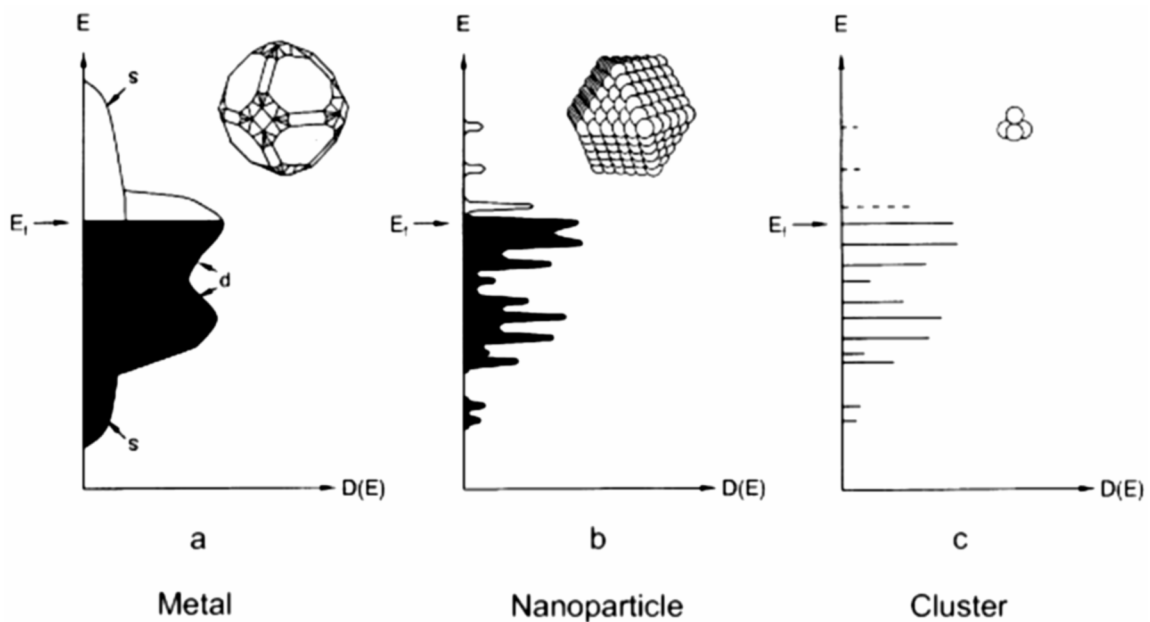


Figure 2. Electronic structures of a metal (plot of energy E versus the density of states $D(E)$) depending on the number of interacting atoms on the way from bulk metal with quasi delocalized valence electrons (a) via nanoparticles (b) to clusters with defined molecular orbitals (c). E_f denotes the Fermi level and the energy of the highest occupied molecular orbital. Adapted from reference [15].

One physical property that changes with the size of the nanoparticle is the capacitance C that decreases with decreasing particle size due to the Coulombic repulsion between the extra electron and the electrons already present on the particle. If the energy, that is required to add a single electron to a nanoparticle $E_c = e^2/2C$ with e as the elementary charge, becomes much larger than the thermal energy $k_B T$, single electron movements to and from the particle can be controlled. By decreasing the size of the nanoparticles down to 1 - 2 nm and hence the capacitance of the particles, single electron movements can be controlled even in the range of room temperature. Thus, gold nanoparticles have become promising candidates for single electron devices which retain their scalability down to the molecular level in a field that was named *Single Electronics*.^[16] For the fabrication of such devices, however, scalable methods for the directed assembly of nanoparticle units are required (*vide infra*).^[17]

A wide variety of further applications have been reported for gold nanoparticles. Especially in live sciences, gold nanoparticles are widely used. One of the traditional methods is immunostaining, where gold particles conjugated to specific antibodies for the molecule of interest serve as contrast agents for TEM investigations.^[18,19] In addition to this technique, the optical properties of gold nanoparticles are used for other sensing and labeling applications.^[20,21] Apart from fluorescence quenching, the most important property of the gold particles for such uses is the significant change of the plasmon resonance frequency with decreasing interparticle distance to less than the particle radius due to dipolar coupling (Figure 3).^[22] The resulting color change from red to purple in aggregated gold nanoparticles was exploited as immunoassay already in 1980.^[23] Mirkin *et al.* used this method then later for the first time for the detection of DNA. A short target DNA strand interlinked the oligonucleotide functionalized gold nanoparticles by complementary base pairing, which led to a clearly visible color change.^[24,25] The same simple concept can also be applied to other biological analytes and is in fact widely used for standard diagnostics such as pregnancy tests.^[26]

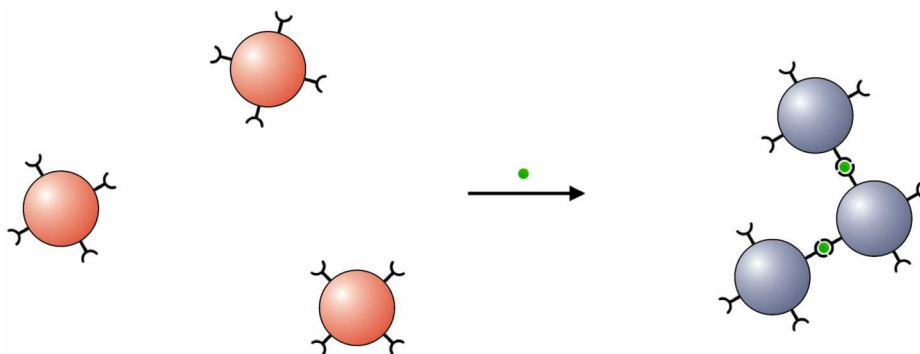


Figure 3. Schematic representation of the basic principle of colorimetric sensing with plasmon resonant gold nanoparticles.

In principle, any interaction between an analyte and a functionality on the surface of gold nanoparticles that is strong enough to lead to particle aggregation with interparticle spacing below the average nanoparticle radius can be used for such colorimetric assays (Figure 3). Some recent examples include selective sensors for heavy metal ions such as Hg^{2+} ^[27] or Pb^{2+} ^[28], but also other cations or anions.^[29]

Another important field of research is centered around the application of gold nanoparticles as catalysts.^[30,31] In the mid 1980s Haruta *et al.* showed that gold nanoparticles that are immobilized on solid surfaces are efficient catalysts for the oxidation of carbon monoxide at very low temperatures.^[32] Since then, industrially relevant reactions like the epoxidation of propene, the oxidation of glucose or the formation of hydrogen peroxide were also found to be efficiently promoted by supported gold particles.^[33] It is therefore believed that the use of gold nanoparticles as catalysts can lead to more efficient and therefore more environmentally friendly large scale industrial processes.^[34] In addition, high selectivities were obtained *i.e.* for the addition of nucleophiles to acetylenes, the selective hydrogenation of N-O bonds or the oxidation of alcohols.^[30,31]

1.3 Clusters and Nanoparticles: Structure and Synthesis

The synthesis of gold nanoparticles and clusters is usually based on the chemical reduction of gold salts by suitable reducing agents similar to the procedure reported by Faraday. An important contribution was made in 1951 by Turkevich.^[35] His method and later improvements^[36] for the preparation of gold nanoparticles with diameters between 16 and 147 nm by the reduction of tetrachloroauric acid (HAuCl_4) with citrate in water are still commonly used when a rather loose shell of stabilizing ligands is required.^[37]

Initial reports on stoichiometrically defined phosphine stabilized Au_5 and Au_6 clusters appeared in 1966.^[38,39] The first complete structural elucidation by single crystal X-ray analysis of a gold cluster - $[\text{Au}_{11}(\text{PPh}_3)_7](\text{SCN})_3$ - was then achieved a few years later.^[40] An almost continuous series of gold clusters was subsequently synthesized and characterized with different phosphine ligands and counterions: Au_6 , Au_7 , Au_8 , Au_9 , Au_{10} up to the full shell icosahedral Au_{13} cluster.^[6] The largest structurally characterized phosphine capped gold cluster $[\text{Au}_{39}(\text{PPh}_3)_{14}]\text{Cl}_8$ was reported in 1992 by Teo *et al.*^[41]

It is assumed that the number of atoms in phosphine stabilized gold clusters is based on the hexagonal close packing of atoms, where each atom is surrounded by 12 nearest neighbors, leading to the so called geometric magic numbers. The smallest full shell cluster is therefore the Au₁₃ core with the following layers containing $10n^2 + 2$ gold atoms (with n being the layer number) (Figure 4).^[42,43]

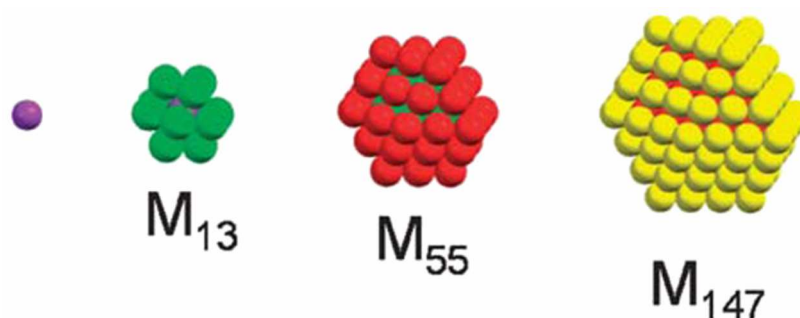


Figure 4. Organization of full shell metal clusters: A single metal atom (purple) is surrounded by 12 others (green) to form a full shell cluster M₁₃. 42 atoms (red) can be densely packed on the first shell to form a M₅₅ two-shell cluster, followed by 92 atoms (yellow) to give M₁₄₇. Adapted from reference [43].

The next full shell cluster [Au₅₅(PPh₃)₁₂]Cl₆ was reported by Günter Schmid and coworkers in 1981.^[44] Although evidence was found that this so called Schmid-cluster might not to be as uniform as the molecular formula suggests,^[45] the uniformity and also the size (1.4 ± 0.4 nm) of this nanoparticle preparation was unique for quite some time.

An important breakthrough was achieved in 1994 by Brust and Schiffrin, who combined Faraday's two-phase preparation of gold nanoparticles with more recent results on ion extraction and monolayer assembly with alkane thiols to form monolayer protected gold nanoparticles.^[46] In the original publication, gold nanoparticles stabilized by dodecanethiol in a size range between 1 and 3 nm with a maximum at 2.0 - 2.5 nm were reported. In addition to the very facile synthesis of small gold nanoparticles with a relatively narrow size distribution, the thiolate monolayer protected particles were highly stable and can be isolated and redissolved in common organic solvents without aggregation or decomposition due to the high stability of the organic shell. Depending on the thiol/gold ratios and the employed conditions, the gold core size can be adjusted between 1.5 and 5.2 nm with good to acceptable size distributions, as was reported in 1998 from Murray and coworkers.^[47] Moreover, the Brust-Schiffrin method is by no means restricted to alkane thiols and allows for the preparation of gold nanoparticles with thiol ligands of very different sizes and polarities.^[48] The surface chemistry of the thiolate protected gold nanoparticles can be changed by ligand

place-exchange reactions, allowing the introduction of functionality to the gold nanoparticles.^[49,50] With very few exceptions (*vide infra*), ligand exchange leads to randomly poly-functionalized gold nanoparticles (Figure 5).

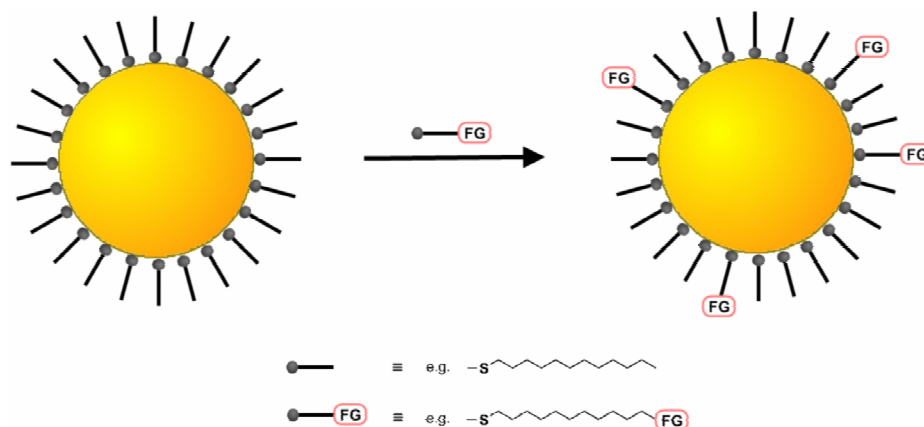


Figure 5. Schematic representation of thiolate ligand exchange reactions. FG represents any chemical or biological functionality and includes e.g. carboxylic acid moieties, DNA or proteins.

First indications for stoichiometrically defined thiolate protected gold clusters were found by Whetten *et al.* in the late 1990s. This group used the cysteine containing tripeptide glutathione (GSH) as stabilizing ligand and succeeded in separating the resulting charged nanoparticles by polyacrylamide gel electrophoresis. The results obtained from the electrospray mass spectra and the electronic spectra of the most abundant cluster were assigned to the formula $\text{Au}_{28}(\text{SG})_{16}$.^[51,52] A more detailed and accurate investigation by similar methods showed in 2005 that a large number of different glutathione protected clusters between Au_{10} and Au_{39} can be found.^[53,54] The exact structure of thiolate protected clusters remained under discussion until very recently, when the single-crystal X-ray structure of the *p*-mercaptobenzoic (*p*-MBA) acid stabilized $\text{Au}_{102}(\text{p-MBA})_{44}$ cluster was reported.^[55] Shortly after this report, the molecular structure of $[\text{N}(\text{C}_8\text{H}_{17})_4][\text{Au}_{25}(\text{SCH}_2\text{CH}_2\text{Ph})_{18}]$ was published as well (Figure 6).^[56] In both structures, the inner core is consistent with gold-gold length and coordination spheres that are found in bulk gold.^[57] In fact, the inner Au_{13} core of the Au_{25} cluster is only slightly distorted from an ideal icosahedral symmetry^[56] and resembles the structure that was found for the phosphine stabilized Au_{13} cluster.^[58] However, the outer shells of the gold cluster structures are formed by RS-Au(I)-SR-Au(I)-SR motifs which have been termed ‘staple’ motif. The nanoparticle is therefore rather a ‘staple-protected’ Au_{13} cluster than a thiolate protected Au_{25} cluster, showing the vast differences between such clusters and clusters

stabilized by other ligands than thiols. Very interestingly, the stabilities of $\text{Au}_{102}(\text{p-MBA})_{44}$ and the Au_{25} cluster seem to arise from closed shells of free 6s electrons.

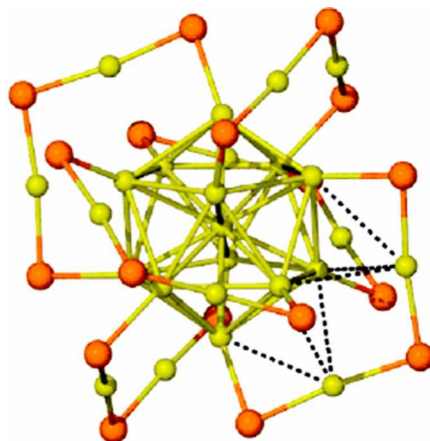


Figure 6. Representation of the gold (yellow) and sulfur (orange) core atoms of the solid state molecular structure of $[\text{N}(\text{C}_8\text{H}_{17})_4][\text{Au}_{25}(\text{SCH}_2\text{CH}_2\text{Ph})_{18}]$. The Au_{13} core is surrounded by six $\text{Au}_2(\text{SR})_3$ ‘staples’. Other atoms than gold and sulfur were omitted for clarity. From reference [56].

1.4 Arrangement and Assembly of Gold Nanoparticles

In view of functional single electron devices based on gold nanoparticles, the controlled and directed spatial assembly of nanoparticles and the adjustment of the electrical transport properties to the desired application still remains a challenge (*vide infra*).^[17,59] Due to the vast variety of techniques and concepts that have been used to address this problem, this topic will mainly be discussed on important examples within this introduction.

Basically, the three-dimensional organization of gold nanoparticles can be achieved directly by crystallization. By varying the nature of the ligand shell, the interparticle spacing can then be controlled in such precipitation processes. This was demonstrated for alkyl thiols^[60,61] as well as quaternary ammonium bromides^[62] of varying chain length. Different generations of poly(amidoamine) (PAMAM) dendrimers proved also to be effective spacers for the assembly of carboxylic acid modified gold nanoparticles. The interparticle spacing of the resulting superlattices of nanoparticles that are formed due to the electrostatic interactions between the particles and the dendrimers correlated well with the sizes of the different generation dendrimers.^[63,64] However, such techniques can only provide regularly packed nanoparticles.

More defined control over the assembly of gold nanoparticles can be achieved by using prearranged templates that can interact with functional groups on the surface of the particles.

In most cases, the introduction of the surface functionality is done by ligand place-exchange reactions (Figure 5).

As templates for a controlled nanoparticle arrangement, synthetic polymers can be used. Rotello and coworkers used modified polystyrene to induce structural control on interlinked nanoparticle assemblies. The interaction of the gold nanoparticles is in this case given by three-point hydrogen bonding between the thymine functionalized particles and diamino-triazine decorated polymers, resulting in spherical nanoparticle assemblies (Figure 7).^[65]

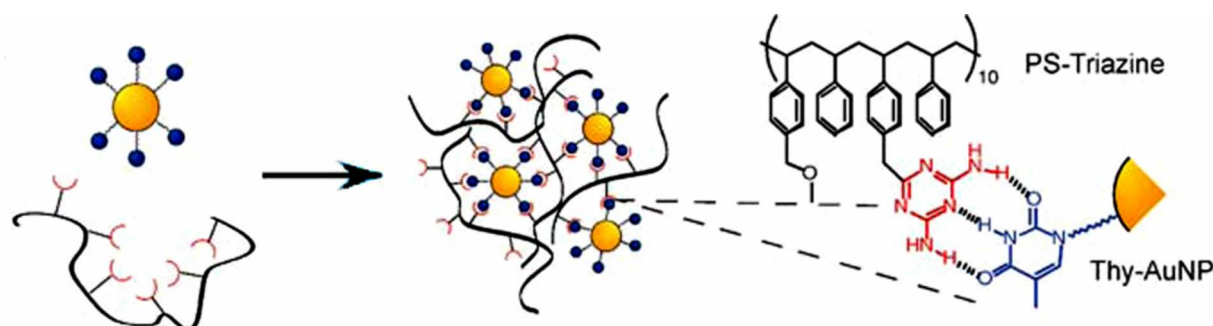


Figure 7. Schematic representation of the polymer-mediated spherical assembly of thymine functionalized gold nanoparticles. Adapted from reference [65].

Similarly, ordered two-dimensional gold nanoparticle arrangements can for instance be obtained by attaching sulfonic acid functionalized Au₅₅ nanoparticles to surfaces coated with thin poly(ethylene imine) (PEI) films. Highly ordered structures with cubic and hexagonal packings of the nanoparticles on the surface were found, which were attributed to two different crystalline phases of the PEI films.^[66] Recently, di-^[67] or triblock^[68] copolymers were used as well to gain some control over the assembly and the arrangement of gold nanoparticles.

A highly versatile platform for the ordered assembly of nanoparticles is given by biomolecules due to their specific binding properties. In general, all of the above mentioned colorimetric biosensing applications can be regarded as biomolecule mediated assembly of gold nanoparticles. The highly specific interactions of biomolecules have also been employed widely for ordered gold nanoparticle assemblies. However, while several reports can be found on protein functionalized gold nanoparticles, combining the intrinsic functionality of many proteins with the distinct properties of nanoparticles,^[69] only few deal with the defined assembly of gold nanoparticles by employing proteins. In a very elegant example by Szuchmacher Blum *et al.*, gold nanoparticles were assembled on the surface of a mutant viral

protein cage which was decorated with thiol containing cysteine moieties at specified positions.^[70] In a subsequent experiment, the highly ordered virus bound nanoparticles were interlinked by conjugated dithiols for electronic investigations (Figure 8).^[71] Another example of protein induced nanoparticle assembly was reported recently by Hainfeld and coworkers. In this work, single 1.3 nm gold particles were bound to the surface of a large protein complex, resulting in highly ordered 2-dimensional nanoparticle-protein superstructures.^[72]

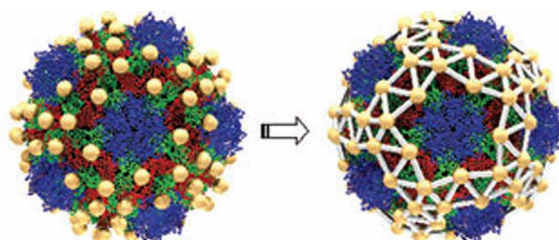


Figure 8. Schematic representation of gold nanoparticle assemblies on the surface of a cowpea mosaic virus (left) and the dithiol interlinked gold nanoparticles (right). From reference [71].

In contrast to these few examples with proteins, DNA has widely been used as construction material for gold nanoparticle superstructures and superlattices.^[73] This can mainly be attributed to the easy artificial programmability of sequences, the selective recognition ability and also the relative rigidity of double-helical DNA. The basic principle for most of the work on DNA-based nanoparticle assembly goes back to the initial reports by Alivisatos^[74] and Mirkin.^[24] These groups used 3'- or 5'-terminus functionalized DNA sequences that were attached to the nanoparticle surface either by thiol ligand exchange^[24] or by selective reaction of the DNA functionality with other nanoparticle functional groups,^[74] resulting in single strand DNA functionalized nanoparticles. These can then be used for instance for the directed formation of nanoparticle dimers, trimers or longer linear structures by DNA hybridization (Figure 9a).^[75,76] However, the interparticle distance can hardly be controlled by that method as these linear DNA-nanoparticle assemblies are highly flexible due to nicks in the DNA structure.



Figure 9. Schematic representation of DNA-directed linear gold nanoparticle assemblies by a) single-strand DNA templates with single strand DNA functionalized nanoparticles or b) functionalized double-strand DNA with subsequent attachment of the nanoparticles.

The power of this technique for the defined assembly of gold nanoparticles was shown by Aldaye and Sleiman, who used preformed DNA templates with rigid organic vertices for the formation of nanoparticle hexagons, squares or triangles (Figure 10a).^[77,78] Furthermore, it was shown very recently that nanoparticle assembly by DNA hybridization can even be used to obtain crystalline nanoparticle superstructures in face centered cubic^[79] or body centered cubic^[80] geometries. Just this year, Alivisatos and coworkers reported the formation of DNA-scaffolded ‘chiral’ nanoparticle pyramids with four nanoparticles of different sizes placed at the tips of the pyramidal structures (Figure 10b).^[81]

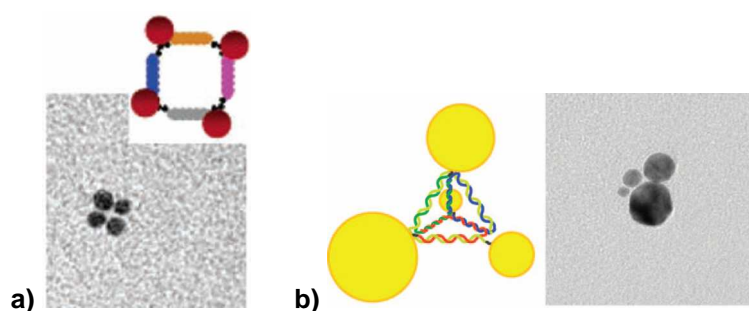


Figure 10. Schematic and TEM images of a gold nanoparticle square (left, from reference [78]) and a ‘chiral’ pyramid (right, from reference [81]).

As was already mentioned above, by using single-strand DNA functionalized gold nanoparticles, nicks are introduced to the produced nanoparticle decorated double-strand DNA, which disfavors this technique for defined linear arrangements of nanoparticles. Especially in view of such linear wire-like arrays, the high mechanical rigidity of intact double-helical DNA is desired (Figure 9b). The gold nanoparticles can be attached to modified DNA bases which can easily be incorporated at defined positions by automated methods.^[73] Linear nanoparticle arrangements were reported i.e. with thiol functionalized DNA, which can bind to the gold nanoparticle surface by exchange of other thiol ligands,^[75,82] but also by using alkyne decorated DNA to covalently attach azide functionalized gold nanoparticles *via* ‘click chemistry’.^[83] Like for sensing applications (*vide supra*), virtually any type of interaction can be used to attach gold nanoparticles to DNA strands. For instance, DNA intercalating agents such as cisplatin^[84] or others,^[85] but also specific protein-receptor interactions^[86,87] have been used for the formation of double-strand DNA based linear nanoparticle arrangements.

These DNA based methods for the ordered arrangement of gold nanoparticles are unexcelled in terms of versatility for the formation of defined nanoparticle superstructures. With regard

Recently, gold nanoparticles were interlinked by oligothiophene dithiols to give nanoparticle aggregates in order to investigate the conductivity as well as the electrochemical behavior of such inorganic/organic hybrid systems.^[92] In 2005, Dadosh and Gordin showed that the ligand exchange approach can indeed also yield defined gold nanoparticle superstructures. They reported nanoparticle dimers which were connected by conjugated dithiols for single molecule electronic investigations where the two particles become part of the electrodes (Figure 12). This dumbbell approach from *bottom up* facilitates thereby the contacting of the single molecule by *top down* methods. The dimers were obtained by reacting a large excess of citrate stabilized 10 nm particles with the dithiol molecules.^[93] Larger nanoparticle aggregates formed also during the ligand exchange reaction, showing that the degree of control is very limited.

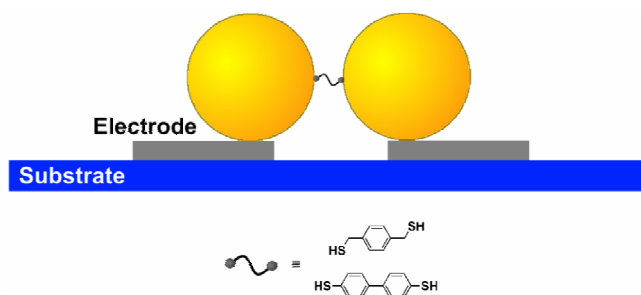


Figure 12. Representation of the *top down* contacting scheme for single molecule investigations with nanoparticle dumbbell structures.

1.5 Defined Functionalization of Nanoparticles

As was pointed out before, complete control over the degree of functionalization of gold nanoparticles as well as the spatial arrangement of surface functional groups cannot be achieved directly by simple ligand exchange. The most common methods to realize monofunctionalized gold nanoparticles involve the attachment of a large label that either prevents further functionalization by steric hindrance or allows the chromatographic separation due to the distinct properties of the label. The latter method is mainly used for gold nanoparticles which are functionalized by biomolecules, using the specific biochemical separation techniques. Statistically functionalized single-strand DNA nanoparticles for instance can be separated from the mono- up to the penta-functionalized particles by agarose gel electrophoresis (Figure 13a).^[94] However, DNA strands of at least 100 base pairs were required for an effective separation. For the formation of small nanoparticle superstructures

such as the ones reported by Aldaye and Sleiman, the nanoparticles were functionalized with much shorter DNA sequences.^[77,78] In these cases, the effective separation of single-strand DNA monofunctionalized gold particles was achieved by reversible extension of the DNA strand. The extension is only complementary to the last 15 bases and is removed upon formation of the superstructures which are formed by 40 base pairs per DNA strand (Figure 13b).^[78]

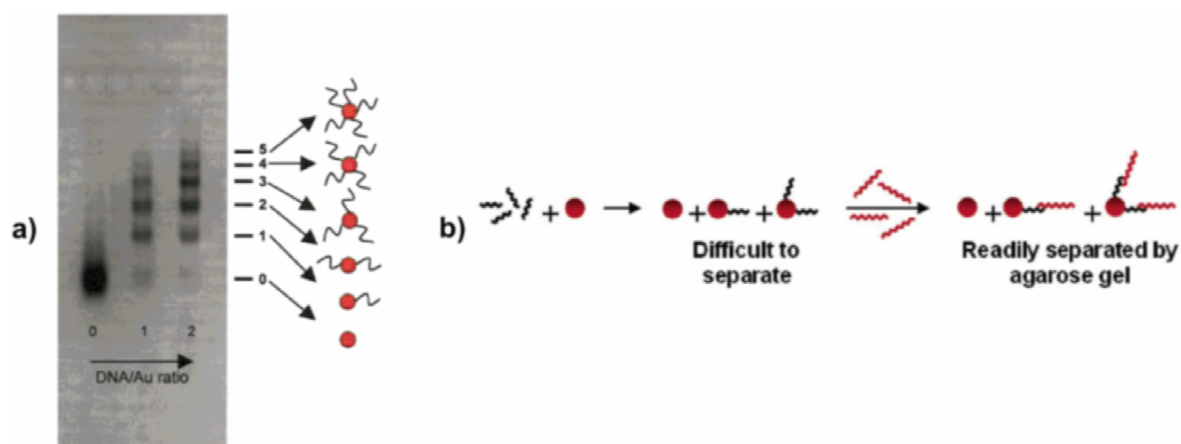


Figure 13. a) Electrophoretic mobility of 5 nm gold nanoparticles that were functionalized with 100 base pair thiolated single-strand. From reference [94]. b) Schematic of the separation concept for 40 base pair single-strand DNA functionalized gold nanoparticles. From reference [78].

Mono-peptide labeled gold nanoparticles were obtained by using immobilized metal ion chromatography. In this special case, the functional peptide sequence contained a sequence of six histidines - a so-called His-tag - which can bind to surface immobilized nickel(II) ions.^[95] This method allows to discriminate only between functionalized and unfunctionalized particles, monofunctionalization can therefore only be achieved if very high nanoparticle to functional peptide ratios are used for the ligand exchange reaction.

Monofunctionalized gold nanoparticles were also obtained by solid phase methods, representing instances for the steric discrimination of higher degrees of functionalization. The initial example from Huo and coworkers is based on resin bound thiol ligands, which can bind to the thiolate protected nanoparticles by ligand exchange (Figure 14). Due to the low functional group density on the solid support, one particle can only bind to a single resin bound thiol. Acidic cleavage of the resin connected ester group of the resin bound thiol provides then mono-carboxylic acid functionalized nanoparticles.^[96] Independent of this contribution, a similar approach was reported for the preparation of lysine monofunctionalized gold nanoparticles.^[97] In both cases, however, the nanoparticle recovery

was quite low after the cleavage from the solid support. Furthermore, the strongly acidic cleavage conditions further limit the usability of this approach.

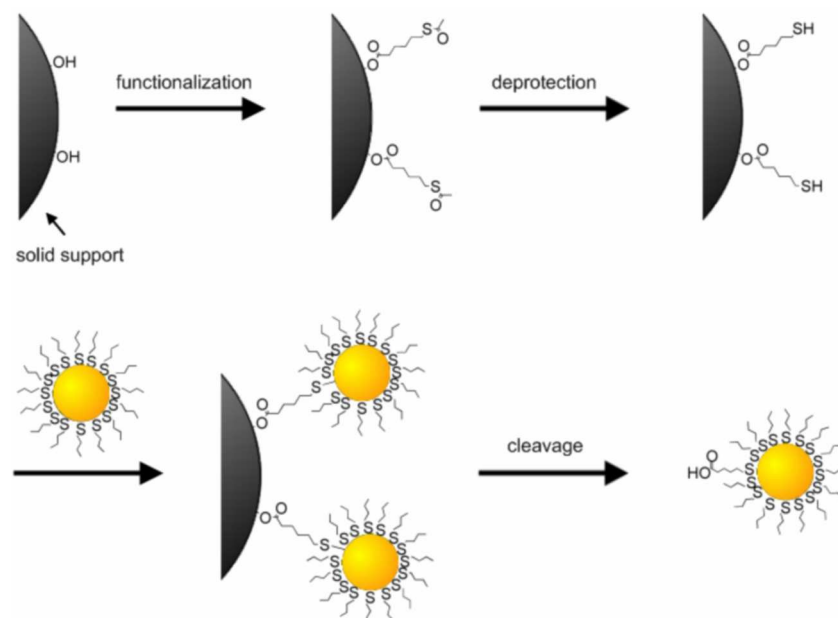


Figure 14. Schematic of the multistep formation of monocarboxylic acid functionalized gold nanoparticles using a thiol functionalized solid polystyrene support. Adapted from reference [96].

Greiner and coworkers showed very recently that a controlled free radical polymerization process on the surface of gold nanoparticles can also lead to mono-carboxylic acid functionalized particles. This group prepared particles stabilized by 4-vinylthiophenol, which were subsequently subjected to radicalic polymerization with very low amounts of an carboxylic acid functionalized initiator under highly diluted conditions. Upon complete polymerization of the surface vinyl groups of the individual particles one single initiator carboxylic acid remains per particle due to the low initiator to nanoparticle ratio (Figure 15).^[98]

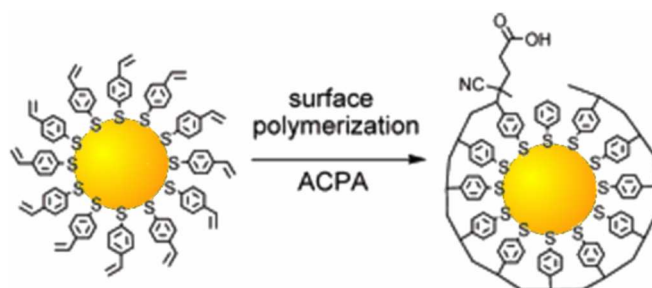


Figure 15. Schematic representation of the surface polymerization process for the formation of monocarboxylic acid functionalized gold nanoparticles. From reference [98]. ACPA: 4,4'-azobis-(4-cyanopentanoic acid).

In 2001, von Kiedrowski *et al.* reported the phase-transfer synthesis of gold clusters stabilized by tridentate benzylic thioether ligands based on 1,3,5-trimethylbenzene scaffolds (Figure 16a).^[99] Starting from an organic solution of the Schmid-cluster $[\text{Au}_{55}(\text{PPh}_3)_{12}]\text{Cl}_6$,^[44] the gold core was transferred completely to a buffered aqueous phase by the thioether ligands after 1 to 7 days depending on the residues on the ligand. The 12 triphenylphosphine ligands that are supposed to be bound at the edges of the cuboctahedron cluster core were thereby exchanged by four of the tridentate ligands and the resulting thioether capped gold clusters were found to be highly stable in the solid phase as well as in aqueous dispersion.^[99] This concept was developed further by interconnecting four tridentate ligands to form one dodecadentate thioether ligand that carried one single functionality allowing for the conjugation to biomolecules (Figure 16b). As before, the thioether stabilized gold clusters were synthesized by phase-transfer, yielding monofunctionalized gold nanoparticles that proved to be stable even at temperatures up to 95°C.^[100]

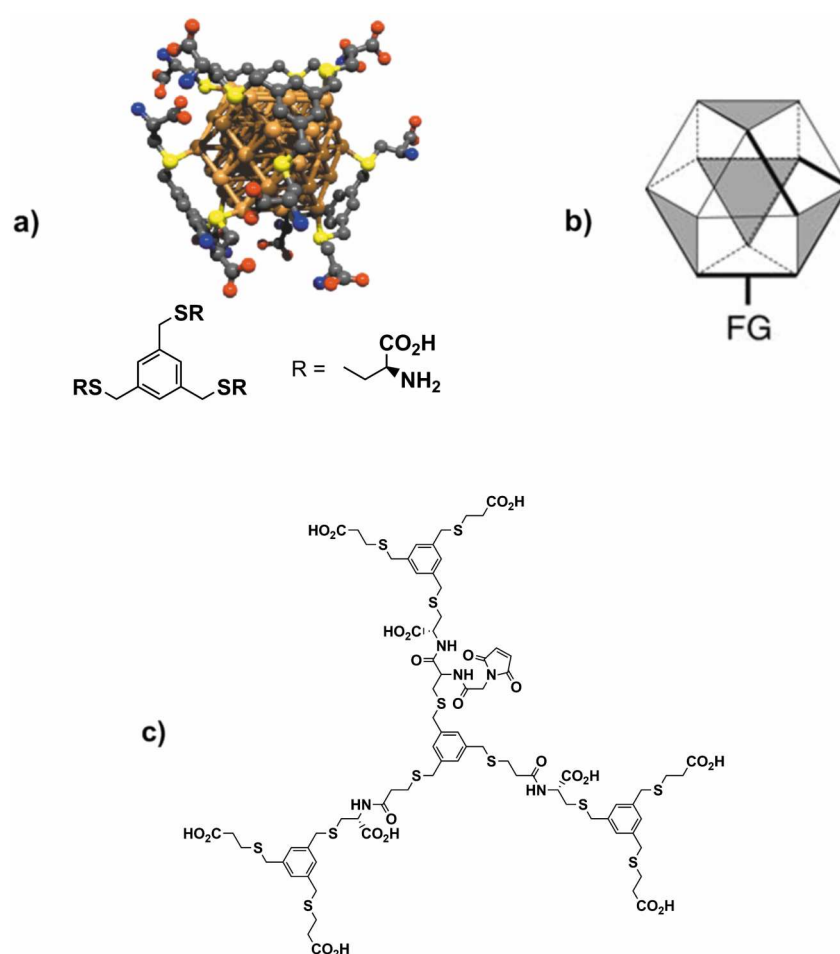


Figure 16. a) Idealized computational model structure of a thioether ligand gold cluster complex and the employed ligand structure. From reference [99]. b) Conceptual picture of a monofunctionalized Au₅₅ cluster with four interlinked tridentate thioether ligands. From reference [100]. c) molecular structure of the dodecadentate thioether ligand for the inclusion of Au₅₅ nanoparticles.

All of the above mentioned methods can provide monofunctionalized gold nanoparticles. However, with regard to gold nanoparticles as ‘artificial molecules’ for nanoengineering purposes, the uses of monovalent particles remain limited.^[59,101] In 2004, the group of Francesco Stellacci found by detailed scanning tunneling microscopy (STM) investigations on mixed thiolate monolayer protected gold nanoparticles that *ordered* alternating domains of the different thiols can form.^[102,103] While phase separation of dissimilar thiol ligands on flat monolayers is well-known, such a high degree of ordering in parallel rings was so far only found on the curved nanoparticle surfaces. The ligands can be viewed as hairs onto a sphere that can be described by the ‘hairy ball theorem’. These hairs cannot be aligned onto the sphere without creating two singularities. In the case of the thiol ligands on curved nanoparticle surfaces this results in two diametrically opposed molecules that do only weakly interact with neighboring ligands (Figure 17).

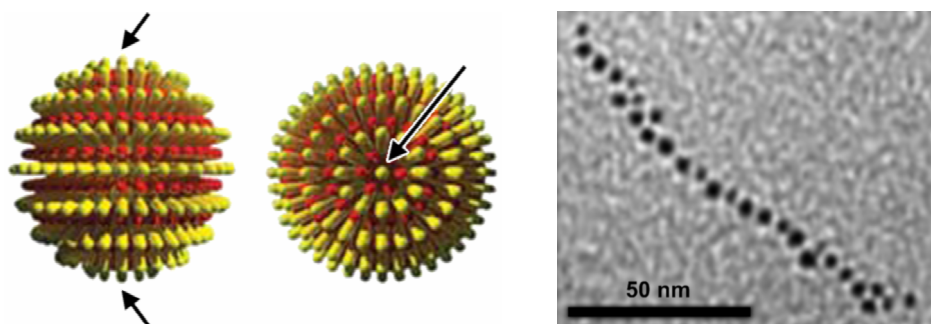


Figure 17. Idealized drawings of 'rippled' gold nanoparticles with mixed thiol monolayers (left), showing the polar defect (arrows). The yellow and the red ripples represent the different thiol ligands. TEM micrograph of linear nanoparticle chains from the polymerization of divalent gold nanoparticles (right). From reference [104].

Based on this concept, Stellacci's group succeeded in replacing the two thiol ligands at the poles with carboxylic acid functionalized thiols.^[104] These divalent nanoparticles were then polymerized with a diamine which results in linear nanoparticle superstructures (Figure 17), clearly showing the effective formation of the particles into molecular building blocks.

In summary, gold nanoparticles have been shown to be versatile functional building blocks for very different applications in medicine, biology, catalysis and materials science. The recent results on the solid state molecular structures of thiolate monolayer protected gold clusters allow for a deeper insight on the mechanisms of nanoparticle stabilization and formation by theoretical methods. However, the effective control of nanoparticle sizes and monodispersity remains a challenge, as does the controlled arrangement of selected functional groups on the surface of a nanoparticle.

2 Research Project and Concept

The aim of this work was the development and investigation of novel concepts for the control of both, the size and the surface functionalization of metal nanoparticles. Size control enables to tune the particles' physical properties while the control over the functionalization allows to adjust its chemical behavior. The conceptual approach to achieve this goal is the stabilization of nanoparticles by large ligands based on multiple thioether moieties which are able to cover defined surface areas (Figure 18).

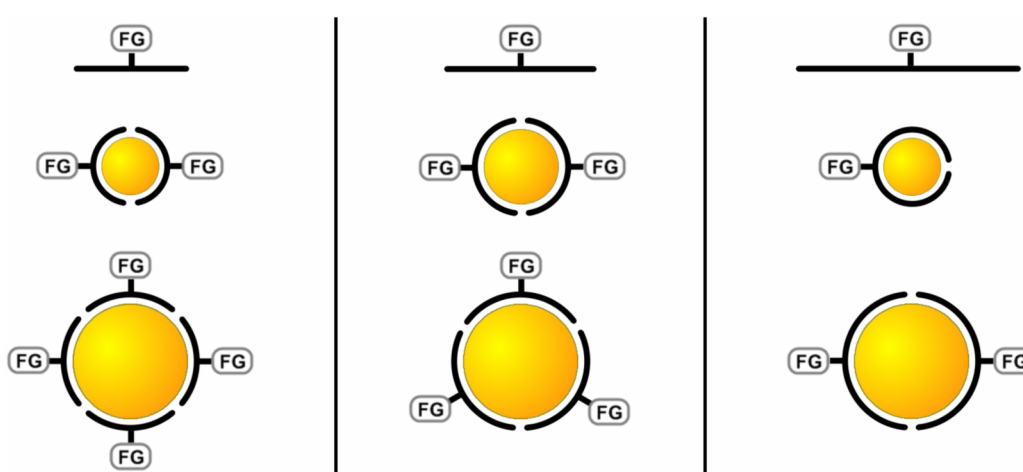


Figure 18. Schematic representation of the basic concept for the selective stabilization and functionalization of gold nanoparticles by multidentate thioether ligands (black) of different sizes. FG: functional group.

Once control over the size and surface functionalization of gold nanoparticles should be achieved, the thioether coated nanoparticles could be employed as synthetic building blocks for the formation of nanoparticle superstructures by standard wet synthetic chemistry methods. Such functionalized nanoparticle building blocks can be perceived as 'artificial molecules' with a defined arrangement of functional groups. Very importantly, this concept allows the controlled introduction of a wide range of functionalities without the need for highly selective separation methods (*vide supra*). In addition, with regard to inorganic/organic hybrid materials for single electronic applications, the controlled introduction of conjugated and rigid functional molecules to form nanoparticle superstructures is not restricted to dithiol molecules. Weakly binding interfaces such as pyridines can also be investigated, because the attachment to the nanoparticle is granted by the multidentate thioether ligand part of the molecule (Figure 19). This allows to enlarge the scope of potential anchoring units for

molecular electronics independent of the strength of the binding interaction to the electrode material.

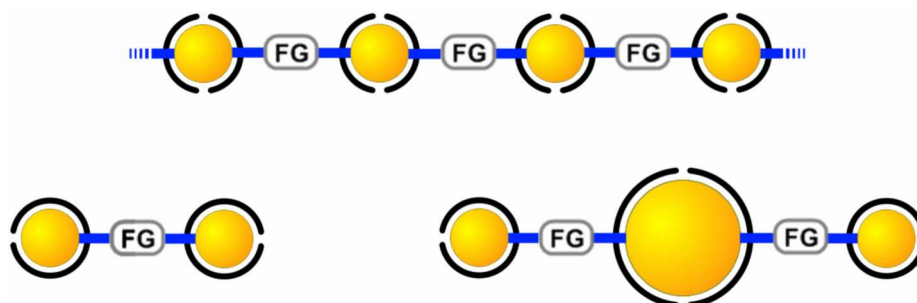


Figure 19. Possible nanoparticle superstructures, interlinked with conjugated and nanoparticle bound functional units (blue), which are part of the thioether ligand molecules (black).

In view of electronic investigations and applications, dumbbell structures are particularly interesting, as such structures allow for single molecule investigations (Figure 20). The nanoparticles of the dumbbell structure become part of the electrodes, making the structure easier accessible by *top-down* approaches compared to single molecules due to the larger overall size of the organic/inorganic hybrid structure. In contrast to similar single molecule investigations reported by Dadosh and Gordin (*vide supra*),^[93] the concept presented here has the advantage that the degree of nanoparticle functionalization and thus also the yield of the dumbbell nanoparticle structure can be controlled directly by the size of the large thioether ligand.

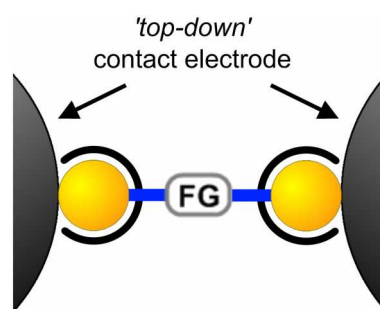


Figure 20. Schematic of a single molecule experiment with a dumbbell structure of nanoparticles stabilized by functionalized thioether ligands.

The focus of this work lies in the exploration of the feasibility of the suggested concepts. Suitable multidentate thioether ligands for the stabilization of gold nanoparticles had to be developed and synthesized. Subsequently, their potential as nanoparticle forming and

stabilizing agents should be investigated in order to find generally applicable methods for differently functionalized thioether ligands. A particular focus is set on the control of the nanoparticle sizes, as this allows the control of the physical properties of the particles. The influence of the size and shape of the thioether ligands on the nanoparticles and the number of thioether ligands per nanoparticle were thus analyzed.

The synthetic methodology for the formation of monofunctionalized thioether ligands had to be developed. The introduced functionalities should thereby allow the wet chemistry processing of the nanoparticles to make them 'artificial molecules' with defined surface functionalities for the formation of nanoparticle superstructures. Suitable functional thioether ligands should be synthesized and be investigated concerning their ability to form functionalized nanoparticles as building blocks for covalently interlinked nanoparticle superstructures.

This doctoral thesis focuses on numerous experiments with a common focus towards the stabilization and functionalization of small gold nanoparticles. Occasionally, experimental details are required which interrupt the evolution of the central theme and thus the readability of the text. To support the reader, each chapter is headed by a short abstract in a grey box to summarize the focus and the achievements of this section.

3 Thioether Coated Gold Nanoparticles

3.1 Linear Thioether Ligands for the Inclusion of Gold Clusters

In this part, the design and synthesis of a octadentate thioether ligand for an Au₉ cluster core will be discussed. Furthermore, preliminary exchange experiments using phosphine stabilized gold clusters will be presented.

As was outlined in the introduction, the aim of this work was the systematic synthesis of gold nanoparticles stabilized by a low, defined number of large monofunctionalized thioether ligands. Based on the results that were reported by von Kiedrowski^[99,100] (see section 1.5), synthesis of the sulfide stabilized gold nanoparticles by ligand exchange seems promising due to the fact that the nanoparticle size and monodispersity can be controlled in the initial nanoparticle formation step, while the degree of functionalization can then be controlled by the size of the employed sulfide ligand by ligand exchange. While von Kiedrowski reported the exchange of the phosphine ligands of the Schmid-Cluster [Au₅₅(PPh₃)₁₂]Cl₆, herein the development of thioether based ligands for other phosphine protected gold cluster ions like *e.g.* [Au₈L₈]²⁺,^[105,106] [Au₉L₈]³⁺,^[107] [Au₁₁L₈]³⁺^[108] or [Au₁₀₁L₂₁]⁵⁺^[109] (with L standing for a triarylphosphine ligand) was envisaged in order to realize a set of selectively functionalized gold clusters which are soluble in organic solvents.

For initial studies on phosphine/sulfide ligand exchange, the [Au₉L₈]³⁺ cluster was chosen. From the different small clusters that are stabilized by monodentate phosphine ligands, the molecular structure of [Au₉L₈]³⁺ displays the highest symmetry with eight surface gold atoms and one central gold atom. The solid state structure, however, is highly sensitive to the nature of the phosphine ligand and the counterion used, resulting in a tetragonal geometry derived from an icosahedron^[107,110-113] or a centered crown geometry^[110,113,114] for the Au₉ core (Figure 21).

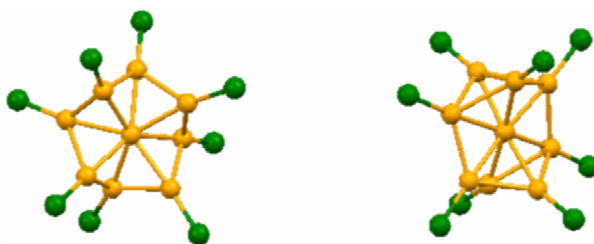


Figure 21. Solid state molecular structures of the central portion of Au₉ cations (orange) with the coordinating phosphorus atoms (green) in a centered crown geometry^[113] (left) or in the icosahedron derived structure (right).^[112] Other atoms than gold or phosphorus were omitted for clarity.

In some cases, both structural isomers were found for the same compound.^[110,112,113] Even more, it was reported that both isomers were found in a single crystallization attempt. The different crystals were separated by their color, dark green for the icosahedron derived structure and brown-red for the centered crown structure.^[110] Accordingly, the spectral shape of the electronic reflectance spectra of the two solid modifications differs strongly. In solution however, NMR^[115] and electronic spectral data^[116,117] indicate that they share a common structure, showing the non-rigidity of these gold clusters, although interconversion of the two structures requires substantial atom movements. It is this structural flexibility that makes these small gold clusters very appealing, as the adaptation to an enwrapping octadentate thioether ligand - able to bind to the eight surface gold atoms - seems likely.

Investigation of the icosahedron derived structure of [Au₉(PPh₃)₈](NO₃)₃ shows P-P distances of 5.5 - 6.8 Å.^[112] Even more interestingly, P-P distances in a very small range between 5.7 and 5.8 Å were found for the centered crown derived structure of the Au₉ cluster. These P-P distances all lie in the distance range of two benzylic thioether moieties which are connected *meta* to each other (Figure 22). An octadentate ligand based on *meta* connected benzylic sulfides was therefore expected to be able to completely enwrap and stabilize an Au₉ cluster core.

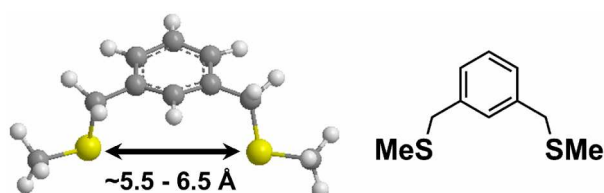
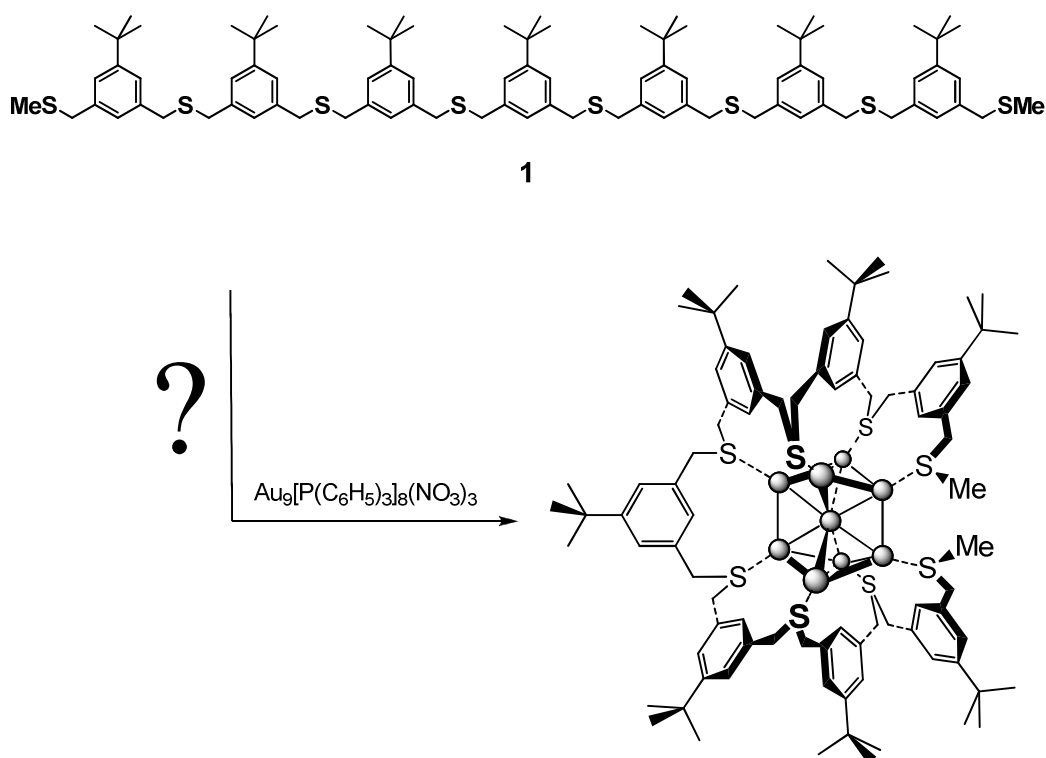


Figure 22. 3D molecular structure (MM2) of *meta*-connected benzylic thioether moieties.

Considerations concerning the solubility of the resulting thioether ligands and the dispersibility of thioether coated nanoparticles implied the necessity for solubilizing groups

attached to the ligands. Furthermore, large solubilizing groups attached to the ligands can also provide more stable gold nanoparticles. Coagulation arising from close contact between nanoparticles can be avoided. The basic design relying solely on benzylic thioethers was therefore altered by *t*-butyl groups *meta* to the benzylic thioether connections of the ligand. In order to allow the ligand to approach the gold core of the phosphine protected cluster easily, the terminal sulfides were capped with relatively small methyl groups. The resulting molecular structure of the heptameric ligand **1** for the inclusion of Au₉ clusters is depicted in Scheme 1.

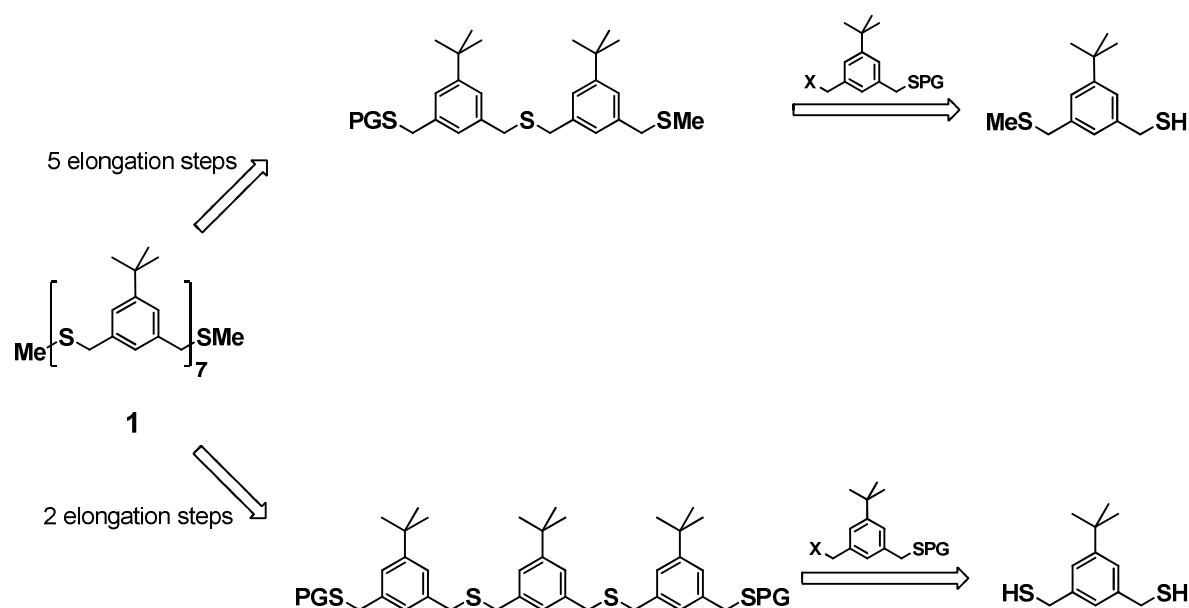
Given the flexibility of both, the benzylic thioether moiety and the gold cluster core, the simple linear octasulfide ligand **1** should be able to act as a multidentate ligand satisfying all eight surface gold atoms of the Au₉ cluster, as is sketched in schematically in Scheme 1 for the icosahedron derived structure.



Scheme 1. Molecular structure of **1** and schematic of the possible 1:1 complex formation of **1** with an icosahedron derived Au₉ cluster core.

3.1.1 Ligand Synthesis

The simple linear design of the heptameric thioether ligand **1** allows in principle for two synthetic strategies: 1) an approach starting from one methyl end of the linear molecule, in which the monomeric units are attached consecutively or 2) starting from the central monomer, where two monomeric units can be attached in one elongation step (Scheme 2).

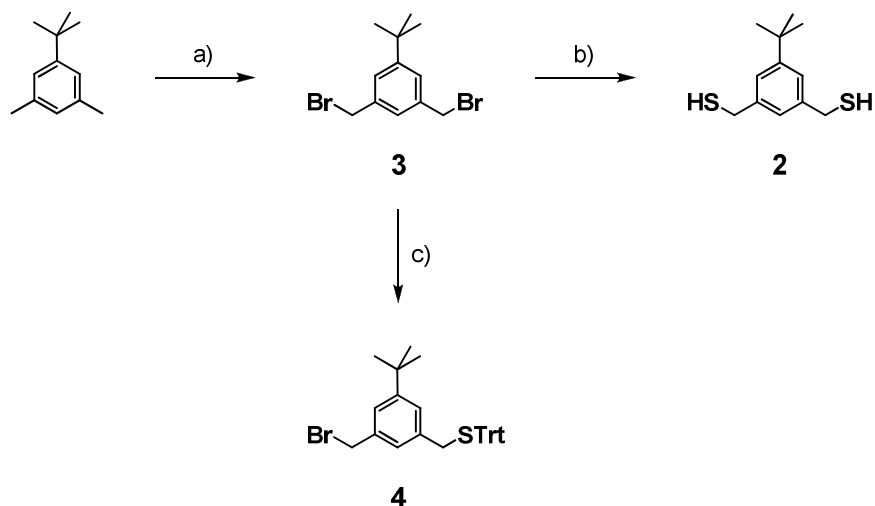


Scheme 2. Retrosynthetic pathways for the synthesis of **1**. X: leaving group; PG: protecting group.

As is obvious from the statements above, the second approach consists of a much lower number of elongation steps. Furthermore, it has to be kept in mind that each elongation step may require more synthetic steps due to protecting group chemistry, which makes the second synthetic strategy starting from the central benzene core much more attractive.

The synthetic strategy is solely based on nucleophilic substitution reactions, which *per se* require a nucleophile and a leaving group. Because benzylic thiols are usually synthesized *via* benzylic halides as leaving groups and a masked or protected thiol precursor,^[118] one extra synthetic step is involved in the synthesis of the nucleophile compared to the leaving group. The central benzene core was therefore chosen to carry the thiol nucleophile in order to save time and material as this building block forms only a small fraction of the molecule and is thus required in smaller quantities than the second required building block. Consequently, (5-*tert*-butyl-1,3-phenylene)dimethanethiol^[119] (**2**) became the starting material for the synthesis of the heptameric ligand **1**.

As second building block a difunctional compound was required, carrying one masked benzylic thiol and one leaving group. As the dithiol **2** can easily be synthesized from 1,3-bis(bromomethyl)-5-*tert*-butylbenzene^[120] (**3**), the dibromide **3** was also chosen as precursor for the synthesis of the second building block.



Scheme 3. Synthesis of **2** and **4**. a) NBS, AIBN, HCOOMe, hv, reflux, 70%; b) thiourea, DMSO, RT, then NaOH aq., 64%; c) TrtSH, K₂CO₃, THF, reflux, 51%.

The precursor for both building blocks for the synthesis of the heptameric ligand **1**, 1,3-bis(bromomethyl)-5-*tert*-butylbenzene (**3**), can be synthesized in a benzylic bromination reaction with *N*-bromosuccinimide (NBS) starting from commercially available 5-*tert*-butyl-1,3-xylene. A very commonly used solvent for radical side chain brominations is carbon tetrachloride, a solvent which is toxic, carcinogenic and exhibits ozone-layer damaging properties (see Material Safety Data Sheet). It was shown that methyl formate works also very efficiently for benzylic brominations.^[121] A procedure that makes use of this solvent^[122] was therefore used for the synthesis of the dibromide **3** (Scheme 3). The radical reaction was initiated by 2,2'-azobis(2-methylpropionitrile) (AIBN) and illumination with a 500 W halogen lamp. The light source emitted enough heat that the mixture was also heated to reflux temperature. After three hours reaction time, the pure product **3** was obtained in a good yield of 70% (literature: 56%^[122]) in multigram scale as colorless crystals after aqueous work up and purification by recrystallization from a dichloromethane (CH₂Cl₂) solution with hexane.

The central dithiol building block **2** was synthesized starting from the dibromide **3** following a slight modification^[123] of the original procedure by Tashiro *et al.*^[119] Using thiourea as sulfur source, the dithiol **2** was obtained after basic and acidic work up. The crude product was

purified by Kugelrohr distillation to give **2** as colorless solid in a yield of 64% (literature: 79%^[123]) (Scheme 3).

As already mentioned above, the second, difunctional building block had to carry one masked benzylic thiol and one leaving group. Especially the protecting group for the masked thiol had to meet several requirements: 1) stability under conditions used for the nucleophilic substitution reaction; 2) cleavage conditions that leave benzylic sulfides undamaged; 3) easy to separate by-products after the deprotection reaction; 4) some degree of control for the monofunctionalization of the dibromide **3** and/or separability of the expected unreacted or difunctionalized by-products. In addition to these requirements, the respective thiol precursor should be commercially available in large enough quantities or at least be synthesized easily in large scale. Also, the reaction conditions needed for the attachment and the deprotection of the thiol should be as simple as possible in order to save time and labor.

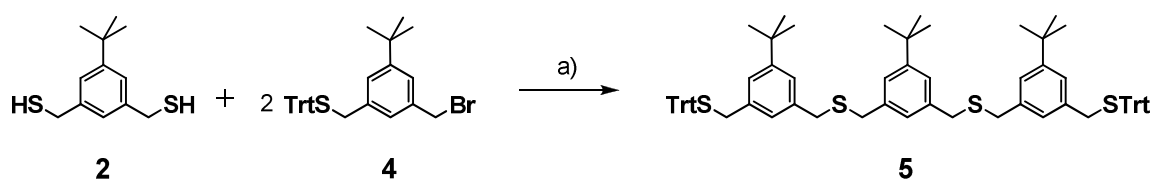
Based on these considerations, the relatively inexpensive trityl thiol seemed to meet the criteria stated above best and was used to synthesize the second building block for the target molecule **1**. This protecting group is sterically highly demanding and can thus provide a good selectivity for the monosubstitution of the dibromide **3**. Furthermore, some examples where trityl thiol was used in order to achieve monosubstitution are already known.^[124,125] Trityl protected thiols are stable under basic, *viz.* nucleophilic substitution conditions and can be cleaved in mildly acidic media which should leave benzylic sulfides intact.^[126] Due to the large size of the trityl group relative to the dibromide **3**, good separability of the desired monofunctionalized compound from the starting material **3** and the disubstituted reaction product by standard silica gel column chromatography can be expected.

The dibromide **3** was thus reacted in a nucleophilic substitution reaction with trityl thiol to form the second building block **4** (Scheme 3). In the literature, only few methods can be found, where trityl thiol was reacted with benzylic bromides, using either *N,N*-dimethylformamide (DMF)^[127,128] or acetonitrile^[129] as solvent. The poor solubility of the dibromide **3** in acetonitrile prevents the use this solvent. Also, the use of the toxic and by evaporation hardly removable solvent DMF was tried to be avoided. In addition, the reaction conditions should be such that monosubstitution of the dibromide **3** can be achieved in high yields. It was therefore tried to use the less polar solvent tetrahydrofuran (THF) with the relatively weak base potassium carbonate in order to get a slow and controllable substitution reaction. The reaction of the starting material **3** and equimolar amounts of trityl thiol in THF in the presence of 1.5 equivalents potassium carbonate was monitored by thin layer chromatography (TLC).

At room temperature, the consumption of trityl thiol was very slow, after 5 days only traces of other compounds than the starting materials were spotted on the TLC plate. For that reason, the mixture was heated to reflux temperature. After 20 hours at that temperature, the trityl thiol was completely consumed and two new spots together with the spot for the starting material **3** were found by TLC. Very importantly, the three spots were well separated, thus indicating an easy separation of the three compounds by standard chromatographic methods. After an aqueous work up, the crude mixture was separated into the components by column chromatography on silica gel. In the order of elution from the column, the starting material **3**, the desired monosubstituted building block **4** and the disubstituted compound were isolated in 19%, 51% and 19% respectively. This result indicates a slight trend towards the monosubstituted product **4**, probably owing to the bulkiness of the trityl thiol nucleophile. These conditions were maintained for syntheses in larger scales starting with up to eight gram of the dibromide **3**. However, in this case, the yield for the desired monofunctionalized building block **4** dropped to 45%, which was mainly due to mixed fractions during the chromatographic separation. As the building block **4** was obtained only as very viscous oil after the evaporation of the solvent CH_2Cl_2 , **4** was precipitated by diluting the concentrated CH_2Cl_2 solution with hexane, followed by evaporation of this solvent mixture. After this procedure the monobromide **4** was obtained as colorless solid which could be conveniently handled in the following synthetic steps.

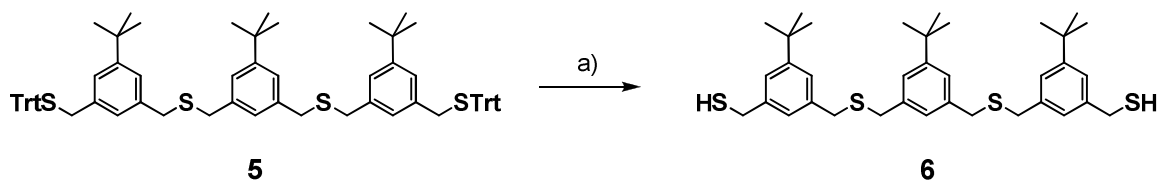
With the two main building blocks **2** and **4** in hand, the elongation procedure to form in an initial step the trimeric trityl protected intermediate **5** had to be developed. Similar to the introduction of the trityl thiol to form **4**, the elongation reaction is a nucleophilic substitution reaction with a thiol nucleophile and a benzylic bromide as leaving group. The conditions that were successfully used before - THF at reflux temperature with potassium carbonate as base - were thus applied to a mixture of the dithiol **2** and the monobromide **4** in a ratio of 1:2. After 30 hours at the elevated temperature, TLC of the reaction mixture still showed mainly the presence of the starting materials **2** and **4**. The reaction rate of such nucleophilic substitution reactions can be increased by changing different parameters such as temperature, solvent and base. Without using a pressure tube, higher temperatures cannot be reached with THF as solvent. Potassium carbonate was therefore changed to the stronger base sodium hydride, which can deprotonate thiol groups to form more nucleophilic sodium thiolates. Furthermore, this base is readily available and easy to handle as dispersion in mineral oil. A 1:2 mixture of **2** and **4** in dry THF under argon was therefore charged with an excess of sodium hydride at room temperature (Scheme 4). These conditions proved to be very effective, as the complete

consumption of the starting materials was already observed after 40 minutes by TLC. After careful quenching of excess sodium hydride by water and an aqueous work up using *t*-butyl methyl ether (MTBE), the crude was purified by column chromatography to give the pure trityl protected trimer **5** in an excellent yield of 96% as colorless solid foam. Particularly with regard to substitution reactions with even larger nucleophiles in later steps of the synthetic pathway to the heptameric ligand **1**, these room temperature conditions seemed to be very promising. Heating would still be possible if the substitution reactions become too slow at room temperature with larger, more sterically demanding nucleophiles.



Scheme 4. Synthesis of the trimer **5**. a) NaH, THF, RT, 96%.

The next fundamental reaction within this sequence was the selective cleavage of the trityl protecting group in the presence of benzylic sulfides. The trityl group can be cleaved easily under acidic conditions in the presence of a cation scavenger, but strong acidic conditions may also cleave the benzylic thioethers.^[126] It was found that triethylsilane can act as cation scavenger very efficiently, thus allowing for very fast deprotection reactions even at low concentrations of trifluoroacetic acid.^[130] Following a procedure developed for a highly functionalized intermediate of a natural macrolactone,^[131] trifluoroacetic acid (TFA) (4% v/v) was added to a solution of the trityl protected trimer **5** and 2.5 equivalents triethylsilane in CH₂Cl₂ (Scheme 5).



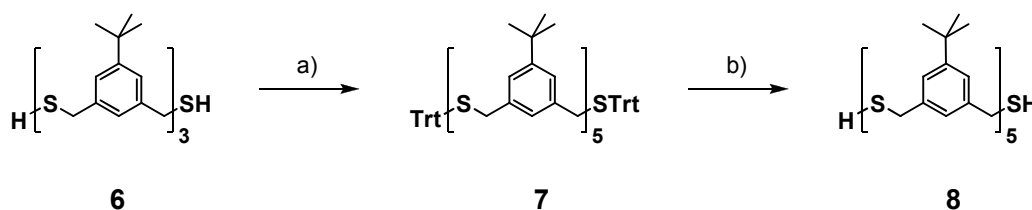
Scheme 5. Deprotection of **5**. a) Et₃SiH, TFA, CH₂Cl₂, RT, quant.

Directly after the addition of the acid the solution turned yellow, indicating the formation of the trityl cation. The color disappeared completely within 5 minutes. TLC analysis after this reaction time confirmed the removal of the trityl groups, as the starting material was

completely consumed and two new spots - one apolar compound and one spot with an R_f value close to the retention factor of the starting material - were observed. A cerium(IV)/ammonium molybdate^[132] reagent that shows the presence of the trityl protecting group by red staining compared to blue staining for compounds that do not easily form carbocations was used to stain the TLC plates. Thereby the removal of the trityl protecting group was shown. Gibbs reagent^[132] stains free thiols in a strong yellow color on TLC plates, while thioethers and most other functional groups remain colorless. The new spot close to the starting material **5** was thereby ascertained to contain the expected thiol functionalities. By use of these two staining reagents, the reaction progress throughout the whole synthetic pathway could be easily monitored, as all intermediates contain either free thiol groups or trityl protected thiols. The deprotection reaction was quenched with sodium hydrogen carbonate and extracted with CH_2Cl_2 . After purification by column chromatography, the trimeric dithiol **6** was obtained as colorless solid in up to quantitative yields. The excellent yields of this reaction and the very apolar and therefore easy to separate by-products made this protocol highly promising for the remaining steps towards the target ligand **1**.

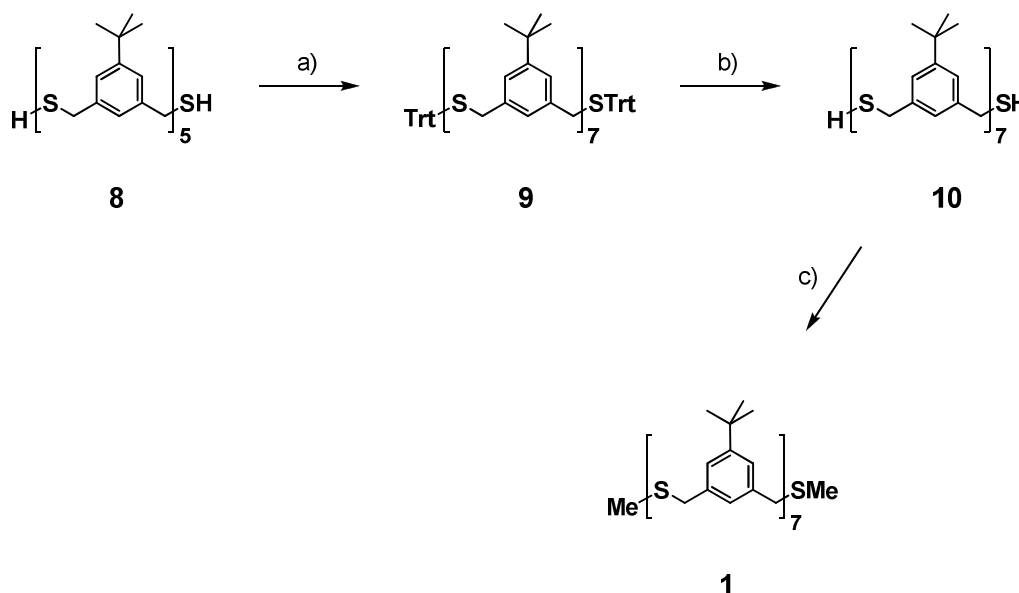
The trityl protected pentamer **7** was synthesized from the trimeric dithiol **6** using the procedure that was used for the synthesis of the trityl trimer **5**. The reaction of the dithiol **6** and 2.2 equivalents of the monobromide **4** in THF with sodium hydride as base successfully gave the pentamer **7** after 1.5 hours at room temperature. After purification by column chromatography, **7** was obtained as colorless solid foam in an excellent yield of 97% (Scheme 6).

The trityl protecting group was then removed from **7** using TFA (4% v/v) in CH_2Cl_2 in the presence of triethylsilane as cation scavenger similar to the deprotection of the trimer **5**. The apolar by-products of the deprotection procedure were removed easily by column chromatography to give the pure pentameric dithiol **8** in a yield of 99% as colorless solid. These results nicely illustrate the generality of the procedures chosen for chain elongation and deprotection of the thiol moieties even for larger nucleophiles.



Scheme 6. Synthesis of the free thiol pentamer **8**. a) **4**, NaH, THF, RT, 97%; b) Et_3SiH , TFA, CH_2Cl_2 , RT, 99%.

Chain elongation was then achieved under similar conditions as before using the pentamer dithiol **8** and the monomeric building block **4**. Under the action of sodium hydride in THF (Scheme 7), the trityl protected heptamer **9** was obtained very efficiently in a yield of 92% after purification of the crude by column chromatography.

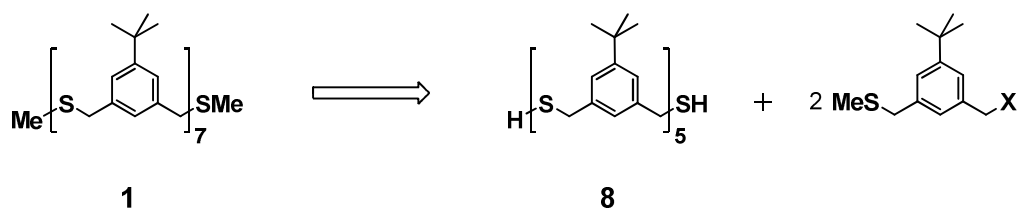


Scheme 7. Synthesis of the target compound **1**. a) **4**, NaH, THF, RT, 92%; b) Et₃SiH, TFA, CH₂Cl₂, RT, 99%; c) NaH, THF, then MeI, RT, 89%.

The general acidic conditions for the removal of the trityl protecting group were applied to **9**, whereby the heptamer dithiol **10** was obtained very efficiently in 99% yield after purification by column chromatography.

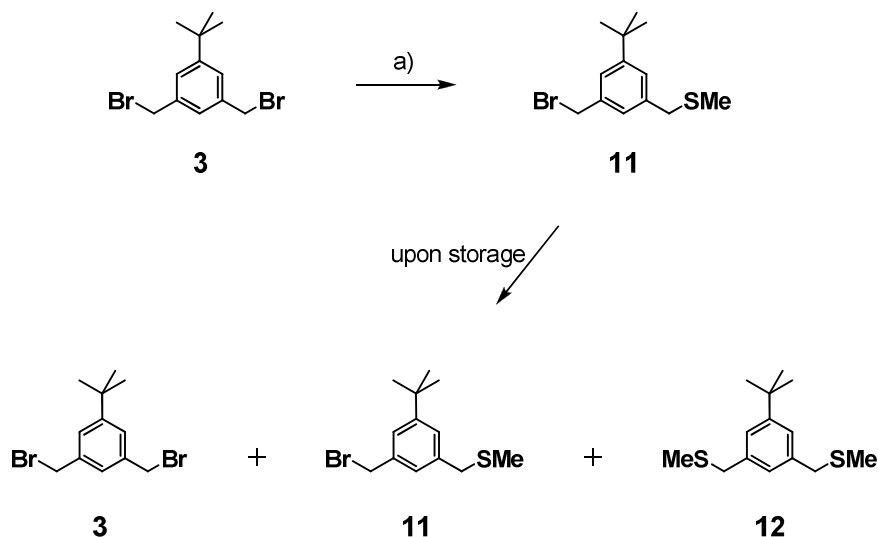
In a final synthetic step, the methyl end-caps were introduced to the heptamer dithiol **10** using iodomethane as electrophile. By using the nucleophilic substitution conditions that were applied successfully before in the elongation steps, the pure methylated target ligand **1** was obtained as colorless solid in a good yield of 89% after chromatographic purification.

In view of larger scale syntheses of the heptameric ligand **1**, an alternative, more divergent synthetic pathway was also explored. Using this route, **1** can be obtained in one step instead of three from the pentameric dithiol **8** (Scheme 8).



Scheme 8. Alternative pathway for the synthesis of **1**.

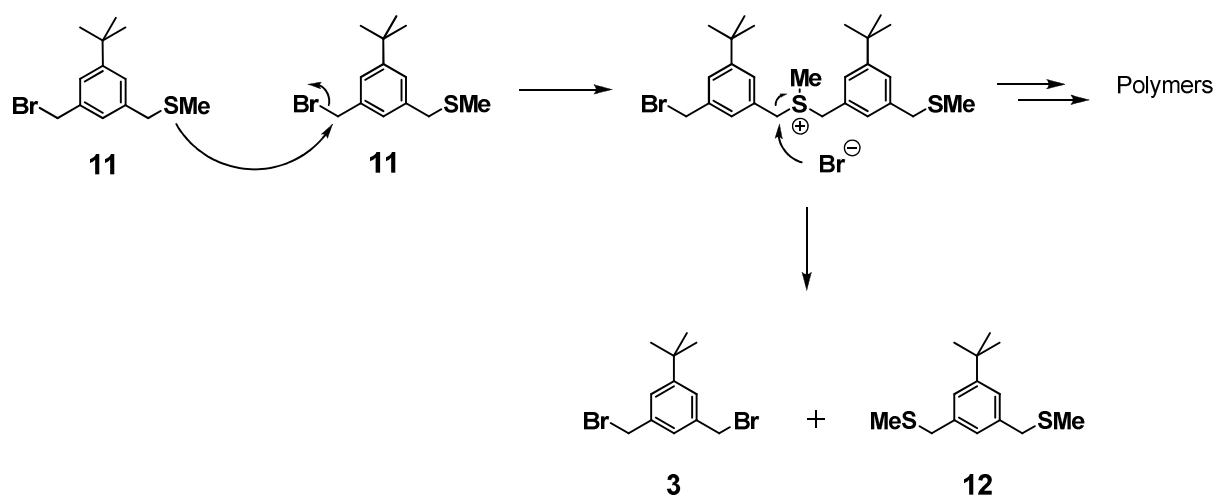
Initially it was tried to synthesize the difunctional compound **11** starting from the dibromide **3** and one equivalent of sodium methanethiolate in dry THF. TLC analysis after two hours revealed the formation of two new spots, probably representing the mono- and dithiolated compound respectively. However, after an aqueous workup and purification by column chromatography, only small amounts (max. 10%) of the desired monobromide **11** were isolated as colorless liquid (Scheme 9). The starting material **3** and the dithiolated compound **12** were also isolated in 20 and 11% respectively. Further investigations showed the very limited stability of **11**: TLC of a sample of purified **11** after storage at 4°C for 24 hours showed again three spots, which appeared to be the dibromide **3**, the monothiolated compound **11** and the dithiolated compound **12** (Scheme 9).



Scheme 9. Attempt to synthesize **11**. a) NaSMe, DMF, RT.

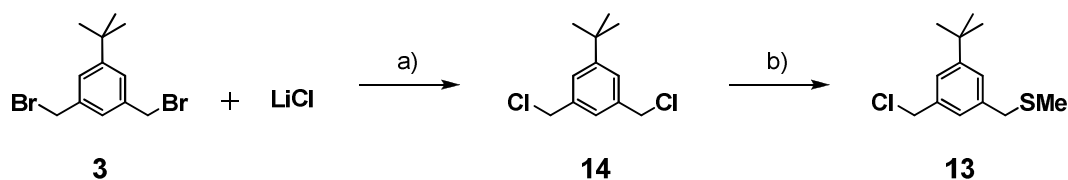
Furthermore, it was noticed that large amounts of the material applied to the TLC plate remained on the baseline when the plate was left for a few minutes at ambient conditions before development. Although several compounds that bear similar structural motifs with benzylic sulfides and benzylic bromides in close proximity were reported in the literature,^{[133-}

^{138]} it is also known that alkyl sulfides can form sulfonium salts with benzylic bromides. This transformation can be done in neat form,^[139] but also in standard organic solvents such as acetone,^[140] chloroform,^[141] acetonitrile^[142] or diethyl ether^[143] without the addition of non-nucleophilic, stabilizing counterions (*e.g.* PF_6^- , BF_4^- , ClO_4^-) at room temperature. Based on this information, it seems very likely that the processes depicted in Scheme 10 take place during the handling of **11**. The sulfonium salts and the polymeric products account probably for the large amount of material that remains on the baseline in TLC investigations



Scheme 10. Possible mechanisms for the degradation of **11**.

The stability observed for the trityl protected building block **4** can therefore be attributed mainly to the sterically demanding trityl group, which prevents the nucleophilic attack of the sulfide moieties to benzylic bromides. However, as was stated in the introduction, the relatively small methyl terminus for the heptameric ligand **1** was chosen on purpose, the exchange to sterically more demanding capping groups was therefore not an option. It was rationalized that the exchange to a weaker leaving group than bromide could give stable compounds containing the leaving group in benzylic position and alkyl sulfides in the same molecule. Indeed, a literature search on the formation of sulfonium ions with benzylic chlorides revealed that this transformation requires elevated temperatures and auxiliary anions,^[144-148] increased stability was therefore expected for the monochloride analogon **13**. 1-*tert*-Butyl-3,5-bis(chloromethyl)benzene^[149] (**14**) was thus synthesized from the dibromide **3** using excess lithium chloride in DMF,^[150] a procedure that gives benzylic chlorides very efficiently (Scheme 11).



Scheme 11. Synthesis of **13**. a) DMF, RT, 99%; b) NaSMe, DMF, RT, 18%.

After one hour stirring at room temperature and aqueous work up, the dichloride **14** was obtained as colorless crystals in quantitative yield and sufficient purity. Under similar conditions that were used for the attempted synthesis of the monobromide **11**, the dichloride **14** was reacted with one equivalent of sodium methanethiolate (Scheme 11). As expected, three main spots were found on the TLC plate. Importantly, no material stayed on the baseline, indicating the suppression of sulfonium salt formation with benzylic chlorides. After separation of the three compounds by column chromatography, the desired monofunctionalized compound **13** was obtained together with the starting material **14** and the dithiomethylated compound in 18%, 42% and 29% respectively. The liquid chloride **13** did not show any signs of decomposition or sulfonium salt formation under ambient conditions. However, as can be seen by the low yield, no selectivity was observed for the monothiolated compound, probably due to the missing steric hindrance of the methyl thiolate compared to tritylthiol. For that reason, this pathway was not investigated to further extent. On the other hand, these findings were important for the development of synthetic pathways for functionalized and dendritic thioether ligands (*vide infra*).

3.1.2 Au₉ Ligand Exchange Experiments

With the target ligand **1** in hand, ligand exchange experiments were conducted using the gold cluster [Au₉(PPh₃)₈](NO₃)₃. This gold cluster is soluble in organic solvents such as methanol, CH₂Cl₂ or THF. Unlike the experiments carried out by von Kiedrowski *et al.*,^[99,100] two-phase experiments at the aqueous/organic interface were not possible, as monofunctionalized gold clusters that are processable by wet synthetic chemistry in organic solvents were targeted within this project. The progress of the ligand exchange is therefore not directly observable by phase transfer of the cluster color and other methods had to be applied in order to verify removal of the phosphine ligands and introduction of the octadentate thioether ligand. A versatile tool to investigate this ligand exchange reaction is given by proton decoupled ³¹P NMR. [Au₉(PPh₃)₈](NO₃)₃ shows one sharp signal at $\delta = 56.9$ ppm,^[112] while free triphenylphosphine gives a signal at $\delta = 5.4$ ppm.^[151] The release of the phosphine ligands should therefore easily be monitored by NMR, considering the large differences of the chemical shifts that can be expected for the initial gold cluster and the free phosphine ligands. Furthermore, the ¹H NMR signals of the gold bound triphenylphosphine are shifted as well compared to free triphenylphosphine.

3.1.2.1 NMR Titration Experiments

Given the structural flexibility of both, the gold cluster and the ligand **1**, a relatively fast exchange rate was anticipated. Hence, a titration of the ligand **1** with the gold cluster was performed directly in an NMR tube. To a solution of the heptameric ligand **1** (1 μ mol) in deuterated dichloromethane (CD₂Cl₂) (1 ml) was added [Au₉(PPh₃)₈](NO₃)₃ (2 μ mol) in 0.2 μ mol portions. After each addition of gold cluster, the ¹H and the ³¹P NMR spectra were recorded. Except for the increase of the signals of the Au₉ cluster relatives to the ligand **1** signals, no changes were observed in the NMR spectra throughout this study.

3.1.2.2 Long Term Ligand Exchange Studies

A slow ligand exchange could be the reason for the negative outcome of this initial attempt for the formation of thioether coated Au₉ clusters. Consequently, the next experiment was performed as a long term NMR study. A CD₂Cl₂ solution of equimolar amounts of [Au₉(PPh₃)₈](NO₃)₃ and the ligand **1** were sealed together with ferrocene as reference substance under argon in an amberized NMR tube and investigated regularly over a period of ten weeks. As control experiment, a solution of the gold cluster alone was monitored under similar conditions. However, similar to the initial NMR titration, the ¹H (Figure 23) and the ³¹P NMR (Figure 24) spectra remained the same in both samples and no evidence for ligand exchange was found.

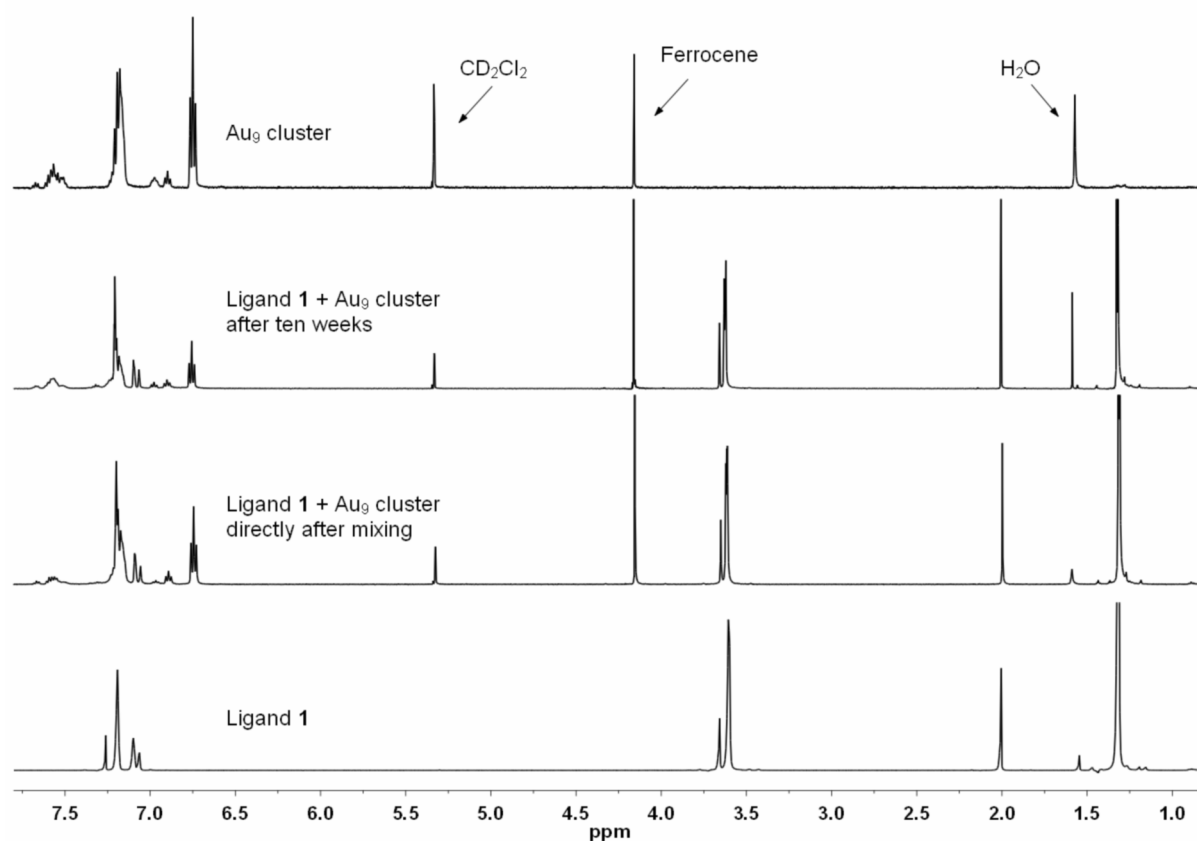


Figure 23. Comparison of ¹H NMR spectra of the mixture of the ligand **1** and [Au₉(PPh₃)₈](NO₃)₃ directly after mixing of the components and after ten weeks. Ferrocene was added as reference for signal integration.

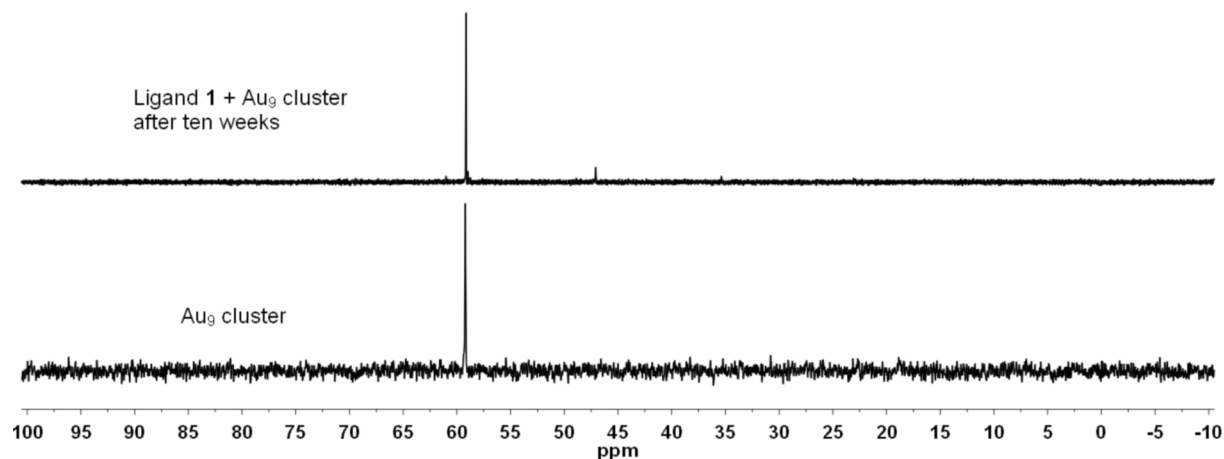


Figure 24. Comparison of ^{31}P NMR spectra of the mixture of the ligand **1** and $[\text{Au}_9(\text{PPh}_3)_8](\text{NO}_3)_3$ directly after mixing of the components and after ten weeks.

In other reported ligand exchange experiments with $[\text{Au}_9(\text{PPh}_3)_8](\text{NO}_3)_3$, large excess of the exchanging ligand was used.^[112,152] Due to the negative outcome of the initial experiments using equimolar amounts of the gold cluster and the octadentate thioether ligand **1**, such conditions were also tried. A mixture of a 15-fold excess of the ligand **1** and $[\text{Au}_9(\text{PPh}_3)_8](\text{NO}_3)_3$ was therefore stirred in dry CH_2Cl_2 under argon. In addition to ^{31}P NMR, the attempted ligand exchange was also investigated by UV/vis spectroscopy. The different known small gold clusters show discrete electronic transitions which are not sensible to the variation of phosphines and anions, but extremely sensitive to changes in the cluster size and geometry.^[153] Since the exchange from phosphines to sulfides may induce structural changes in the gold core, UV/vis spectroscopy was employed as fast tool to monitor the ligand exchange reaction. However, no changes were observed in the UV/vis and ^{31}P NMR spectra within 2 days. After this time, the mixture was heated to 35°C for 12 hours. A fine black precipitate formed during that time, indicating a partial thermal decomposition of the gold cluster and the formation of bulk gold. After this procedure, the ^{31}P NMR spectrum of the remaining colored solution with additional CD_2Cl_2 showed two new signals at $\delta = 45$ ppm and $\delta = 33$ ppm in addition to the original $[\text{Au}_9(\text{PPh}_3)_8](\text{NO}_3)_3$ signal at $\delta = 57$ ppm (Figure 25). The mixture was then left for another week at the elevated temperature. During that time, more of the black precipitate was formed and the liquid phase became colorless. Also, relative to the ^{31}P resonance for the Au_9 cluster, the two new signals at $\delta = 45$ ppm and $\delta = 33$ ppm became stronger. As much more upfield shifts would be expected for free triphenylphosphine ligands, the new signals that were observed in the ^{31}P NMR spectra must probably be attributed to triphenylphosphine ligands which are bound to other gold species. The ^{31}P resonances of the larger gold clusters $[\text{Au}_{55}(\text{PPh}_3)_{12}]\text{Cl}_6$ and $[\text{Au}_{101}(\text{PPh}_3)_{21}]\text{Cl}_5$ were reported

to be at $\delta = 32$ ppm^[154] and $\delta = 43$ ppm,^[155] respectively. It is therefore possible that similar clusters with NO_3^- anions were formed before the precipitation to bulk gold took place. Another possibility is the formation of $\text{Au}(\text{PPh}_3)\text{Cl}$ in a reaction with the chlorinated solvent, as this compound was reported to show a ^{31}P resonance at $\delta = 34$ ppm.^[155]

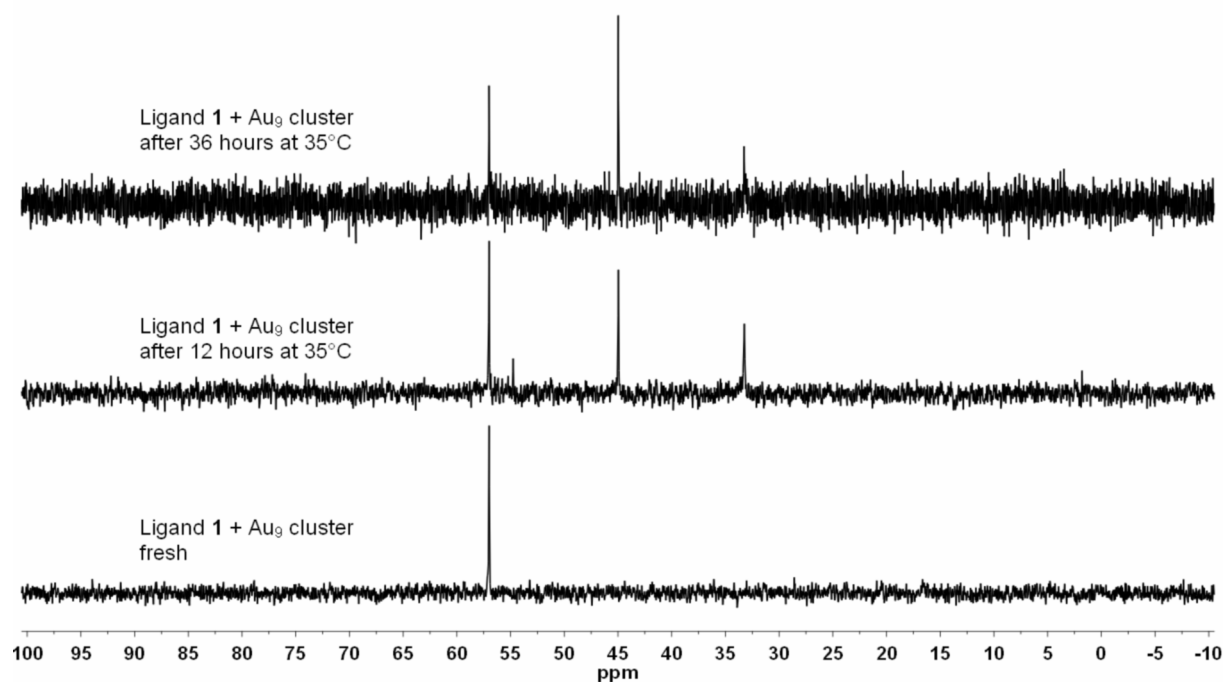


Figure 25. ^{31}P NMR spectra of the ligand exchange experiment with the heptamer **1** and $[\text{Au}_9(\text{PPh}_3)_8](\text{NO}_3)_3$ in CH_2Cl_2 .

However, in the UV/vis spectrum that was obtained after 36 hours at the elevated temperature, only the appearance of a peak centered at 340 nm can be observed in addition to the original signals of $[\text{Au}_9(\text{PPh}_3)_8](\text{NO}_3)_3$ (Figure 26). This is not in accordance with the formation of Au_{55} or Au_{101} clusters, for which decreasing absorbances between 300 and 800 nm were reported.^[45,109] The origin of the absorbance at 340 nm could not be assigned to a known gold cluster, the nature of the formed compounds remained therefore puzzling. In any case, no suitable conditions for the direct ligand exchange to form thioether coated Au_9 clusters were found. Furthermore, the coagulation to bulk gold was observed, even indicating the possibility of destabilization of the Au_9 cluster by the thioether ligand.

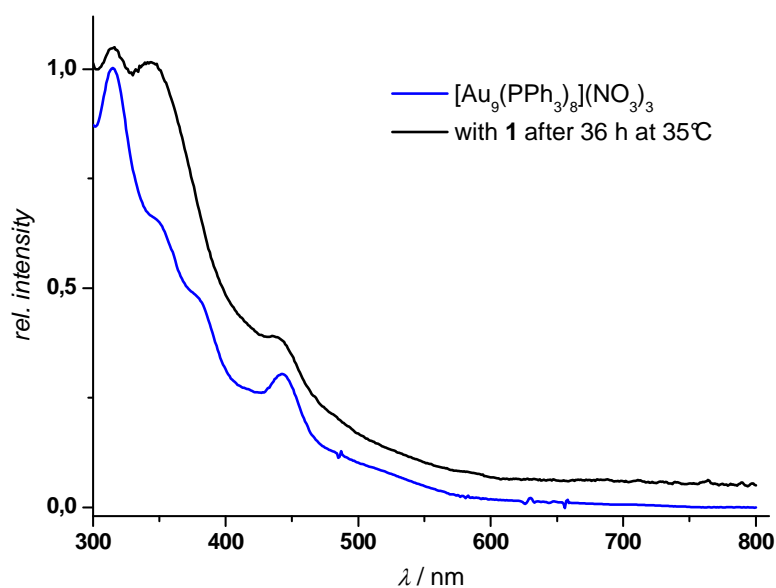


Figure 26. UV/vis spectrum of the ligand exchange experiment with the heptamer **1** and $[\text{Au}_9(\text{PPh}_3)_8](\text{NO}_3)_3$ in CH_2Cl_2 in comparison with the spectrum of pure $[\text{Au}_9(\text{PPh}_3)_8](\text{NO}_3)_3$.

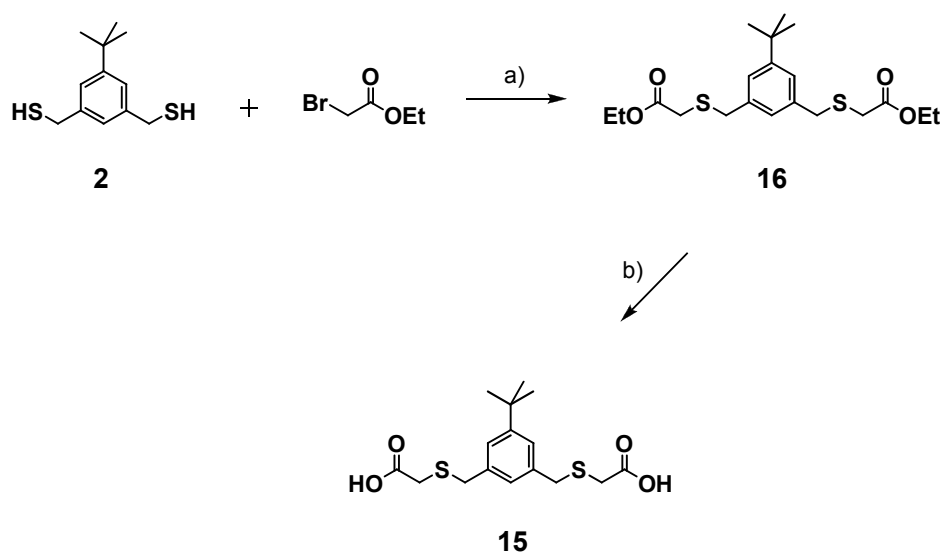
These unsuccessful experiments in CH_2Cl_2 and CD_2Cl_2 led to the conclusion that a change of the employed solvents could help to facilitate the ligand exchange. Given the relative high polarity of $[\text{Au}_9(\text{PPh}_3)_8](\text{NO}_3)_3$ and the low polarity of the thioether ligand **1**, it was tried to use a biphasic mixture of organic solvents, where a ligand exchange could be observed directly by a phase exchange of the colored gold cluster. Using again a 15-fold excess of the ligand **1** in hexane, a solution of $[\text{Au}_9(\text{PPh}_3)_8](\text{NO}_3)_3$ in methanol was added and the resulting two-phase mixture was stirred for one week. Similarly, a two-phase mixture of ethylene glycol and toluene was used in order to achieve ligand exchange. In both cases, the less polar phase stayed colorless, while the reddish color of the gold cluster solution remained unchanged in the more polar phase. This result was further corroborated by the ^{31}P NMR spectra of the colored solutions, which did not show any changes compared to the spectrum of pure $[\text{Au}_9(\text{PPh}_3)_8](\text{NO}_3)_3$.

3.1.2.3 Two-Phase Ligand Exchange Experiments with Water Soluble Gold Clusters

The phosphine ligands of $[\text{Au}_9(\text{PPh}_3)_8](\text{NO}_3)_3$ can be exchanged by water soluble triphenylphosphine monosulfonate^[112] and trisulfonate^[152] sodium salt ligands, resulting in water soluble gold clusters. The UV/vis spectra after the ligand exchange reactions were no more consistent with the Au_9 cluster cores, but resembled the spectra that were obtained for

phosphine stabilized Au₈ clusters. So far, the exact composition of these clusters remains unsolved.^[112,152] Nevertheless, these water soluble gold clusters seemed highly promising for two-phase ligand exchange experiments with the octadentate thioether ligand **1** and were used in attempts to form thioether stabilized gold clusters. Aqueous solutions of the freshly prepared water soluble gold clusters with the triphenylphosphine monosulfonate or trisulfonate ligands were added to solutions of 15 equivalents of the heptamer **1** in CH₂Cl₂ and the biphasic mixtures were stirred vigorously under argon for 4 days. As in all other attempts before, no indication for ligand exchange was observed in both cases, neither by transfer of the gold cluster color to the organic phase nor by ³¹P NMR investigations.

In a final attempt to synthesize small sulfide protected gold clusters by ligand exchange reactions, it was investigated whether carboxylic acid moieties, which were present in the ligands employed for the phosphine sulfide exchange of the Schmid-Cluster,^[99,100] were crucial for a successful ligand exchange. In this case, a small, easy to synthesize ligand was wanted for an initial test reaction. Hence, the bicarboxylic acid ligand **15** was synthesized in two steps starting from the dithiol **2** (Scheme 12). The alkylation with ethyl bromoacetate proved to be straightforward in CH₂Cl₂ with triethylamine (TEA) as base. The diester **16** was obtained as colorless oil in 62% yield after column chromatography. Saponification under basic conditions using sodium hydroxide in a water/ethanol mixture gave the desired diacid **15** quantitatively as colorless solid in high purity after an aqueous work up.



Scheme 12. Synthesis of the diacid **15**. a) TEA, CH₂Cl₂, RT, 62%; b) NaOH aq., EtOH, RT, quant.

To test the ligand exchanging properties of the diacid ligand **15**, a biphasic water/CH₂Cl₂ setup was used with the water soluble triphenylphosphine monosulfonate gold cluster and a large excess of the ligand **15**. This mixture was stirred vigorously under argon for 3 weeks and investigated by NMR weekly. As in all other experiments before, no phase transfer and no changes in the ³¹P NMR spectrum were observed during that time period.

Based on these results for ligand exchange experiments with small Au₉ clusters it was concluded that the phosphine sulfide exchange is not that straightforward in this case as it was reported for the Au₅₅ cluster. This could be explained by the nature of the investigated gold cluster: while [Au₉(PPh₃)₈](NO₃)₃ can be perceived as defined molecular species with molecule-like electronic levels,^[112] “[Au₅₅(PPh₃)₁₂]Cl₆” was found to be polydisperse.^[45] Furthermore, the phosphine ligands of larger “Au₅₅” or “Au₁₀₁” clusters proved to be labile and are easily exchanged.^[45,155-157] For the larger clusters, rapid movement of the phosphine ligand along the particle surface is discussed as being the reason for the single phosphine resonance observed in ³¹P NMR spectra.^[156] In the case of a small Au₁₁ cluster, no evidence for such dynamic behavior was found,^[158] highlighting the different type of Au-P interaction for the small, molecule-like gold clusters compared to the larger phosphine protected gold nanoparticles.

In view of the negative outcome of the attempts to synthesize thioether protected Au₉ clusters by phosphine sulfide exchange, no further experiments were done regarding this goal.

3.1.3 Thioether Coated Gold Nanoparticles by Ligand Exchange

As the experiments concerning the preparation of thioether coated small gold clusters by phosphine-sulfide ligand exchange were not successful, it was tried if gold nanoparticles that are stabilized by more weakly bound protecting agents than phosphines can be enwrapped and stabilized by multidentate thioether ligands.

It was reported that gold nanoparticles prepared by an inverse micelle synthesis using didodecyldimethylammonium bromide as surfactant can be modified after the synthesis by dialkyl sulfides.^[159] The particles obtained by this procedure, however, had a mean diameter of 7 nm and were thus rather big for the envisaged ligand exchange with multidentate thioether ligands to form nanoparticles with defined numbers of ligands. Furthermore, the distribution of particle sizes was very broad. More interestingly, the surfactant-free synthesis of gold nanoparticles in diethylene glycol dimethyl ether (diglyme) with sodium naphthalenide as reducing agent was reported in 2005.^[160] The by the solvent only weakly stabilized nanoparticles were not stable for a longer time, but addition of alkyl thiol or alkyl amine ligands led to stable, dispersible nanoparticles. The particle sizes were adjusted by the amount of reducing agent in a range of 1.9 to 5.2 nm with satisfactory size distributions. Given the rather weak binding of diglyme to the nanoparticle surface, this method seemed very promising with regard to stabilization of the particles with multidentate thioether ligands.

Using the heptameric ligand **1**, it was tested whether this method allows for the size selective synthesis of gold nanoparticles stabilized by multidentate thioether ligands. Following the literature procedure,^[160] the weakly protected gold nanoparticles were synthesized by adding 2.5 equivalents of a sodium naphthalenide solution to a solution of tetrachloroauric acid in diglyme. After 2 minutes, aliquots of the dark red-brown colored nanoparticle dispersion were then added to solutions of different amounts of the thioether ligand **1** in toluene. The amount of ligand was thereby varied from 1 to 10 equivalents of thioether moieties compared to the amount of tetrachloroauric acid employed. Similar to the exchange with alkyl thiol or alkyl amine ligands described in the literature,^[160] this procedure led to precipitation of the gold nanoparticles, leaving the liquid phases nearly colorless. After centrifugation and removal of the supernatants, it was tried to redisperse the black precipitates in CH₂Cl₂. In all cases, the residues were only redispersible to a very small extent in CH₂Cl₂, giving very slightly pink colored nanoparticle dispersions. Most of the material remained in the solid phase, indicating either a very weak stabilization by the thioether ligand **1** or only incomplete displacement of

the diglyme from the nanoparticle surface. Apart from the formation of bulk gold by coagulation of nanoparticles, the formation of large, indispensible assemblies of intact nanoparticles has to be taken into account. In principle, one octadentate ligand **1** can cross-link two or more nanoparticles, whereby the formation of large nanoparticle aggregates could be triggered. Similar behavior was observed in the case of gold nanoparticles that were stabilized by the weak capping agent tetra-*n*-octylammonium bromide (TOAB) upon addition of silane based tri- or tetradentate thioether ligands.^[161-163] UV/vis analysis of the slightly colored CH₂Cl₂ dispersions of the initial precipitate reveals a very broad and red shifted surface plasmon resonance band, which is indicative of close nanoparticle-nanoparticle interactions.^[9,10]

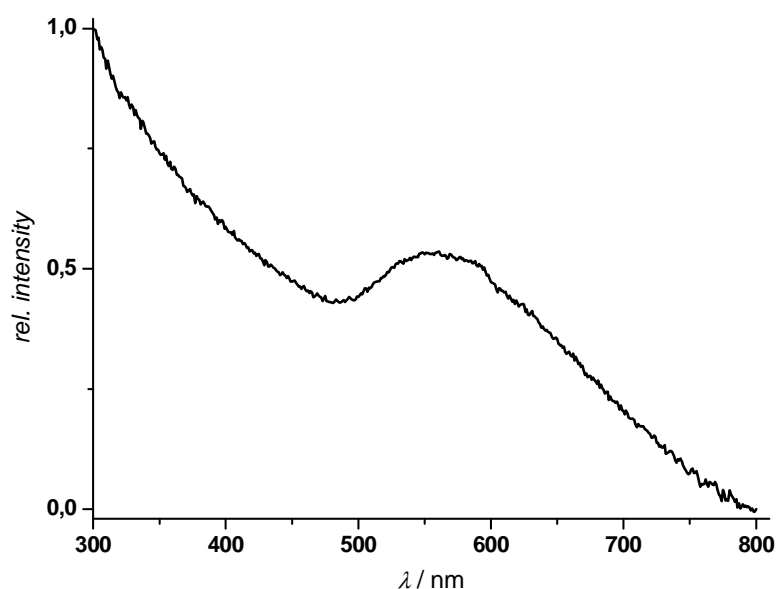


Figure 27. UV/vis absorption spectrum of the redispersed (CH₂Cl₂) nanoparticle precipitate in the presence of the heptameric ligand **1**.

The observed spectral shape was thereby independent of the amount of thioether ligand **1** used. Under otherwise similar conditions as the experiments employing the thioether ligand **1**, the diglyme stabilized particles were added to pure toluene. Compared to the experiments employing the thioether ligand **1**, the complete precipitation of the nanoparticles was slower and the formed precipitate was not redispersible in CH₂Cl₂ at all. These results show that the bidentate thioether ligands do have an effect on the diglyme stabilized gold nanoparticles, even if the influence may be small. A clear picture of the nature of the observed precipitate cannot be obtained just by UV/vis investigations and the conclusions drawn are highly speculative. In any case, it was not possible to obtain stable and dispersible thioether coated

gold nanoparticles by this method. For this reason, the application of thioether ligands to weakly diglyme stabilized gold nanoparticles was no more pursued.

3.1.4 Summary and Conclusions

In summary, the synthesis of gold clusters or nanoparticles stabilized by multidentate thioether ligands *via* ligand exchange reactions was not successful. Different attempts for ligand exchange using the heptamer **1** with a variety of conditions left the gold clusters either untouched or led to the decomposition of the gold species. Also the introduction of carboxylic acid end groups to the thioether ligands did not provide thioether stabilized gold clusters. Even the very weakly binding diglyme as stabilizer for gold nanoparticles could not be replaced to form stable thioether coated particles. However, in this case the UV/vis results indicate the formation of nanoparticle aggregates mediated by the octadentate thioether ligand **1**. The plasmon resonance that was observed by UV/vis spectroscopy is thereby a sign for the formation of nanoparticles with diameters larger than 2-3 nm. This shows that the thioether ligands do indeed partially bind and interlink gold nanoparticles, but do not enwrap and efficiently stabilize single particles. In contrast to the results that were obtained by von Kiedrowski,^[99,100] these observations indicate that multidentate thioether ligands might not be well suited for the formation of thioether stabilized gold nanoparticles by ligand exchange reactions.

3.2 Direct Synthesis of Thioether Stabilized Gold Nanoparticles

In this section, the direct preparation of gold nanoparticles in the presence of multidentate linear thioether ligands of different length will be shown. The results concerning the stabilization and surface coverage of gold nanoparticles by these ligands will be discussed.

The ability of thioether based ligands to stabilize gold nanoparticles was reported in the literature for a few examples. In particular, with exception of the two-phase ligand exchange synthesis reported by von Kiedrowski^[99,100] and the inverse micelle synthesis from Sorensen,^[159] all of the thioether stabilized gold nanoparticles were directly synthesized from water soluble gold(III) precursors by reduction in the presence of the stabilizing thioether ligands.^[135,164-171] However, by comparing the different studies it becomes evident that the nature of the employed thioether ligands and hence the obtained results concerning nanoparticle sizes and stability differ strongly.

In the early reports of thioether stabilized gold nanoparticles from the laboratories of David Reinhoudt^[164] and Jon Preece,^[165] dialkyl sulfide ligands such as **17** (Figure 28) were used in similar protocols as were used for the synthesis of alkyl thiolate protected gold nanoparticles. The dialkyl sulfide stabilized gold nanoparticles were found to be much less stable than alkyl thiolate protected ones. Irreversible aggregation of the particles occurred within hours in dispersion or upon removal of the solvent. Also in comparison to the dialkyl sulfide stabilized gold nanoparticles obtained by an inverse micelle method (see section 3.1.3),^[159] a much lower stability was found. This was attributed to the stabilizing properties of the micelle forming surfactant that was not removed from the particle surfaces.^[164] Compared to alkyl thiolate protected gold nanoparticles, the particles stabilized by dialkyl sulfides showed much larger core sizes and broader size distributions. For example, decanethiol yielded gold nanoparticles with a mean diameter of 2.2 ± 0.1 nm, while the synthesis of didecyl sulfide capped particles under similar reaction conditions yielded nanoparticles with a mean core diameter of 5.3 ± 0.8 nm.^[165] On the other hand, it was also shown that by using a sterically demanding calix(4)arene derived tetradentate thioether ligand **18** (Figure 28), significantly smaller (1.8 ± 0.4 nm) and also more stable nanoparticles were obtained.^[164]

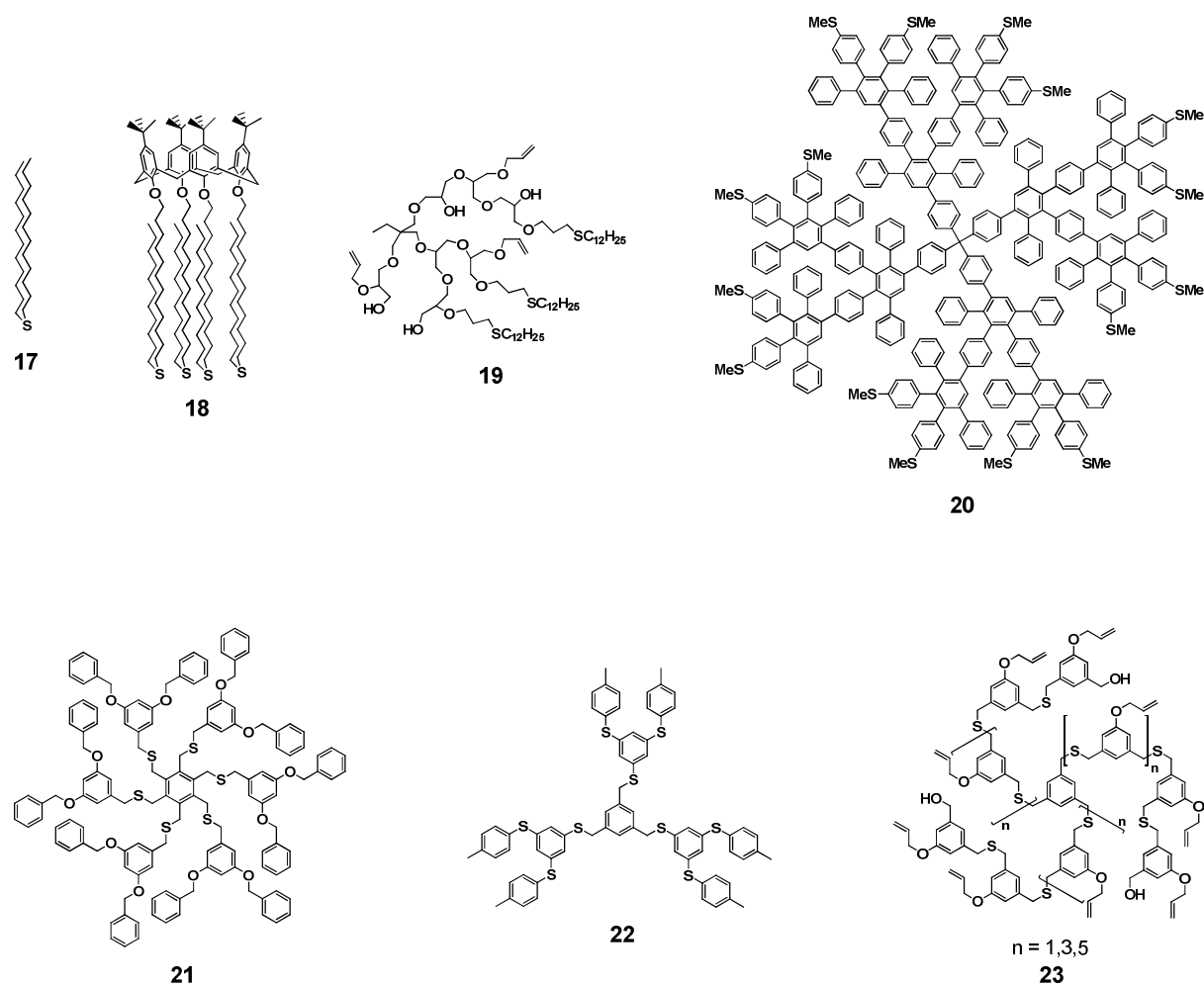


Figure 28. Examples of thioether structures that were employed for the stabilization of gold nanoparticles.

More complex thioether containing structures were also used for the formation of gold nanoparticles. However, the results obtained for gold nanoparticles stabilized by thioether containing polymers^[168-171] cannot be compared with the outcome of the studies with dialkyl sulfides. The effect of the polymer matrix regarding the stabilization of the gold nanoparticles could be even greater than the impact of the thioether moieties. Even relatively small glycols such as diglyme can be employed for the stabilization of gold nanoparticles (*vide supra*).^[160] A strong effect of the polymer backbone can thus be expected especially in the example of Huang *et al.*,^[169] where the thioether modified hyperbranched polyglycerol **19** (Figure 28) was utilized as template and stabilizing agent for gold nanoparticles. In other cases, the thioether moieties were only used as end-caps for the employed polymers and account therefore only for a small part of the stabilizing molecule.^[170,171] According to what was said, the results of the different reports on gold nanoparticles stabilized by thioether containing polymers diverge strongly from well dispersible and monodisperse particles^[170,171] to very broadly distributed particle sizes.^[168,169] and no conclusions on the nanoparticle stabilizing properties of thioether ligands can be drawn.

The use of thioether dendrimers for the stabilization of gold nanoparticles was reported as well.^[166,167] As is the case for polymeric thioethers, the employed thioether dendrimers and the obtained results can hardly be compared and cannot be taken as reference for a general picture of thioether stabilized gold nanoparticles due to significant structural diversity of the employed ligands. In the report of Müllen *et al.*,^[166] the stiff thiomethyl terminated polyphenylene dendrimer **20** (Figure 28) was utilized for the stabilization and the synthesis of gold nanoparticles. The particle sizes found within this study range from 1 to 30 nm with a main population around 4 nm with no deviation value given due to the highly polydisperse mixture obtained. Interestingly, these dendrimer stabilized gold nanoparticles were found to be highly stable under ambient conditions and well dispersible in CHCl₃ and toluene.

In contrast to the stiff thioether terminated dendrimers reported by Müllen,^[166] the dendrimer structures used by Vögtle and de Cola^[167] for the synthesis of thioether stabilized gold nanoparticles consist of benzylic or phenylic thioethers located mainly in the centers of the structures (*e.g.* **21** or **22**) (Figure 28). However, even within this single study, a clear comparison of the thioether structures for requirements for monodisperse, size controlled and well dispersible gold nanoparticles is not possible. The gold nanoparticle stabilizing properties of structures consisting solely of benzylic thioethers were compared to structures built of phenylic ethers or thioethers within one molecule, whereby the electronic and structural differences of benzylic and phenylic thioethers were not taken into account. The gold nanoparticles obtained in the presence of the thioether dendrimers **21** or **22** were highly polydisperse with particle diameters in the range of 1 - 5 nm in all cases. It was also found that the phase transfer agent tetra-*n*-octylammonium bromide (TOAB) that was used during the synthesis of the particles cannot be completely removed by repeated precipitation of the nanoparticles. TOAB is therefore needed for the stabilization of the nanoparticles synthesized in the presence of the thioether dendrimers **21** or **22**, indicating an incomplete coverage of the particle surface by the dendrimers.

A last report on the direct synthesis of thioether stabilized gold nanoparticles appeared in 2005 from the group of Toshi Nagata.^[135] Multidentate star-shaped ligands **23** (Figure 28) with 9 to 21 benzylic thioethers per molecule were employed for the stabilization of gold nanoparticles. The mean particle sizes were found to be between 1.5 and 1.7 nm with a fairly low deviation of 0.5 nm. Remarkably, the stability, the core sizes and the narrow dispersity of the nanoparticles stabilized by these thioether ligands seemed to be relatively independent of the size of the ligand used. The universal validity of the results was however somewhat diminished by the fact that one allyl phenyl ether moiety was present per thioether moiety in

the stabilizing molecules. The impact of these ether moieties concerning the stabilization of gold nanoparticles remains unclear as does the influence of the three acetal protecting groups present at the termini of the molecules.

Despite the large differences of the thioether ligands employed in the different studies regarding the direct synthesis of gold nanoparticles with thioether ligands as stabilizers, some general conclusions can be drawn. The surrounding of the thioether moieties and the rest of the stabilizing molecule seem to play much more important roles in the case of thioether ligands compared to thiol stabilizers. The procedures that were used for the preparation of gold nanoparticles were very similar in all presented cases, but very diverse nanoparticle core sizes and stabilities were found for the different thioether ligands. In comparison to thiol stabilized nanoparticles prepared by the same Brust-Schiffrin method,^[46] it becomes obvious that the size and stability differences for diverse thiol ligands is much smaller. For instance, thiophenol protected gold particles^[172] which were prepared by this method were determined to be in the same size range as nanoparticles stabilized by alkyl thiols.^[46,47] Even thiol terminated peptides,^[173] fluorinated alkyl chains^[174] or dendrons of different generations^[175-180] yielded gold nanoparticles in a comparable size range of 1.5 to 2.6 nm, which illustrates the vast independence of the nanoparticle sizes from the employed thiol ligand compared to the thioether ligands. In particular, the number of binding thioether moieties seems to play an important role on the stabilizing properties of the thioether ligand employed for the stabilization of gold nanoparticles. This manifests in the good stability of the nanoparticles that were prepared in the presence of the tetradentate calix(4)arene derived thioether ligand **18** from Reinhoudt *et al.*^[164] and the results obtained for the large star-shaped benzyl thioether ligands **23**.^[135]

In this context, the octadentate thioether ligand **1** seemed to be well suited for the direct synthesis of gold nanoparticles. Especially the flexibility of the linear system and the multiple binding sites should allow for an efficient stabilization of gold particles. Furthermore, this ligand system brings by design the sterically demanding *tert*-butyl groups, which are expected to provide further stabilizing properties and also to make the resulting gold nanoparticles more easily dispersible in organic solvents. In contrast to the other described thioether ligands used for the synthesis of gold nanoparticles, the thioether ligand **1** is based solely on benzylic thioether moieties and does not have any other functional groups such as ethers or acetals which may interfere with the weakly binding thioether groups.

3.2.1 Initial Studies

In an initial attempt it was tried to synthesize gold nanoparticles in the presence of the octadentate heptamer thioether **1** by using the two-phase method developed by Brust and Schiffrin^[46] for the synthesis of alkyl thiolate protected gold particles. To an aqueous solution of the gold(III) precursor tetrachloroauric acid (HAuCl₄) was added a solution of the phase transfer agent TOAB in toluene. The resulting biphasic system was vigorously stirred, whereupon the gold(III) salt was transferred to the organic phase, apparent by the discoloration of the aqueous phase and the strong orange color of the organic phase. A solution of the ligand **1** was then added to the system. Unlike the original procedure, where a 1:1 ratio of gold to thiol was used,^[46] the amount of the thioether ligand **1** was chosen such that two equivalents sulfide moieties were present per gold(III) equivalent in the mixture. With the octasulfide **1**, this resulted in 4 equivalents HAuCl₄ compared to 1 equivalent of the ligand **1**. The reduction of gold(III) in the presence of the thioether ligand **1** was then carried out by adding an aqueous solution of the reducing agent sodium borohydride to the strongly stirred two-phase system. Immediately after the addition of the reducing agent, the toluene phase turned dark brown, indicating the formation of dispersed gold nanoparticles. The spectral shape of the UV/vis spectrum (Figure 29) of the toluene phase obtained shortly after the reduction of gold(III) is very similar to other thiol^[46] or sulfide^[135,164,165,167] stabilized nanoparticles systems. The absence of a plasmon resonance band centered around 520 nm indicates that mainly nanoparticles with core diameters smaller than ~2-3 nm^[181] were formed by this procedure in the presence of the heptameric ligand **1**. The **Au-1** nanoparticle dispersion was left at ambient conditions for two days. During this time, no changes were detected; neither by the bare eye nor by UV/vis spectroscopy (Figure 29).

It is known that the phase transfer agent TOAB can itself act as stabilizer for gold nanoparticles.^[182] The gold nanoparticle stabilizing abilities of the octadentate thioether ligand **1** were thus further corroborated by comparing the results to a test experiment using only the phase transfer agent TOAB without the thioether ligand present. In this case, a strongly red colored organic phase was obtained after the addition of the reducing agent sodium borohydride. As already indicated by the color, a strong plasmon resonance centered at 520 nm was found in the UV/vis spectrum that was recorded shortly after the nanoparticle formation procedure (Figure 29). This result indicates the formation of nanoparticles with core diameters larger than ~2-3 nm^[181] and shows therefore the influence of the thioether ligand **1** on the formed nanoparticles. Furthermore, the formation of a black precipitate was

observed within 30 minutes after the addition of the reducing agent in the case TOAB stabilized particles. After 24 hours at ambient conditions, the organic phase was nearly colorless and more of the precipitate was formed. This precipitate was not dispersible in common solvents including water and was most likely bulk gold which formed by coagulation of the initially formed gold nanoparticles due to the very limited stabilizing properties of the amphiphilic phase transfer agent. Accordingly, the formation of smaller and more stable nanoparticles in the initial experiment can be fully attributed to the presence of the multidentate thioether ligand **1** and is not due to the presence of the ammonium salt TOAB.

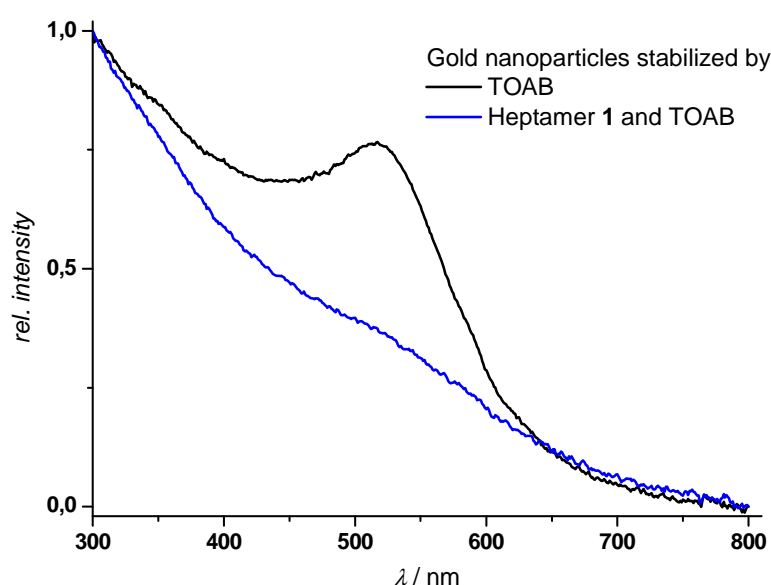


Figure 29. UV/vis absorption spectra (toluene) of the nanoparticle preparations directly after the reduction with sodium borohydride in the presence of TOAB and in the presence of TOAB and the heptamer ligand **1**.

A direct and commonly applied method to observe the core sizes of gold nanoparticles is Transmission Electron Microscopy (TEM). The precise size of the gold core can be determined directly by measuring the diameters of the observed spherical structures due to the strong contrast pictures obtained by this method. In order to get a first overview of the core sizes and size distributions of the heptamer stabilized **Au-1** nanoparticles, TEM was performed. For that, a single drop of the diluted **Au-1** dispersion in toluene was carefully transferred onto a carbon coated copper grid and then dried under a stream of nitrogen. A quick survey of 250 nanoparticles revealed that the main population of particles had core sizes between 0.8 and 1.8 nm (Figure 30), confirming the initial conclusions that were made based on the UV/vis spectroscopic investigations.

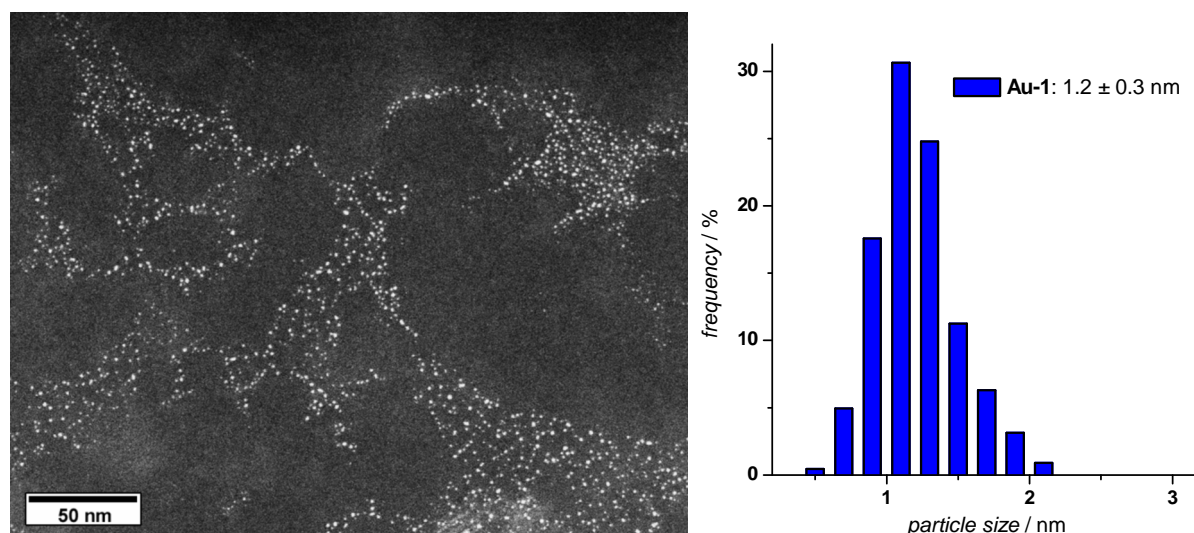


Figure 30. Representative TEM micrograph of Au-1 (left) and nanoparticle size distribution of Au-1 (right).

3.2.2 Thioether Oligomers for the Stabilization of Gold Nanoparticles

Based on these results it was decided to study the dependence of the nanoparticle sizes, dispersities and stabilities on the nature of the stabilizing thioether ligand in more detail. For a comprehensive investigation, the respective di-, tetra- and hexathioether ligands were included. In order to ensure the comparability of the ligands, the terminal sulfur atoms were end-capped with benzyl groups. With these end groups, the multidentate thioether ligands are solely based on dibenzyl thioethers, which should bind equally to the nanoparticle surface. The resulting target structures **24** - **27** are displayed in Figure 31.

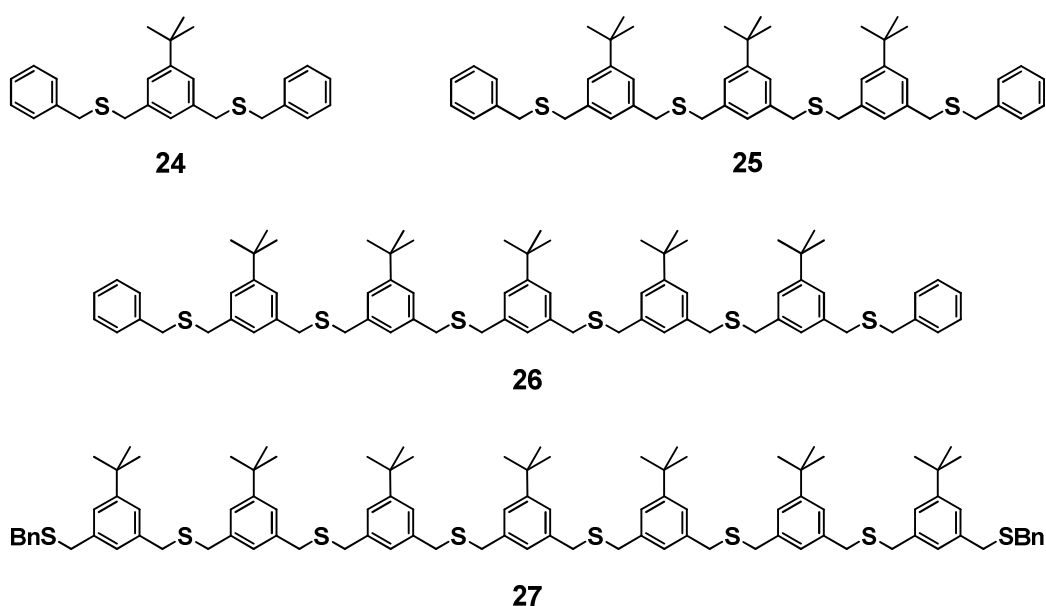


Figure 31. Linear thioether ligands for the stabilization of gold nanoparticles.

low solubility of the heptameric ligand **27** in toluene, the organic solvent was changed and CH_2Cl_2 was used instead of toluene. Under otherwise similar conditions as before, gold nanoparticles were synthesized in the presence of the different thioether ligands **24** - **27** by the reduction of the gold(III) precursor tetrachloroauric acid with sodium borohydride in the presence of TOAB as phase transfer agent. In the case of the monomeric ligand **24**, the organic phase turned brown-red. In the other three cases, the organic phases were dark brown after the addition of the reducing agent. Accordingly, the UV/vis spectrum of the particles stabilized by the monomer **24** shows the presence of a surface plasmon resonance band around 520 nm, while the particles stabilized by the larger ligands **25** - **27** have very similar UV/vis spectra that do not show such an absorption band (Figure 32). The appearance of the weak plasmon resonance band in the case of the **Au-24** particles points at the presence of nanoparticles with core diameters larger than $\sim 2\text{-}3$ nm.^[181] From these data, no conclusions can be drawn regarding the monodispersity of the gold nanoparticles, *viz.* whether mainly particles smaller than 2 nm were obtained with a small population considerably larger than 2 nm or if a large fraction of the particles is slightly larger than 2-3 nm. However, the monomer stabilized **Au-24** particles displayed a very limited stability. After approximately 1 hour at ambient conditions, the formation of a black precipitate became evident in coincidence with a gradual color change to red, indicating the coagulation of gold nanoparticles to larger particles and eventually bulk gold. This was further corroborated by the increasing surface plasmon resonance centered at 520 nm (Figure 32), which is indicative for the formation of larger gold nanoparticles.^[181,183]

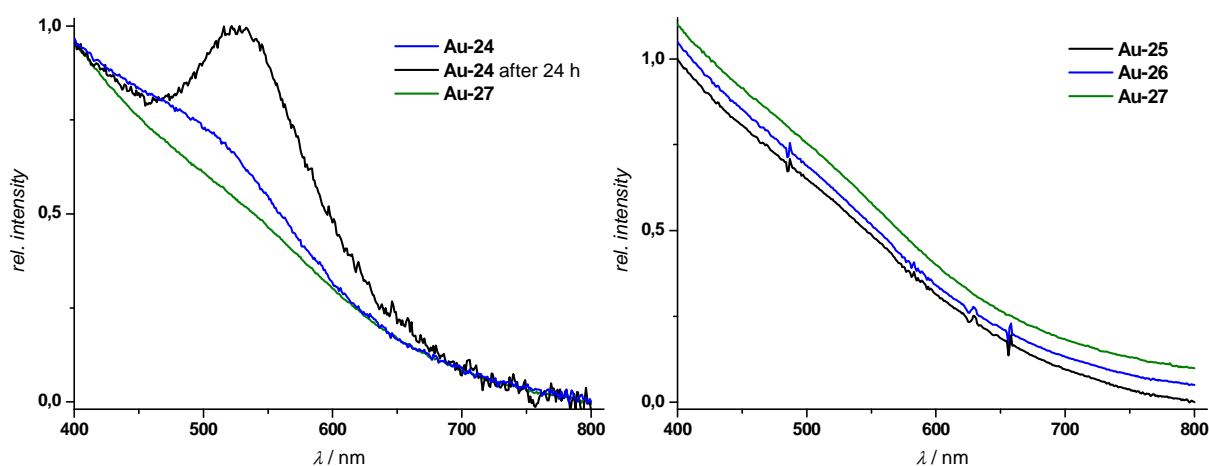


Figure 32. Normalized UV/vis absorption spectra (CH_2Cl_2) of **Au-24** and **Au-27** (left) and **Au-25**, **Au-26** and **Au-27** after one month in dispersion (right, these spectra were shifted vertically in 0.05 increments with respect to the relative absorption).

In the other three cases **Au-25**, **Au-26** and **Au-27**, the organic phases were separated, dried over magnesium sulfate and then filtered. These dispersions were monitored over a period of one month by UV/vis. Compared to the monomer stabilized **Au-24** particles, a much greater stability was already found for the **Au-26** nanoparticles stabilized by the tetradentate trimer **26**. No significant changes were observed in the UV/vis spectra of **Au-26** within this time period, indicating the suppression of nanoparticle growth by the trimeric ligand **26**. However, after a few days, the formation of a fine gold layer on the glass surface of the storage vessel was noted, showing the somewhat limited stability of the trimer protected **Au-26** nanoparticles. The trend towards an increasing stability of the thioether stabilized nanoparticles with increasing length of the coating ligand is further confirmed by the particles stabilized by the penta- or heptameric ligands **26** and **27**. In these cases, no formation of bulk gold was observed within one month. Also, the shape of UV/vis spectra remained the same during this period (Figure 32).

Nanoparticle Purification

It has to be noted that during this first investigation of the stabilities of thioether-coated nanoparticles the phase transfer agent TOAB was present. As was said before, TOAB can act as stabilizer for gold nanoparticles itself^[182] and had to be removed from the mixtures in order to receive a clear picture of the stabilizing properties of the oligomeric thioether ligands **25** - **27**. The removal of TOAB was achieved by precipitation of the nanoparticles from a CH₂Cl₂ dispersion with ethanol, similar to the purification procedure for thiolate protected gold nanoparticles.^[46] The dispersions of the **Au-25** - **Au-27** nanoparticles in CH₂Cl₂ were therefore concentrated to approximately 1 ml by using a rotary evaporator with a water bath at a temperature of ca. 35°C. The concentrated nanoparticle dispersions were then transferred to centrifuge tubes and 24 ml ethanol was added while stirring. In all three cases, a fine precipitate formed immediately after the addition of ethanol. The precipitates were separated from the liquid phase by centrifugation at 10°C, leaving slightly brown colored liquid phases. After removal of the supernatants, it was tried to redisperse the black residues in CH₂Cl₂. In the case of the nanoparticles stabilized by the penta- and heptameric ligands **26** and **27**, the solid residues were completely dispersible in small amounts of the organic solvent. However, the trimer stabilized particles were not fully dispersible in CH₂Cl₂ and other organic solvents such as toluene or THF after this procedure. The removal of TOAB could have led to

destabilization and then coagulation of the **Au-25** particles to bulk gold, indicating the limited stability of these trimer stabilized nanoparticles. In the cases of the **Au-26** and **Au-27** nanoparticles stabilized by hexa- or octadentate ligands, the precipitation/centrifugation procedure was repeated two more times in order to completely remove the phase transfer agent TOAB from the mixtures.

The purified nanoparticles were obtained as black-brown waxy solids. Independent of the ligand used (**26** or **27**), the particles remained dispersible when stored in the solid phase. Furthermore, even after removal of the phase transfer agent, the gold nanoparticles were stable as CH_2Cl_2 dispersions for more than one month, as neither precipitation nor color changes were observed during this period. Accordingly, the UV/vis spectra of the **Au-26** and **Au-27** dispersions directly after the purification procedure and one month later resembled the spectra obtained in the presence of TOAB (Figure 33), showing the suppression of nanoparticle coagulation to particles larger than 2-3 nm.

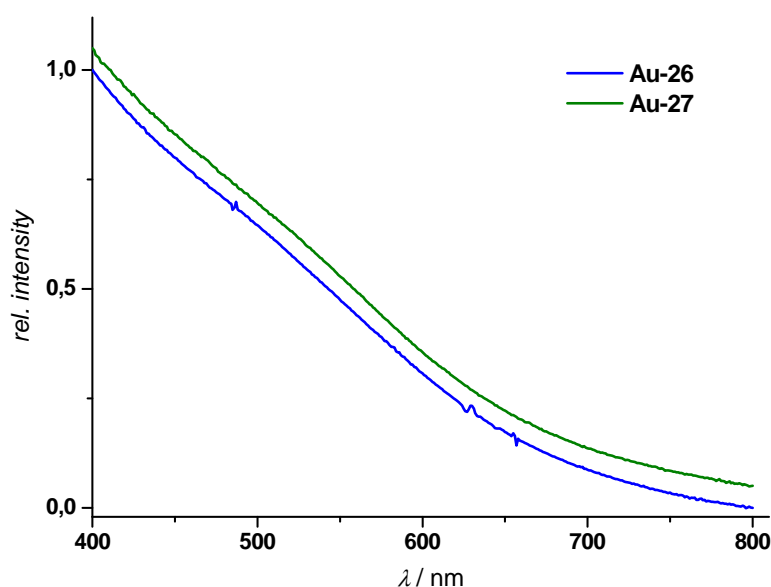


Figure 33. Normalized UV/vis absorption spectra (CH_2Cl_2) of **Au-26** and **Au-27** after purification by precipitation from ethanol. For better visibility, the spectrum of **Au-27** was shifted vertically.

Both, the heptamer stabilized **Au-27** nanoparticles and the heptameric ligand **27** itself, show very similar solubilities and are not or only weakly soluble in ethanol as well as other polar solvents such as acetonitrile or acetone. For that reason, excess, unbound thioether ligand **27** cannot be removed by the precipitation method that was employed for the removal of the highly polar TOAB. For a clear picture on the stoichiometry of the thioether stabilized particles though, excess ligand had to be removed from the system. It was therefore tried if a

standard chromatographic separation using silica gel or basic aluminum oxide could be used. Unfortunately, TLC revealed the low stability of the **Au-27** nanoparticles on both materials. On silica gel, the particles stayed on the baseline, even when the very polar solvent methanol was used as eluent. In contrast to that, the color of the nanoparticles moved on basic aluminum oxide when a 4:1 mixture of CH_2Cl_2 and methanol was used as eluent. But a strong tailing was found, with most of the brown nanoparticle color remaining in the tail, indicating the limited stability of the particles on this material. Thus, both methods proved to be inapplicable for the separation of the thioether coated **Au-27** nanoparticles and excess ligand **27**.

Gel Permeation Chromatography (GPC) was then applied to the heptamer stabilized **Au-27** nanoparticles, as this method is solely based on size exclusion. Strong, destabilizing interactions between the chromatographic material and the gold nanoparticles were not expected. Indeed, by the use of *Bio-Rad Bio-Beads S-X1* (molecular weight range: 600 to 14000 g/mol) with toluene as eluent, a sharp and narrow black-brown colored band moved through the column. Small fractions were collected, whereby the pure excess ligand **27** was separated efficiently from the strongly colored nanoparticle fractions as was shown by TLC and NMR.

NMR

The heptamer stabilized **Au-27** nanoparticles were investigated by ^1H NMR in CD_2Cl_2 after each purification step (Figure 34). The spectrum that was obtained after phase separation and drying over magnesium sulfate shows the presence of the signals of the ligand **27** and strong signals of the phase transfer agent TOAB that was used in excess. After the purification procedure, only the signals of the ligand **27** can be found, confirming the efficient removal of TOAB by the precipitation procedure. Unlike the gold nanoparticles stabilized by the thioether dendrimers **21** or **22** that were reported by Vögtle and De Cola,^[167] TOAB was therefore not required for the stabilization of the nanoparticles by the octadentate ligand **27**. Only the signals of the pure ligand were found in the spectra. The **Au-27** particles after removal of excess ligand show very broad signals underneath the original ligand signals. The broadening of proton signals of ligands bound to gold nanoparticle surfaces is well known for alkane thiols^[47,184-186] as well as for sulfide ligands.^[164,165]

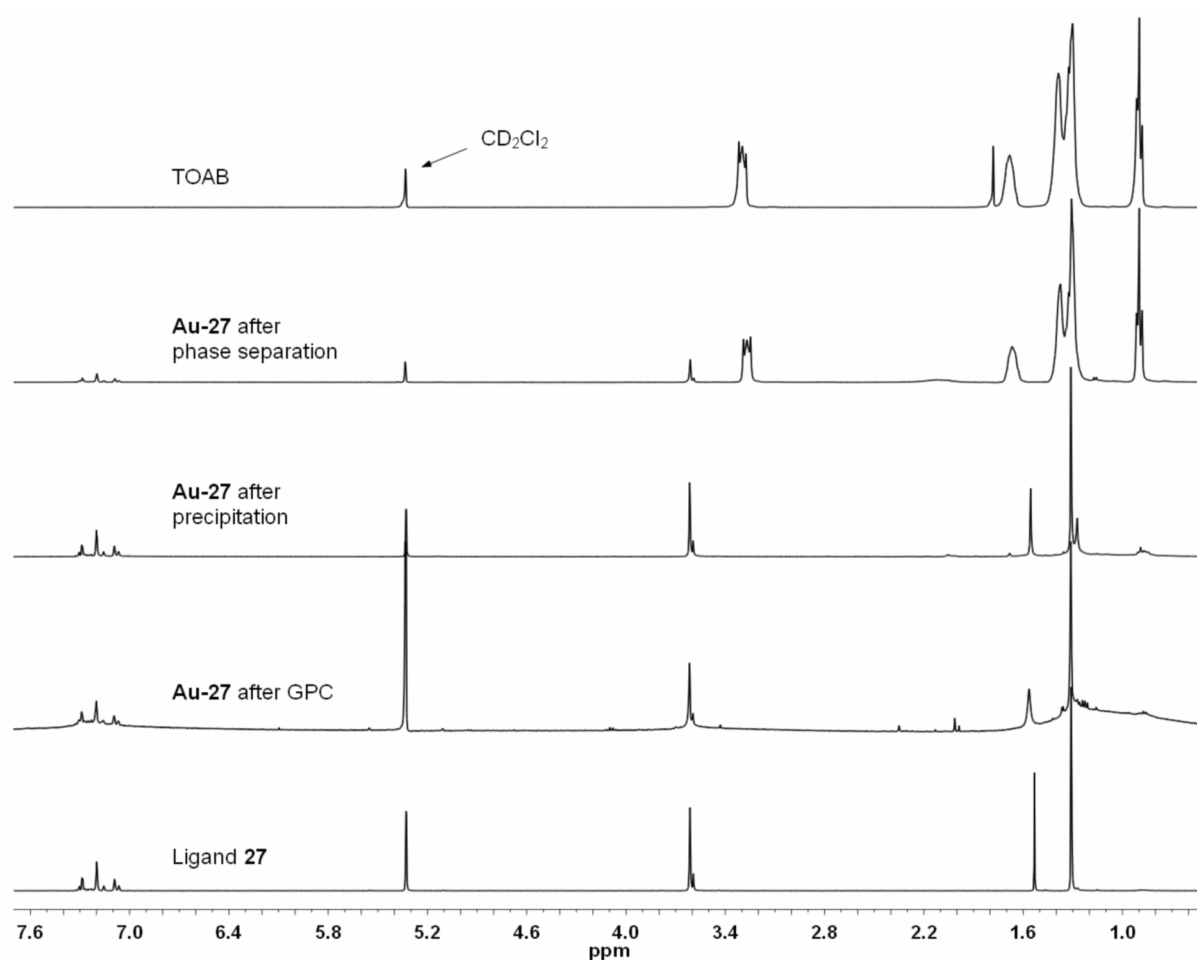


Figure 34. ^1H NMR spectra (CD_2Cl_2) of **Au-27** at different stages of purification in comparison with the spectra of TOAB and the pure ligand **27**.

Nanoparticle Sizes and Size Distributions

The **Au-26** and **Au-27** particles stabilized by the penta- and heptameric ligands were investigated by High Resolution Scanning Transmission Electron Microscopy (HRSTEM). As before, single drops of diluted CH_2Cl_2 **Au-26** and **Au-27** dispersions were carefully transferred to carbon coated copper grids. The grids were dried in air and then investigated by HRSTEM.

The micrographs obtained with the pentamer stabilized **Au-26** nanoparticles after the precipitation procedure show a rather broad distribution of nanoparticle sizes. Gold nanoparticles were found with diameters between 1 and 5 nm with an average diameter of 1.8 nm over a population of 430 particles (Figure 35).

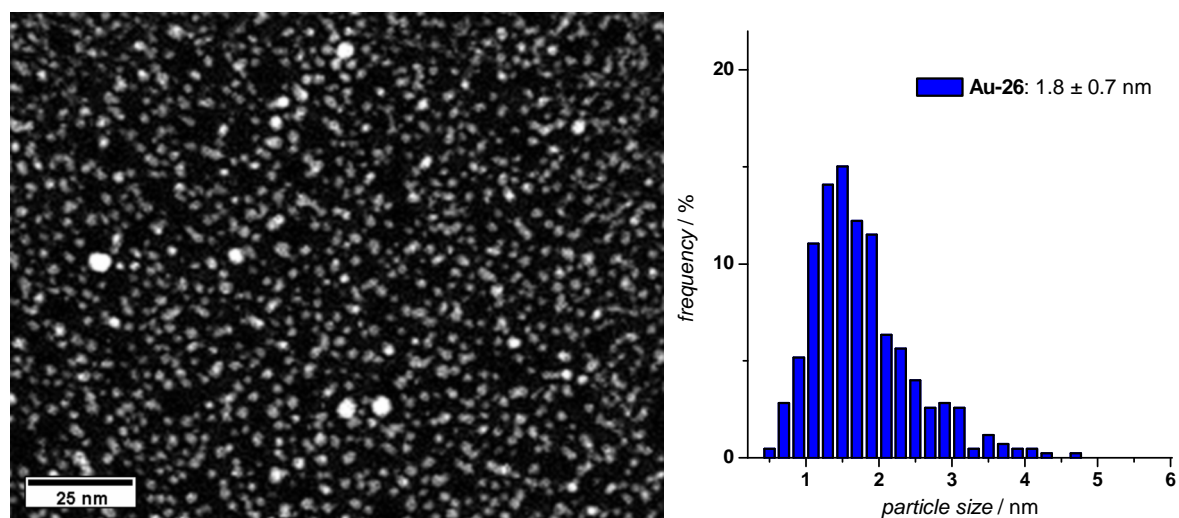


Figure 35. HRSTEM micrograph of **Au-26** after precipitation (left) and size distribution histogram of **Au-26** (right).

In the case of the **Au-27** particles stabilized by the heptameric ligand, HRSTEM was performed before and after the purification procedure. In both cases, much narrower size distributions were found compared to the pentamer stabilized **Au-26** nanoparticles. The histogram in Figure 37 shows that the main fraction of the heptamer stabilized **Au-27** nanoparticles in the presence of TOAB has sizes around 1 nm with a tail towards larger sizes up to 2.1 nm. Interestingly, a different size distribution was observed after removal of the phase transfer agent by precipitation. In addition to the parent accumulation with core diameters around 1 nm a second accumulation with a maximum at about 1.9 nm was found (Figure 37).

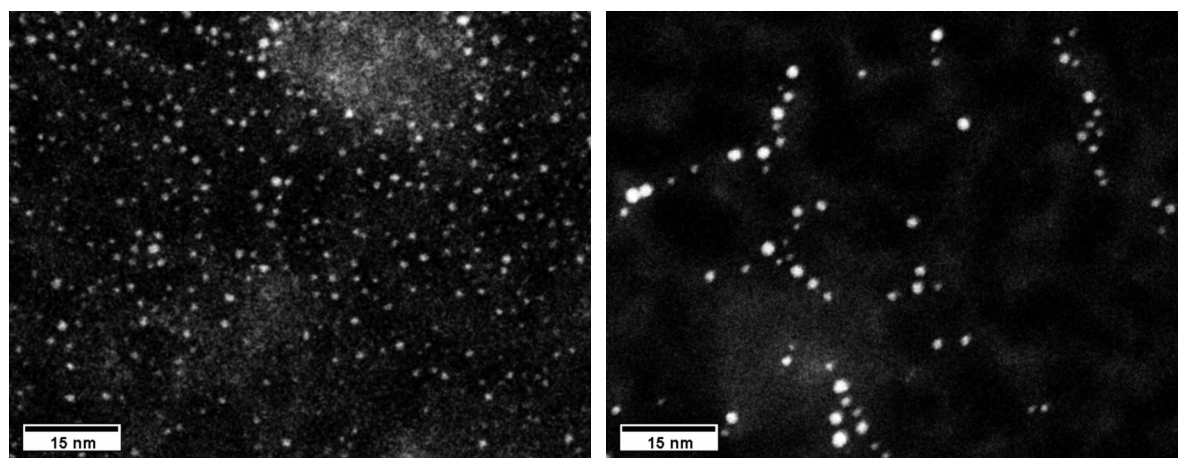


Figure 36. HRSTEM micrographs of **Au-27** before (left) and after purification by precipitation (right).

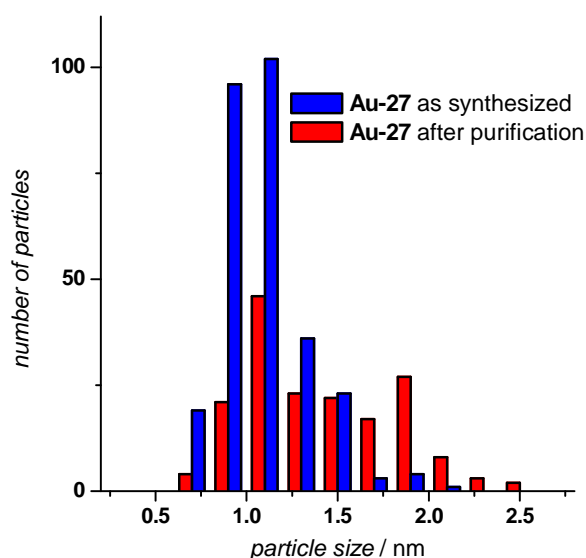


Figure 37. Nanoparticle size distribution histograms of **Au-27** before and after the purification by precipitation.

These results suggest that the removal of TOAB induces a partial destabilization of the particles, resulting in the coalescence of some small 1 nm particles to larger particles. However, the formation of particles with core diameters larger than 2.5 nm seems to be suppressed by the heptameric thioether ligand **27**, as no particles were found with larger sizes.

Due to the long time period (approx. 2 months) between application of the samples to the TEM grid and the actual measurement, it cannot be ruled out that aging occurred and the particles, especially the pentamer stabilized **Au-26** ones, coagulated on the grid.^[187] If coagulation of the **Au-26** nanoparticles took place on the carbon surface of the TEM grid while the **Au-27** particles did not coagulate to a similar extent, this would further support the importance of multiple thioether binding sites for the formation of stable thioether coated gold nanoparticles.

Elemental Analysis, Calculations Concerning the Nanoparticle/Ligand Ratio

Elemental analysis was performed with the heptamer stabilized **Au-27** nanoparticles after the removal of TOAB in order to obtain the ratio of ligand **27** to gold. From the elements present in the stabilized nanoparticles (Au, S, C, H), this method allows solely the determination of the carbon and hydrogen content of the sample. However, based on the NMR spectra, it was shown that TOAB was completely removed from the system. Apart from gold nanoparticles and excess ligand molecules, no other mass sources were present. For the nanoparticle

sample, proportions of 35.3% carbon and 3.7% hydrogen were found. Compared to the theoretical results expected for the heptamer **27** - 75.4% carbon and 8.1% hydrogen - very similar carbon to hydrogen ratios were found, also pointing at the absence of other hydrogen or carbon sources. From these values, a mass proportion of 45.7 % or 46.8% ligand (based on the hydrogen or the carbon proportions respectively) can be calculated. Using these proportions, a nanoparticle yield of 79 - 85 % is obtained with respect to the gold equivalents used for the synthesis of the nanoparticles. Some losses probably arise from the purification procedure by precipitation, whereby the supernatant remained neither completely clear nor colorless after centrifugation, indicating the presence of nanoparticles remaining in the liquid phase. However, this shows that even higher nanoparticle yields were obtained during the synthesis and thus further indicates the ability of the heptameric thioether ligand **27** to efficiently form and stabilize gold nanoparticles with a narrow size distribution.

With regard to the stoichiometry of the nanoparticle thioether complexes, elemental analysis was also performed with the gold nanoparticles purified by GPC, where excess unbound ligand **27** was removed. A carbon proportion of 23.0% and a hydrogen proportion of 2.4% were found for the so purified **Au-27** nanoparticles. These results were again compared to the theoretical values for the pure ligand **27**, whereby a ligand proportion between 29.6% and 30.5% was obtained depending on which element was used for the calculation. From these values, an average of 18.1 to 18.8 gold atoms can be calculated to be present per ligand molecule.

By combining these data with the bimodal size distribution of the nanoparticles after purification by precipitation, the number of thioether ligands per nanoparticle can be roughly estimated based on several assumptions.

If a spherical shape of the nanoparticles is assumed, the surface of the nanoparticles with a diameter of 1.9 nm is approximately four times larger than the surface of the 1.0 nm particles. Given a complete surface coverage of the nanoparticles, this allows the conclusion that four times more thioether ligands **27** are probably required to stabilize one 1.9 nm particle compared to one 1.0 nm particle. Au₂₅ particles were reported to have a core diameter of 1.1 nm,^[188] which is slightly larger than the 1.0 nm observed for the small nanoparticle fraction. On the other hand, TEM analysis of Au₁₁ clusters revealed a significantly smaller core size of 0.8 nm.^[189] For the calculations presented here, an average value of 20 gold atoms per 1.0 nm was therefore used in a first approximation. The gold atom content of the larger 1.9 nm particles was calculated by assuming a spherical shape of the particles and by using

the density of bulk gold. A value of 195 gold atoms per 1.9 nm particle was thereby estimated. Taking into account the actual distribution of core sizes that was received by TEM analysis of the purified nanoparticles, the number of 1.0 nm particles was found to be approximately twice the number of 1.9 nm particles. According to these assumptions, the following formula can be used for the determination of the ligand coverage of the nanoparticles:

$$\frac{2N_{1.0nm} + N_{1.9nm}}{2n_{1.0nm} + n_{1.9nm}} = N_{calc.}$$

n_{Xnm} : Number of heptamer **27** ligands per X nm nanoparticle.

$N_{calc.}$: Number of gold atoms per ligand, calculated from elemental analysis data.

N_{Xnm} : Number of gold atoms per gold cluster of the diameter X nm.

With $n_{1.9nm} = 4n_{1.0nm}$, this equation can be transformed to give the number of ligands that stabilize one 1.0 nm particle $n_{1.0nm}$:

$$n_{1.0nm} = \frac{2N_{1.0nm} + N_{1.9nm}}{6N_{calc.}}$$

By introducing the number of gold atoms assumed for the gold nanoparticles ($N_{1.0nm} = 20$; $N_{1.9nm} = 195$) and the average number of gold atoms per ligand ($N_{calc.} = 18.1$ or 18.8), $n_{1.0nm}$ is found to be 2.16 or 2.08 respectively. These results strongly imply that only a low number of heptameric thioether ligands **27** is needed to stabilize a single gold nanoparticle in the size range of 1-2 nm. As an integer number of ligands can be expected, only two of these ligands are required to enwrap one 1.0 nm particle, while eight to nine ligands can stabilize one 1.9 nm particle.

3.2.3 Summary and Conclusions

It was shown that multidentate thioether ligands can indeed be used for the preparation of gold nanoparticles that are stabilized by a low number of ligands. In particular, the benzyl end-capped mono- to heptameric linear thioether ligands **24** - **27** were prepared efficiently and investigated on their nanoparticle stabilizing properties. Gold nanoparticles were prepared by using a two-phase protocol with TOAB as phase transfer agent. Thereby, mainly particles smaller than 2-3 nm were obtained. The stabilities of the nanoparticles were strongly dependent on the size of the ligand: while the monomer stabilized **Au-24** particles coagulated fast, the particles stabilized by longer oligomers remained stable. However, upon removal of the phase transfer agent, only the heptamer coated **Au-27** particles were stable and did not coagulate to particles with diameters larger than 2.5 nm. Further investigations showed that only two heptameric thioether ligands **27** are required to stabilize the main fraction of nanoparticles with diameters around 1.0 nm.

3.3 Functionalized Gold Nanoparticles

This chapter deals with the synthesis of monofunctionalized thioether ligands and the application of such ligands for the preparation of functionalized gold nanoparticles as building blocks for wet chemistry processing. In the first part of this chapter, the development of synthetic methodologies for the modular synthesis of functionalized thioether ligands will be presented. In a second part, initial studies concerning the usability of thioether stabilized nanoparticles as 'artificial molecules' for the formation of nanoparticle superstructures will be shown.

Based on the encouraging results obtained with the heptameric ligand **27** concerning gold nanoparticle stability and surface coverage, monofunctionalized thioether ligands were designed. Basically, the attached functionality should make the resulting nanoparticles accessible by wet chemistry and therefore allow the selective attachment of virtually anything of interest to the nanoparticle surface. The considerable fraction of the nanoparticle surface coated by the oligomeric thioether ligand (*vide supra*) provides a hybrid system with a low integer number of ligands per particle. An additional functional group at the ligand thus provides coated nanoparticles comprising a low integer number of peripheral functional groups. As long as these particles remain dispersible in appropriate solvents, these additional functional groups are addressable by wet chemistry allowing *e.g.* for the controlled formation of nanoparticle superstructures such as dimers or linear chains. (Figure 38, see also section 2).

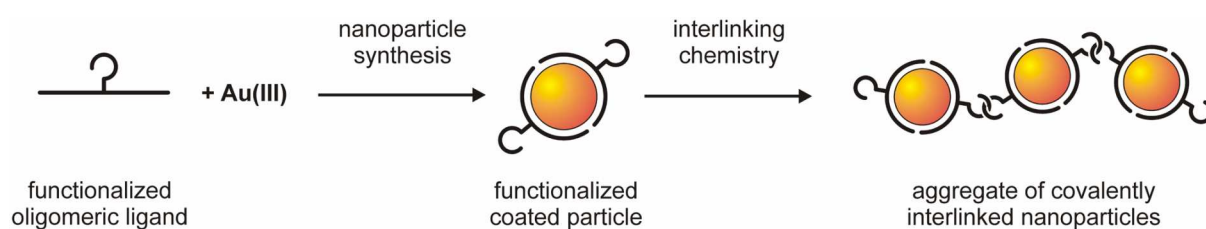
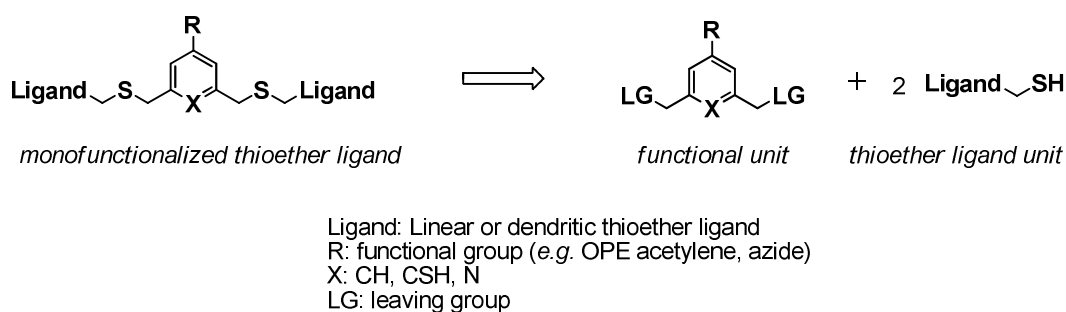


Figure 38. Basic concept of coating gold nanoparticles with oligomeric thioether ligands comprising a peripheral functional group to provide building blocks for subsequent wet chemistry processing. Inorganic/organic hybrid aggregates are formed by covalent chemistry of the additional functionalities.

Thiolate protected gold nanoparticles have been shown to be stable under a wide range of reaction conditions. Rather mild transformations include the copper catalyzed version of the azide-alkyne Huisgen cycloaddition,^[190,191] today referred to as 'click' chemistry,^[192,193]

which was employed for the functionalization of gold nanoparticles.^[194-196] This procedure was also employed to attach gold nanoparticles to biomolecules,^[83,197] to surfaces^[198] or as visual sensor for copper(II) ions by nanoparticle aggregation.^[199] Other cycloaddition reactions like the 1,3-dipolar addition of nitrones to electron deficient double bonds^[200,201] or Diels-Alder reactions^[202-206] were also used to attach further functionalities to gold nanoparticles. Olefin metathesis was mostly employed to encage and therefore stabilize gold nanoparticles by surface polymerization of multiple olefin groups,^[207-210] but recently it was also shown that cross metathesis allows for the efficient introduction of functional molecules to olefinated nanoparticles and dendrimers.^[211] However, in this case, the ‘intramolecular’ reaction on the particle surface could not be completely suppressed. Nucleophilic substitution reactions^[49] and esterifications^[98,212] were less commonly used, which may be explained by the reduced reactivity owing to the steric hindrance on the crowded nanoparticle surface.^[48,49] All of the reactions mentioned so far were performed under very mild conditions in the absence of strongly basic, acidic or nucleophilic reagents. In this context it is very interesting to note that the functionalization of Weinreb amide modified gold nanoparticles with strongly nucleophilic Grignard or organolithium reagents was reported recently.^[213] The utility of these reactions is limited, as the reaction yields and the degree of particle decomposition are strongly dependent on the concentration of the organometallic reagent. Optimization on a case-to-case basis would probably be required.

In principle, the methods described above are all interesting candidates for the targeted functionalization of thioether stabilized gold nanoparticles or for the formation of ordered nanoparticle superstructures, although mild reaction conditions were a prerequisite to reduce the risk of losing the ligand shell during wet chemistry processing. In order to be able to explore a wide range of functionalities and also different designs of the thioether ligand parts, the synthesis of the monofunctionalized thioether ligands was performed as modular as possible. The modular synthetic concept is shown schematically in Scheme 15, whereby the functional building block is synthesized separately from the thioether containing ligand building block, allowing for easy structural modifications of both building blocks. This allows the introduction of the desired functionality in a late step of the synthetic pathway. If necessary, modifications of the employed functional moiety could also be achieved on the assembled thioether ligand.

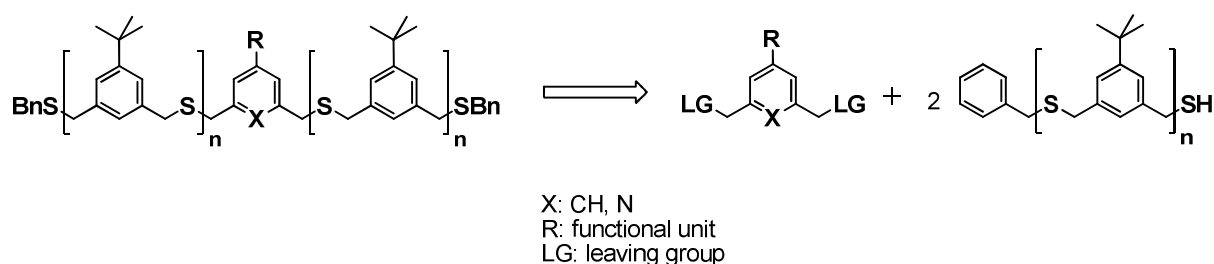


Scheme 15. General scheme for the modular synthesis of monofunctionalized oligomeric dibenzylthioether ligands .

3.3.1 Monofunctionalized Thioether Ligands

3.3.1.1 Synthesis of Linear Thioether Building Blocks

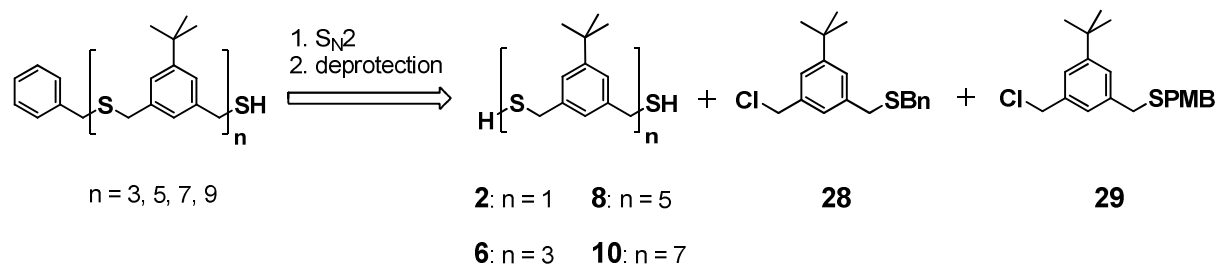
In order to ensure full comparability with previous results, the design of the monofunctionalized thioether ligands was kept very similar to the linear ligands **24** - **27** for initial experiments. The basic ligand structure was maintained, only the *t*-butyl group of the central benzene moiety was exchanged by the functional group. According to the general modular strategy, linear oligomeric monothiols were needed as thioether building blocks (Scheme 16).



Scheme 16. Modular synthetic pathway for functionalized linear thioether ligands.

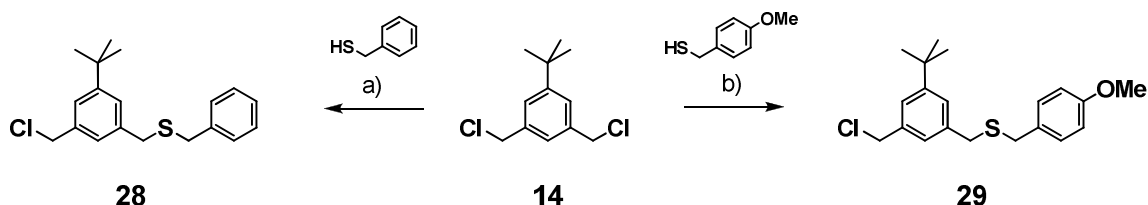
Initially, it was tried to find a general strategy, which would allow to synthesize also longer monothiols starting from the respective dithiols **2**, **6**, **8** or **10**. Attempts to introduce just one benzyl group would lead to inseparable mixtures for the longer oligomers, thus a functionality that allows for the chromatographic separation of the mixture and that can be removed easily from the ligands had to be introduced. For this purpose the *p*-methoxybenzyl (PMB) protecting group was chosen, as the polar methoxy group should allow for the

chromatographic separation of the expected mixtures even for larger thioether oligomers. As main building blocks, the monochlorides **28** and **29** were selected (Scheme 17). Chloride was chosen as leaving group due to the instabilities that were found for the thiomethyl bromide building block **11** (*vide supra*).



Scheme 17. Retrosynthetic pathway for the formation of linear monothiol building blocks starting from the oligomeric dithiols **2**, **6**, **8** or **10**. PMB = *p*-methoxybenzyl.

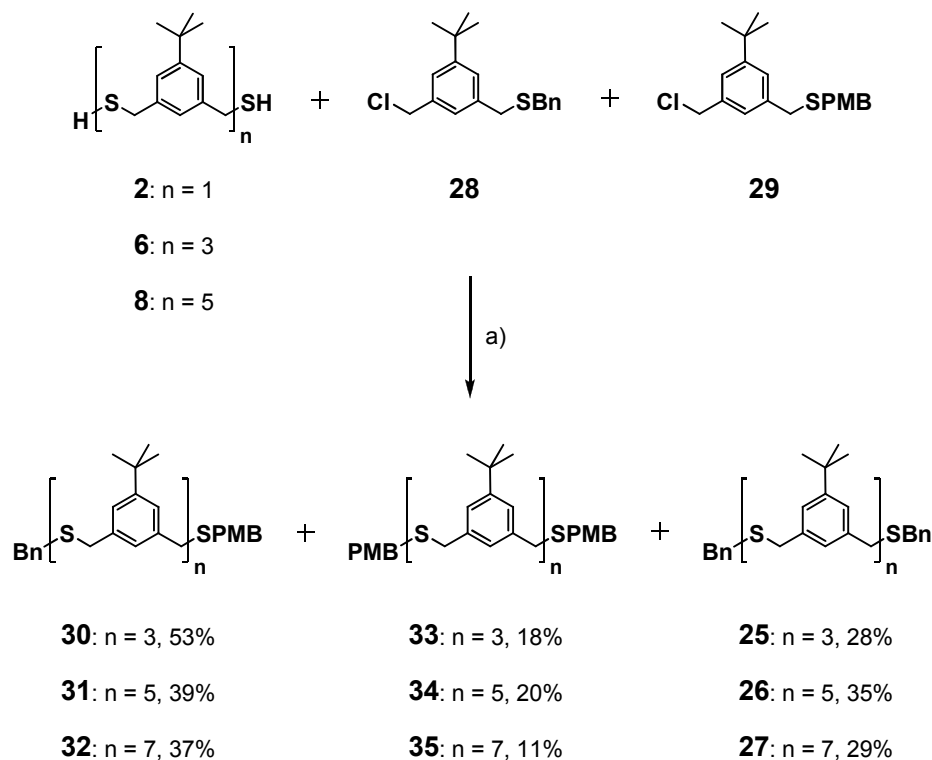
The two monochlorides **28** and **29** were synthesized under similar conditions that were used for the trityl building block **4**. A mixture of 1,3-bis(chloromethyl)-5-*tert*-butylbenzene (**14**), potassium carbonate and the respective thiol (benzyl mercaptan or 4-methoxybenzyl mercaptan) was therefore heated under reflux for 30 hours. After an aqueous work up and purification by column chromatography, the desired monochlorides **28** and **29** were obtained as colorless oils in 52% and 42% yield respectively (Scheme 18).



Scheme 18. Synthesis of the monochlorides **28** and **29**. a) K_2CO_3 , THF, reflux, 52%;
b) K_2CO_3 , THF, reflux, 42%.

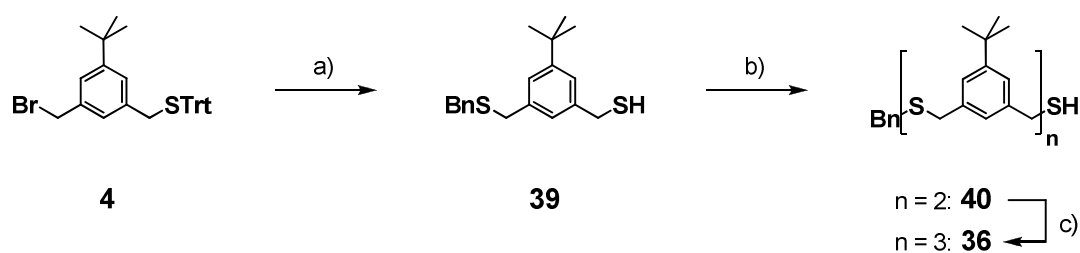
Starting from the dithiols **2**, **6** and **8**, the differently protected thioether oligomers **30** - **32** were obtained by using an equimolar mixture of the benzyl and the PMB capped monochlorides **28** and **29** (Scheme 19). Like in the elongation step for the unfunctionalized linear ligands, the reactions were carried out in THF under the action of sodium hydride as strong base. As expected, mixtures composed of the dibenzyl, the benzyl-PMB and the di-PMB compounds were obtained. However, in all cases the mixtures were easily separated by column chromatography. The benzyl-PMB trimer **30** was thereby obtained as colorless oil in a yield

of 53%, while the other mixed oligomers **31** and **32** were received as colorless solids in 39% and 37% yield respectively. The di-PMB oligomers **33** - **35** were also isolated and could be used for test reactions concerning the selective cleavage of the PMB protecting group.



Scheme 19. Synthesis of the differently PMB-Bn end-capped linear oligomers **30** - **32**. a) NaH, THF, RT.

The standard conditions for the removal of the protecting group of PMB and benzyl protected thiols differ only slightly.^[126] It was therefore carefully tried to find the right conditions for a selective cleavage of the PMB group in the presence of benzylic thioethers. The di-PMB protected trimer **33** was used for all test reactions. Like the trityl protecting group, PMB is sensitive to acid.^[126] Hence, the conditions that were employed for the trityl removal were tried in this case, too. However, no conversion of the starting material was observed, even when pure TFA was used in the presence of triethylsilane as cation scavenger. When excess of anisole was used instead of triethylsilane as cation scavenger, the formation of a new spot on the TLC plate was observed after 36 hours in addition to the spot of the starting material **33**. However, when the mixture was heated overnight to 50°C to accelerate the conversion, a large number of compounds was found on the TLC plate, indicating the decomposition of the benzylic thioethers. Similar results were obtained when methanesulfonic acid was added to a solution of **33** in a 1:1 mixture of TFA and CH₂Cl₂ in the presence of anisole at 0°C.



Scheme 21. Synthesis of the monothiol trimer **36**. a) 1. BnSH, NaH, THF, RT; 2. Et₃SiH, TFA, CH₂Cl₂, RT, 82%; b) 1. BnSH, NaH, THF, RT; 2. Et₃SiH, TFA, CH₂Cl₂, RT, 83%; c) 1. BnSH, NaH, THF, RT; 2. Et₃SiH, TFA, CH₂Cl₂, RT, 88%.

By applying similar reaction conditions to the SH-SBn-monomer **39** and the benzylic bromide **4**, the trityl protected dimer was formed initially, which was again deprotected without further purification steps to provide the dimeric monothiol **40**. This compound was isolated by column chromatography in a yield of 83% as colorless oil. To elongate the dimer, these reaction conditions were applied again to the dimeric monothiol **40** and the bromide **4**. After deprotection of the trityl protected intermediate, the trimeric monothiol **36** was isolated as colorless oil in 88% yield after column chromatography. The increasing yields with increasing chain lengths were attributed to the formation of small amounts of disulfides, which were not easy to separate from the desired monothiols. In the case of the monomer **39** and the dimer **40**, some mixed fractions were found after column chromatography, while the trimer **36** was well separable from the disulfide by-product. Longer oligomers were not prepared by this method.

3.3.1.2 Acetylene Functionalized Thioether Ligands

As was pointed out before, mild reaction conditions are preferable for the processing of functionalized gold nanoparticles by wet synthetic chemistry. Particularly interesting are functional groups that enable coupling chemistry with each other or with additional compounds. In this context, acetylene functionalized building blocks seemed highly promising. Acetylenes are known for numerous chemical transformation reactions under rather mild copper catalyzed reaction conditions. These include 'click' chemistry,^[192,193] the oxidative ethynyl dimerization (Glaser-Hay coupling),^[215] the Sonogashira coupling reaction between ethynyls and arylhalides^[216-218] or the formation of dialkynyl platinum complexes.^[219] For all these transformations, mild reaction conditions have already been reported. In particular the smooth performance of the reactions at room temperature in solvents like

CH_2Cl_2 or THF in which the unfunctionalized **Au-27** particles already displayed good stability and dispersibility makes these procedures very interesting.

For the formation of acetylene functionalized nanoparticles, rigid-rod type oligophenylene-ethynyl (OPE) structures were chosen. The structural rigidity and the variation in length of these OPE spacer units were expected to be ideal features, as they allow for the control of the distance between the surface of the nanoparticle and the functional group. In particular, these features allow to investigate the validity of the concept of thioether stabilized gold nanoparticles as 'artificial molecules' with defined and ordered surface functionalities. By interlinking of OPE functionalized nanoparticles to superstructures by wet synthetic chemistry, the length of the rigid functional unit should be reflected in the spacing between the particles in the formed nanoparticle aggregates.

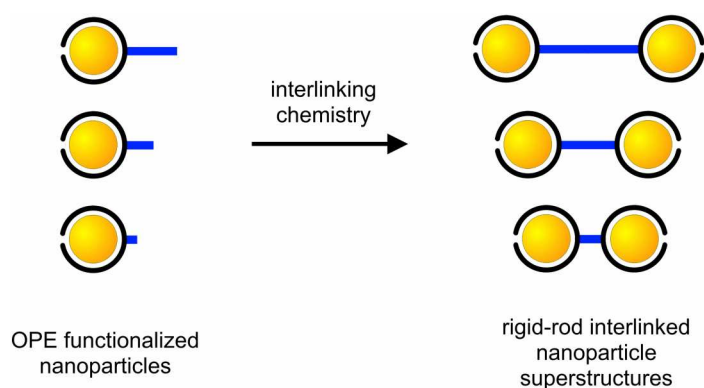


Figure 39. Schematic of the formation of rigid-rod interlinked nanoparticle dumbbell superstructures with OPE functionalized gold nanoparticles. The thioether ligands are represented in black, while the functional OPE units are drawn as blue bars.

Additional advantages of the OPE units were their delocalization, which enables their detection by UV/vis spectroscopy and their straightforward accessibility by acetylene scaffolding chemistry.^[220,221] Furthermore, the acetylene as functional group can be protected during the formation of the gold nanoparticles with trialkylsilyl protecting groups^[126] to prevent uncontrollable side reactions like the formation of gold alkyne bonds^[222] and also to compensate the missing steric demands of *t*-butyl group that was present in the parent ligand **27** (Figure 40). To activate the acetylenes as functional groups on the surface of the particles, the silyl protecting groups can easily be removed under mild conditions by fluoride anions or under weakly basic conditions.^[126]

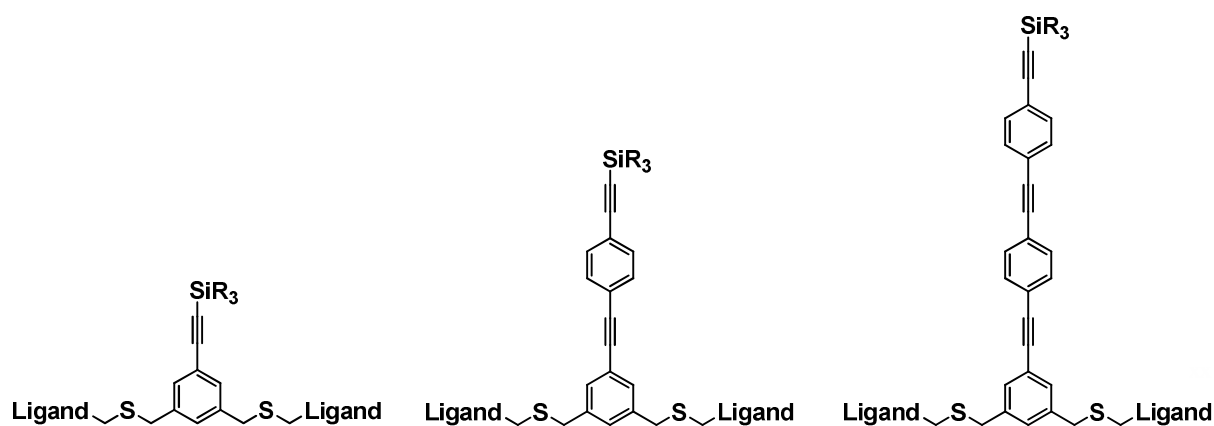
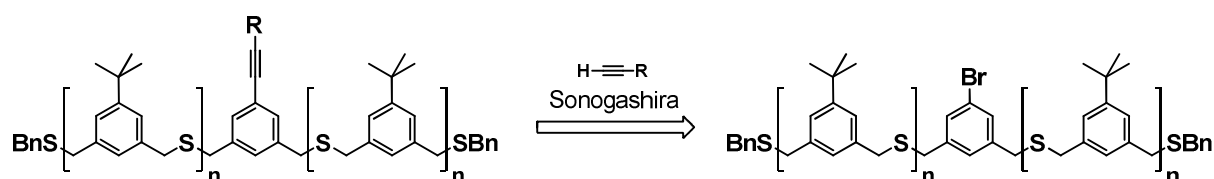


Figure 40. General structure of OPE functionalized thioether ligands.

Synthesis *via* Bromo Functionalized Thioether Ligands

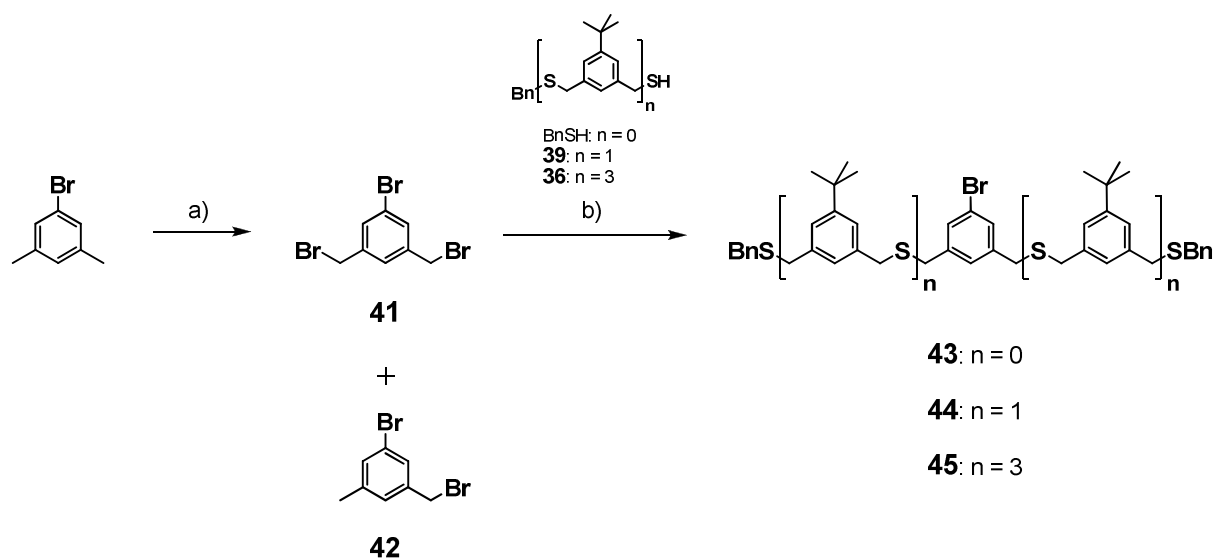
Initially it was tried to form the bromide functionalized thioether ligands, which could then be transformed to acetylene functionalized ligands by Sonogashira coupling reactions^[223] (Scheme 22).



Scheme 22. Retrosynthesis of acetylene functionalized linear thioether ligands starting from the bromo functionalized ligands.

The central bromide building block 1-bromo-3,5-bis(bromomethyl)benzene^[224] (**41**) was synthesized starting from 5-bromo-*m*-xylene *via* α -bromination with NBS and methyl formate as solvent, closely following a literature procedure.^[225] As in the synthesis of the dibromide **3**, AIBN was used as radical starter and a 500 W halogen lamp was used to induce the radical reaction. Bromination reactions with aryl halides were reported to be inefficient,^[226] and this was also found in this case. Even after a reaction time of 20 hours, full conversion to the desired product was not observed by TLC. After an aqueous work up, the crude mixture was subjected to column chromatography, whereby the desired product **41** was isolated in 33% yield as colorless crystals. The major product of this reaction was the monobrominated compound **42**, which was obtained in 60% yield (Scheme 23).

The bromide building block **41** was then reacted with benzyl mercaptan or the monothiols **39** or **36** to form the mono-, tri- or heptameric bromide functionalized ligands **43**, **44** and **45**. The reactions were performed under the standard nucleophilic substitution conditions that were used for the synthesis of the linear thioether ligands, namely by using sodium hydride as base to deprotonate the thiols and THF as solvent. After an aqueous work up and purification by column chromatography, the monobromo thioether ligands **43**, **44** and **45** were obtained in excellent yields of 96%, 97% and 93% respectively (Scheme 23).



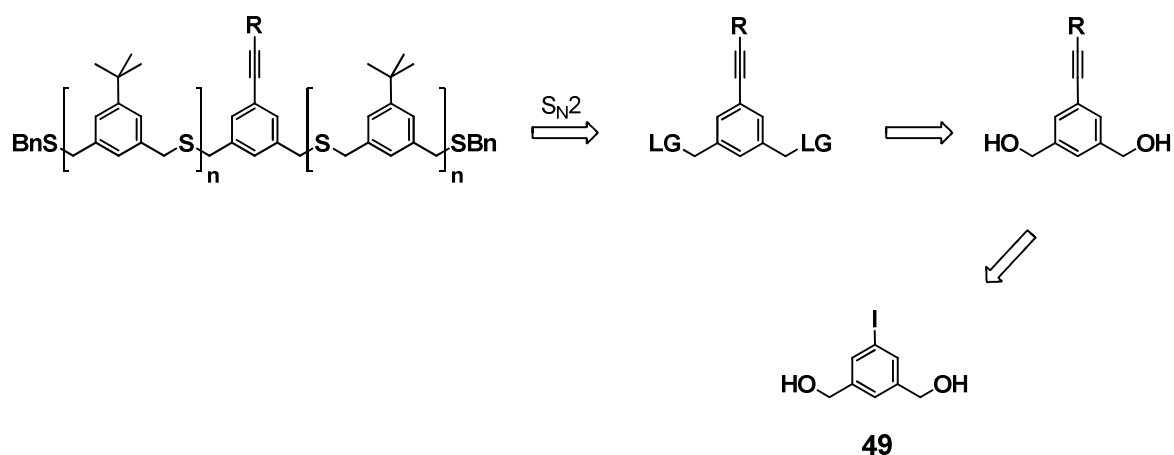
Scheme 23. Synthesis of the bromo functionalized ligands **43**, **44** and **45**. a) NBS, AIBN, HCOOMe, hv, reflux, **41**: 33%; **42**: 60%; b) NaH, THF, RT, **43**: 96%; **44**: 97%; **45**: 93%.

For the introduction of the acetylene moiety to the thioether ligands, trimethylsilyl (TMS) monoprotected ethyne was chosen. The TMS protecting group can be removed under very mild basic conditions to form the free alkyne moiety.^[126] Only few reports of Sonogashira coupling reactions in the presence of benzylic thioethers were found in the literature. In contrast to the present case, these reactions were done with aryl iodides^[227,228] or pyridine derivatives,^[229] which are both more reactive in C-C coupling reactions with ethynyls than aryl bromides.^[223,230] In order to find a general Sonogashira protocol for bromide functionalized thioether ligands, test reactions were carried out with the trimer **44**. By following a procedure that was reported for sulfide containing aryl iodides,^[227] no conversion of **44** was observed during the reaction of **44** and TMS acetylene. Thus, similar conditions - triethylamine (TEA) as solvent with copper(I) iodide and bis(triphenylphosphine)-palladium(II) chloride (Pd(PPh₃)₂Cl₂) as catalysts - were applied, but this time the mixture was heated to 45°C. After 15 h at that temperature, no changes were observed by TLC, but

Synthesis *via* Acetylene Building Blocks

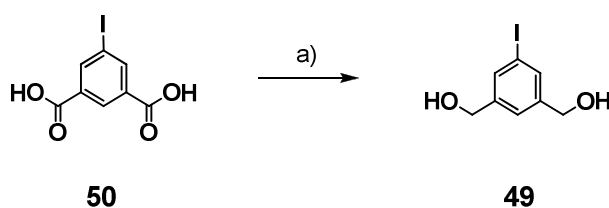
Consequently, the synthetic strategy was changed such, that the functional acetylene moiety is introduced to the central functionalized building block before the assembly of the actual ligand (Scheme 25). This cannot be achieved directly from the bromo building block **41**, because the nucleophilic acetylene intermediates that are formed during the Sonogashira coupling reaction can also react with the benzylic bromides.

Benzylic alcohols can be used as masked leaving groups alternatively, as these functional groups can be easily transformed to leaving groups suitable for nucleophilic substitution reactions *i.e.* by the formation of a sulfonate or by halide substitution.^[231] However, a literature search on phenylene acetylenes with two benzylic hydroxides in the *meta* positions revealed that these compounds were prepared exclusively by reduction of a benzoic acid ester derivative *after* the introduction of the terminal acetylene moiety by Sonogashira coupling reactions.^[232-234] On the other hand, a more detailed literature search which included single benzylic hydroxides *meta* to the acetylene moiety showed that the alcohols should not interfere with the palladium catalyzed coupling of the acetylene.^[235-237] Also, the polar hydroxides can provide good solubility of the substrate in the polar amine solvents that are regularly employed for Sonogashira coupling reactions. A number of synthetic steps can be saved as well by introducing the different acetylenes to the dihydroxide **49** rather than to the diester **50**. If the acetylenes would be introduced to **50**, the reduction to the respective acetylene functionalized dialcohols would have to be carried out for each OPE unit separately.



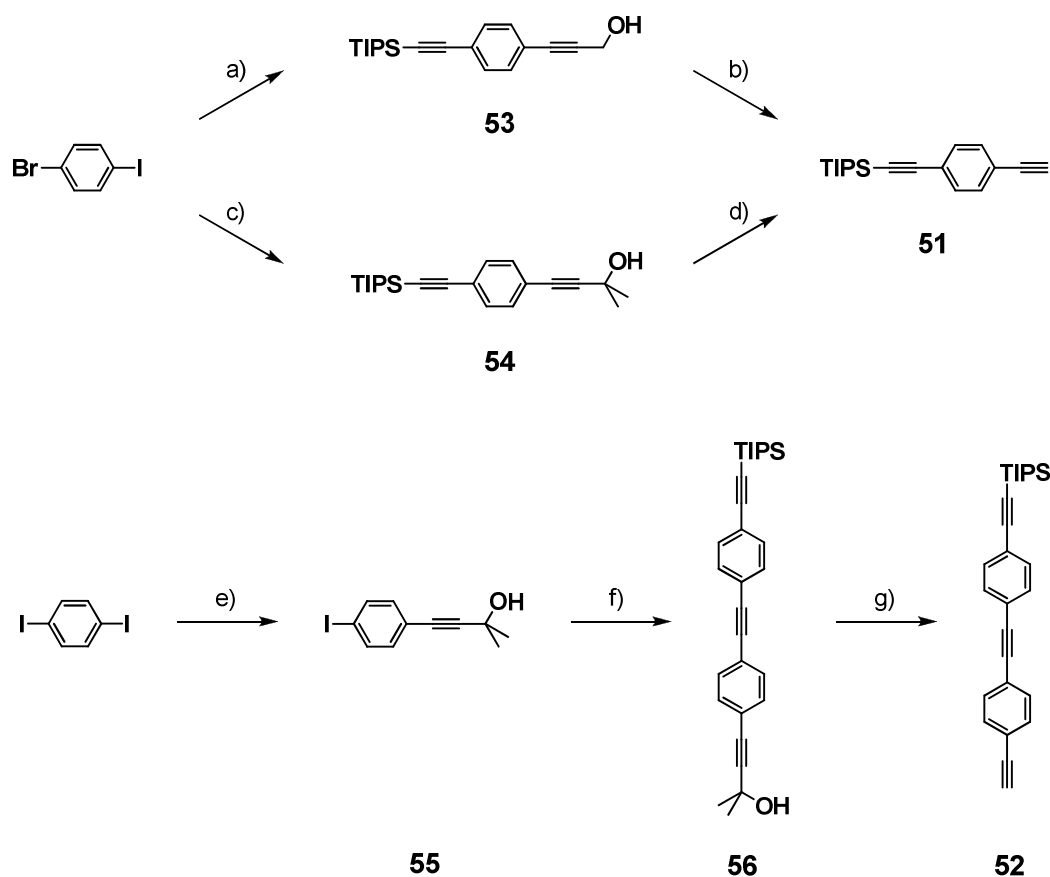
Scheme 25. Retrosynthesis of acetylene functionalized linear thioether ligands starting from the dihydroxybenzyl iodide **49**.

Due to the better reactivity towards the copper catalyzed introduction of acetylenes, an iodo aryl derivative was used instead of the bromide. Thus (5-iodo-1,3-phenylene)dimethanol^[238] (**49**) was synthesized as precursor for acetylene building blocks. The commercially available dimethyl 5-iodoisophthalate (**50**) was reduced with diisobutylaluminium hydride (DIBAL-H) in THF at -40°C, closely following a known procedure.^[239] However, the work up by quenching the reaction with water, followed by filtration through a pad of celites proved to be troublesome and the diol **49** was obtained as colorless crystals in only 57% yield (literature: 65%^[239]). In a second attempt to synthesize **49** in a larger scale, the work up procedure was changed by quenching the reaction with 1M hydrochloric acid to completely dissolve the precipitated aluminum salts. The resulting mixture was then extracted with *t*-butyl methyl ether (MTBE) to give the desired aryl iodide **49** in a yield that was significantly increased to 99% (Scheme 26).



Scheme 26. Synthesis of **49**. DIBAL-H, hexane, THF, -40°C, 99%.

Unlike the first attempt to synthesize acetylene functionalized oligomeric ligands, the in general more stable tri-*iso*-propylsilyl (TIPS) protecting group was chosen for this synthetic pathway instead of the TMS group in order to prevent unwanted cleavage during the nucleophilic introduction of the thioether ligand building blocks. In addition, the TIPS protecting group is sterically more demanding than the TMS group and can thus provide more stable and better dispersible acetylene functionalized gold nanoparticles. The TIPS protecting group can also be removed under mild conditions by using fluoride anions.^[126] While TIPS-acetylene is commercially available, the mono TIPS protected OPE rod-type structures **51**^[240] and **52**^[240] had to be synthesized (Scheme 27).



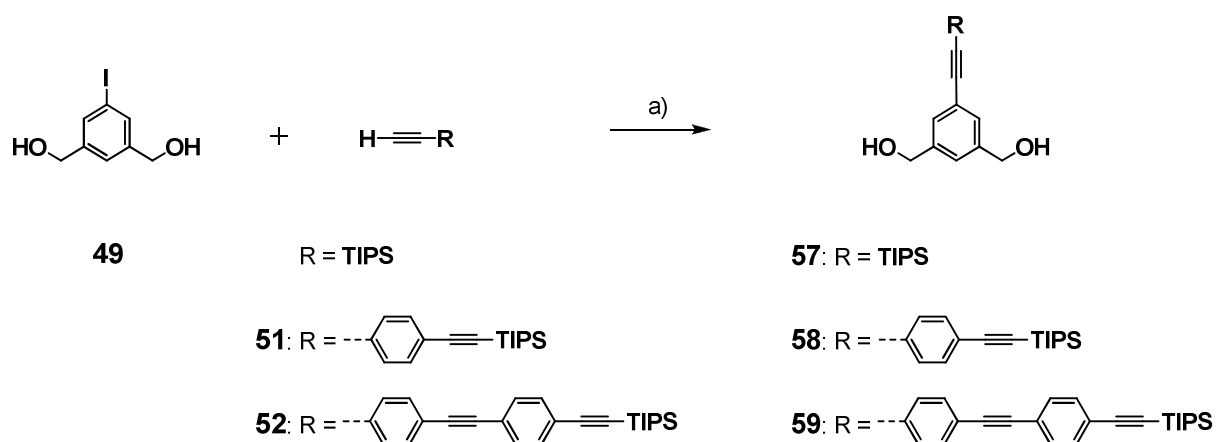
Scheme 27. Synthesis of **51** and **52**. a) TIPS-acetylene, Pd(PPh₃)₂Cl₂, CuI, TEA, 45°C, then propargyl alcohol, reflux, 75%; b) MnO₂, KOH, Et₂O, 83%; c) TIPS-acetylene, Pd(PPh₃)₂Cl₂, CuI, TEA, 45°C, then 2-methyl-3-butyn-2-ol, reflux, 91%; d) NaOH, toluene, reflux, 93%; e) 2-methyl-3-butyn-2-ol, Pd(PPh₃)₂Cl₂, CuI, TEA, 45°C, 48%; f) **51**, Pd(PPh₃)₂Cl₂, CuI, TEA, 45°C, 99%, g) NaOH, toluene, reflux, 99%.

The original procedure for the synthesis of **51** and **52** that was published by Dixneuf *et al.* is based solely on TIPS and TMS protecting groups.^[240] However, the polarities of both groups are very comparable, which makes the chromatographic isolation of the desired differently protected intermediates from the respective di-TIPS and di-TMS protected side products rather difficult. Thus, a strategy that makes use of polar hydroxide containing acetylene precursors was chosen. Initially, **51** was synthesized *via* the propargyl alcohol derivative **53**.^[241] Starting from 1-bromo-4-iodobenzene, the two different acetylenes were introduced under Sonogashira conditions. To a solution of 1-bromo-4-iodobenzene and equimolar amounts of TIPS acetylene in degassed TEA were added the catalysts Pd(PPh₃)₂Cl₂ and copper(I) iodide at room temperature. After two hours, excess of propargyl alcohol was added and the mixture was heated to reflux for another two hours. The desired differently protected diacetylene **53** was thereby obtained in 75% yield after purification by column chromatography. Selective removal of the propargyl group was achieved oxidatively under the action of manganese dioxide with potassium hydroxide in diethyl ether (Et₂O). After

column chromatography, the monoprotected diacetylene **51** was isolated in 83% yield. For preparations in larger scale, the strategy was changed slightly in order to avoid the extensive use of manganese dioxide. 2-Methyl-3-butyn-2-ol was used as second acetylene precursor to form the differently protected intermediate **54**^[242] in a good yield of 91% using otherwise identical reagents and conditions as for the synthesis of **53**. The propan-2-ol protecting group was removed smoothly by ground sodium hydroxide in refluxing toluene, to give **51** in 93% yield after column chromatography without the necessity of an aqueous work up procedure.

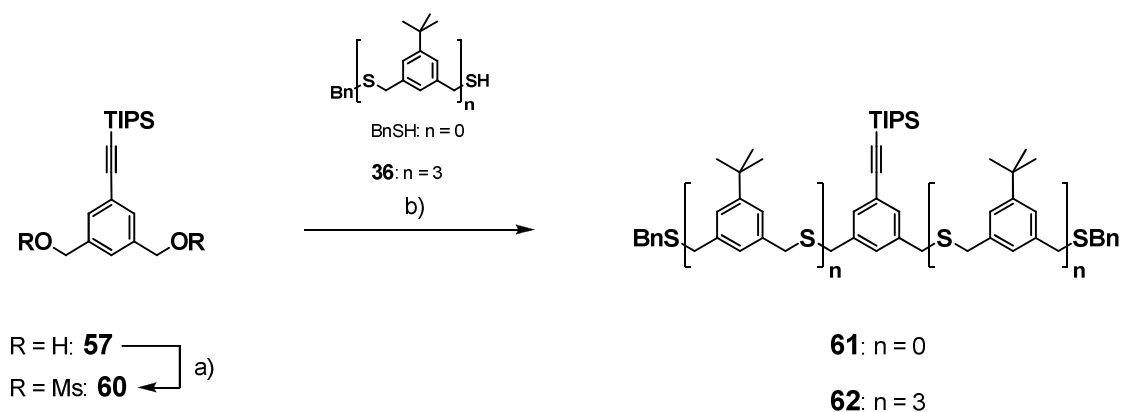
As second building block for the synthesis of the longer OPE rod **52**, 4-(4-iodophenyl)-2-methylbut-3-yn-2-ol^[243] (**55**) was synthesized starting from 1,4-diiodobenzene, closely following a literature procedure.^[244] Unlike 1-bromo-4-iodobenzene, the diiodobenzene does not allow for selective monoacetylation. On the other hand, due to the polar protecting group, the chromatographic separation of the expected mixture was straightforward and the highly reactive iodo aryl **55** can be used conveniently for the next coupling step. After column chromatography, the iodo acetylene **55** was isolated in 48%. **55** was then reacted with the monoprotected diacetylene **51** under acetylene aryl halide coupling conditions in degassed TEA at 45°C in the presence of copper(I) iodide and Pd(PPh₃)₂Cl₂. These conditions were found to be highly general and were used in all following Sonogashira coupling reactions described within this work unless otherwise noted. The differently protected OPE rod **56** was thereby obtained very efficiently in 99% isolated yield after column chromatography. Removal of the propan-2-ol protecting group was achieved under similar conditions that were used for the shorter OPE unit **54**. This way, the mono TIPS protected OPE rod **52** was synthesized in 99% yield.

With the acetylenes **51** and **52** in hand, the three central dihydroxybenzyl subunits **57** - **59** were synthesized following the general Sonogashira coupling protocol (Scheme 28). Excellent yields were obtained in all three cases. The shortest member of the series **57** was obtained quantitatively, while the two OPE structures **58** and **59** were both isolated in 98% yield after column chromatography. The presence of benzylic hydroxides proved therefore to be entirely unproblematic for the introduction of acetylenes to aryl halides by Sonogashira reactions.



Scheme 28. Synthesis of the acetylene building blocks **57 - 59**. a) $\text{Pd}(\text{PPh}_3)_2\text{Cl}_2$, CuI , TEA , 45°C , **57**: quant.; **58**: 98%; **59**: 98%.

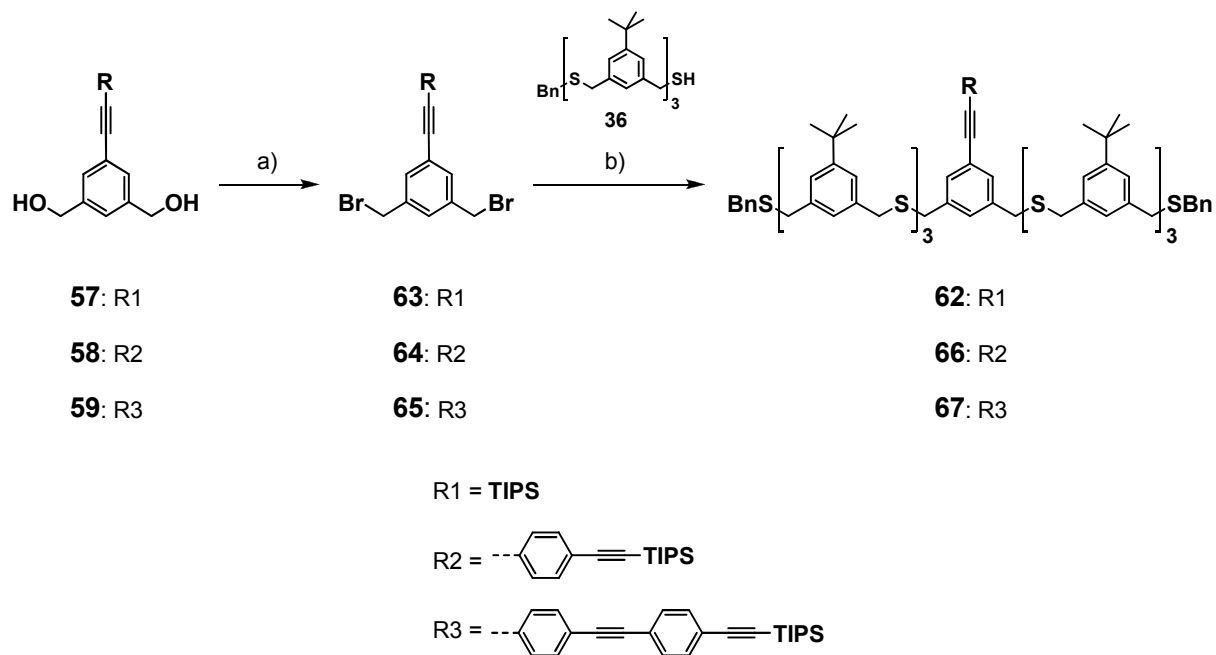
The conversion of the benzylic hydroxides into leaving groups suitable for nucleophilic substitution reactions was then necessary in order to get acetylene functionalized thioether ligands. Sulfonate leaving groups can be introduced under mild basic conditions, under which the TIPS protecting groups should be stable. To test suitable reaction conditions, mesyl groups were introduced to the shortest acetylene building block **57**. Hence, the diol **57** was reacted with three equivalents methanesulfonyl chloride in dry CH_2Cl_2 at 0°C with TEA as base (Scheme 29). After the complete consumption of the starting material **57**, the reaction mixture was extracted with water. After evaporation of the organic phase, the dimesyl compound **60** was obtained quantitatively in good purity without further purification steps. This material was then directly used in the next step and reacted with benzyl mercaptan in THF with sodium hydride as base. The TIPS acetylene monomer **61** was isolated after column chromatography in 86% yield. However, when this sequence was repeated with the SH-SBn-trimer **36** instead of benzyl mercaptan, no conversion of the starting materials **60** and **36** was observed by TLC after one hour under similar conditions. Only after heating to reflux temperature for 2 hours, the desired acetylene functionalized heptamer **62** was formed and could be isolated in 77% yield after purification by column chromatography.



Scheme 29. Synthesis of the acetylene functionalized oligomers **61** and **62** via mesyl leaving groups.

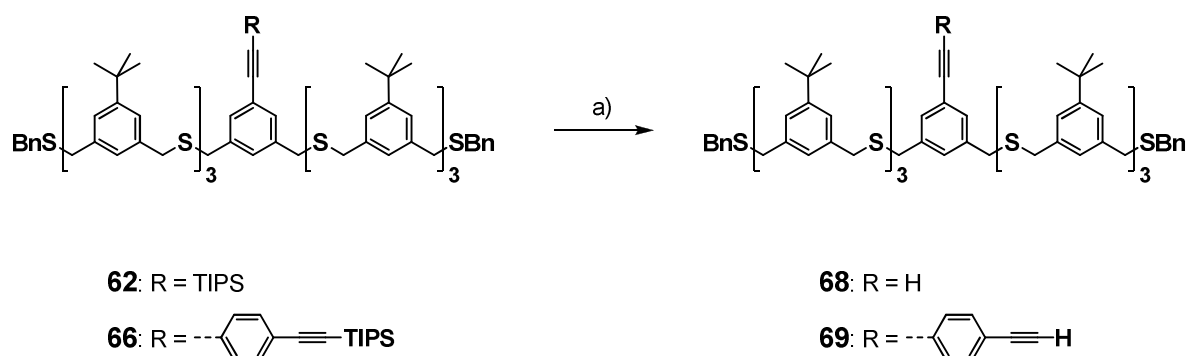
a) MsCl, TEA, CH_2Cl_2 , RT, quant.; b) NaH, THF, RT, **61**: 86%; **62**: after reflux, 77%.

Compared to the results obtained before with benzylic bromides (*vide supra*), mesyl leaving groups seem to work less efficiently as leaving groups towards thiolate nucleophiles. Suitable conditions for the direct substitution of the benzylic hydroxides with bromides were thus investigated, under which the TIPS protecting group is neither cleaved nor takes part in other reactive pathways. It is possible to exchange benzylic hydroxides with bromides under strong acidic conditions with hydrobromic acid. However, the acid labile TIPS protecting group does not allow for such conditions in the cases of **57** - **59**. A neutral method for the direct substitution of hydroxides with bromides is the so called Appel reaction with carbon tetrabromide and triphenylphosphine. With these reagents, triphenylphosphine oxide serves as good leaving group which gets substituted by nucleophilic bromide anions that are generated during the reaction. Treatment of the dihydroxybenzyl derivative **57** with excess of carbon tetrabromide and triphenylphosphine in dry THF provided the corresponding benzyl bromide **63** in 97% yield after column chromatography (Scheme 30). With the better bromide leaving groups, the heptamer **62** was synthesized very efficiently from the reaction of **63** with the thiol trimer **36** with sodium hydride in THF at room temperature in quantitative yield after aqueous work up and column chromatography. Similarly, the longer OPE building blocks **58** and **59** were converted to the bromides **64** and **65**. The apolar bromides **64** and **65** were only filtered through a pad of silica with hexane and then directly reacted with slightly more than two equivalents of the trimeric monothiol **36** in THF in the presence of sodium hydride. Work up and subsequent column chromatography provided the TIPS-acetylene functionalized ligands **66** and **67** as colorless, very viscous oils in good yields of 87% and 71% for the two steps respectively.



Scheme 30. Synthesis of the OPE functionalized heptameric ligands **62**, **66** and **67**. a) PPh_3 , CBr_4 , THF, RT; b) NaH, THF, RT, **62**: 97%; **66**: 87%; **67**: 71% for the two steps respectively.

In order to verify the necessity of the TIPS protecting groups for the synthesis of acetylene functionalized gold nanoparticles, the ligands **68** and **69**, carrying free acetylenes, were also synthesized (Scheme 31). Thus, **62** and **66** were treated with tetra-*n*-butylammonium fluoride (TBAF) in wet THF. After approximately one hour, TLC revealed the complete consumption of the starting materials and the formation of one new spot in both cases. Aqueous work up followed by column chromatography gave the free acetylenes **68** and **69** in nearly quantitative yields.



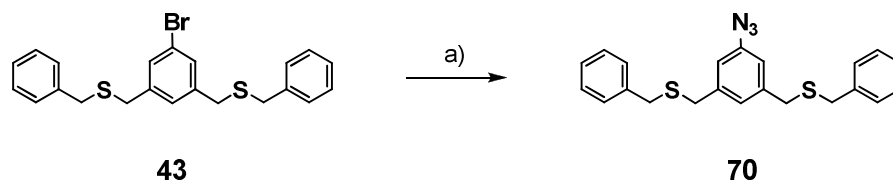
Scheme 31. Deprotection of the OPE heptamers **62** and **66**. a) TBAF, THF, RT, **68**: 98%; **69**: quant.

3.3.1.3 Aryl Azide Functionalized Thioether Ligands

The mild reaction conditions and the versatility of azide-alkyne ‘click’ chemistry (*vide supra*) made such procedures highly interesting for the subsequent functionalization of thioether coated nanoparticles. Azide functionalized nanoparticles could for instance be employed as complementary building blocks to acetylene functionalized nanoparticles. In view of such defined nanoparticle building blocks, the preparation of azide modules for the synthesis of monofunctionalized thioether ligands was explored.

The standard ‘click’ chemistry procedures were reported to be very general and do allow for the cycloaddition of alkyl acetylenes and azides as well as phenyl derivatives thereof.^[245] To keep the synthesis of the functionalized thioether ligands for the stabilization of gold nanoparticles as modular as possible, it was decided to attach the azide functionality directly to the central phenyl ring of the ligand. Although such azides were mostly made starting from aniline derivatives *via* diazonium salts and subsequent treatment with sodium azide,^[246] some procedures were described starting from aryl halides. However, nucleophilic aromatic substitution reactions of aryl chlorides with sodium azide^[247] require electron withdrawing substituents on the aromatic core. Also not desired were strongly basic conditions that are required to form Grignard^[248] or organolithium^[249,250] intermediates, that can be quenched with tosyl azide to form the desired arylazides. Quite recently, two new modifications of the copper(I) catalyzed Ullmann-type preparation^[251] of aryl azides from aryl halides were reported.^[252-254] These procedures make use of amine or amino acid additives, which allow for significantly milder and therefore much more general applicable reaction conditions compared to the original procedure. Due to the high reported yields, the functional group tolerance and the simple and fast reaction conditions, the synthetic procedure reported by Liang and coworkers^[254] seemed particularly interesting. In order to test this method for thioether ligands, the bromo monomer **43** was reacted with excess of sodium azide in the presence of 10 mol% copper(I) iodide, 5 mol% sodium ascorbate and 15 mol% of the ligand *N,N'*-dimethylethylenediamine (Scheme 32). In the original procedure, the reactions were carried out in a 7:3 mixture of ethanol and water and this solvent mixture was also used initially. The thioether monomer was however not soluble in this mixture, not even at elevated temperatures. 50% v/v THF was therefore added to the reaction mixture and the resulting slurry was heated to reflux for one hour. After this reaction time, TLC showed the complete consumption of the starting material **43** and the formation of one new spot. After purification

by column chromatography, the desired azide monomer **70** was obtained in a good yield of 86% as slightly yellow oil.

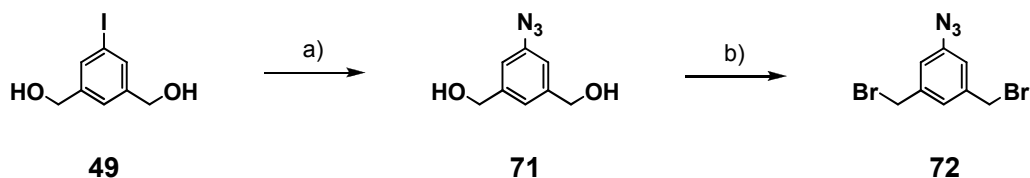


Scheme 32. Synthesis of the azide monomer **70**. a) NaN₃, CuI, sodium ascorbate, *N,N'*-dimethylethylenediamine, EtOH/H₂O/THF, 86%.

This result confirms the general applicability of this procedure, but solubility problems were still supposed to be an issue especially for the larger bromo functionalized thioether oligomers. Hence, other high boiling solvents such as toluene, DMF or dimethylsulfoxide (DMSO) were tried under otherwise similar reaction conditions. Unfortunately, none of these solvents proved to be useful for this Ullmann-type reaction, and only starting material **43** with traces of the azide monomer **70** could be found by TLC even after several days at temperatures up to 135°C. This outcome can probably mainly be attributed to the low solubility of sodium azide in these organic solvents.

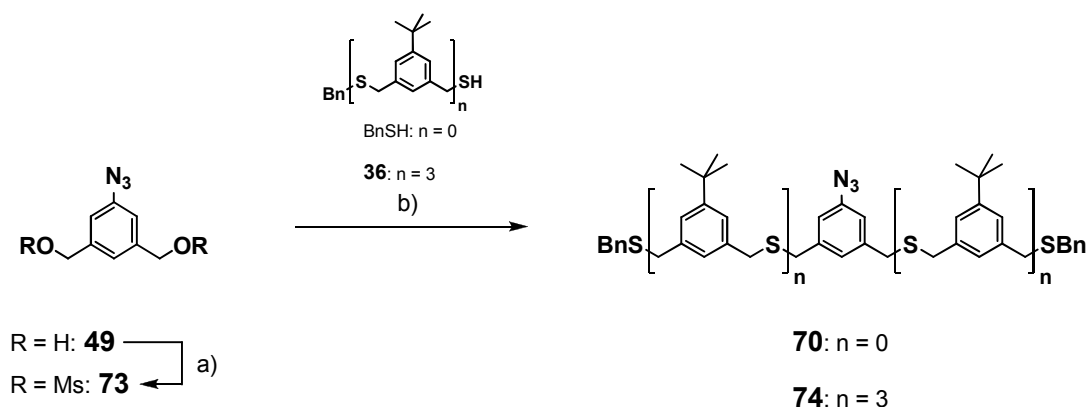
Parallel to the change of the synthetic strategy for the synthesis of the acetylene functionalized thioether ligands (*vide supra*), it was rationalized that the iodo precursor **49** could also be used for the synthesis of azide functionalized ligands. Thus, (5-iodo-1,3-phenylene)dimethanol (**49**) was reacted with sodium azide in a 7:3 ethanol/water mixture under the conditions reported by Liang and coworkers^[254] (Scheme 33). In this case, the addition of THF was not necessary due to the hydroxide groups that provided good solubility in this polar solvent mixture. The desired aryl azide (5-azido-1,3-phenylene)dimethanol^[255] **71** was isolated by column chromatography without the necessity of an aqueous work up in an excellent yield of 96%. It was then tried to introduce bromide leaving groups under similar Appel conditions in THF that were used for the synthesis of the acetylene building blocks **63** - **65**. Unfortunately, the reaction proceeded mainly to the monobrominated compound and the desired dibromide **72** was only isolated in 7% yield. In another attempt, the solvent was changed to DMF, a better solvent for nucleophilic substitution reactions than THF. Thereby, the reaction performed smoothly and the azide dibromide **72** was obtained in a yield of 81% as off white solid. This compound proved to be very unstable. Even when kept at 4°C in a

dark fridge, the compound turned black within hours and TLC analysis revealed the decomposition of the initial dibromide **72**.



Scheme 33. Synthesis of the azide building block **72**. a) NaN_3 , CuI , sodium ascorbate, *N,N'*-dimethylethylenediamine, $\text{EtOH}/\text{H}_2\text{O}$, 96%; b) PPh_3 , CBr_4 , THF, RT, 81%.

Transformation of the hydroxides to mesyl leaving groups, directly followed by the attack of the thiol nucleophile was then envisaged. Thus, the diol **71** was reacted with mesyl chloride in CH_2Cl_2 with TEA as base to quantitatively yield the dimesyl compound **73** after aqueous work up. The azide monomer **70** was then obtained in a good yield of 91% by applying the standard nucleophilic substitution conditions - sodium hydride in THF - to a mixture of **73** and benzyl mercaptan (Scheme 34).



Scheme 34. Synthesis of the azide functionalized oligomers **70** and **74**. a) MsCl , TEA, CH_2Cl_2 , RT, quant.; b) NaH , THF, RT, **70**: 91%; **74**: 45%.

Due to the discouraging results obtained in the attempt to synthesize the heptamer **62** from the dimesyl acetylene **60** (*vide supra*), other substitution conditions with the more polar solvent DMF were tried for the introduction of the trimer thiol **36** to the azide building block **73**. The freshly prepared dimesyl azide **73** was therefore dissolved in dry DMF and the trimeric thiol **36** and the weak base potassium carbonate were added (Scheme 34). TLC revealed the complete consumption of the starting materials after 1.5 hours. After an aqueous work up to remove most of the DMF, the desired azide heptamer **74** was isolated as colorless

solid by column chromatography. The obtained yield of 45% was however quite low. This low yield came rather unexpected because full conversion was observed by TLC. It is therefore possible that decomposition took place on the silica gel column although this was not investigated to further extent.

3.3.2 Towards Functionalized Building Blocks for Electronic Applications

In view of gold nanoparticles or gold nanoparticle superstructures for electronic applications, such as single molecule investigations with nanoparticle dumbbell structures (Figure 41, see also section 2), further functionalization was required on the stabilizing thioether ligands to allow the electronic coupling between gold nanoparticles and the functional molecule.

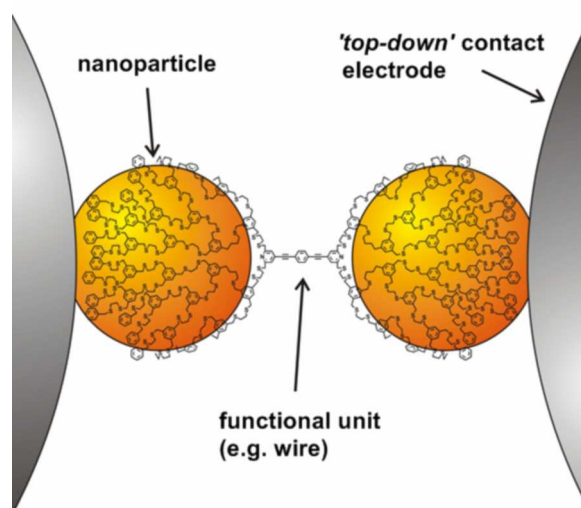


Figure 41. Schematic of a possible single molecule experiment employing pyridine functionalized thioether ligands.

In order to be able to integrate different molecular structures for electronic investigations between gold nanoparticles, the design of the functionalized building blocks should be - as before - as modular as possible. Similar to the 'simple' functionalized ligands based on functionalized benzene rings, aryl halides were therefore integrated to the molecular structures, as these allow for the introduction of functionality by Sonogashira coupling. In particular, this reaction gives conjugated OPE structures that show a relatively high conductance and were regularly used for single molecule electronic measurements. Of course, aryl halides do also allow for other reactions such as other Pd catalyzed C-C coupling

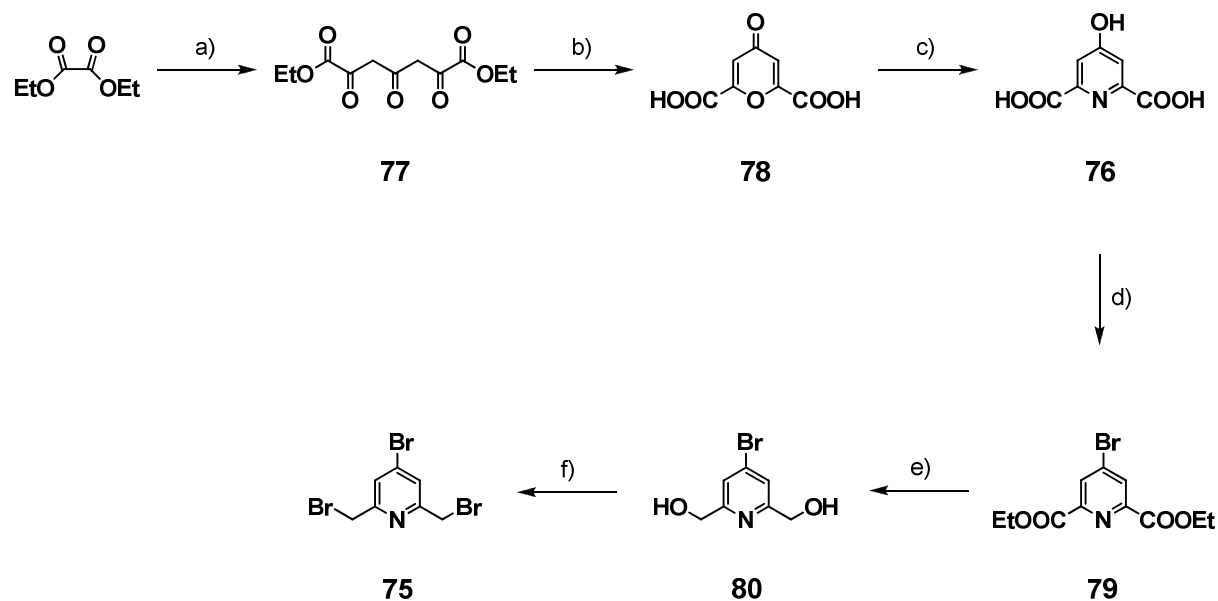
reactions like *e.g.* for the formation of biaryl structures. A plethora of functional molecules can thus be introduced to the thioether ligands and then be investigated on a single molecule level.

3.3.2.1 Pyridine Building Blocks

As was sketched in the section 2, pyridines are interesting candidates for functional building blocks as this moiety can provide the electronic coupling to the electrode material. On the other hand, pyridines do only bind weakly to gold, which makes single molecule investigations difficult. Initially, 4-bromo-2,6-bis(bromomethyl)pyridine^[256] (**75**) (Scheme 35) was chosen as main building block to synthesize bromo functionalized linear thioether ligands. These ligands should then be further functionalized by Sonogashira coupling or other protocols.

The bromo pyridine **75** can be synthesized in three steps starting from the commercially available chelidamic acid (**76**).^[256,257] However, this precursor is relatively expensive and also sold in small quantities only. Starting from the very inexpensive compounds diethyl oxalate and acetone, chelidamic acid (**76**) can be prepared in large quantities in just three steps.^[258,259]

The original procedure for the synthesis of diethyl 2,4,6-trioxoheptanedioate (**77**) is rather complicated and requires multiple flasks that have to be maintained at high temperatures. Also, the transfer of boiling sodium ethanolate solutions is required, when this procedure is followed.^[258,260] It was therefore tried if the synthesis of **77** could not be simplified considerably by adding the complete amounts of diethyl oxalate and acetone directly to a freshly prepared solution of sodium ethanolate. After evaporation of excess ethanol and addition concentrated hydrochloric acid and crushed ice, the resulting yellow precipitate was filtered and dried under vacuum. ¹H NMR showed that this solid was indeed the desired product **77**, which was obtained in a yield of 56% (Lit.: 96%^[260]). The relatively low yield is thereby compensated by the simplified and very fast procedure. The synthesis was done on a multigram scale and was thus not optimized further.



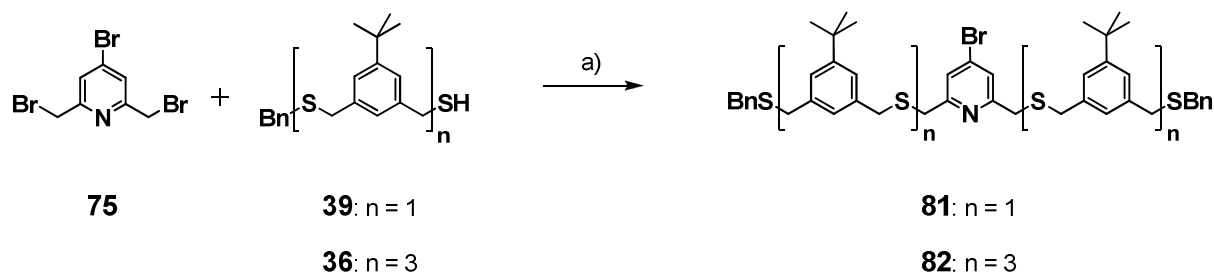
Scheme 35. Synthesis of the pyridine building block **75**. a) NaOEt, acetone, EtOH, reflux, then HCl conc. 56%; b) HCl conc., reflux, 46%; c) NH₄OH aq., reflux, 87%; d) PBr₅, 90°C, then EtOH, 79%; e) NaBH₄, EtOH, reflux, 93%; f) 48% HBr aq., H₂SO₄ conc., reflux, 96%.

For the formation of chelidonic acid (**78**), the linear precursor **77** was suspended in concentrated hydrochloric acid and heated to reflux temperature overnight. After cooling to room temperature, the desired product **78** was directly isolated by filtration as off white powder in 46% yield. This compound was readily converted to chelidamic acid (**76**) by heating in an aqueous ammonia solution. Chelidamic acid (**76**) was precipitated with hydrochloric acid and isolated by filtration. After washing with water, the product was obtained in 87% yield in sufficient purity.

The introduction of the aryl bromide moiety was achieved by heating chelidamic acid (**76**) with freshly prepared phosphorus pentabromide without solvent, closely following a literature procedure.^[257] The intermediate acid bromide was then quenched with dry ethanol to obtain the diester **79** in a good yield of 79% as colorless crystals after recrystallization from ethanol. The reduction of the diester **79** to the diol **80** was efficiently achieved by the action of sodium borohydride in refluxing ethanol, similar to a literature procedure.^[256] After the evaporation of the solvent, the crude remains were extracted thoroughly with acetone. The extract was then evaporated to yield the desired product as colorless powder in 55% yield. As TLC showed the presence of the diol **80** in the already extracted solid, an additional aqueous work up of the remaining solid was therefore performed with ethyl acetate. After evaporation of the organic solvent, more of the pyridine diol **80** was isolated, raising the overall yield for this reaction to excellent 93% (Lit. 53%^[256]).

The substitution of the hydroxide moieties of **80** with bromide leaving groups was reported either with phosphorous tribromide^[256] or a 33% hydrogen bromide solution in acetic acid,^[261] both procedures providing the bromo pyridine **75** only in comparatively low yields. Herein, the bromo pyridine building block **75** was synthesized by heating a solution of the diol **80** in 48% hydrobromic acid with additional concentrated sulfuric acid. After five hours, the mixture was basified with hydrogen carbonate and then extracted with CH₂Cl₂, to give the pyridine **75** as colorless solid in a very good yield of 96% in high purity.

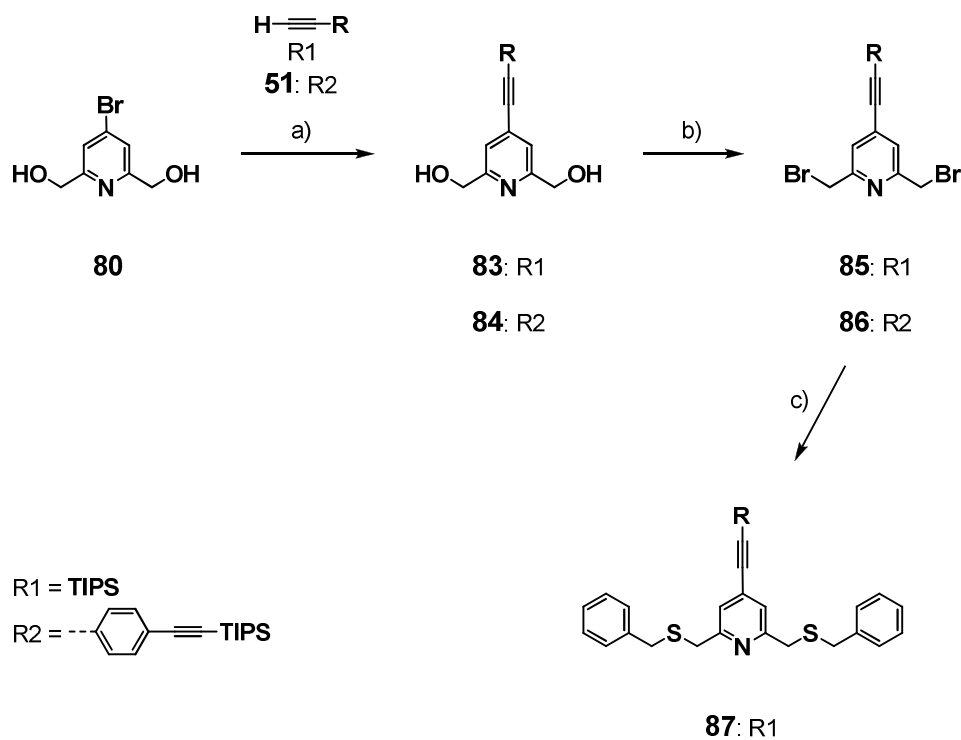
In order to achieve functionalized thioether ligands for electronic applications, the pyridine building block **75** was reacted with the linear thioether building blocks **36** and **39** in DMF with potassium carbonate as base (Scheme 36). The tri- and heptameric ligands **81** and **82** were thereby obtained as colorless oils in 88% and 85% yield after purification by column chromatography. However, due to the unsatisfying bad results obtained in Sonogashira coupling reactions with the bromide functionalized thioether ligands **43** - **45** (*vide supra*), it was not tried to introduce the OPE building blocks to these ligands.



Scheme 36. Synthesis of the pyridine thioether oligomers **81** and **82**. a) K₂CO₃, DMF, RT, **81**: 88%; **82**: 85%.

Similar to the OPE building blocks **57** - **59** (*vide supra*), acetylene functionalized pyridine building blocks were then synthesized starting from the diol **80**. Under standard Sonogashira coupling conditions in TEA at 80°C, **80** was reacted either with TIPS acetylene or the OPE rod **51**, to yield the TIPS protected acetylenes **83** and **84** in 81% as colorless solids in both cases (Scheme 37). Purification was achieved by column chromatography. The hydroxide moieties were then substituted with bromides under Appel conditions. To solutions of the diols **83** and **84** in THF were thus added triphenylphosphine and carbon tetrabromide and the resulting mixtures were stirred for two hours at room temperature. After an aqueous work up and purification by column chromatography, the dibromides **85** and **86** were obtained in 69% and 63% as slightly yellow oils respectively. These reactions were just done once and the reasons for the low yields were not investigated. In a small scale test reaction, the shorter

pyridine-acetylene building block **85** was reacted with benzyl mercaptan in DMF with potassium carbonate as base. Thereby, the functionalized monomer **87** was obtained efficiently in a yield of 83% after column chromatography. The longer pyridine OPE building block **86** was then used for dendritic thioether ligand structures (see section 3.4.3.2).



Scheme 37. Synthesis of the acetylene functionalized pyridine building blocks **85**, **86** and **87**. a) CuI, Pd(PPh₃)₂Cl₂, TEA, 80°C, 81%; b) PPh₃, CBr₄, THF, RT, **85**: 69%, **86**: 63%; c) BnSH, K₂CO₃, DMF, RT, 83%.

3.3.2.2 Monothiol Building Blocks

Thiophenol building blocks for monofunctionalized thioether ligands are not only interesting for electronic investigations. Such building blocks could also allow for ligand exchange with weakly stabilized nanoparticles, something that was not achieved with ligands based solely on thioethers (*vide supra*). Due to the strong interaction between thiols and gold surfaces, one single thiol moiety in a large multidentate thioether ligand could act as ‘spearhead’ that binds the thioether ligand to a nanoparticle surface and could therefore allow for an ‘intramolecular’ ligand exchange due to the large entropic gain by releasing multiple ligands (Figure 42).

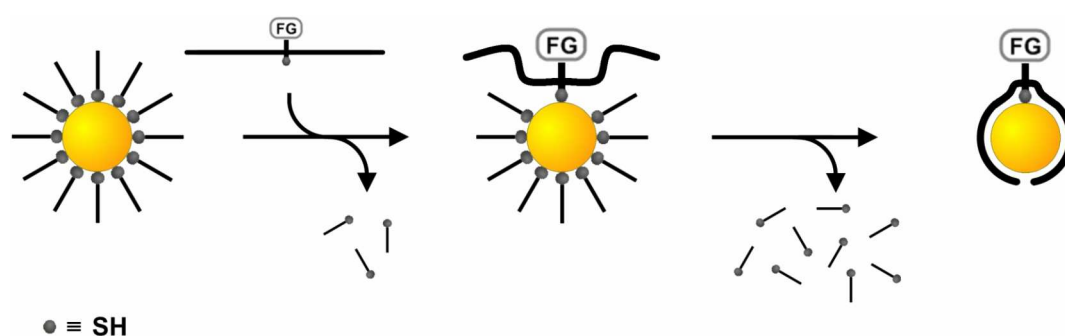
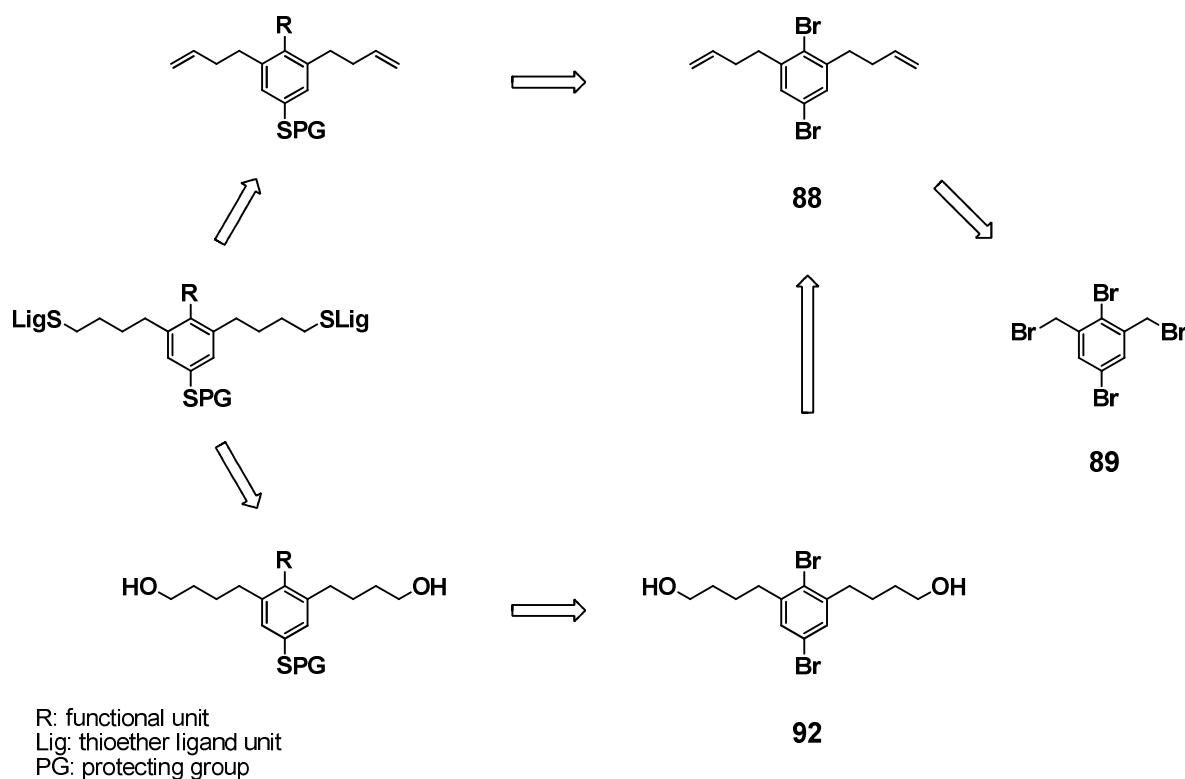


Figure 42. Schematic of the exchange of multiple thiol ligands by a large monothiol thioether ligand to form monofunctionalized thioether coated gold nanoparticles. FG: functional group.

Compared to pyridine based functionalized building blocks, the benzene core of thiophenol based building blocks can be expected to be much further away from the nanoparticle surface due to the additional length of the C-S bond. In order to prevent tilting of the functional building block by interaction of the neighboring thioether moieties with gold, short benzylic thioethers could not be used for the attachment of the ligand subunits in such cases. A more flexible system was therefore developed based on butyl chains that are attached *meta* to the thiophenol (Scheme 38). The introduction of the thioether ligand parts should be possible from the double bonds either by direct reaction with the thiols *via* a thiol-ene coupling^[262,263] or by hydroboration, conversion of the hydroxides to leaving groups and subsequent nucleophilic substitution.



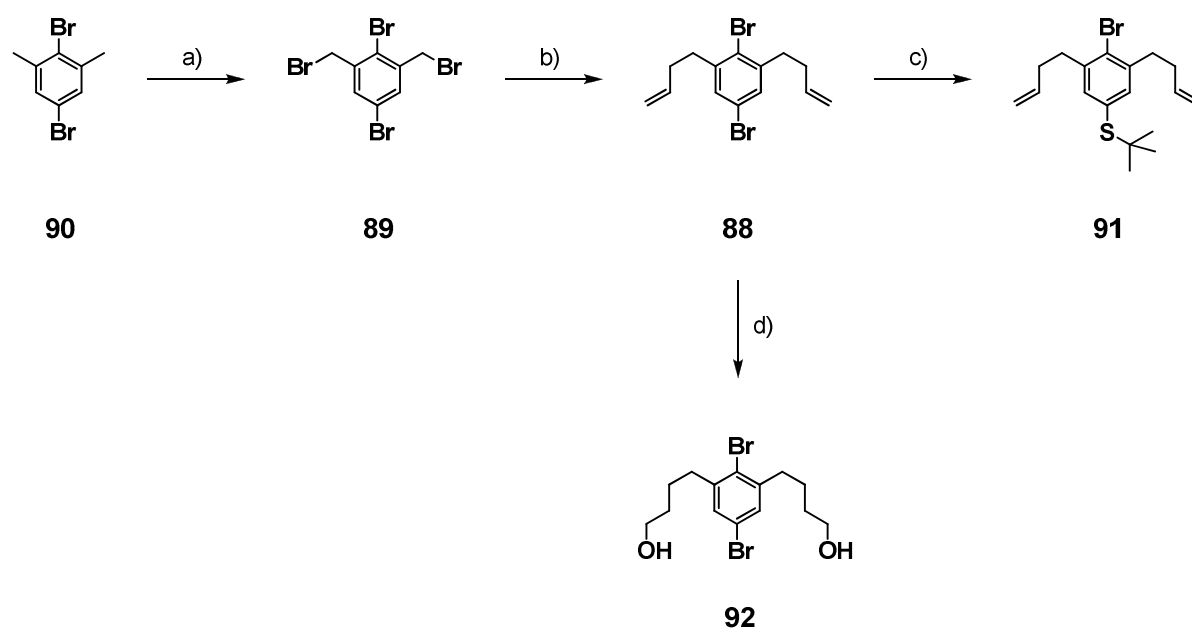
Scheme 38. Retrosynthetic analysis for monothiol thioether ligands.

It was envisaged to introduce the thiophenol precursor selectively to the sterically less crowded and electronically favored position *meta* to the alkyl chain by bromine lithium exchange and subsequent reaction with elemental sulfur.^[264] Other possibilities include the direct nucleophilic aromatic substitution or a palladium catalyzed version thereof.^[265] The butene derivative **88** should be easily accessible from the known compound 2,5-dibromo-1,3-bis(bromomethyl)benzene^[266] (**89**) by reaction with an commercially available allyl Grignard reagent.^[267]

The tetrabromide **89** can be synthesized *via* a radicalic side chain bromination starting from the commercially available 2,5-dibromo-*m*-xylene (**90**). Due to reports on very low yields in such reactions with aryl bromides in non-chlorinated solvents,^[226] the reaction was performed in carbon tetrachloride with NBS and AIBN as radical starter, closely following a literature procedure (Scheme 39).^[266] In addition to heating under reflux, the mixture was also illuminated by a 500 W halogen lamp. Also, the reaction time was increased to 24 hours instead of the reported two hours, as TLC revealed the incomplete formation of the desired product after the short reaction time. After basic aqueous work up with sodium hydrogen carbonate solution and two recrystallization procedures from CH₂Cl₂/hexane, the tetrabromide **89** was isolated as colorless crystals in a good yield of 72% (Lit.: 55%^[266]). With this material in hand, it was attempted to perform the bromination reaction in the less toxic and more

environmentally friendly solvent methyl formate. However, even with large excess of NBS and long reaction times, the bromination was not brought to completion and a mixture of starting material **90**, the monobrominated derivative and minor amounts of the dibrominated product was found.

The introduction of the alkene chains to the tetrabromo precursor **89** was achieved by nucleophilic substitution of the benzylic bromides with the commercially available allyl magnesium bromide, following a published procedure for a related compound.^[268] Thus, a solution of the Grignard reagent in diethyl ether was slowly added to a solution of **89** in THF at 0°C. After 3 hours, the reaction was quenched with water, extracted with MTBE and then purified by column chromatography to yield the dialkene **88** in 56%.

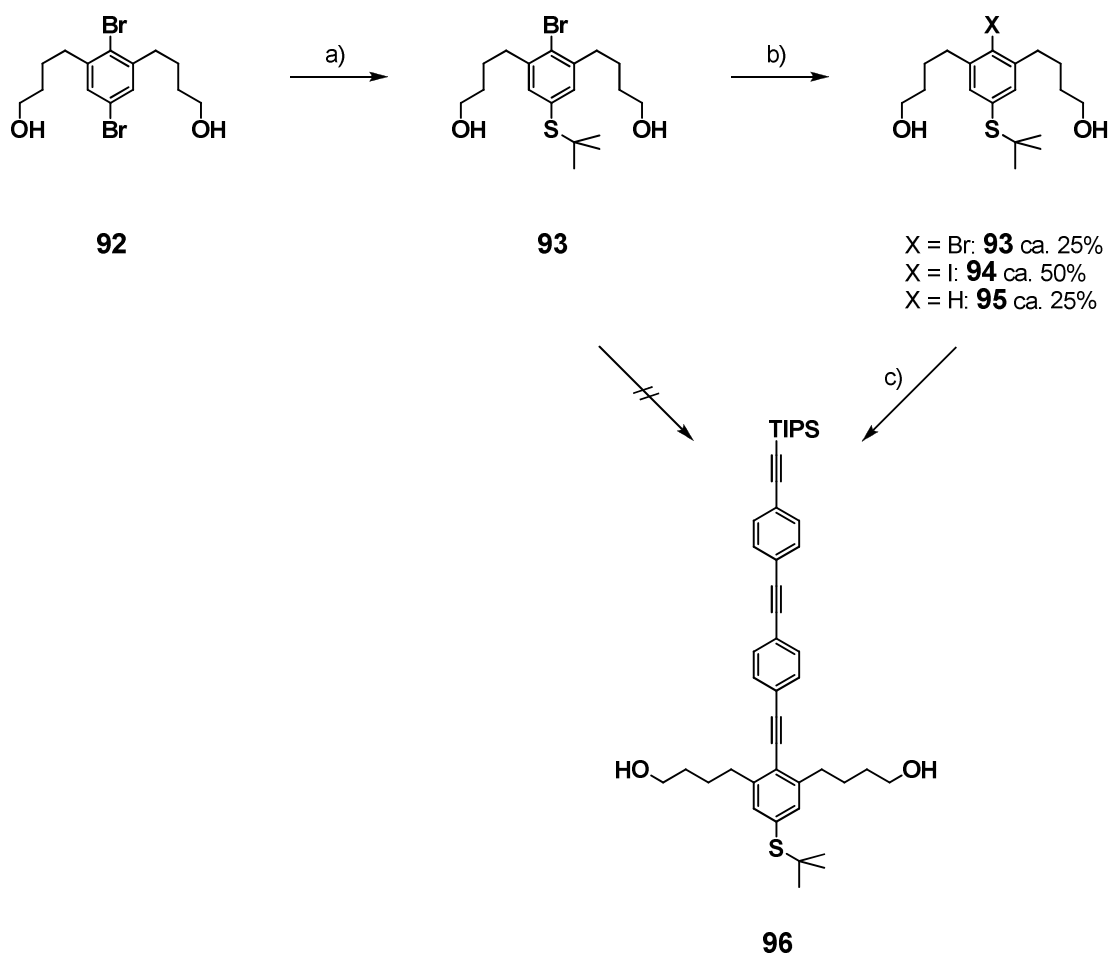


Scheme 39. Towards monothiol building blocks. a) NBS, AIBN, CCl_4 , $h\nu$, reflux, 72%; b) allyl magnesium bromide, Et_2O , THF, RT, 56%, c) $\text{NaS}t\text{-Bu}$, $\text{Pd}(\text{PPh}_3)_4$, $n\text{-BuOH}$, reflux, 46% with impurities; d) $\text{BH}_3\cdot\text{THF}$, THF, RT, then H_2O_2 aq., NaOH aq., RT, 61%.

Starting from **88**, different attempts including bromine lithium exchange and subsequent quenching with sulfur or palladium catalyzed reactions with different thiophenol precursors were made to selectively introduce a thiol moiety *meta* to the alkyl chains using different conditions and precursors.^[269-271] The most promising results were obtained with a palladium catalyzed reaction of **88** with sodium *t*-butyl thiolate, which gave the desired product **91** regioselectively, albeit in low yield due to the formation of side products from the reaction of

the thiolate with the double bonds.^[271] It was also tried to add sulfides to the termini of the alkene chains, although with limited success due to low yields and complicated procedures.^[269-271] Based on these results, it was decided to introduce hydroxy groups to the alkene chains prior to the reaction with sodium *t*-butyl thiolate (Scheme 39). The alcohols should neither influence the introduction of the thiol nor the introduction of further functionality by palladium catalyzed cross coupling reactions. Furthermore, transformation of the hydroxide moieties to leaving groups suitable for nucleophilic substitution reactions should be easily achievable. The diol **92** was synthesized *via* a hydroboration/oxidation/hydrolysis sequence, which selectively provides the *anti*-Markovnikov hydrated products. To a solution of the diene **88** in THF was slowly added a borane/THF complex, which directly led to the formation of a precipitate, probably due to the formation of polymers. The initial reaction products were oxidized with a mixture of sodium hydroxide and hydrogen peroxide, which provided the desired dihydroxy product **92**. After purification by column chromatography, the diol **92** was isolated in 61% yield as colorless oil. The low yield of the reaction probably arises from the precipitation of polymeric intermediates, which prevented the intermixture of the reagents. By using for instance 9-borabicyclo[3,3,1]nonane, which can only add to one double bond and can therefore not form polymeric boranes with the diene **88**, higher yields of **92** can be expected in future attempts.

The diol **92** was then reacted with equimolar amounts of sodium *t*-butylthiolate in refluxing *n*-butanol in the presence of catalytic amounts of tetrakis(triphenylphosphine)palladium(0) (Scheme 40). After an aqueous work up procedure with MTBE, the major product was isolated by column chromatography in 66% yield. ¹H NMR revealed that just one of the possible regioisomers was obtained. However, 1D NMR methods did not allow to distinguish clearly between the two isomers. A NOESY experiment was therefore performed, which undoubtedly showed the proximity of the aryl protons and the protons of the *t*-butyl protecting group. Moreover, no cross-peak was found between the signals of *t*-butyl protons and the signal of the protons attached to the alkyl side chains. The main product of the reaction is thus the desired thiophenol derivative **93**.



Scheme 40. Towards monothiol functionalized building blocks. a) Na*S**t*-Bu, Pd(PPh₃)₄, *n*-BuOH, reflux, 66%; b) *n*-BuLi, hexane, THF, -78°C, then I₂, -78°C → RT; c) **52**, CuI, Pd(PPh₃)₂Cl₂, TEA, 50°C, 20% for two steps.

To test the applicability of the thiophenol building block for the synthesis of functionalized thioether ligands, several procedures had to be validated: the introduction of the ligand building blocks, the introduction of the desired functionality and the deprotection of the thiophenol moiety. All of these procedures were done on a very small scale and were shown to be feasible. However, these test reactions were partially performed with mixtures and were therefore not cleanly characterized. Nevertheless, the desired transformation was in all cases clearly observable by NMR. The main results are described in the following section.

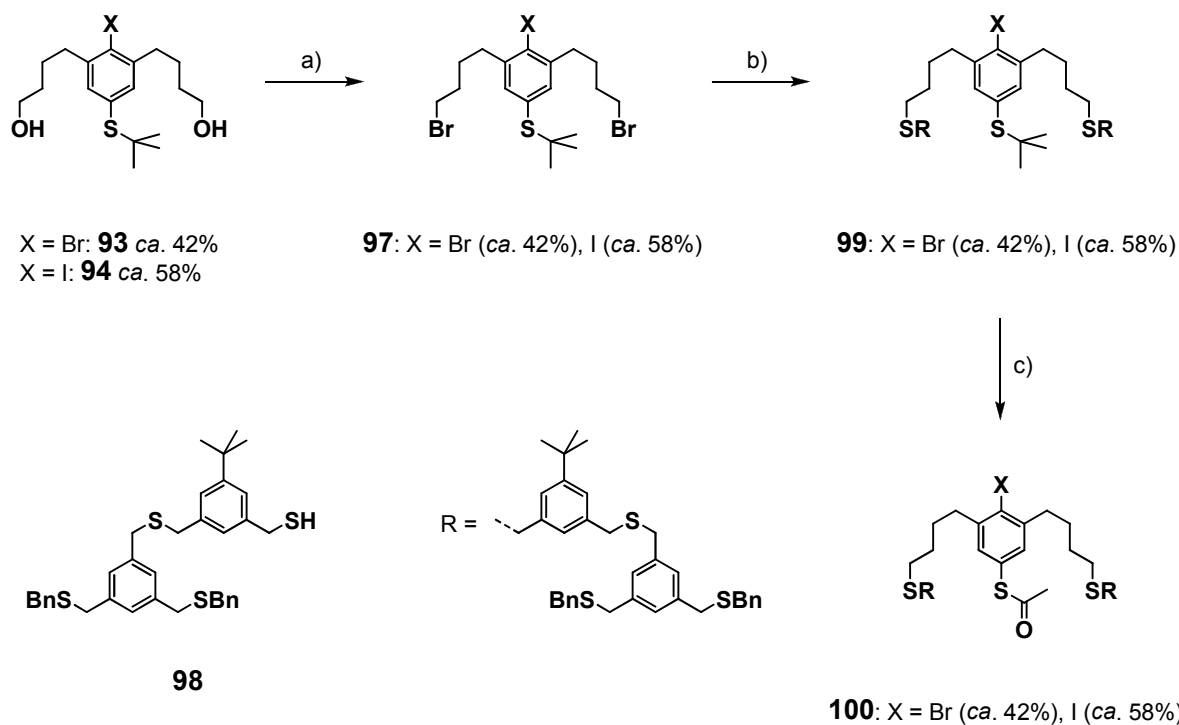
The bromide **93** is a rather bad substrate for Sonogashira coupling reactions with acetylenes due to the sterically demanding alkyl chains in *ortho* position to the bromide. By applying the standard Sonogashira coupling conditions (*vide supra*) to a mixture of **93** and the OPE **52** in refluxing TEA, only the starting materials were recovered (Scheme 40). Only very few methods were reported so far for the efficient introduction of acetylenes to comparable crowded bromide substrates.^[272-275] In order to avoid the highly specialized and harsh reaction conditions required, the synthesis of the more reactive iodide **94** was envisaged. In a small

scale test reaction, the bromide **93** was reacted in THF with 3.5 equivalents of *n*-butyl lithium at -78°C in order to deprotonate the hydroxide groups and to form the aryl lithium intermediate, which was subsequently iodinated by adding excess iodine to the mixture. After an aqueous work up, ^1H NMR of the crude product revealed a mixture of compounds. The signals found were assigned to the iodinated product **94**, the starting material **93** and the debrominated compound **95** in a ratio of *ca.* 2:1:1 respectively. By TLC, just one spot was found, indicating that separation of the three compounds by silica gel column chromatography would be challenging. To test whether the iodo derivative **94** can indeed be used efficiently for the introduction of acetylenes, the crude mixture was subjected to the standard Sonogashira coupling conditions (*vide supra*) with the OPE **52** in triethylamine with copper(I) iodide and $\text{Pd}(\text{PPh}_3)_2\text{Cl}_2$ at 50°C . The reaction was stopped after one hour, as the formation of a new spot was observed on the TLC plate. The desired building block **96** was isolated by column chromatography in 20% yield for the two steps. A *ca.* 1:1 mixture of the bromide **93** and the iodide **94** (44% yield for the two steps) was also isolated, indicating that the reaction was not brought to completion after the short reaction time.

The 1:1 mixture of **93** and **94** was subjected to Appel conditions to introduce bromide leaving groups. Under the action of triphenylphosphine and carbon tetrabromide, the mixture of the bromides **97** was obtained efficiently in 95% yield (Scheme 41). **97** was then reacted with the starting generation dendritic thioether building block **98** (see also section 3.4.3.1) in THF with sodium hydride as base. At room temperature, no conversion was observed by TLC within three hours. The mixture was therefore heated to reflux. After another two hours at the elevated temperature, the reaction was quenched with water and extracted with MTBE. The crude was purified by column chromatography to give the *t*-butyl protected thioether ligand **99** quantitatively.

The *t*-butyl protecting group can be removed by lewis acids such as boron tribromide. These conditions could also lead to disassembly of benzylic thioethers. In a final test reaction it was therefore tried if the *t*-butyl protected thiol of **99** can be selectively transprotected *in situ* with an acetyl protecting group. Acetyl protected thiols can be deprotected under very mild conditions without the necessity of complicated work up procedures. The *t*-butyl protected ligand **99** was thus added to a mixture of toluene and acetyl chloride, to which was slowly added the lewis acid boron tribromide. After one hour reaction time, a new compound was observed by TLC. The reaction was then quenched with water and extracted with CH_2Cl_2 . The organic extracts were subjected to column chromatography, whereby the acetyl protected thiol **100** was isolated in 60% yield. As the reaction was not brought to completion, the

starting material **99** was also present and was isolated in 40%. It is therefore very likely that longer reaction times would lead to a quantitative conversion of **99** to the acetyl protected compound **100**.



Scheme 41. Towards monothiol functionalized building blocks. a) PPh_3 , CBr_4 , THF, RT, 95%, b) **98**, NaH, THF, reflux, quant.; c) BBr_3 , AcCl, toluene, RT, 60% (incomplete reaction, **99** was isolated in 40%).

Even when only performed with compound mixtures, this short test sequence shows that the thiol building block **93** can be indeed used very efficiently as building block for the formation of monothiol thioether ligands. Except for bromine/iodine exchange reaction, the procedures provide the desired products in high yields and do not require further improvement. Due to time constraints, monothiol functionalized thioether ligands were not synthesized in larger scale.

3.3.3 Preparation of Acetylene Functionalized Gold Nanoparticles

To investigate and validate the concept of thioether stabilized gold nanoparticles as 'artificial molecules' carrying surface functionalities at defined positions and as building blocks for wet chemistry processing, gold nanoparticles were formed in the presence of acetylene functionalized heptameric thioether ligands. The particles were prepared with the TIPS protected OPE ligands **62**, **66** and **67** as well as the free acetylene heptamer **69** (Figure 43). As was pointed out before (*vide supra*), the interparticle distances of nanoparticles interlinked by the OPE structures should reflect the lengths of the rigid rod type acetylene linkers. Also, due to the very similar heptameric ligand structures, the results concerning nanoparticle stabilization with these acetylene functionalized ligands can be directly compared to the unfunctionalized heptamer ligand **27** to investigate the influence of the functional OPE rods of **62**, **66**, **67** and **69**.

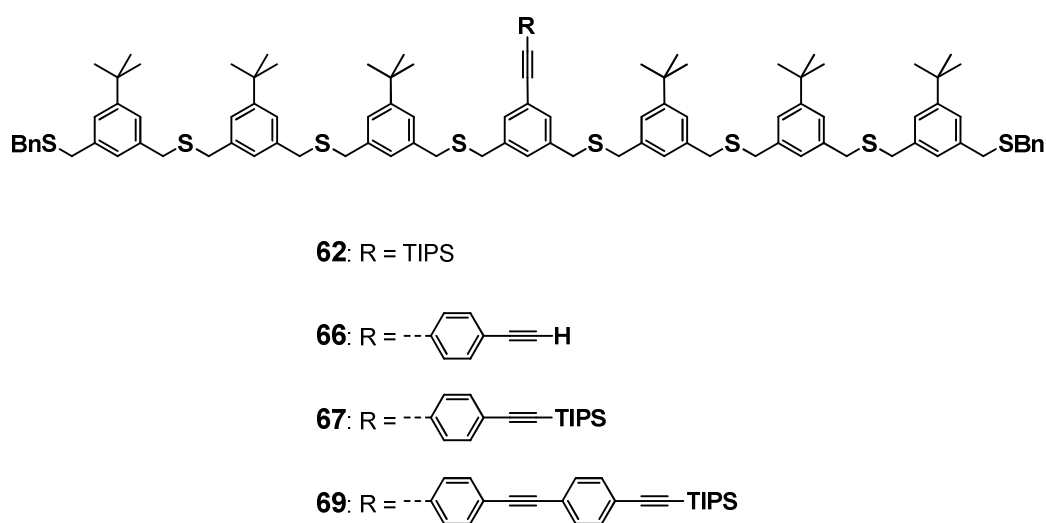


Figure 43. Acetylene functionalized thioether ligands **62**, **66**, **67** and **69** for the stabilization of gold nanoparticles.

The gold nanoparticle syntheses were performed according to the same two-phase protocol that was used for the syntheses of the particles coated by the unfunctionalized heptamer **27** (*vide supra*). However, in contrast to the preparation of the unfunctionalized particles **Au-24** – **Au-27**, solvent removal was not performed at elevated temperatures. In the following cases, the solvents were evaporated by a stream of nitrogen at room temperature. For the synthesis of functionalized gold nanoparticles, the gold(III) precursor tetrachloroauric acid was transferred from the aqueous phase to the organic CH_2Cl_2 phase by TOAB. The respective

ligand **62**, **66**, **67** or **69** was added, whereby a 1:1 ratio of gold equivalents to sulfide moieties was maintained (8 equivalents HAuCl_4 to 1 equivalent of the octadentate thioether ligand). The gold(III) was then reduced by adding an aqueous sodium borohydride solution to the quickly stirred system. In all cases, the organic phases were strongly dark brown colored after the addition of the reducing agent, indicating the formation of gold nanoparticles. After separation of the CH_2Cl_2 and the aqueous phase, the particles were precipitated from a concentrated CH_2Cl_2 dispersion with ethanol. The precipitated particles were separated from the liquid phase by centrifugation. This procedure was repeated two more times in order to completely remove the phase transfer agent TOAB. The dispersibilities of the acetylene functionalized nanoparticles were thereby very similar to the unfunctionalized heptamer coated **Au-27** nanoparticles. As was pointed out before, excess ligand cannot be removed by this method due to very similar solubility properties of the heptameric ligands **62**, **66**, **67** and **69** and the nanoparticles stabilized with these ligands. As for the unfunctionalized gold nanoparticles **Au-27**, excess, unbound ligand was removed by GPC in all cases. However, while the nanoparticles stabilized by the TIPS protected acetylene ligands **62**, **66** and **67** moved in a narrow brown colored band through the GPC column, some material of the free acetylene particles **Au-69** stayed on the column as was indicated by the brown tail and the brown color of the column material after the purification procedure. Furthermore, the free acetylene particles were not fully dispersible in CH_2Cl_2 after removal of the eluent toluene. In the cases of the TIPS protected acetylenes, the particles remained fully dispersible in common organic solvents such as CH_2Cl_2 , toluene or THF.

UV/vis Investigations

UV/vis investigations of **Au-62**, **Au-66**, **Au-67** and **Au-69** (Figure 44) show the formation of gold nanoparticles. Between wavelengths of 400 and 800 nm, all spectra resemble the spectrum obtained for the unfunctionalized heptamer coated nanoparticles **Au-27**, indicating the similar nanoparticle stabilization properties of the different heptameric ligand structures. As for **Au-27**, no plasmon resonances were found at around 520 nm in the UV/vis spectra of **Au-62**, **Au-66** and **Au-67**, pointing towards particles with diameters smaller than 2-3 nm.^[181] This was also true for the **Au-69** particles that carry free acetylene functional groups (Figure 44). The low dispersibility of these particles after purification by GPC was therefore probably not due to coagulation of nanoparticles to larger particles or bulk gold. On the contrary, the

absence of a plasmon resonance and therefore larger particles points towards the formation of nanoparticle aggregates. This may be due to direct acetylene gold bonds^[222] or diacetylene formation. The removal of excess ligand molecules by GPC was conveniently monitored by the reduction of the intensity of the UV/vis band between 290 and 400 nm, where the phenylene ethynyl subunits of the acetylene functionalized ligands **62**, **66**, **67** and **69** absorb light. Importantly, compared to the unfunctionalized gold particles **Au-27**, a signal in this region remained in all cases after the purification by GPC, indicating the presence of the functional group in the coating ligand (Figure 44). Even after one month in dispersion at ambient conditions, the UV/vis spectra of the acetylene functionalized particles **Au-62**, **Au-66**, **Au-67** and **Au-69** remained unchanged, pointing at the long term stability of these coated hybrid structures. In particular the absence of a plasmon resonance band demonstrated the stability provided by their heptameric ligands **62**, **66**, **67** and **69**, as has already been found for the parent ligand **27**.

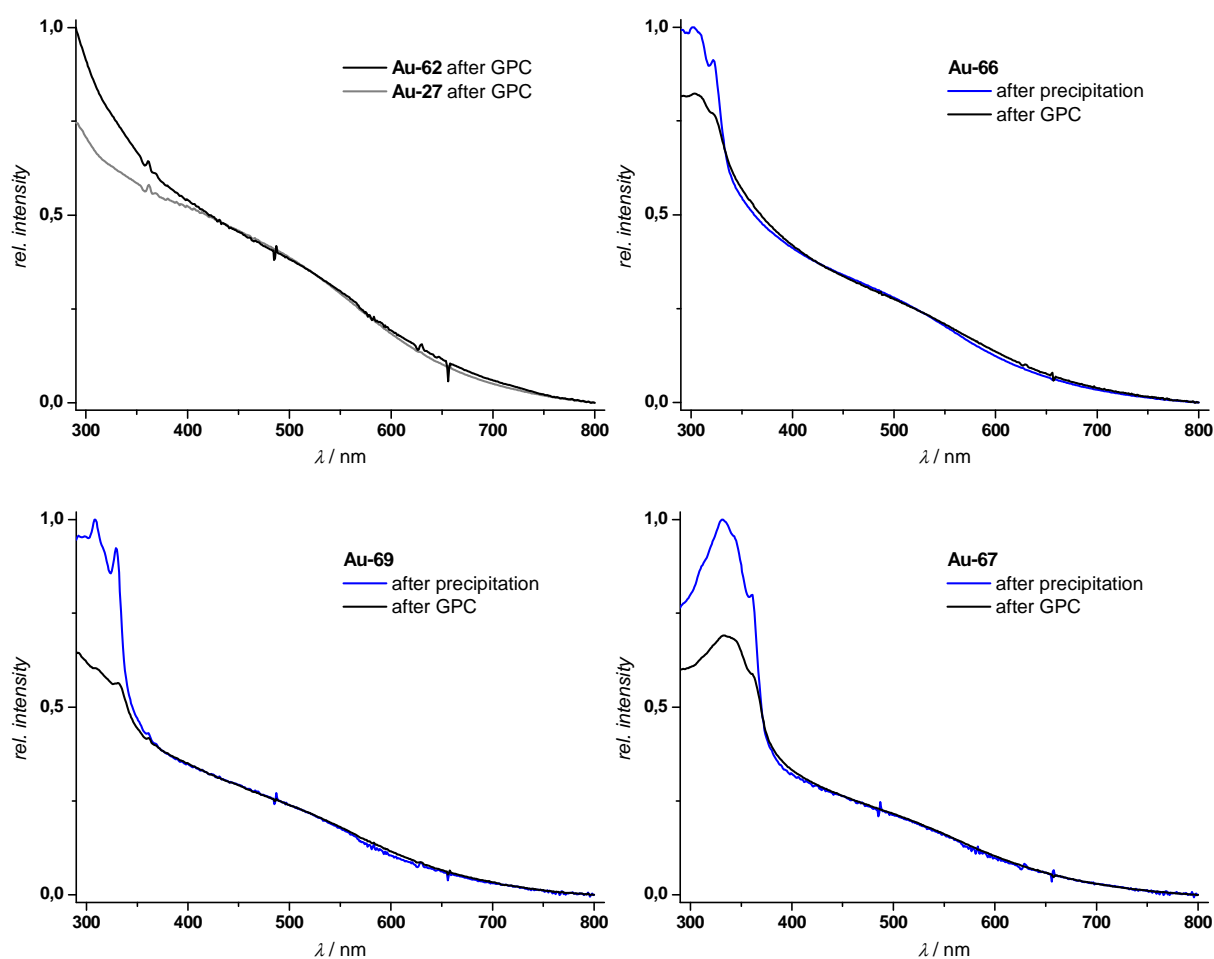


Figure 44. UV/vis absorption spectrum (CH_2Cl_2) of **Au-62** after purification by GPC in comparison with the spectrum of **Au-27** and UV/vis absorption spectra of **Au-66**, **Au-67** and **Au-69** before and after purification by GPC. The spectra were normalized at 520 nm.

The direct comparison of the UV/vis spectra of the TIPS protected nanoparticles **Au-62**, **Au-66** and **Au-67** nicely shows the red shift of the absorption of the functional OPE unit due to the increase in conjugation length (Figure 45).

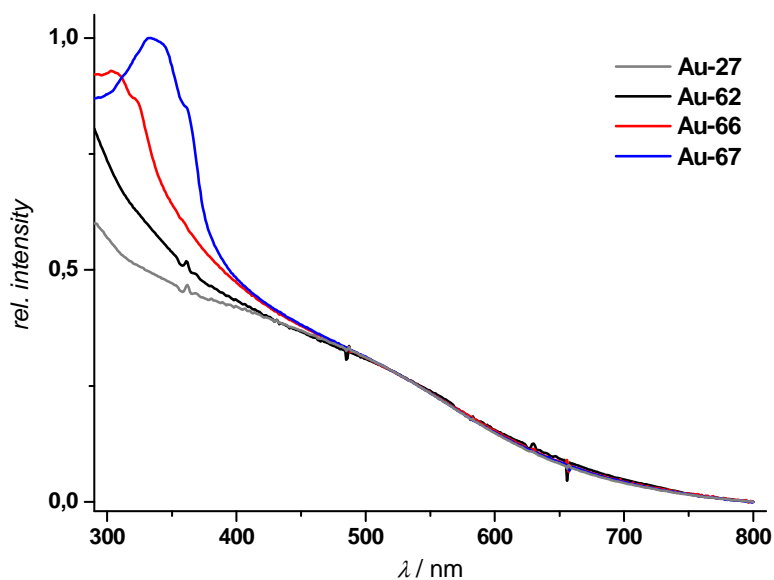


Figure 45. Direct comparison of the UV/vis absorption spectra of **Au-27** and **Au-62**, **Au-66** and **Au-67** in CH_2Cl_2 after purification by GPC. The spectra were normalized at 520 nm.

NMR

^1H NMR was performed with the medium size OPE functionalized **Au-66** and **Au-69** particles after purification by GPC (Figure 46). In both cases, very broad signals are found similar to the unfunctionalized **Au-27** nanoparticles, indicating again the similar nanoparticle stabilizing properties of the different heptameric ligands. Also, TOAB signals cannot be found, showing that the phase transfer agent TOAB is not required for the stabilization of the OPE functionalized nanoparticles.

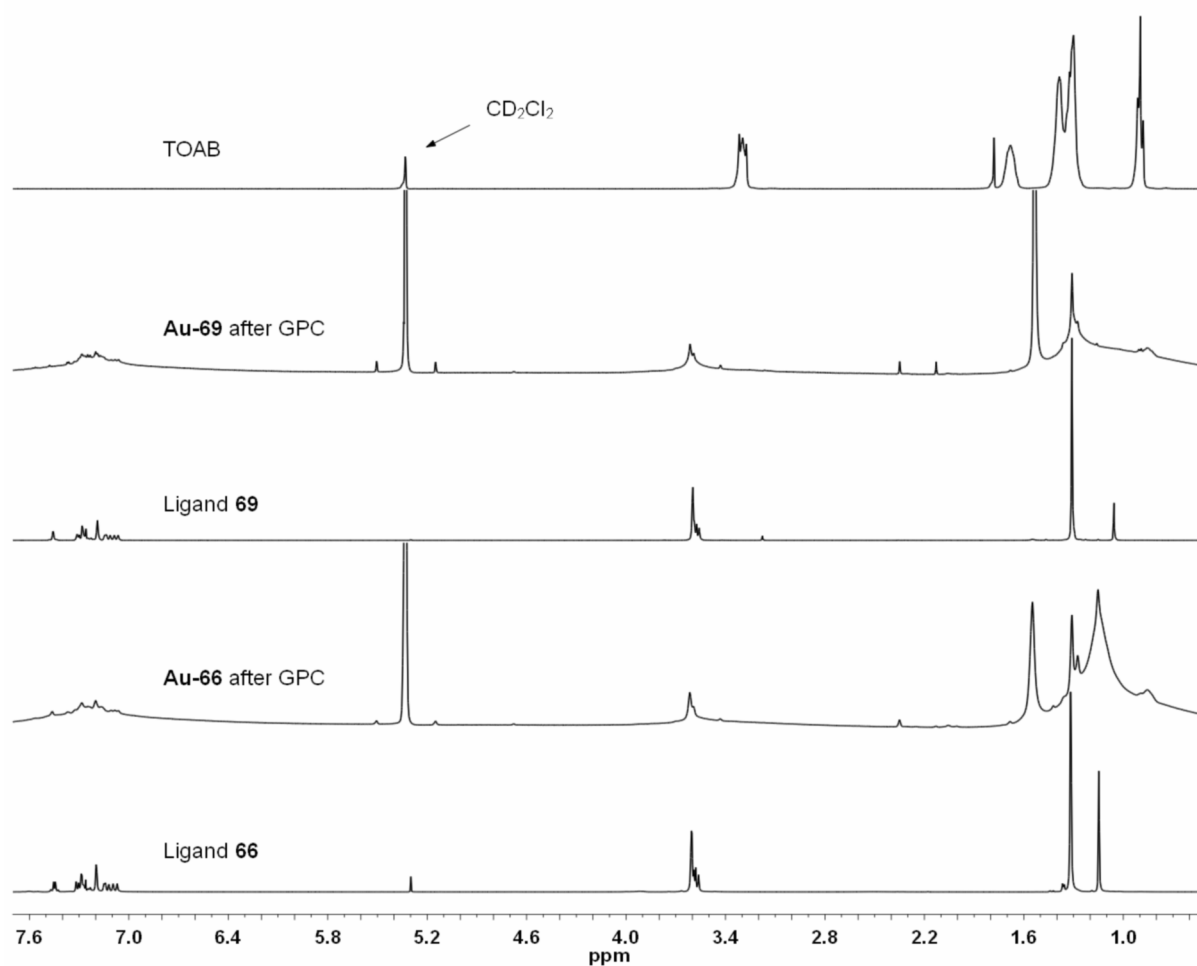


Figure 46. ^1H NMR spectra of **Au-66** and **Au-69** on comparison with the spectra of the pure ligands **66** and **69** and pure TOAB.

Nanoparticle Sizes and Size Distributions

To investigate the size distribution of the formed particles, TEM was performed with **Au-62**, **Au-66**, **Au-67** and **Au-69** after purification by GPC on carbon coated copper grids (Figure 47). In the normal TEM mode, positive images are obtained initially in contrast to the negative images that were obtained by HRSTEM for the unfunctionalized **Au-24 - Au-27** nanoparticles (*vide supra*). Similarly, the contrast of these pictures was used for the determination of the precise size of the gold cores. As displayed in Figure 48, very comparable and rather narrow particle size distributions were obtained for the TIPS acetylene particles **Au-62**, **Au-66** and **Au-67**, with a majority of particles with diameters between 1 and 1.1 nm and with standard deviations of around 0.2 nm. Similar results were obtained for the free acetylene particles **Au-69**. In these cases some aggregates of nanoparticles can be found in the TEM micrographs. Such aggregates were not found with the TIPS protected particles **Au-62**, **Au-66** and **Au-67**.

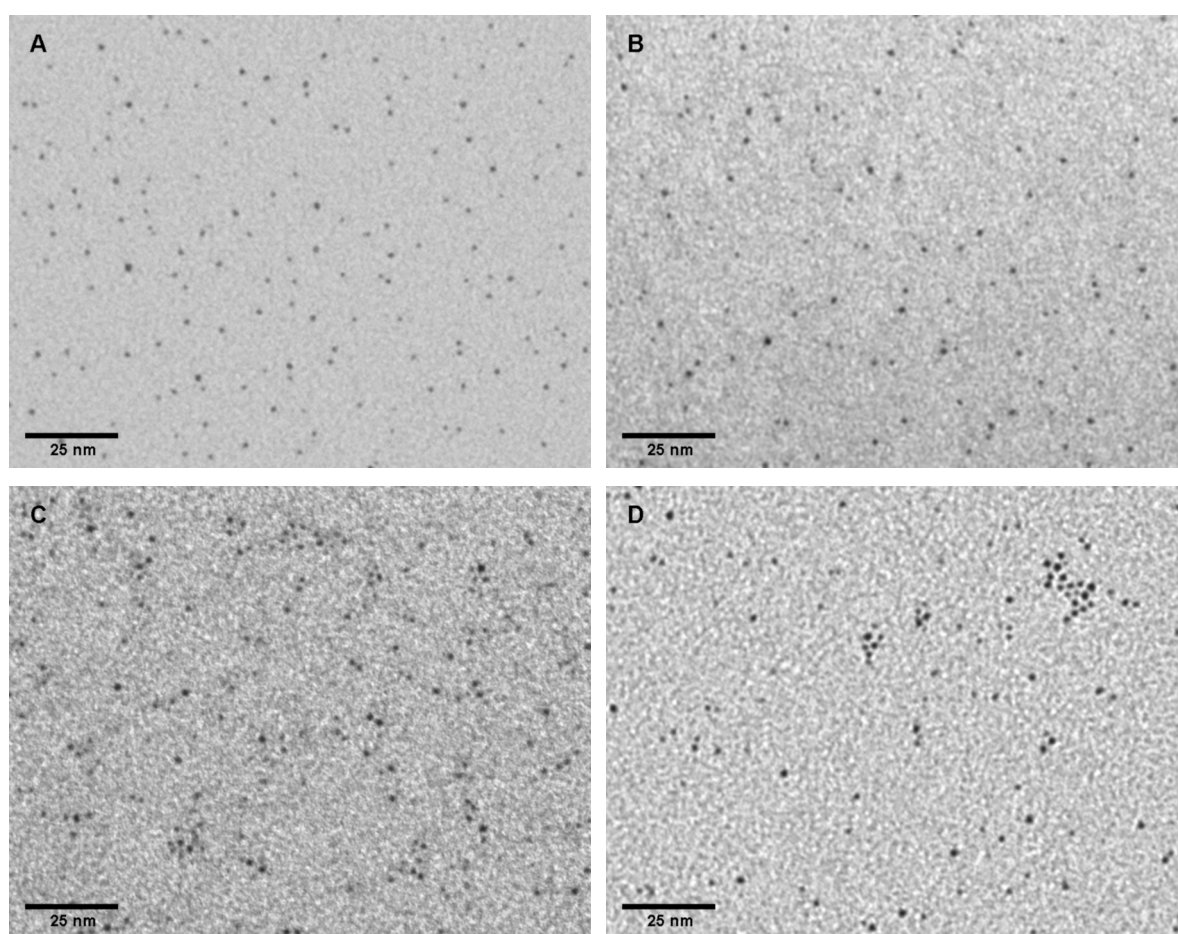


Figure 47. Representative TEM micrographs of **Au-62** (A), **Au-66** (B), **Au-67** (C) and **Au-69** (D). TEM micrographs of larger areas of the TEM grids can be found in the appendix.

As can be seen in the size distribution histograms (Figure 48), a small population of larger particles up to 2 nm can be found. However, coagulation of particles to a population with larger core sizes as was the case for the unfunctionalized **Au-27** particles was not observed. This can probably be attributed to the improved preparation procedure for the functionalized gold nanoparticles that avoids increased temperatures for the evaporation of solvents. Even though within the experimental error, there seems to be a slight trend towards a smaller average particle size with increasing length of the functionalizing OPE rod. Even more interesting is the marginal narrowing of the size distribution and thus increasing the ‘monodispersity’ of the **Au-67** particles which are functionalized with the longest OPE rod. These findings were attributed to the increased steric repulsion from the bulky TIPS protected functional units. This assumption is further supported by the direct comparison of the TIPS protected **Au-66** and the free acetylene **Au-69** particles. The **Au-69** particles that do not carry the protecting group were found to be slightly bigger than the **Au-66** particles.

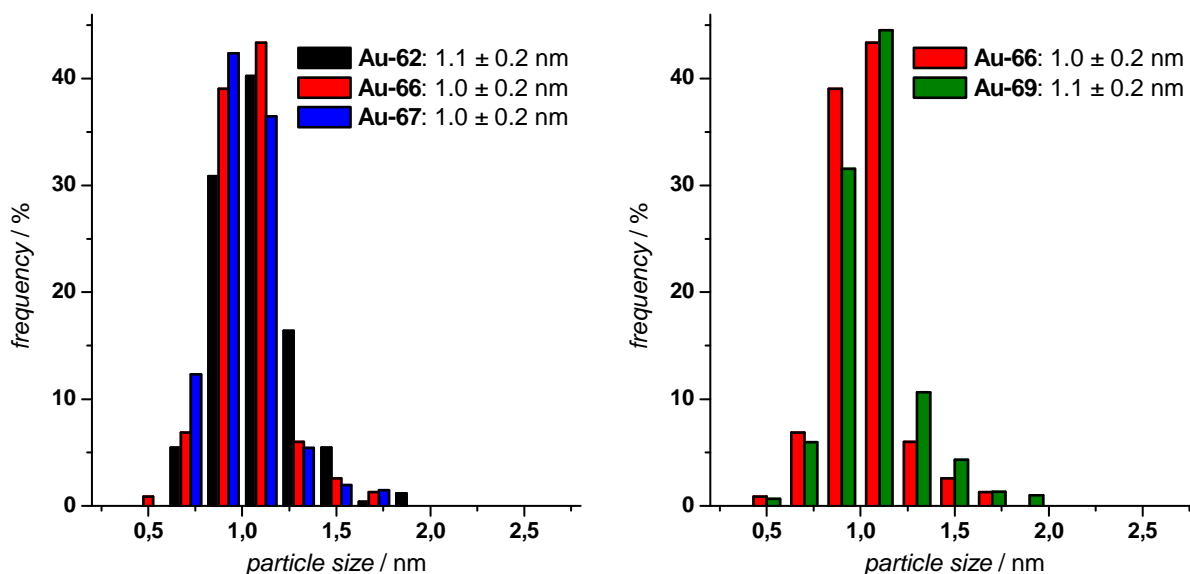


Figure 48. Comparison of the size distributions of **Au-62**, **Au-66** and **Au-67** TIPS acetylene functionalized nanoparticles (left) and of **Au-66** with the free acetylene **Au-69** nanoparticles (right).

Thermogravimetric Analysis

For the investigation of the ligand/nanoparticle ratios, thermogravimetric analysis (TGA) was performed with the **Au-62**, **Au-66** and **Au-67** nanoparticles. The analysis was made with a heating rate of 10°C/minute in a temperature range between 50 and 950°C. The shapes of the obtained curves are in all cases very similar with three horizontal steps starting at around 175°C, 260°C and 420°C (Figure 49).

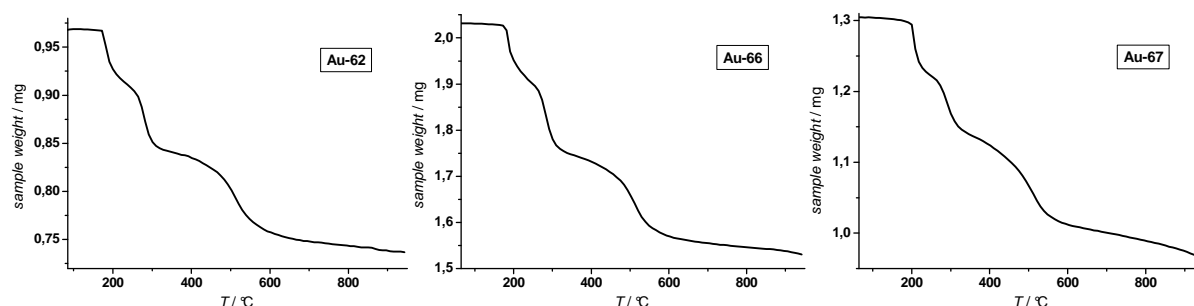


Figure 49. Weight loss diagrams of **Au-62**, **Au-66** and **Au-67**.

The observed weight losses between the start and the end temperatures were between 25 and 27%. If the complete removal of organic material from the gold surface is assumed, 25 – 27 gold atoms can be calculated to be present per functional thioether ligand. By assuming a spherical shape of the **Au-62**, **Au-66** and **Au-67** nanoparticles and by taking the density of bulk gold, one 1.1 nm gold nanoparticle consists of 42 gold atoms. Based on these data it can be assumed that the smallest nanoparticles with diameters below 0.9 nm are stabilized by a single heptameric thioether ligand, while the main fraction of **Au-62**, **Au-66** and **Au-67** nanoparticles with diameters between 0.9 and 1.2 nm is stabilized by two or three ligands per particle. Thereby these results show that mainly nanoparticles with a small number of functionalities were obtained. These observations parallel nicely the results that were obtained for the unfunctionalized **Au-27** particles (*vide supra*). However, a continuing decrease of sample mass can be observed in all cases between 600 and 950°C. It is therefore possible that not all of the organic material was removed in the observed temperature range.

In general, the gold nanoparticle stabilizing properties of the acetylene functionalized heptamer ligands **62**, **66**, **67** and **69** are very similar to the unfunctionalized ligand **27**. This includes similar particle diameters and nanoparticle surface coverages by the thioether ligands

as well as similar dispersibilities of the nanoparticles stabilized by the different functionalized and unfunctionalized heptameric thioether ligands. The nanoparticle sizes and main properties can therefore be controlled by the thioether ligand part while the functional unit of the ligand molecule provides the synthetic accessibility of the nanoparticles.

In contrast to the **Au-27** nanoparticles, no bimodal size distributions were found for the acetylene functionalized **Au-62**, **Au-66**, **Au-67** and **Au-69** nanoparticles after removal of the phase transfer agent TOAB. This suppression of nanoparticle coagulation can probably mainly be attributed to the improved nanoparticle preparation and purification procedures that avoid elevated temperatures.

3.3.4 Diacetylene Interlinked Nanoparticle Superstructures

With the OPE functionalized **Au-62**, **Au-66** and **Au-67** nanoparticles in hand, the ability of surface functionalized gold nanoparticles as 'artificial molecules' processable by wet synthetic chemistry was demonstrated by interlinkage of the nanoparticles using the acetylene functionality. The length of the rigid rod interparticle spacer should thereby determine the interparticle spacing in the linked nanoparticle superstructures.

As most direct chemical tool to interlink acetylene functionalized gold nanoparticles, oxidative diacetylene formation of terminal alkynyl groups was chosen. The diacetylene link is as rigid as the OPE functional units and can therefore provide the desired rigid nanoparticle linker (Figure 50). Furthermore, the diacetylene linked OPE structures have an increased conjugation length compared to the unreacted OPE units, which is traceable by UV/vis.

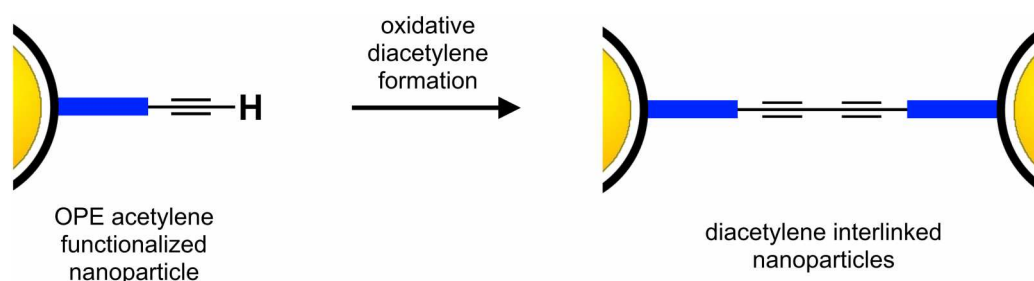
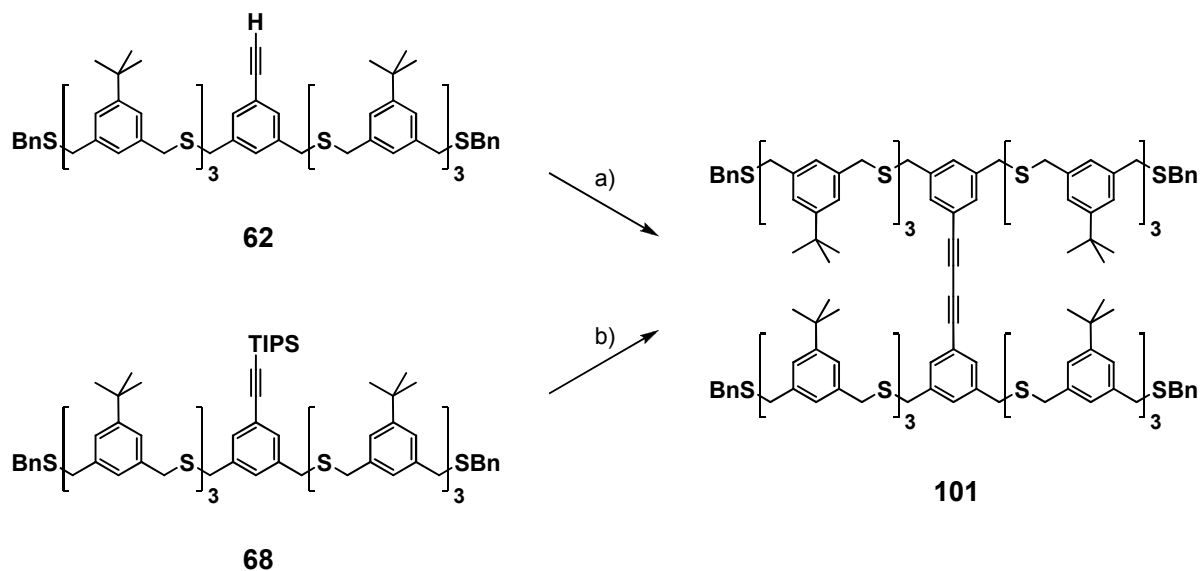


Figure 50. Schematic representation of the formation of diacetylene interlinked nanoparticles from OPE acetylene functionalized thioether coated nanoparticles. The thioether ligands are represented in black, while the functional OPE units are drawn as blue bars.

Numerous catalytic protocols for the homocoupling of terminal acetylenes have been reported.^[215] Recently, very mild palladium catalyzed coupling reactions gained some attention.^[276-279] As palladium black particles that could interfere with the employed analytical tools might be formed during the coupling reaction, more classical copper catalyzed protocols appeared to be more interesting. However, the increased temperature and the polar ethanol as solvent disqualified the original Glaser conditions.^[280,281] The same is true for the coupling conditions in hot pyridine that were reported by Eglinton and Galbraith.^[282] In particular heating has to be avoided to maintain the ligand coating and the particle sizes during the coupling reaction. Even chemisorbed thiolates can desorb from gold surfaces at temperatures as low as 100°C.^[283] Sulfides on the other hand do only physisorb on gold surfaces,^[135,161,284-286] and the stability of sulfide monolayers on gold is therefore rather weak.^[287] In order to test these assumptions, the unfunctionalized **Au-27** particles were heated to 55°C in pyridine, corresponding to the Eglinton conditions. This procedure led to coagulation of the particles as was evidenced by a color change to red and the formation of a black precipitate within 1 hour, pointing at the limited stability of the particles coated with such heptameric ligands. A mild alternative are the coupling conditions that were developed by Hay, who performed oxidative acetylenic couplings with oxygen in the presence of catalytic amounts of the bidentate ligand *N,N,N',N'*-tetramethylethylenediamine (TMEDA) and copper(I) chloride.^[288] The major advantage of this method is the enhanced solubility of the reactive species, which allows the coupling reaction to proceed satisfactorily at room temperature in various organic solvents.

To investigate the suitability of the envisaged conditions for the interlinking of acetylene functionalized gold nanoparticles, the chemistry was first studied with the free alkyne ligand **68** in small scale (Scheme 42). To a solution of **68** in CH₂Cl₂ was thus added TMEDA (2.5% v/v), followed by copper(I) chloride (CuCl). The homogenous mixture was stirred vigorously in an open reaction vessel to allow for the reaction with oxygen (Scheme 42). After 15 minutes, **68** was completely consumed and the diethyne **101** was formed, as was shown by TLC, UV/vis spectroscopy and ¹H NMR spectroscopy. The copper ions and the TMEDA were efficiently removed in a work up procedure with aqueous ammonium chloride. However, due to the partial aggregation that was observed with the free acetylene particles **Au-69** (*vide supra*), the TIPS protected particles **Au-62**, **Au-66** and **Au-67** were used for the preparation of nanoparticle superstructures. It was therefore investigated whether the interlinking procedure can be facilitated by combining the deprotection procedure and the coupling step in a one-pot protocol. Indeed, the TIPS protected ligand **62** was readily converted to the diethyne derivative **101** in CH₂Cl₂ after addition of TBAF in wet THF,

followed by TMEDA and CuCl one hour later (Scheme 42). Similarly, the diethynes of the TIPS acetylene ligands **66** and **67** were obtained in small scale test reactions.



Scheme 42. Dimerization of **62** and **68**. a) CuCl, TMEDA, air, CH₂Cl₂, RT;
b) 1. TBAF, CH₂Cl₂, RT; 2. TMEDA, CuCl, air, RT.

To investigate the stability of the nanoparticles coated by heptameric thioether ligands and also for comparison with coupling experiments of acetylene functionalized nanoparticles, these one-pot reaction conditions were applied to the unfunctionalized **Au-27** particles. The particles were investigated by UV/vis spectroscopy as well as TEM and no differences were found after 1 hour under these conditions compared to as prepared **Au-27**. This shows the good stability of these thioether ligand coated particles under such reaction conditions.

Similar one-pot deprotection/Hay reaction conditions were then applied to the TIPS acetylene functionalized gold nanoparticles **Au-62**, **Au-66** and **Au-67**. The particles were thus dispersed in CH₂Cl₂ and solutions of TBAF in wet THF were added. After stirring at room temperature for 1 hour, TMEDA (2.5% v/v) and copper(I) chloride were added and the mixtures were stirred vigorously in open reaction vessels. In the case of the **Au-62** particles comprising the shortest acetylene unit, the formation of a black precipitate *ca.* 1.5 hours after the addition of CuCl was observed. In the other two cases **Au-66** and **Au-67** with longer OPE rods, a black precipitate formed immediately after the addition of the copper salt, leaving the liquid phases nearly colorless. Importantly, such precipitations were not observed when the unfunctionalized **Au-27** particles were subjected to similar reaction conditions. Furthermore, the direct addition of TMEDA and copper(I) chloride to CH₂Cl₂ dispersions of the TIPS protected

Au-62, **Au-66** and **Au-67** particles did also not lead to the formation of precipitates. However, when these oxidative coupling conditions were applied directly to the free acetylene particles **Au-69**, precipitation did occur as well. These observations strongly point at the formation of diacetylenes as the reason for nanoparticle aggregation and precipitation. Coagulation of nanoparticles would also be accompanied by a color change to red, as was observed with the nanoparticles stabilized by the monomeric ligand **24** (*vide supra*).

UV/vis Investigations

The hypothesis is further supported by the UV/vis spectra of the remaining colored dispersions of the one-pot deprotection/coupling reactions with **Au-62**, **Au-66** and **Au-67**. In the absorption region between wavelengths of 400 and 800 nm, the electronic spectra resemble exactly the spectra of the particles before the reaction (Figure 51).

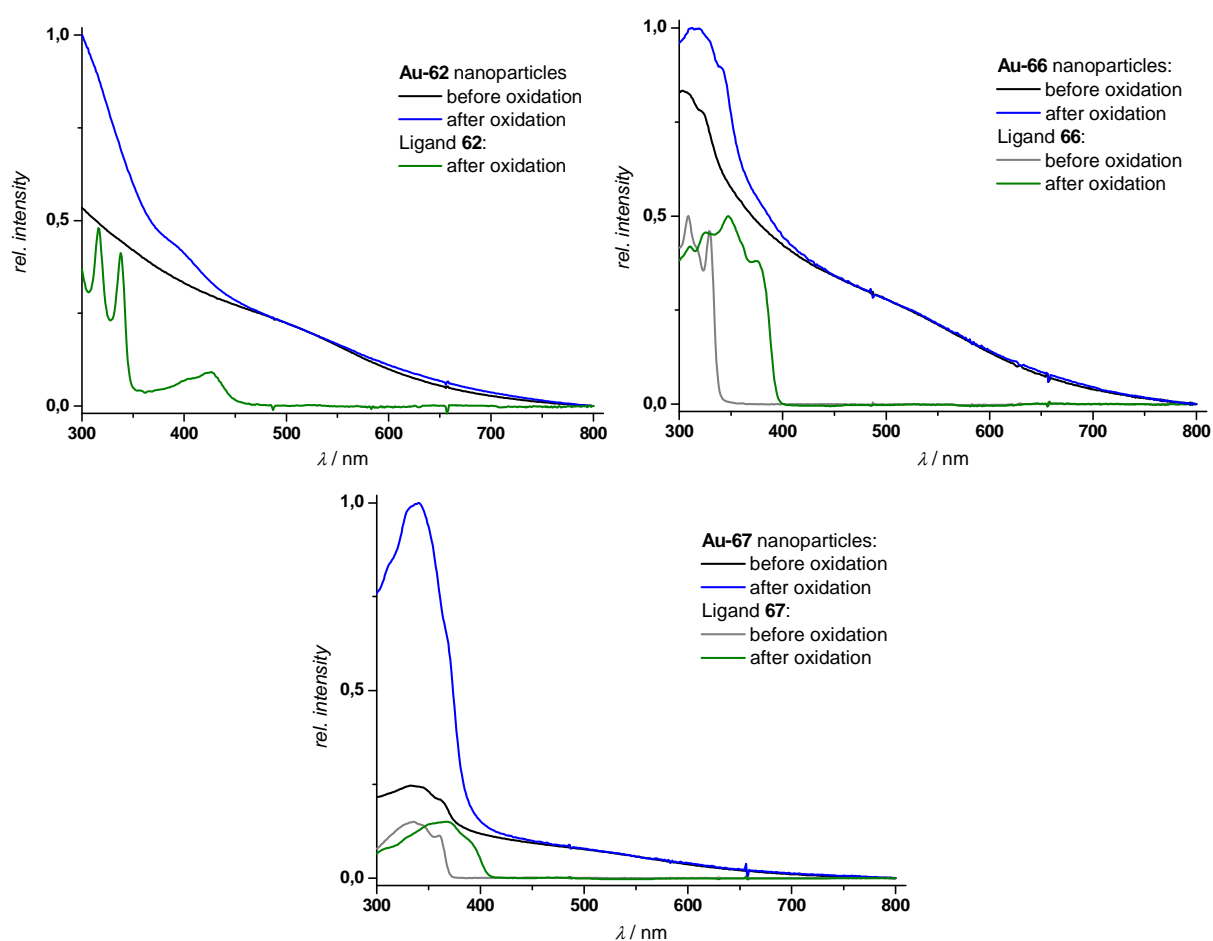


Figure 51. UV/vis absorption spectra (CH_2Cl_2) of **Au-62**, **Au-66** and **Au-67** before and after the deprotection/Hay procedure.

As was pointed out before, the absence of a plasmon resonance centered at 520 nm shows that the gold nanoparticles did not coagulate to particles with diameters larger than 2 nm.^[181] At wavelengths below 400 nm, a red shift of the OPE bands was observed in all cases compared to the TIPS protected particles **Au-62**, **Au-66** and **Au-67**. Comparison with the free ligands **62**, **66** and **67** and the respective diacetylene dimers clearly shows the presence of the diacetylenes in the different reaction mixtures, as similar shifts of the absorption edges towards longer wavelengths were found. The striking similarity of the shifts observed during the transition from the coated particles to nanoparticle aggregates corroborates the interlinking of the particles by oxidative acetylene coupling as the chemical process forming these precipitating aggregates.

TEM Investigations and Discussion

The reaction products of the one-pot deprotection/Hay conditions were investigated by TEM. The reaction mixtures were therefore highly diluted with CH₂Cl₂ and then directly transferred onto carbon coated copper grids. As can be clearly seen in the TEM micrographs, the gold nanoparticles retain their integrity and do not coagulate to larger particles in all cases (Figure 52). This parallels the results obtained by UV/vis spectroscopy. Obviously, these particles form large aggregates of nanoparticles that lie flat on the carbon surface of the TEM grid. This also points at interlinking of the **Au-62**, **Au-66** and **Au-67** particles by diacetylene formation, as such clusters were not observed when the unfunctionalized nanoparticles **Au-27** were exposed to the same procedure. Similar nanoparticle aggregates were already observed to some extent on TEM grids of the free acetylene nanoparticles **Au-69** (*vide supra*). The fact that these aggregates of particles are lying flat on the surface is supporting the hypothesis of a low number of functional groups per particle, as otherwise the formation of 3 dimensional networks would be expected.

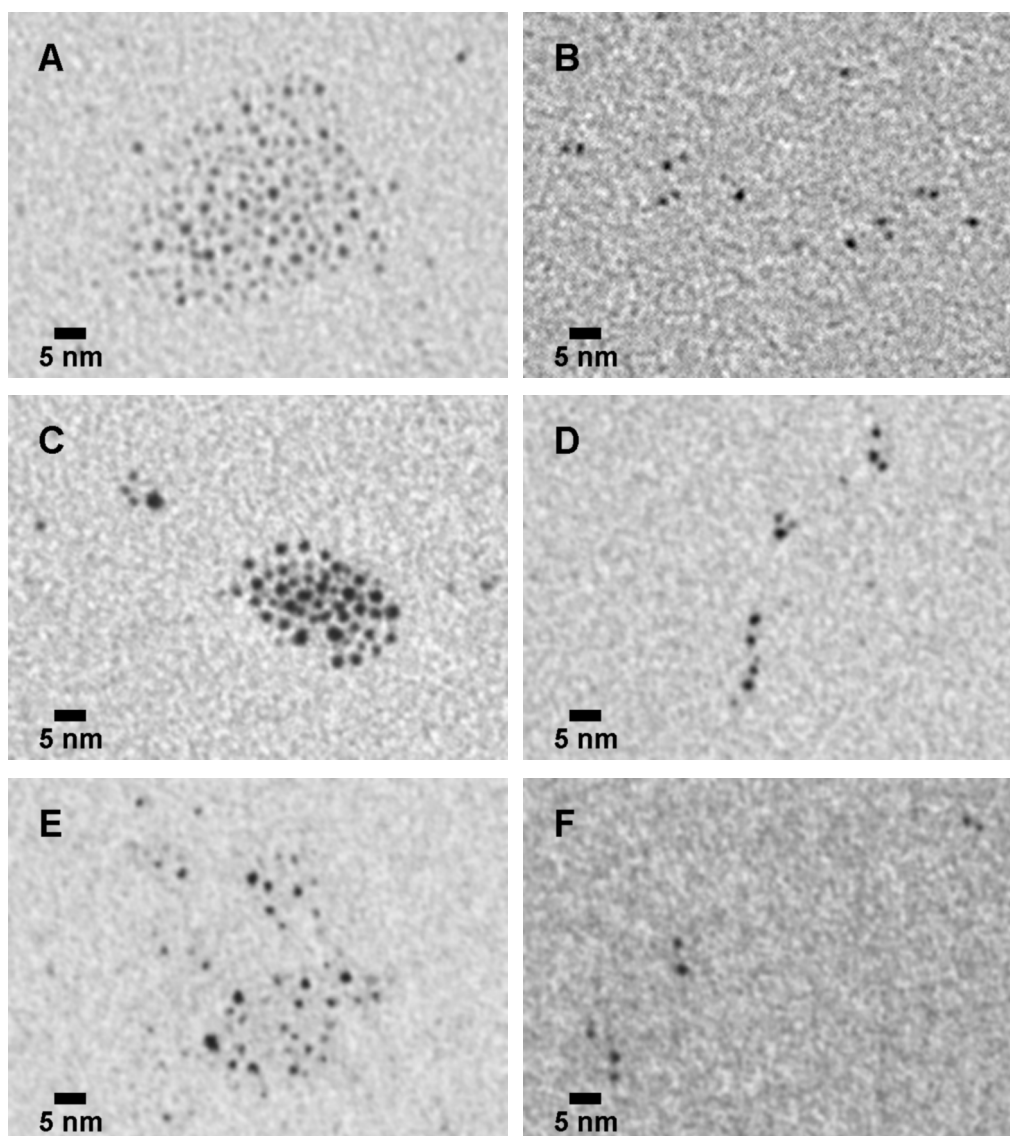


Figure 52. Representative TEM micrographs of $(\text{Au-62})_n$ (A), $(\text{Au-62})_{2-4}$ (B), $(\text{Au-66})_n$ (C), $(\text{Au-66})_{2-4}$ (D), $(\text{Au-67})_n$ (E) and $(\text{Au-67})_{2-4}$ (F). TEM micrographs of larger areas of the can be found in the appendix.

By direct comparison of the nanoparticle aggregates comprising the shortest acetylene linker $(\text{Au-62})_n$ and the aggregates of the particles with the longest OPE rod $(\text{Au-67})_n$, the higher density of the $(\text{Au-62})_n$ aggregates becomes evident (Figure 52). This is in good agreement with the expectation for covalently linked nanoparticle superstructures, as the interparticle distance should vary with the length of the rigid spacer between the heptameric ligand and its functional acetylene moiety in the series **62**, **66** and **67**. Quantification of the different interparticle distances is however not possible from the large aggregates. A considerable fraction of neighboring particles in the deposited clusters are probably not covalently linked but only separated by the steric repulsion of their coating ligand as an effect of the arranging of the interlinked network during deposition on the flat substrate.

To remove the large nanoparticle aggregates as well as the copper ions and the TMEDA present in the reaction mixture, the acetylenic coupling reactions with **Au-62**, **Au-66** and **Au-67** were subjected to an aqueous work up procedure 15 minutes after the addition of copper(I) chloride. The mixtures were thus diluted with CH_2Cl_2 and then extracted twice with an aqueous ammonium chloride solution. The organic phases were then dried over magnesium sulfate and filtrated. The dispersion of the **Au-62** particles after this procedure was strongly colored, indicating the presence of relatively large amounts of dispersed gold nanoparticles. This dispersion was strongly diluted before the transfer to a carbon coated TEM grid. On the other hand, due to the aggregation of most of the material, the dispersions that were obtained from the oxidative coupling reactions of **Au-66** and **Au-67** were nearly colorless. These dispersions were applied directly to TEM grids.

Inspection of the TEM micrographs after the work up procedure revealed small superstructures like nanoparticle dimers, trimers or other small oligomers as the origin of the remaining color of the dispersions of **Au-62**, **Au-66** and **Au-67** after the deprotection/Hay procedure. Also some unreacted single particles can be found (Figure 52). As the nanoparticle dispersions were highly diluted before the transfer to the TEM grids, the observed superstructures arise mainly from interlinked particles and were not formed by coincidence during deposition. Furthermore, such structures of nanoparticles were rarely found by TEM investigations of unreacted thioether coated nanoparticles.

However, as two acetylene functional groups were expected to be present per nanoparticle, the complete oxidative coupling would lead solely to polymeric nanoparticle structures. An incomplete removal of the TIPS protecting group might account for the presence of single particles and small nanoparticle superstructures after the deprotection/Hay conditions as well as an incomplete diacetylene formation. Also, it cannot be ruled out that some nanoparticles are only stabilized by one functionalized thioether ligand or that two acetylene moieties situated on the same nanoparticle formed a diacetylene bond. Both processes can account for the formation of end-caps that stop the nanoparticle polymerization process. TEM does only allow to investigate the gold cores and not the organic coating, this method is therefore not suitable to unambiguously distinguish between the different processes discussed.

The small nanoparticle superstructures that were observed after the aqueous work up of $(\text{Au-62})_n$, $(\text{Au-66})_n$ and $(\text{Au-67})_n$ are ideally suited to read out the interparticle spacing mainly for two reasons. First, due to their low dimensionality, the interlinked structure can be

expected to lay parallel to the substrate surface. And second, contributions from non-covalently linked nanoparticle superstructures can be neglected.

The interparticle distances of the reacted acetylene functionalized nanoparticles **Au-62**, **Au-66** and **Au-67** were thus measured from the TEM micrographs after aqueous reaction work up. Only small nanoparticle superstructures $(\text{Au-62})_n$, $(\text{Au-66})_n$ and $(\text{Au-67})_n$ with $1 < n < 5$ were used for this investigation to minimize the contribution of incidentally formed neighboring particles. Larger nanoparticle aggregates were in any case only rarely found in the TEM micrographs that were obtained after the work up procedure. For the same reason, only nanoparticle pairs with a spacing below the theoretical maximum length of the diacetylene linked OPE spacers (1.2 nm for $(\text{Au-62})_{2-4}$, 2.6 nm for $(\text{Au-66})_{2-4}$ or 3.7 nm for $(\text{Au-67})_{2-4}$) were considered. As the largest of the measured dispersible nanoparticle superstructures after aqueous work up and filtration comprise four nanoparticles, this number is assumed to separate between aggregates $(\text{Au-X})_n$ and superstructures $(\text{Au-X})_{2-4}$. These terms will be used throughout this thesis for reasons of simplicity, even if the boundary between large aggregates and small superstructures is probably not that sharp.

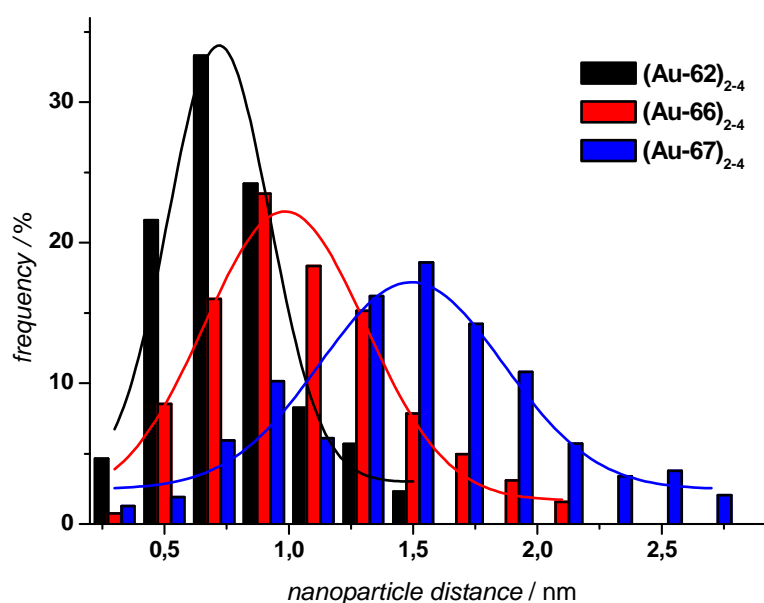


Figure 53. Interparticle distance distributions of nanoparticle superstructures $(\text{Au-62})_{2-4}$, $(\text{Au-66})_{2-4}$ and $(\text{Au-67})_{2-4}$. The Gaussian fits were included for a better visibility of the trend found.

For the three hybrid systems, almost Gaussian interparticle distance distributions were observed (Figure 53). The maxima were found to be at about 0.8 nm for $(\text{Au-62})_{2-4}$, 1.0 nm for $(\text{Au-66})_{2-4}$ and 1.6 nm for $(\text{Au-67})_{2-4}$. The distributions were leveling off towards the theoretical maximum of the different linkers respectively. A perfect correlation between the

observed particle spacing and the increasing length of the rigid linkers was therefore found, further corroborating the formation of covalently interlinked nanoparticles as the origin of the hybrid superstructures. A closer examination of the interparticle distances of **(Au-62)**₂₋₄, **(Au-66)**₂₋₄ and **(Au-67)**₂₋₄ reveals a broadening of the distance distribution rather than just a shift to longer distances for the elongated rigid diacetylenes in **(Au-66)**₂₋₄ and **(Au-67)**₂₋₄. Furthermore, the observed values for the interparticle distances are considerably shorter than the full stretched theoretical length of the rigid OPE linkers. However, the central benzene units of the ligands where the functional linkers are attached are likely to adopt a tilted arrangement with respect to the nanoparticle surface due to the steric repulsion between the hydrogen atom *para* to the OPE unit and the nanoparticle surface (Figure 54). These shorter interparticle distances are therefore not surprising. The very narrow interparticle distance distribution that was found for **(Au-62)**₂₋₄ probably reflects the increased steric repulsion provided by the sterically demanding *t*-butyl groups of the thioether ligand. Due to the short functional acetylene spacer in **62**, a less tilted arrangement of the footing central benzene unit is probably induced, while the proximity of the second particle becomes less important for both longer members of the series **(Au-66)**₂₋₄ and **(Au-67)**₂₋₄.

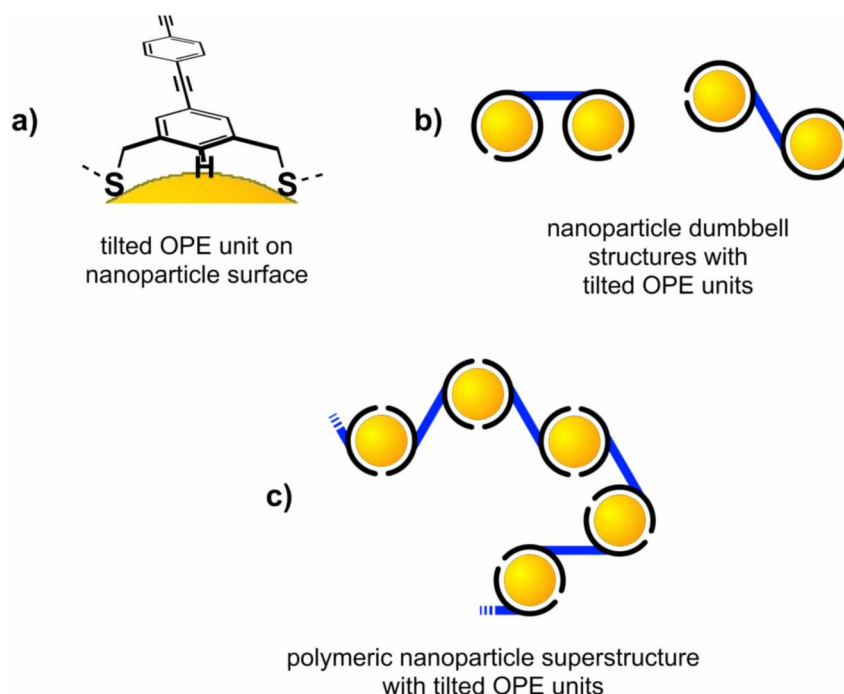


Figure 54. Schematic representations of a) the tilted arrangement of the OPE functional unit relative to the surface of a gold nanoparticle and the consequences of such an arrangement on b) dumbbell or c) linear nanoparticle superstructures. The thioether ligands are represented in black, while the functional OPE units are drawn as blue bars.

Another interesting feature was observed in the distance distribution solely for **(Au-67)₂₋₄**. At a distance about 1 nm, a second minute maximum was found. This might be attributed to the formation of direct acetylene-gold bonds (Figure 55), as have already been reported by Gorman and coworkers.^[222] The particles functionalized with both shorter acetylenes **Au-62** and **Au-66** either do not allow for this type of nanoparticle-nanoparticle interaction due to steric repulsion or the shorter interparticle distances originating from the direct acetylene-gold interaction cannot be observed in the distance histograms as a result of relatively small distance differences for the two binding modes.

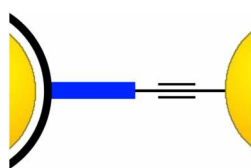


Figure 55. Schematic of the direct acetylene-gold interlinkage of OPE-thioether stabilized gold nanoparticles. The thioether ligand is represented in black, while the functional OPE unit is drawn as blue bars.

Steric repulsion might also be the reason for the considerably slower formation of precipitating aggregates of **(Au-62)_n** compared with the particles **Au-66** and **Au-67** comprising larger distances between the nanoparticle surface and the functional acetylene unit. The alkyne function of the thioether ligand **62** with the short OPE unit is close to the ligand crowded nanoparticle surface in the case of **Au-62**, which impedes the reaction between two nanoparticles and even more the reaction of an already large nanoparticle aggregate and a nanoparticle. The longer OPE units of **Au-66** and **Au-67** are much more accessible and the oxidative diacetylene formation is therefore much faster. These considerations also imply that the observed formation of small nanoparticle superstructures such as dimers or trimers could be to a large extent due to unreacted free acetylenes. However, deceleration of the deprotection process of the TIPS groups due to sterical hindrance cannot be ruled out and might also contribute to the slow formation of precipitating aggregates during the deprotection/coupling reaction of **Au-62**. Also, some acetylene monofunctionalized gold nanoparticles might be present, which can stop the polymerization process.

These investigations with the acetylene functionalized gold nanoparticles **Au-62**, **Au-66** and **Au-67** clearly show the feasibility of the concept to selectively functionalize gold nanoparticles by large thioether ligands. It was also shown that these particles can become

suitable building blocks for wet chemistry. The increasing levels of complexity emerging from the organic ligand molecule are depicted schematically for the heptameric thioether ligand **66** in Figure 56. Gold nanoparticles **Au-66** were formed in good monodispersity with the ligand **66** as stabilizing agent. In average, these particles are coated by two functionalized ligands. As this is an average calculated amount, particles stabilized by three or more ligands cannot be excluded. By a one-pot deprotection/oxidative coupling procedure, mainly chains of covalently interlinked gold nanoparticles (**Au-66**)_n are provided. Long, folded chains form precipitating aggregates (n>4), while smaller discrete hybrid superstructures (n=1-4) remain in dispersion.

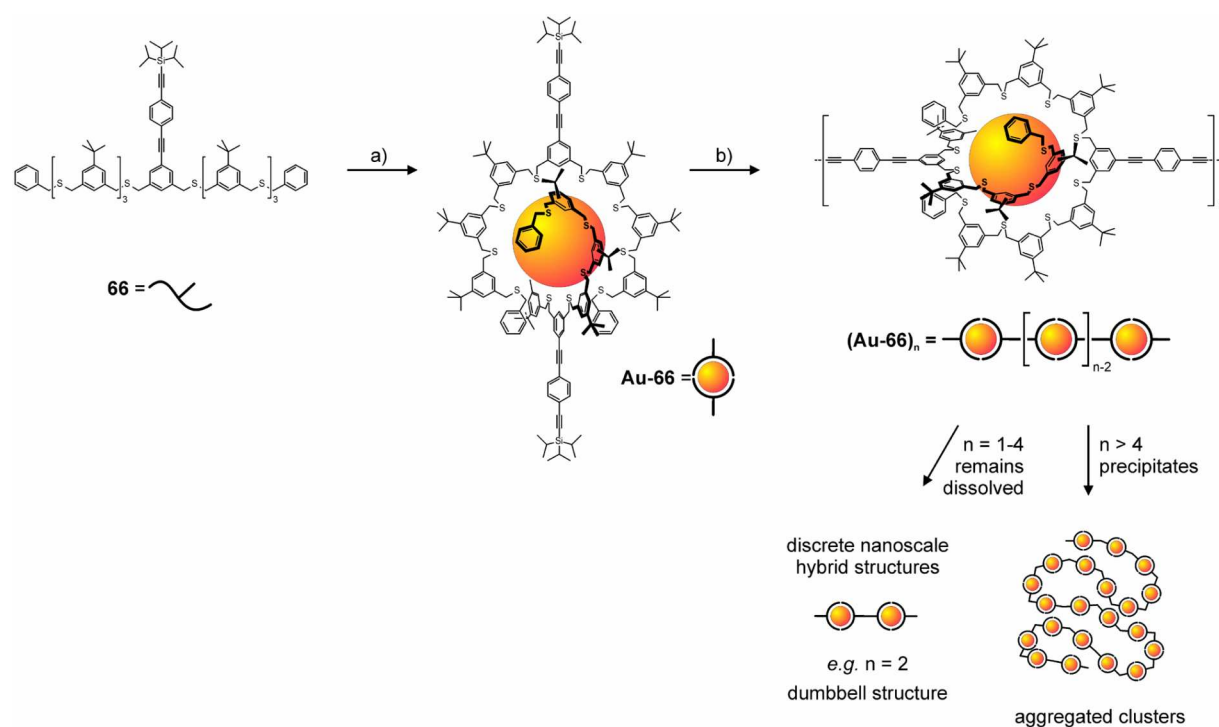


Figure 56. Increasing levels of structural complexity emerging from the ligand **66**. a) The thioether heptamer stabilizes gold particles of a given size and a low number of ligands at its surface (reaction conditions: HAuCl_4 , TOAB, NaBH_4 , $\text{CH}_2\text{Cl}_2/\text{H}_2\text{O}$; GPC.) b) Deprotection of the acetylene enables the formation of organic/inorganic hybrid chains by oxidative acetylene coupling (reaction conditions: 1. TBAF in CH_2Cl_2 , RT; 2. TMEDA, CuCl , RT). While longer chains aggregate and precipitate, short hybrid superstructures comprising up to approximately four interlinked particles remain in dispersion.

3.3.5 Summary and Conclusions

The synthetic methodology for the highly modular formation of monofunctionalized thioether ligands was developed. In particular, the monothiol trimer **36** as thioether ligand building block was synthesized efficiently. This building block allows for the formation of monofunctionalized thioether ligands based on the structure of the heptamer thioether ligand **27**, which was effectively used for the formation and stabilization of gold nanoparticles. Furthermore, the iodo-dihydroxide **49** was found to be a versatile starting material for the formation of functionalized modules that allow the easy synthesis of monofunctionalized thioether ligands. The iodo moiety allows for the introduction of different functionalities such as OPE units or azides, which can be used for the formation of selectively surface functionalized gold nanoparticles. Similarly, efficient synthetic methods for the preparation of functionalized thioether ligands for electronic applications based on pyridine or thiophenol coupling units were developed.

OPE functionalized gold nanoparticles were prepared in high yields and could be used as building blocks for covalently interlinked nanoparticle superstructures by oxidative diacetylene formation. The interparticle spacing of small superstructures varies thereby with the length of the functional OPE unit of the stabilizing thioether ligand, showing the ability of functionalized thioether coated gold nanoparticles to act as 'artificial molecules' for wet chemistry processing. Furthermore, the results that were obtained with the different acetylene functionalized heptameric thioether ligands concerning the formation and stabilization of gold nanoparticles show that the control of the nanoparticle sizes is given by the thioether ligand parts of the molecules rather than the attached functional units.

3.4 Dendritic Thioether Ligands

This part deals with the investigation of the size steering properties of multidentate thioether ligands. The synthesis of thioether dendrons as modular building blocks for the preparation of monofunctionalized thioether dendrimers will be presented followed by studies on the nanoparticle stabilizing and coating properties of these dendritic molecules.

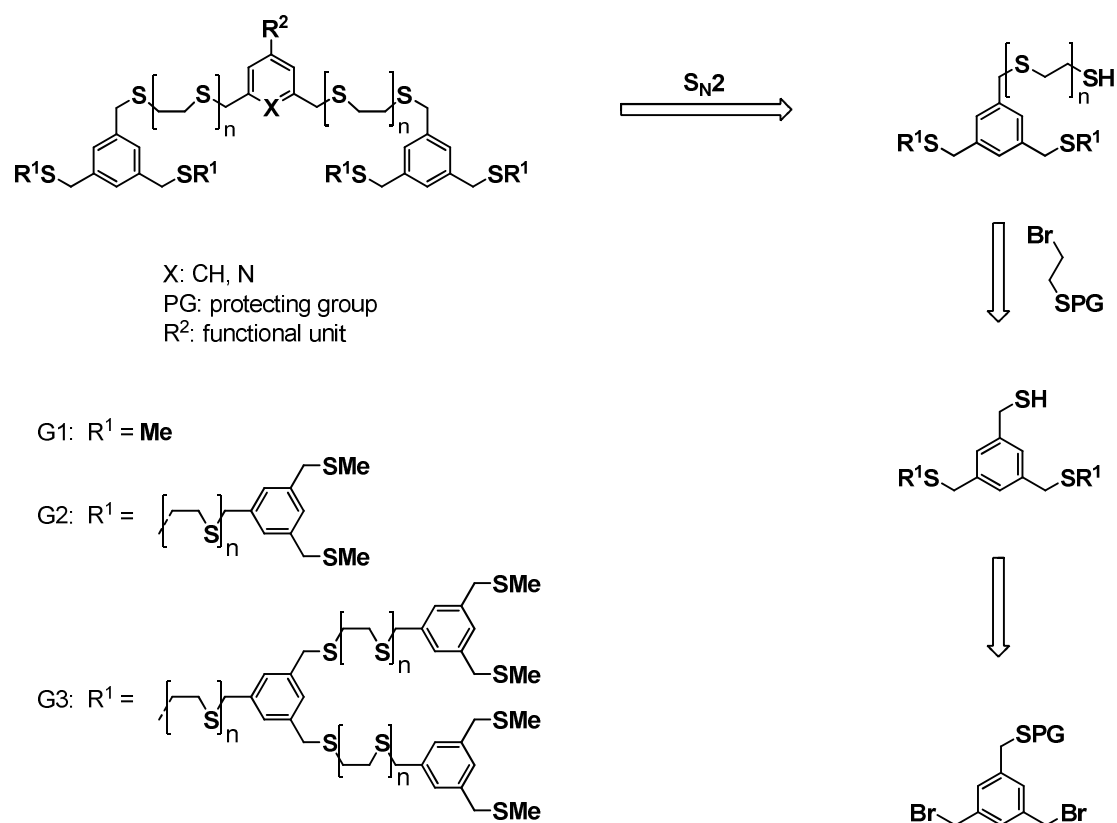
With regard to monofunctionalized gold nanoparticles coated by large thioether based ligands, linear ligand structures can hardly provide complete coverage of spherical nanoparticles by just one ligand. Due to their branched nature, much better nanoparticle surface coverage and also higher nanoparticle stability can be expected for dendritic thioether structures. The linear thioether ligands seem to control the sizes of the stabilized nanoparticles (*vide supra*). Even more control on the nanoparticle sizes could be provided by different generations of large dendritic thioether ligands.

Encapsulation of metal nanoparticles was mainly reported for poly(amidoamine) (PAMAM)^[289-291] or poly(propylene imine) (PPI)^[292,293] derived dendrimers so far. In these cases, the nanoparticles were formed directly by reduction of a metal salt in the presence of the respective dendrimer. The formed metal particles were however only stable in dispersion in the presence of excess dendrimer. Also, very broad size distributions were found for the PAMAM or PPI dendrimer stabilized nanoparticles. Except for the example from Vögtle and De Cola^[167] that was already discussed in section 0, dendrimers or dendritic structures based on sulfides have not been used for the formation and stabilization of nanoparticles. However, the sulfide dendrimers (*e.g.* **21** or **22**) that were used within this study were rather stiff and relatively small. Encapsulation of nanoparticles and therefore controlled functionalization would not be possible with such structures. Moreover, the stability of the sulfide dendrimer stabilized gold nanoparticles was reported to be very limited.^[167]

In general, only very few examples of thioether containing dendrimers or dendritic structures were reported in the literature. Most of these few examples are based on aryllic sulfides and form therefore stiff dendritic structures.^[167,294-296] Only one example was found where a dendrimer based on flexible benzylic thioethers was reported.^[297] In this case, the sulfides were used as intermediates for the formation of oligo(phenylenevinylene) dendrimers by dendrimer metamorphosis and not for the stabilization of gold nanoparticles.

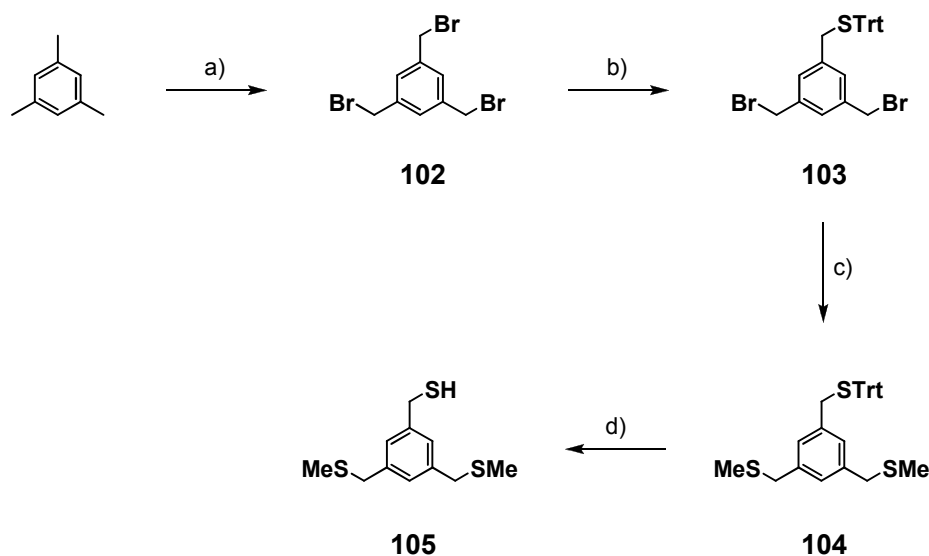
3.4.1 Synthetic Strategy and Synthesis

For the preparation of thioether coated nanoparticles, highly flexible dendritic structures were desired in order to have a system that can adapt to the curved nanoparticle surface and bind with all thioether moieties present in the ligand. A high degree of branching should also be avoided for similar reasons. On the basis of the structures that were reported by von Kiedrowski *et al.* for the phase-transfer synthesis of thioether stabilized Au₅₅ clusters,^[99,100] mesitylene based benzylic thioethers were chosen as lead structure for the formation of dendrimers for the coating of gold nanoparticles. To enlarge the distance between neighboring mesitylene branching units, flexible ethylene dithiol units were introduced. Thus, higher flexibility of the dendritic structures is assured. Furthermore, a theoretical study concerning thioether stabilized gold nanoparticles reported thioethers of such ethylene dithiol units as being very promising candidates for nanoparticle stabilization.^[298] Benzyl methyl sulfides were chosen as end groups of the dendrimers. The target dendritic structure is depicted in Scheme 43 together with the modular convergent synthetic strategy. This strategy does not only allow to freely alter the functional central unit, but also the number of ethylene dithiol subunits to adjust the spacing between two branching units.



Scheme 43. Retrosynthetic pathway for monofunctionalized thioether dendrimer ligands.

The literature known starting material 1,3,5-tris(bromomethyl)benzene^[299] (**102**) was prepared in one synthetic step starting from mesitylene by radicalic side chain bromination with NBS (Scheme 44). Methyl formate was used as solvent and AIBN as radical starter. After 6 hours illumination with a 500 W halogen lamp, the solvent was evaporated and an aqueous work up was performed. The crude was then recrystallized from CH₂Cl₂/hexane five times to yield the desired product as colorless crystals. The supernatants of the last three recrystallization procedures were combined and the solvent mixture was removed by evaporation. The residue was then recrystallized three times to yield more of the target compound **102**. After this procedure, the pure tribromide **102** was obtained in a good overall yield of 45% on a 40 g scale for this one step process. This is a very good result for this direct threefold side chain bromination of mesitylene, as this reaction was often reported to be very inefficient with isolated yields ranging between 2 and 30% due to the formation of a large number of side products.^[300-302] Methyl formate seems therefore to be more selective in this bromination reaction compared to the commonly used carbon tetrachloride. For comparison, the alternative route for the synthesis of 1,3,5-tris(bromomethyl)benzene (**102**) is starting from 1,3,5-benzenetricarboxylic acid and involves three synthetic steps.

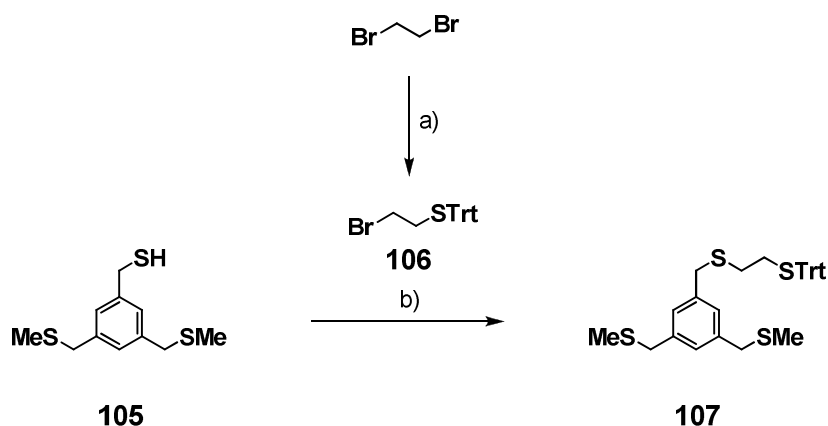


Scheme 44. Synthesis of **105**. a) NBS, AIBN, HCOOMe, hv, reflux, 45%; b) TrtSH, K₂CO₃, THF, reflux, 47%; c) NaSMe, DMF, RT, 90%; d) Et₃SiH, TFA, CH₂Cl₂, RT, 82%.

Monothiolation of **102** was achieved similar to the formation of the monobromide building block **4** (see section 3.1.1) by the use of one equivalent of the sterically demanding trityl thiol in refluxing THF with potassium carbonate as base. The desired dibromide **103** was isolated in 47% yield after purification by column chromatography. The starting material **102** was also

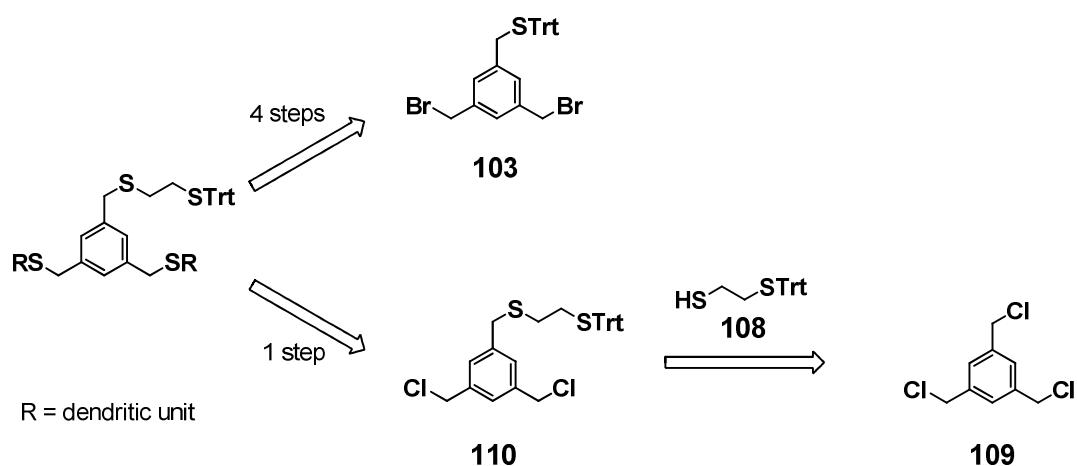
isolated and could be used again. The reaction of **103** with sodium methanethiolate in DMF provided then the end capped building block **104** in 90% yield after column chromatography. Under the acidic trityl deprotection conditions that were already used for the synthesis of the linear thioether ligands (*vide supra*) the monothiol **105** was formed efficiently in 82% yield (Scheme 44). Removal of the side products of the deprotection procedure was achieved by column chromatography.

The monobromo ethylene building block (2-bromoethyl)(trityl)sulfane^[124] (**106**) was synthesized starting from 1,2-dibromoethane according to a literature procedure^[124] in THF with sodium hydride as base. The monobromide was obtained quantitatively after an aqueous work up and was reacted with the monothiol **105** without further purification. The substitution reaction was carried out in dry THF with sodium hydride, to give the monoethylene starting generation (G0) dendron **107** as colorless oil in 85% yield. These initial results were very encouraging with respect to the envisaged synthetic pathway (Scheme 43).



Scheme 45. Synthesis of the G0 dendron **107**. a) TrtSH, NaH, THF, 0°C, quant.; b) NaH, THF, RT, 85%.

However, for a first investigation, the thioether dendrimers containing only one ethylene dithiol moiety per branching unit were envisaged. In order to save two synthetic steps for each generation synthesized, it seems reasonable to introduce the ethylene thiol unit before building up the next generation of the dendron (Scheme 46 bottom). This cannot be done directly from the branching monomer **103**, because deprotection of the benzylic thiol followed by conditions suitable to introduce the bromo ethylene block **106** would mainly lead to the formation of polymeric products by nucleophilic attack of the thiol to the benzylic bromides. It was therefore envisaged to introduce the monoprotected ethylene dithiol **108** directly to the trichloride **109**.



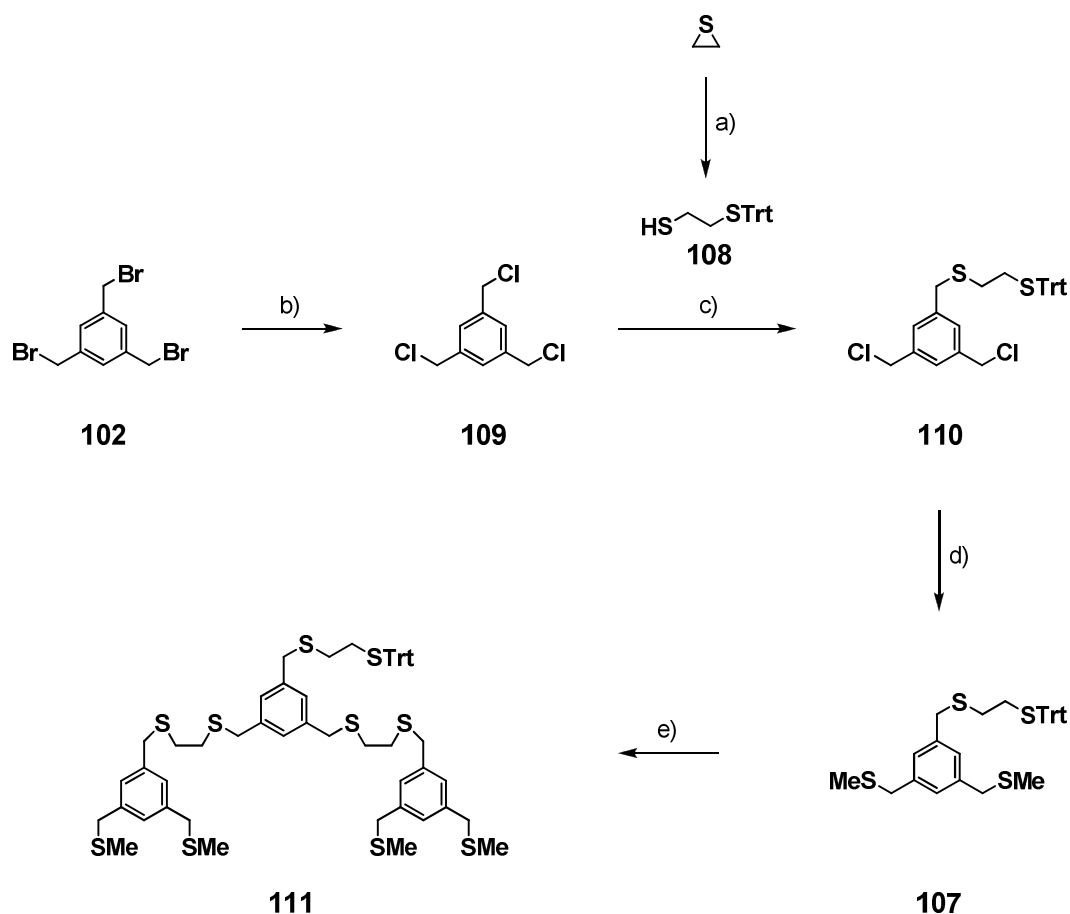
Scheme 46. Retrosynthesis of thioether dendrimers carrying only one ethylene dithiol moiety per branching unit.

1,3,5-tris(chloromethyl)benzene^[303] (**109**) was chosen for the synthesis of the branching unit **110** due to the low stability that was observed with compounds carrying sterically non-demanding sulfides and benzylic bromide leaving groups (see section 3.1.1). The branching unit **110** can then be reacted with the methyl sulfide end caps or the free thiol dendrons to form the trityl protected next generation. Only one synthetic step is required to form the next generation free thiol dendrons that are required for the synthesis of the functionalized thioether dendrimers carrying one ethylene linker per branching unit compared to three steps in the more general pathway (Scheme 46).

The monotrityl-protected dithiol **108** was already reported in the literature,^[304] but only as unwanted side product in an attempt to synthesize a thioketal starting from ethylene dithiol. For a targeted synthesis of this compound, ethylene sulfide was reacted under basic conditions with a two fold excess of trityl thiol, based on procedures that were reported for ring-opening reactions of thiiranes (Scheme 47).^[305,306] The excess of the thiol was necessary to minimize the formation of longer ethylene dithiol chains which can form in a reaction of the product **108** with ethylene sulfide. TEA was used as base and DMF^[306] as well as dimethyl sulfoxide (DMSO)^[305] were used as solvents in different attempts. Independent of the solvent used, the monoprotected dithiol **108** was obtained very efficiently in more than 90% yield as colorless solid after purification by column chromatography. The employed excess of trityl thiol was nearly completely recovered in good purity and was reused.

The trichloride starting material **109** was prepared directly from the tribromide **102** in a nucleophilic substitution reaction with lithium chloride in DMF. As this reaction is highly exothermic, ice-cooling was necessary. After an aqueous work up procedure and

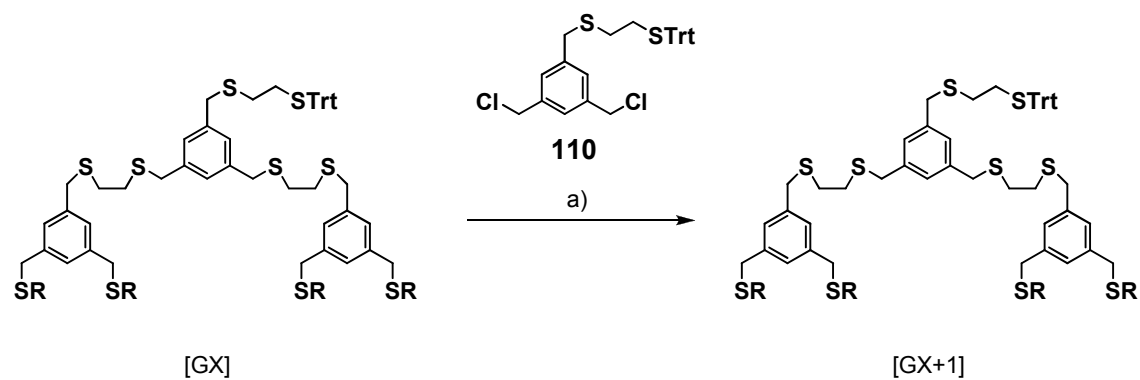
recrystallization from CH_2Cl_2 /hexane, the pure trichloride **109** was obtained in multigram scale and good purity in 90% yield from the tribromide **102**. An equimolar mixture of the monothiol **108** and the trichloride **109** was then refluxed in dry THF in the presence of potassium carbonate to give a mixture of differently substituted mesitylene derivatives. The desired key intermediate **110** was isolated as convenient to handle colorless solid from the mixture in a good yield of 46% after purification by column chromatography. From **110**, the trityl protected monoethylene G0 dendron **107** was synthesized easily in 88% isolated yield by a reaction with excess sodium methanethiolate in dry DMF. From **107**, the G1 dendron **111** was synthesized by a reaction with excess sodium methanethiolate in dry DMF.



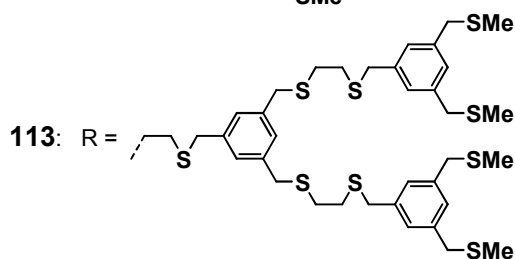
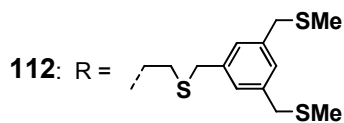
Scheme 47. Synthesis of the G1 dendron **111**. a) TrtSH, TEA, DMF, RT, 92%; b) LiCl, DMF, 0°C, 90%; c) K₂CO₃, THF, reflux, 46%; d) NaSMe, DMF, RT, 88%; e) 1. Et₃SiH, TFA, DCM, RT; 2. **110**, NaH, THF, RT, 88%.

The trityl protecting group of the G0 dendron **107** was removed under acidic conditions (4% v/v TFA in CH₂Cl₂) with triethylsilane as cation scavenger (Scheme 47). The free thiol was isolated by column chromatography in 90% yield. Unfortunately, this compound was found to decompose slowly, as was shown by TLC. The reaction of the free thiol with the branching unit **110** was therefore performed directly after the aqueous work up procedure of the deprotection reaction without further purification. Excess of the crude oily mixture was directly transferred to the reaction vessel in dry THF. The dichloride **110** was then added, followed by sodium hydride. After quenching with water, the mixture was extracted with MTBE. It was then tried to purify the crude product by column chromatography. However, the desired G1 dendron **111** eluted very slowly and a broad distribution over the column material was found when CH₂Cl₂ was used as eluent, although a retention factor of 0.5 was found by TLC in the same solvent. Different eluent systems were then tried in order to find a better purification procedure for the dendron **111**. In terms of separability and also solubility of the crude mixture, the best results were obtained when small percentages of the relative polar eluent ethyl acetate were added to 3:2 mixtures of CH₂Cl₂ and hexane. This way, the side products of the deprotection reaction and excess of the deprotected G0 dendron **107** were removed easily without the addition of ethyl acetate during the chromatographic purification procedure. The addition of 2% v/v ethyl acetate to the CH₂Cl₂/hexane mixture allowed then to receive the pure G1 dendron **111** efficiently as colorless oil in 88% yield.

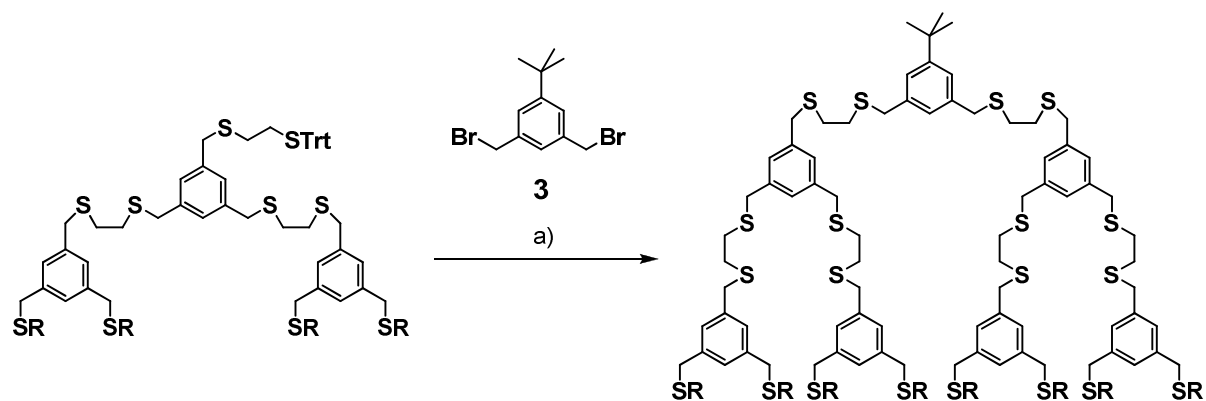
The second generation (G2) dendron **112** was synthesized under similar conditions by deprotection of **111**, followed by the reaction with the branching unit **110** directly after an aqueous work up of the deprotection reaction (Scheme 48). After aqueous work up and column chromatography, the G2 dendron **112** was isolated as colorless oil in 79% yield. The excess of the deprotected G1 dendron was thereby removed in the presence of 2% ethyl acetate in a 3:2 mixture of CH₂Cl₂ and hexane, while the desired G2 **112** eluted with 4% ethyl acetate. This procedure was repeated with **112** in order to receive the G3 dendron **113**, which was obtained as colorless oil in 75% yield after column chromatography (CH₂Cl₂/hexane 4:1 with 4% ethyl acetate).



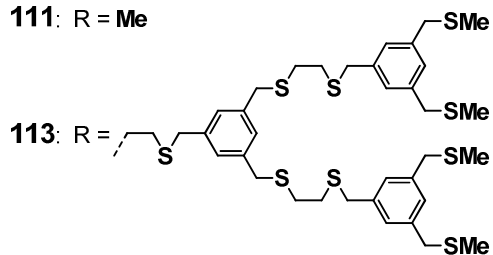
111: R = Me



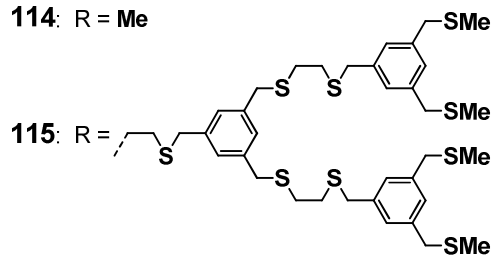
Scheme 48. Synthesis of higher generation dendrons. a) 1. Et_3SiH , TFA, CH_2Cl_2 , RT; 2. NaH, THF, RT, **112**: 79%; **113**: 75%.



111: R = Me



114: R = Me



Scheme 49. Synthesis of the *t*-butyl terminated dendrimers **114** and **115**. a) 1. Et_3SiH , TFA, CH_2Cl_2 , RT; 2. NaH, THF, RT, **114**: 88%; **115**: 57%.

For initial experiments concerning the stabilization of gold nanoparticles, the ethylene dithiol dendrons were reacted with the dibromide **3**, as the *t*-butyl group is easily observable in ^1H NMR experiments. Under otherwise similar reaction conditions that were used for the synthesis of the ethylene dithiol dendrons, the second and fourth generation *t*-butyl terminated dendrimers **114** and **115** were prepared in 88% and 57% isolated yields respectively (Scheme 49).

3.4.2 Gold Nanoparticle Formation Experiments

For the investigation of the gold nanoparticle size steering and stabilizing properties of the thioether dendrimer ligands **114** and **115**, gold nanoparticles were prepared in the presence of these ligands. In order to ensure the comparability with the studies on nanoparticles stabilized by linear thioether ligands (see sections 0 and 1.1), the same Brust/Schiffrin protocol^[46] was employed for the synthesis of gold nanoparticles in the presence of thioether dendrimers. The syntheses were performed in a two-phase water/ CH_2Cl_2 mixture with TOAB as phase transfer agent. As for the synthesis of gold nanoparticles stabilized by linear thioether ligands, a 1:1 ratio of sulfide moieties to gold was maintained in an initial attempt, resulting in 20 equivalents of the gold(III) precursor HAuCl_4 compared to 1 equivalent of the G2 ligand **114**. The reduction of gold(III) with sodium borohydride led however to the formation of a black precipitate in the presence of the G2 dendrimer **114** directly after the addition of the reducing agent. The organic phase was nearly colorless with a slight red color. The results were very similar to the results that were obtained with the monomeric ligand **24** (see section 0), it was therefore concluded that bulk gold was probably formed. In a following experiment, the amount of ligand **114** was doubled relative to the gold(III) precursor, resulting in a gold to sulfide ratio of 1:2. As before, a black precipitate formed directly after the addition of the reducing agent, indicating the formation of bulk gold.

Since the second generation dendrimer showed only very weak gold nanoparticle stabilizing properties, a 1:2 ratio of gold to sulfide was also used for the synthesis of gold particles in the presence of the fourth generation dendrimer **115** with 92 thioether moieties (46 equivalents HAuCl_4 to 1 equivalent of **115**). In this case, no precipitate was formed after the addition of the reducing agent. The reduction of the gold(III) precursor did indeed lead to the formation of gold nanoparticles, as was evidenced by the reddish brown color of the organic phase. By UV/vis, the presence of a weak plasmon resonance was observed directly after the synthesis

(Figure 57), which indicated the presence of particles larger than 2-3 nm.^[181] The two phases of the reaction mixture were separated and the colored organic phase was dried over magnesium sulfate. The organic dispersion was then left under ambient conditions and was investigated by UV/vis spectroscopy regularly. After three days, no significant changes were observed in the UV/vis spectra.

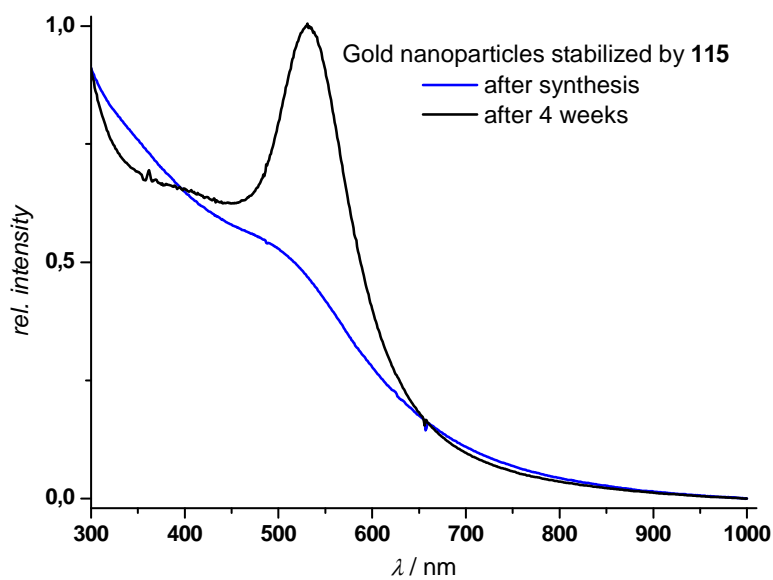


Figure 57. UV/vis absorption spectra (CH_2Cl_2) of the gold nanoparticles stabilized by **115** directly after the preparation and after four weeks in CH_2Cl_2 dispersion.

Three weeks later however, the dispersion was dark red colored, which also mirrored in the UV/vis spectrum that showed a very strong and narrow plasmon resonance band (Figure 57). These changes indicate the formation of larger gold nanoparticles by coagulation. However, the particles were still dispersible in CH_2Cl_2 and the coagulation process did not lead to precipitation of bulk gold.

TEM Investigations

HRSTEM was performed in order to investigate the obtained particle sizes and dispersities, which could be dictated by the size of the large thioether dendrimer **115**. However, the HRSTEM micrographs revealed a very broad distribution of particle sizes in a range between 1 and 15 nm (Figure 58) with a mean diameter of 6.2 ± 2.5 nm. Also, no distinct particle sizes were found which could be assigned to particles stabilized by different integer numbers of the large G4 dendrimer ligand **115**.

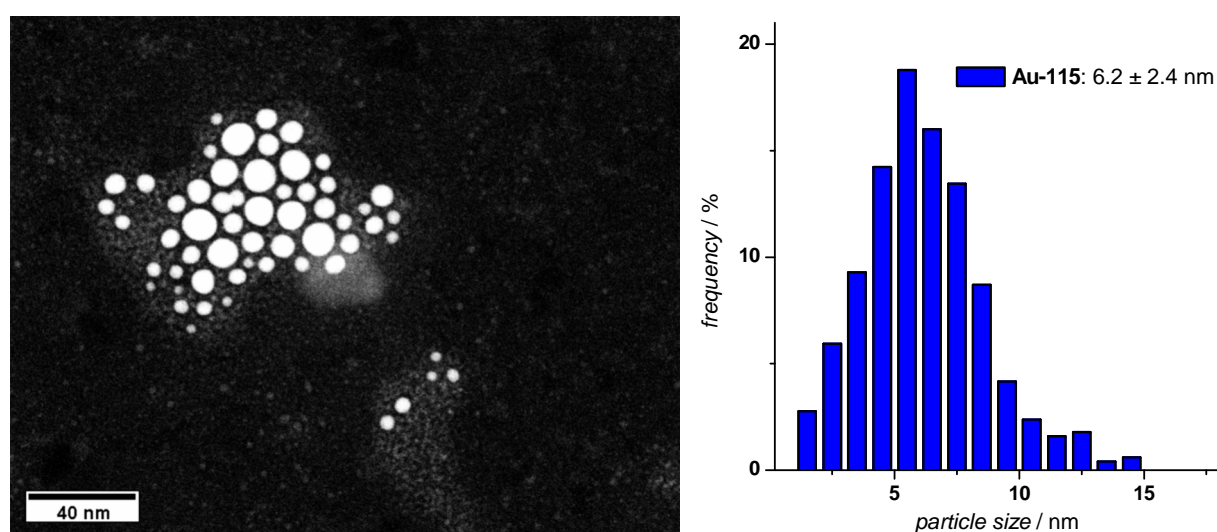
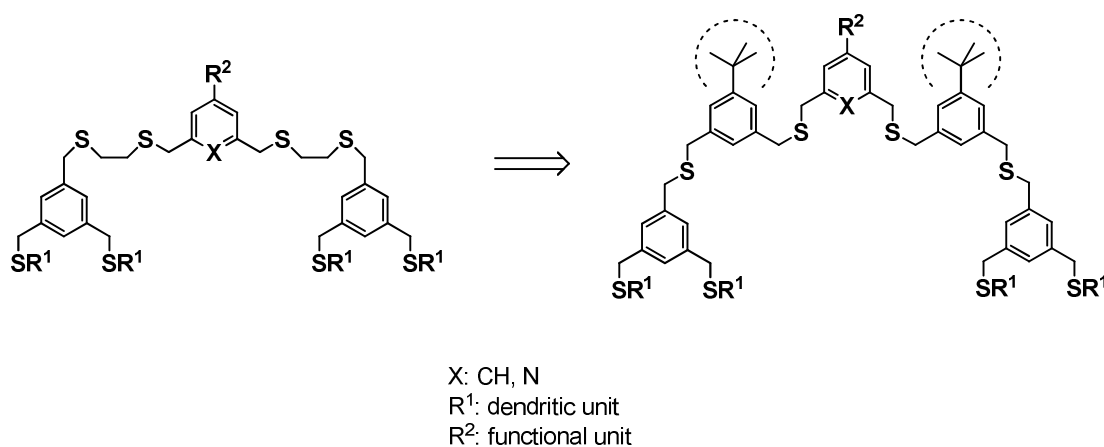


Figure 58. Representative HRSTEM micrograph of **Au-115** (left) and size distribution histogram of **Au-115** (right) after four weeks in CH_2Cl_2 dispersion.

3.4.3 Further Development of the Thioether Dendrimers

Based on the comparison of the results obtained for the linear thioether ligands **24** – **27** and the dendrimer ligands **114** and **115**, it was hypothesized that the missing steric hindrance of the dendritic ligands might be the reason for the low degree of nanoparticle stabilization provided by the dendrimer ligands **114** and **115**. In particular, these dendrimers do only provide benzene rings and ethylene bridges, which presumably lie flat on the nanoparticle surface and can therefore not provide an efficient coating layer for the gold nanoparticles. Much more stable and monodisperse gold nanoparticles were obtained with the octadentate ligand **27** compared to the fourth generation dendrimer **115** with 92 thioether moieties. It is therefore not only the large number of thioether moieties that is responsible for the stabilization of the nanoparticles. As main difference between the linear ligands and the

dendritic ligands, the sterically demanding *t*-butyl groups were noticeable. Together with the surface binding of the thioether moieties, these groups could prevent the direct contact of nanoparticles and therefore inhibit the coagulation of small nanoparticles to larger structures. These considerations led to a different design for dendritic thioether ligands for the stabilization of gold nanoparticles, which makes use of the successfully employed structural motifs of the linear thioether ligands **24** – **27**. Thus, the flexible ethylene dithiol chains were exchanged with a building block based on the sterically demanding *t*-butyl benzene dithiol **2** (Scheme 50).



Scheme 50. Sterically demanding thioether dendrimers.

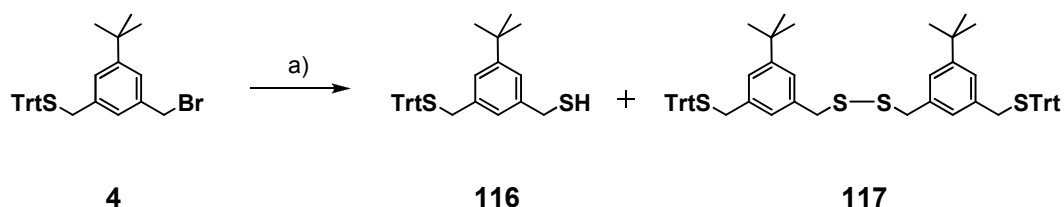
In addition, the end caps were exchanged from methyl sulfides to benzylic sulfides (Scheme 50). Overall, this should provide the required bulkiness of the ligand, while the flexibility of the dendritic system is still maintained due to the connection at the flexible benzylic position. Furthermore, the overall ligand size is increased to considerable extent compared to the initial ethylene dithiol dendrimer ligands. A second generation thioether dendrimer with the *t*-butyl benzene bridges has already a molecular weight which is approximately double the weight of the linear heptamer ligand **27** and should therefore be able to cover a considerably larger part of the surface area of nanoparticles.

3.4.3.1 Dendron Synthesis

The synthetic strategy was kept similar to the successful synthesis of the ethylene dithiol dendrimers. Thus, the different modular functional units (see section 3.3.1) can be easily

attached in a final synthetic step to form monofunctionalized dendrimers by nucleophilic substitution reactions with the thiol terminated dendrons.

The monoprotected dithiol **116** was prepared efficiently starting from the already monofunctionalized bromide **4**, closely following a mild one-pot procedure for the conversion of benzylic bromides to thiols.^[118] An acetate protected thiol was introduced first by the reaction of **4** with potassium thioacetate in dry THF, followed by *in situ* deprotection by addition of potassium carbonate and methanol to the reaction mixture (Scheme 51). The desired monothiol **116** was thereby obtained in 80% yield after column chromatography. It was found that the losses can be attributed to the formation of the disulfide **117**, which was also isolated.



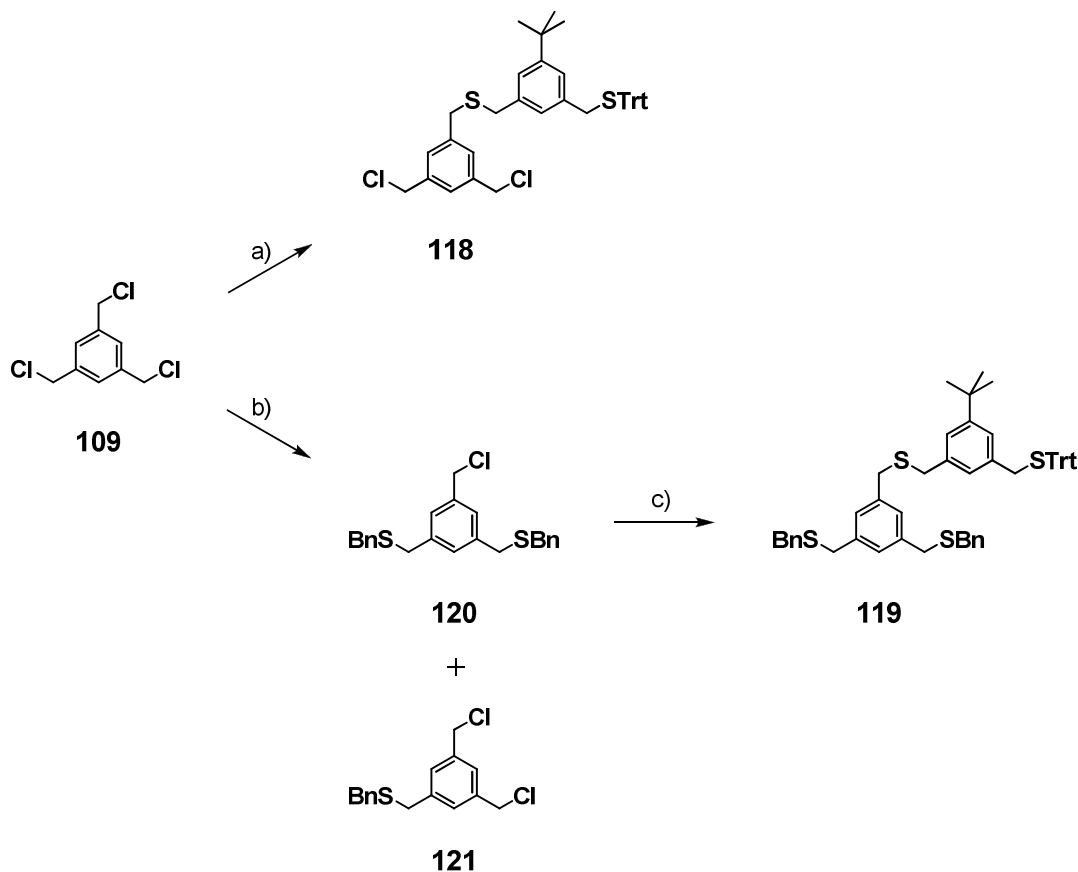
Scheme 51. Synthesis of **116**. a) KSAc, THF, RT, then K₂CO₃, MeOH, RT, **116**: 80%.

To prevent the formation of the unwanted side product **117** upon storage, the monothiol **116** was stored under argon at 4°C.

The dichloride branching unit **118** was then obtained from the reaction of **116** with a slight excess of the trichloride **109** in refluxing THF with potassium carbonate (Scheme 52). The excess of the trichloride **109** was used in order to minimize the formation of di- or trisubstituted reaction products. The desired monosubstituted branching unit **118** was isolated in a good yield of 49% after purification by column chromatography. The trichloride starting material **109** was also isolated and was reused.

In order to prevent losses of the monothiol **116**, which had to be synthesized in three synthetic steps, the starting generation dendron **119** was not synthesized directly from the branching unit **118**. Rather the benzyl end-caps were introduced to the trichloride **109** prior to the *t*-butyl benzene unit (Scheme 52). This reaction was performed by using commercially available benzyl mercaptan in dry THF with sodium hydride as base. After purification by column chromatography, the desired monochloride **120** was obtained as colorless liquid in a good yield of 44%. The dichloride **121** was also obtained and was isolated in 28% yield. This compound was used in further attempts to synthesize the monochloride **120**. In a second step, the monothiol **116** was then introduced very efficiently under standard nucleophilic

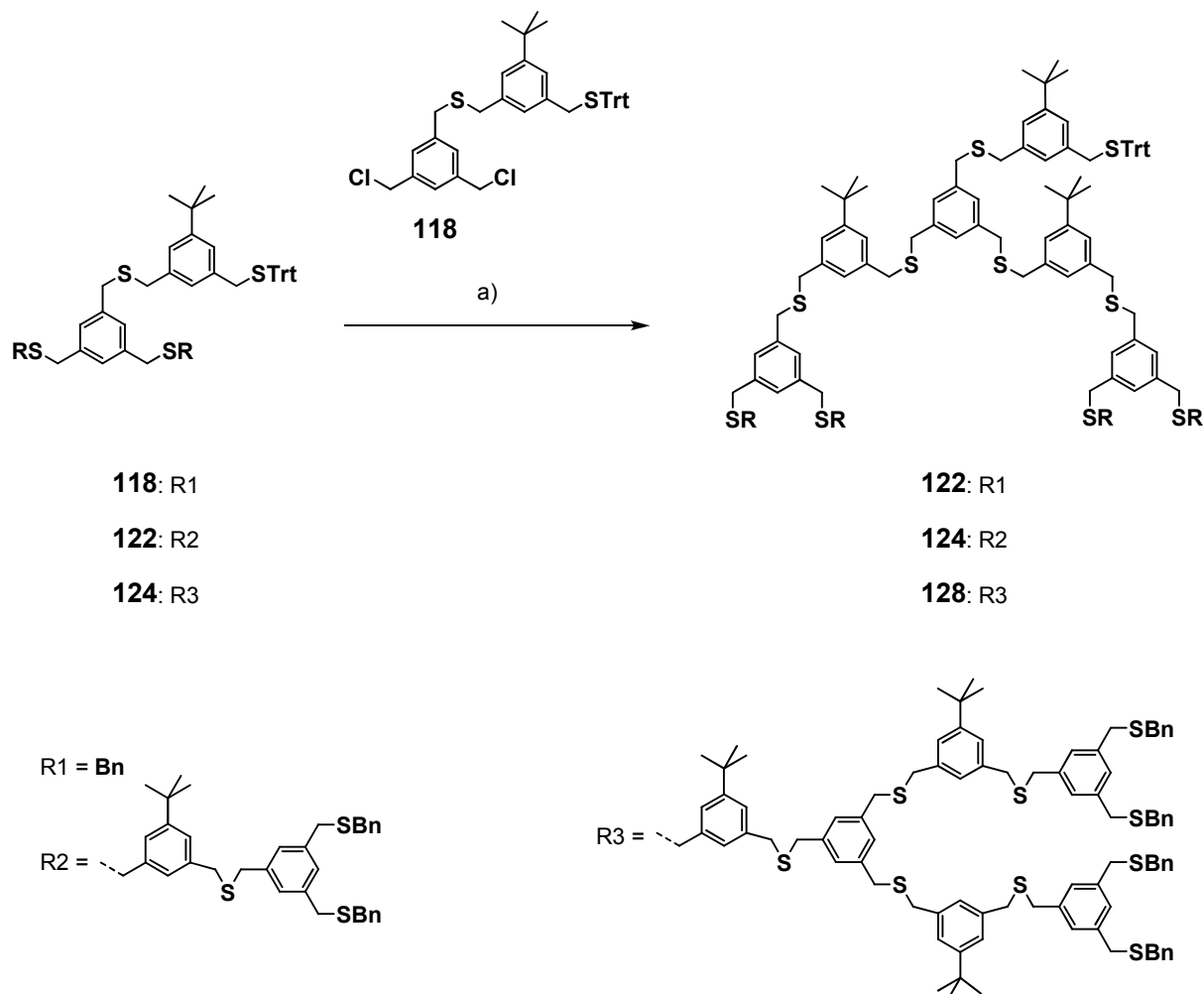
substitution conditions in THF with sodium hydride. By column chromatography, the G0 dendron **119** was isolated as colorless oil in quantitative yield.



Scheme 52. Synthesis of **118** and **119**. a) **116**, NaH, THF, RT, 49%; b) BnSH, NaH, THF, RT, **120**: 44%; **121**: 28%; c) **116**, NaH, THF, RT, quant.

With the main building blocks **118** and **119** in hand, the first generation dendron **122** was synthesized in a similar fashion as the ethylene dithiol dendrons. The trityl protecting group of the G0 dendron **119** was deprotected with 4% v/v TFA in CH_2Cl_2 with triethylsilane as cation scavenger (Scheme 53). After an aqueous work up procedure, the free thiol intermediate **98** was directly reacted with substoichiometric amounts of the branching unit **118** in THF with sodium hydride as base. This reaction led to the G1 dendron **122** in 81% yield after column chromatography based on the amount of the branching unit **118**. The purification by column chromatography appeared to be much more straightforward compared to the G1 ethylene dithiol dendron **111**, as mixtures of CH_2Cl_2 and hexane provided good results and the addition of ethyl acetate was not necessary. However, it was found that the major by-product of this reaction sequence was the disulfide **123** (Scheme 54), which can be formed oxidatively by the reaction of two free thiol intermediates **98**. The reaction mixture of the nucleophilic

substitution reaction was degassed by bubbling argon through the solution prior to the addition of sodium hydride. The yield of this reaction was thereby increased to up to 90%.



Scheme 53. Synthesis of the higher generation dendrons **122**, **124** and **128**. a) 1. Et_3SiH , TFA, CH_2Cl_2 , RT, **98**: 97%; **127**: 89%; 2. NaH, THF, RT, **122**: 90%; **124**: 90%; **128**: 29%, but not pure.

Using similar reaction conditions, the G1 dendron **122** was deprotected and the crude was then - after an aqueous work up - transferred directly with THF to the reaction flask with the branching unit **118** for the formation of the next generation dendron **124**. Without degassing of the solution, sodium hydride was added. TLC showed the formation of two major products, one with an R_f value which was very close to the R_f value of the G1 starting material **122** and another product which moved considerably slower on the TLC plate. These two compounds were separated by column chromatography and unfortunately none was the desired G2 dendron **124**. $^1\text{H NMR}$ of the compound that eluted first revealed the presence of the trityl protected branching unit. However, relative to these signals, only signals fitting for one dendron and one additional singlet at 4.5 ppm were found. The additional signal lies exactly

The second major product of this reaction was found to be the disulfide **126**, as was shown by the formation of the free thiol **127** upon reduction with tri-*n*-butylphosphine in THF and methanol (Scheme 54).^[307]

Considering these results, it seems that the disulfide formation was faster than the reaction with the branching unit **118**, leaving excess chloride leaving groups, which led to the formation of the monochloride **125**. In order to have more control over the formation of the second generation dendron **124**, the crude mixture of the deprotection procedure with **122** was purified by column chromatography prior to the nucleophilic substitution reaction. The free thiol **127** was thus obtained in up to 89%, showing that some of the losses can also be attributed to the deprotection procedure. A mixture of slightly more than two equivalents of the thiol **127** and the dichloride **118** was then carefully degassed with argon to suppress the oxidative disulfide formation. The reaction was initiated with the addition of sodium hydride. After aqueous work up and purification by column chromatography, the desired second generation dendron was isolated in up to 90% yield (Scheme 53). However, much lower yields were also obtained in other attempts to synthesize **124**, showing the importance of perfect reaction conditions for the synthesis of such thioether dendrimers.

The third generation dendron **128** was also synthesized under the optimized reaction conditions that were used for the second generation **124**. Purification of the crude by column chromatography provided the G3 dendron **128** in only 29% yield (Scheme 53). However, this assignment was solely based on the ¹H NMR spectrum, which showed well fitting ratios between the trityl group and the other signal groups. The presence of the disulfide **129** of the free thiol G2 dendron **130** cannot be ruled out based only on this evidence.

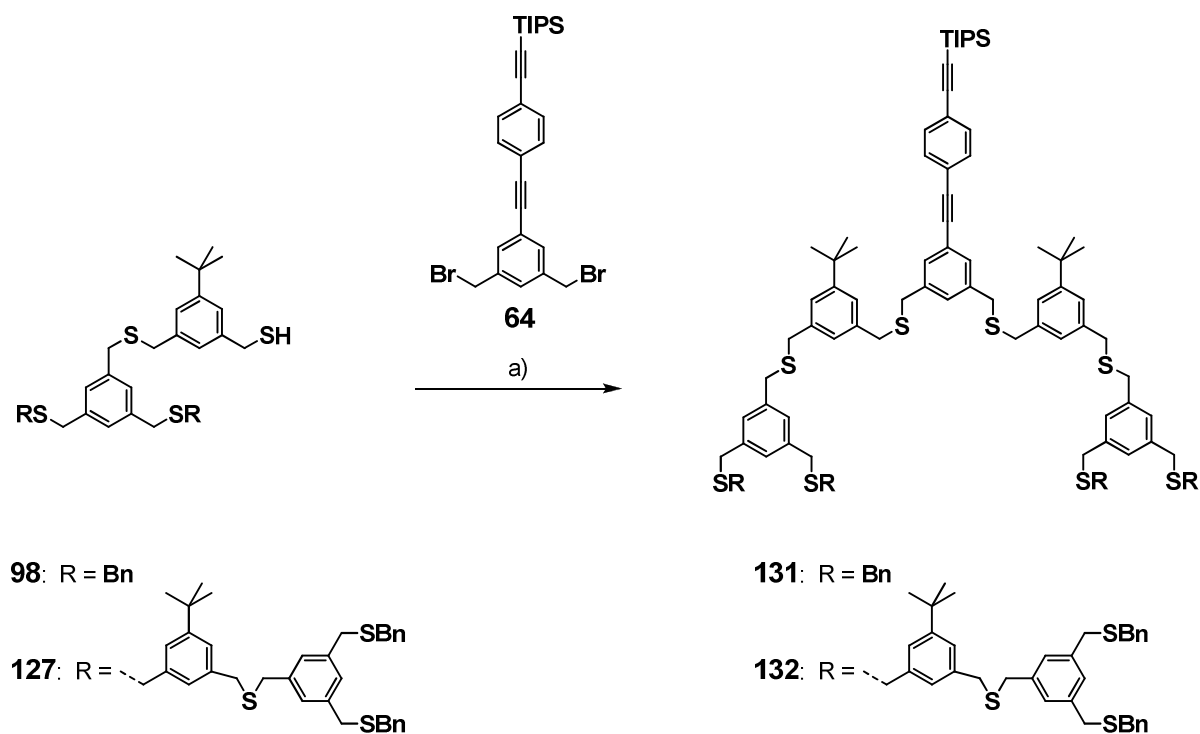
In future attempts to synthesize higher generation dendrons, a reversal of the functionalities of the building blocks may provide better results: if the thioether dendron carries the leaving group and the branching unit free thiols, the formation of the disulfides **123**, **126** and **129** can be prevented.

3.4.3.2 Synthesis of Acetylene Functionalized Dendrimers

For initial experiments on the gold nanoparticle stabilizing and size steering properties of the sterically demanding thioether dendrimer structures, the medium length OPE functional unit **64** was integrated as central unit of the dendrimer structures (Scheme 55). Due to the

fluorescence of the OPE rod, the dendrimer formation becomes easily traceable by TLC and the desired dendrimer can be clearly distinguished from the disulfide side products that may be formed. Furthermore, this acetylene functionalization allows for the formation of OPE functionalized nanoparticles that can give further insight to the applicability of dendrimer coated nanoparticles as building blocks for wet synthetic chemistry processing.

The first generation dendrimer **131** was obtained from the reaction of excess of the deprotected G0 dendron **98** with the OPE dibromide **64** in degassed THF with sodium hydride as base. The crude was purified twice in order to completely remove the disulfide by product. Thus, the G1 OPE dendrimer **131** was obtained in 98% yield as colorless, very viscous oil. Similarly, the second generation OPE dendrimer **132** was obtained in 99% yield after repetitive purification by column chromatography.



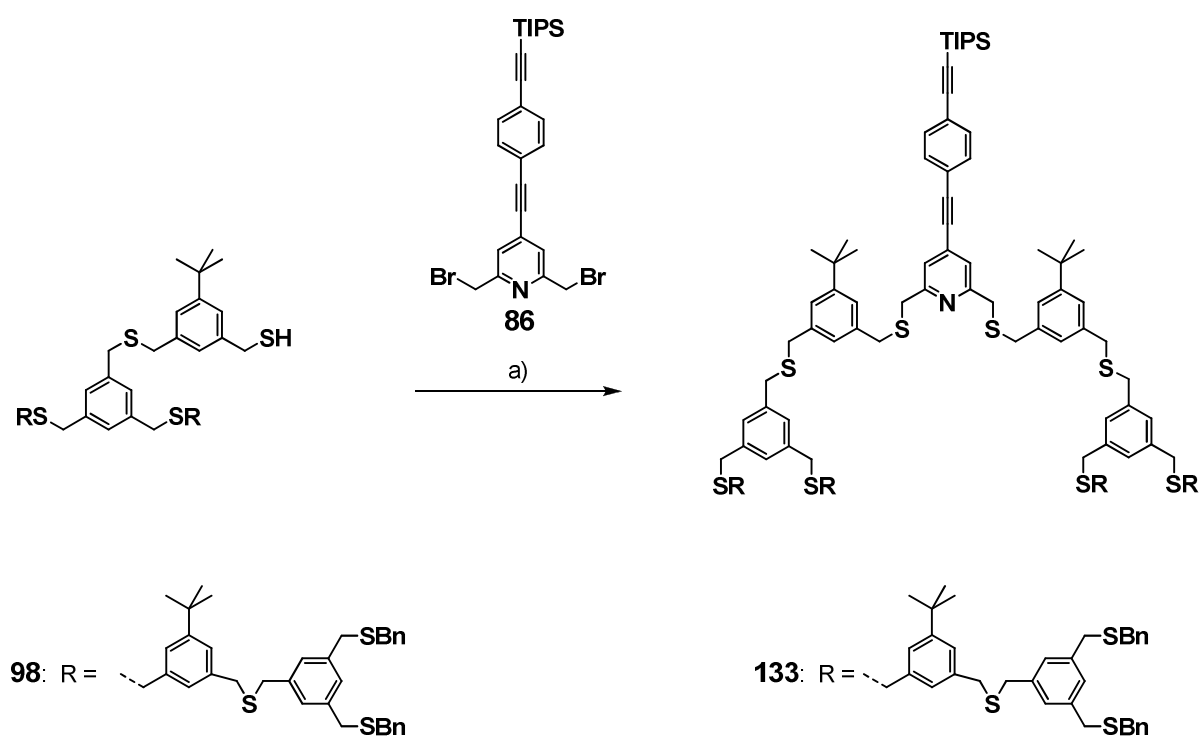
Scheme 55. Synthesis of the OPE functionalized dendrimers **131** and **132**.

a) NaH, THF, RT, **131**: 98%; **132**: 99%.

Attempts to obtain the third generation dendrimer failed however. Column chromatography after the deprotection procedure of the G2 dendron **124** provided only small amounts of mixtures of compounds with the G2 disulfide **129** among them. The presence of free thiol groups were observed by ^1H NMR, but integration of the obtained signals revealed that most of the material of the observed mixture did not contain free thiol moieties. Also, the direct

reaction of **124** with the OPE unit **64** after the deprotection procedure without purification by column chromatography led to inseparable mixtures. It was found out later that the G1 and G2 dendrimers **131** and **132** are not stable, even when stored at 4°C. Attempts to further characterize these structures after a storage time of approximately three months revealed the decomposition of **131** and **132**. This instability might also explain in part the unsuccessful attempts to synthesize the G3 dendrimer.

The second generation pyridine OPE dendrimer **133** was synthesized as well (Scheme 56). In addition to the features provided by the rigid rod OPE unit, the polar pyridine moiety was expected to allow for the easier chromatographic separation of disulfide by-products. Using similar reaction conditions that were used for the other dendrimers, **133** was obtained quantitatively after purification by column chromatography. In this case, removal of disulfide by products proved to be simple, as these compounds eluted from the column with pure CH₂Cl₂, while the addition of 2% triethylamine was necessary to receive the pyridine functionalized dendrimer **133**. Interestingly, this compound was found to be stable, even when stored under ambient conditions. At this point however, it remains unclear if the stability differences between the benzene OPE dendrimers **131** and **132** and the pyridine derivative **133** arise from the intrinsic properties of the molecules or might be attributed to the presence of minor amounts of disulfide by-products in the preparations of **131** and **132**.



Scheme 56. Synthesis of the G2 pyridine OPE dendrimer **133**. a) NaH, THF, RT, quant.

3.4.4 Dendrimer Stabilized Gold Nanoparticles

To investigate the properties of dendrimeric thioether ligands concerning nanoparticle stabilities, surface coverage and sizes, gold nanoparticles were formed in the presence of OPE functionalized dendrimer ligands **132** and **133** by applying the two-phase protocol that was used for the synthesis of the OPE functionalized nanoparticles coated with linear heptameric ligands (*vide supra*). As before, a 1:1 ratio between gold(III) and sulfide moieties was used, resulting in 20 equivalents of tetrachloroauric acid compared to the second generation ligands **132** and **133**. Thus, tetrachloroauric acid was transferred with TOAB from an aqueous phase to a CH₂Cl₂ phase. A CH₂Cl₂ solution of the respective dendrimer ligand **132** or **133** was added and the gold(III) precursor was then reduced after 10 minutes by an aqueous solution of sodium borohydride. In both cases, the organic phases turned dark brown immediately after the addition of the reducing agent, indicating the formation of nanoparticles. The CH₂Cl₂ phases were separated and were then dried over magnesium sulfate. After concentration of the dispersions to approximately 1 ml, the **Au-132** and **Au-133** nanoparticles were precipitated by addition of ethanol. The particles were separated by centrifugation, leaving the supernatants nearly colorless. This is in contrast to the gold nanoparticles coated by linear heptameric ligands (**Au-27**, **Au-62**, **Au-66** and **Au-67**), where the supernatants were slightly brown colored after centrifugation, indicating the presence of gold nanoparticles in the liquid phases. The remaining solid dendrimer coated nanoparticles were redispersed in CH₂Cl₂ and the precipitation/centrifugation procedure was repeated twice to completely remove the phase transfer agent TOAB. Notably, the **Au-132** particles were obtained very efficiently in 90% based on the gold equivalents used. The lower nanoparticle yield of 76% that was found for the pyridine-OPE G2 ligand **133** might be attributed to the partial removal of excess free ligand by this procedure due to the polar pyridine unit. To remove further excess ligand, GPC was performed with the **Au-132** and **Au-133** particles using toluene as eluent. In all three cases the dendrimer coated gold nanoparticles eluted in a narrow brown colored band. However, late eluting colored nanoparticle containing fractions of second generation dendrimer particles **Au-132** and **Au-133** were found to contain the free ligands **132** and **133** by TLC and fluorescence analysis. These fractions were therefore not combined with the main nanoparticle containing fractions.

UV/vis Investigations

The UV/vis spectra of the dendrimer stabilized **Au-132** and **Au-133** particles (Figure 60) are very similar to the spectra of the OPE functionalized **Au-66** nanoparticles (*vide supra*). In all cases, no strong plasmon resonance band can be observed, indicating the formation of nanoparticles with diameters smaller than 2-3 nm.^[181] Also, the presence of the functionalized ligands is evident by the absorption between 300 and 400 nm. After removal of excess ligand **132** or **133** by GPC, the signals in this region become weaker compared to the signals originating from the gold nanoparticles. This shows that the efficient removal of unbound ligand from the nanoparticles by size exclusion is possible even with the relatively large second generation dendrimer ligands **132** and **133**.

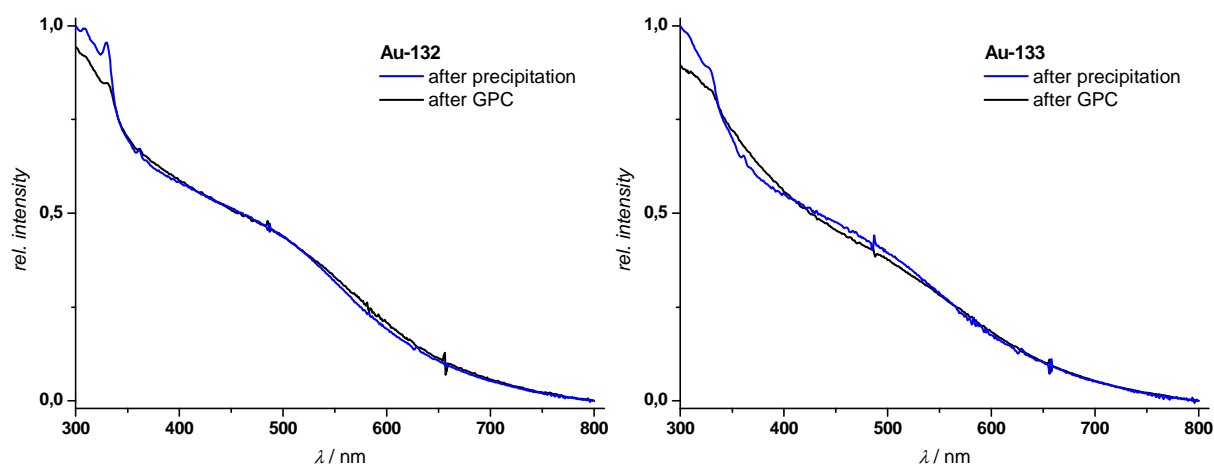


Figure 60. Normalized UV/vis absorption spectra (CH_2Cl_2) of **Au-132** and **Au-133** before and after purification by GPC.

NMR

The ^1H NMR spectra of the thioether dendrimer stabilized **Au-132** and **Au-133** particles after purification by GPC show very broad signals (Figure 61), similar to other thioether stabilized gold nanoparticles (*vide supra*). Also, no signals for the phase transfer agent TOAB can be found, indicating that only the thioether dendrimers are required for the stabilization of **Au-132** and **Au-133** nanoparticles.

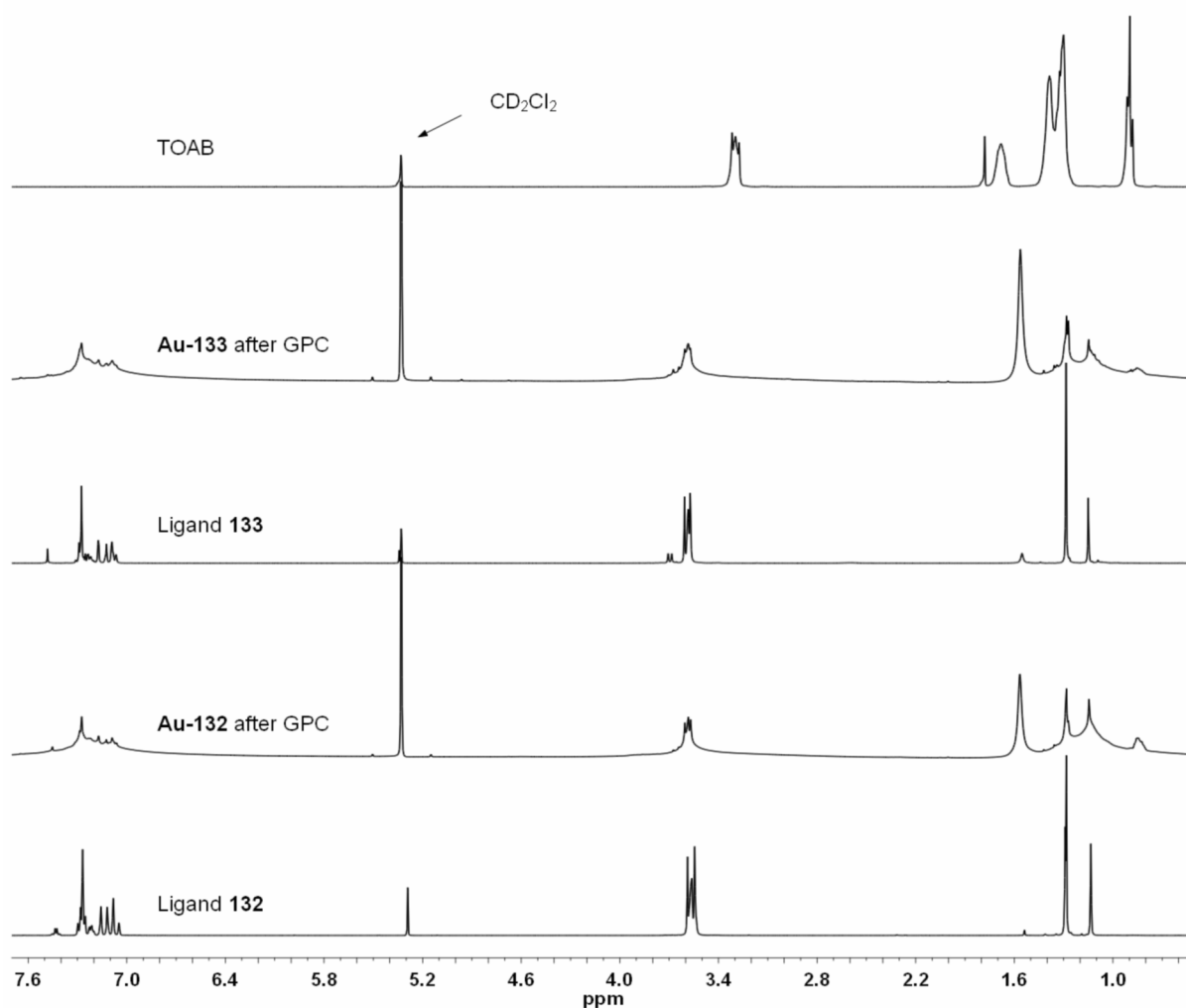


Figure 61. ^1H NMR spectra of **Au-132** and **Au-133** in comparison with the spectra of the pure ligands **132** and **133** and pure TOAB.

TEM Investigations

The dendrimer coated gold nanoparticles **Au-132** and **Au-133** were investigated by TEM on carbon coated copper grids (Figure 62 top). Thereby it was found that the **Au-132** particles stabilized by the second generation dendrimer have a mean diameter of 1.3 nm with standard deviation of 0.2 nm (Figure 62 bottom). The pyridine dendrimer particles **Au-133** were found to be slightly larger with a mean diameter of 1.35 nm, but notably with a smaller deviation of 0.14 nm. Compared to the heptamer coated OPE particles **Au-27**, these particles are considerably larger, which can be attributed to the increased size of the second generation dendrimer ligands **132** and **133** and their size steering properties. Furthermore, better monodispersities were found for the thioether dendrimer coated **Au-132** and **Au-133** particles, which further supports the goal of controlling nanoparticle sizes by ligand design.

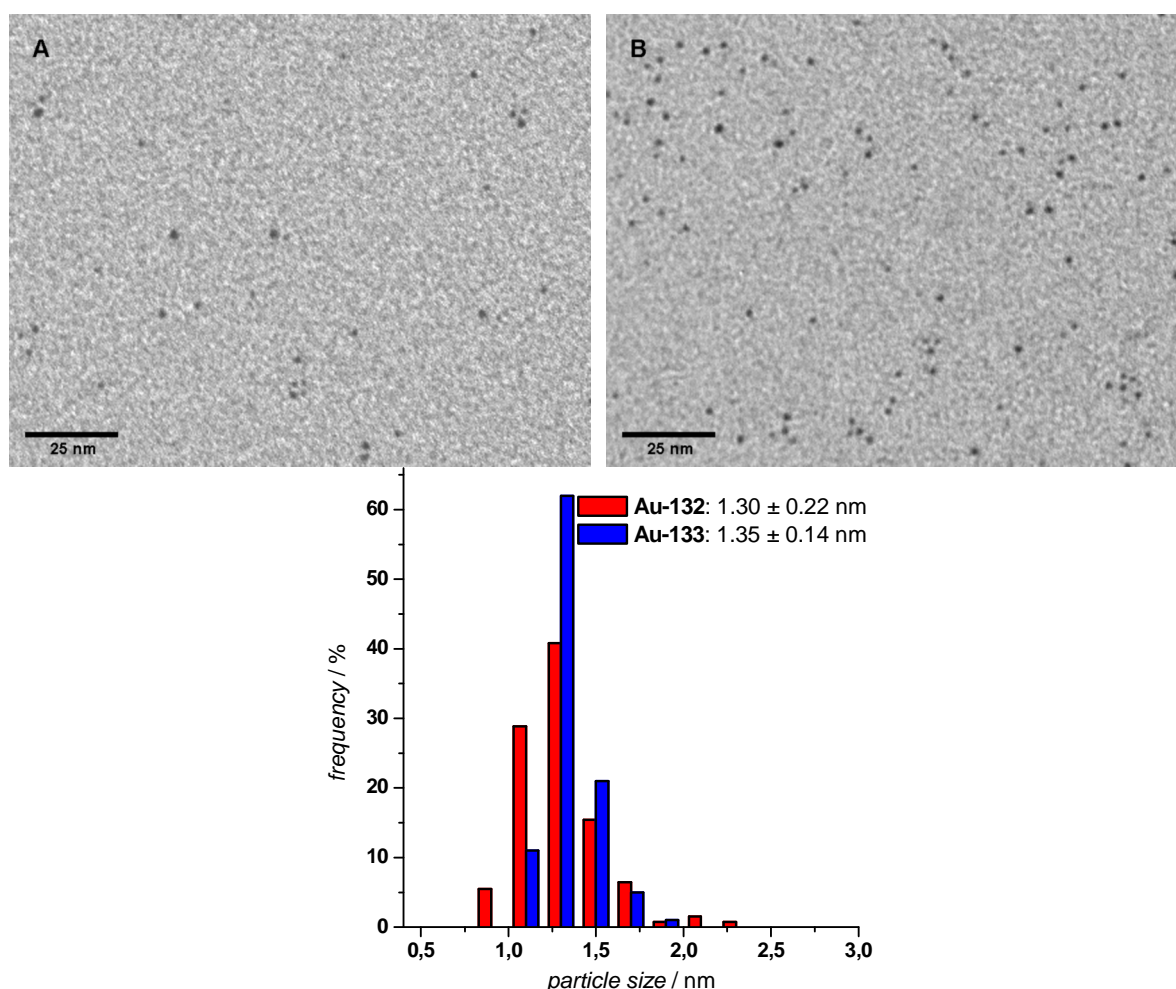


Figure 62. TEM micrographs and size distribution histograms of **Au-132** (A) and **Au-133** (B) (top). TEM micrographs of larger areas of the TEM grids can be found in the appendix. Size distribution histograms of **Au-132** and **Au-133** (bottom).

Elemental Analysis

In order to obtain a deeper insight to the nanoparticle surface coverage of the second generation dendrimer ligands **132** and **133**, elemental analyses were performed with the dendrimer coated **Au-132** and **Au-133** nanoparticles.

After removal of excess ligand by GPC, ligand weight proportions of 34.0% for **Au-132** and 32.5% for **Au-133** respectively. These values are based on the assumption that only gold nanoparticles and the coating ligands are present. From these weight proportions, the presence of 34 gold atoms per coating ligand **132** and 36 gold atoms per pyridine ligand **133** can be calculated. Similar to before (*vide supra*) the average number of gold atoms per nanoparticle was calculated by using the density of bulk gold. 68 gold atoms can thus be assumed for the 1.3 nm **Au-132** particles, while 76 gold atoms form larger 1.35 nm **Au-133** particles. In contrast to the heptamer stabilized **Au-27** particles, a second nanoparticle size distribution had not to be taken into account. Therefore, the number of coating ligands per particle was calculated directly by dividing the number of atoms per particle with the average number of gold atoms per ligand. The average number of dendrimer ligands per particle is thereby found to be 2.0 for **Au-132** and 2.1 for **Au-133**. Based on these calculations, it can be assumed that mainly difunctionalized nanoparticles were formed with the G2 dendrimers **132** and **133**.

3.4.5 Formation of Gold Nanoparticle Superstructures

The ability of the dendrimer coated **Au-132** and **Au-133** nanoparticles to act as 'artificial molecules' with functional groups in defined positions was demonstrated by the formation of nanoparticle superstructures similar to the OPE heptamer stabilized **Au-62**, **Au-66** and **Au-67** nanoparticles (*vide supra*). The focus in these investigations lies mainly in the comparison of the properties of the pyridine OPE units with the properties of the benzene derived functional OPE rods and the validation of the assumptions that were made concerning the broad particle-particle distance distributions that were found for superstructures of **Au-66** and **Au-67** (see section 3.3.4).

Nanoparticle superstructures were formed by using the one-pot deprotection/oxidation conditions that were already used before with linear heptamer stabilized nanoparticles (see section 3.3.4). The TIPS acetylene functionalized **Au-132** and **Au-133** particles were thus dispersed in CH₂Cl₂ and a solution of TBAF in wet THF was added. After stirring at room

temperature for one hour, TMEDA (2.5% v/v) and copper(I) chloride were added and the mixtures were stirred vigorously in open reaction vessels. Very interestingly, no precipitates were formed after this procedure within one hour and no other visible changes were observed in the reaction mixtures. This is in sharp contrast to the observations that were made with the **Au-66** particles which carry OPE units of similar length. In this case, a black precipitate was formed very shortly after the addition of the copper salt (*vide supra*).

UV/vis Investigations

UV/vis spectroscopic investigation of the reaction mixtures shows in both cases the desired diacetylene formation (Figure 63). Obvious red-shifts for the signals of the OPE functional units in the range between 300 and 450 nm can be observed in comparison with the unreacted **Au-132** and **Au-133** nanoparticles, indicating the formation of large conjugated diacetylene-OPE structures. Between 450 and 800 nm no significant changes can be seen, indicating the stability of the dendrimer coated nanoparticles under the Hay reaction conditions.

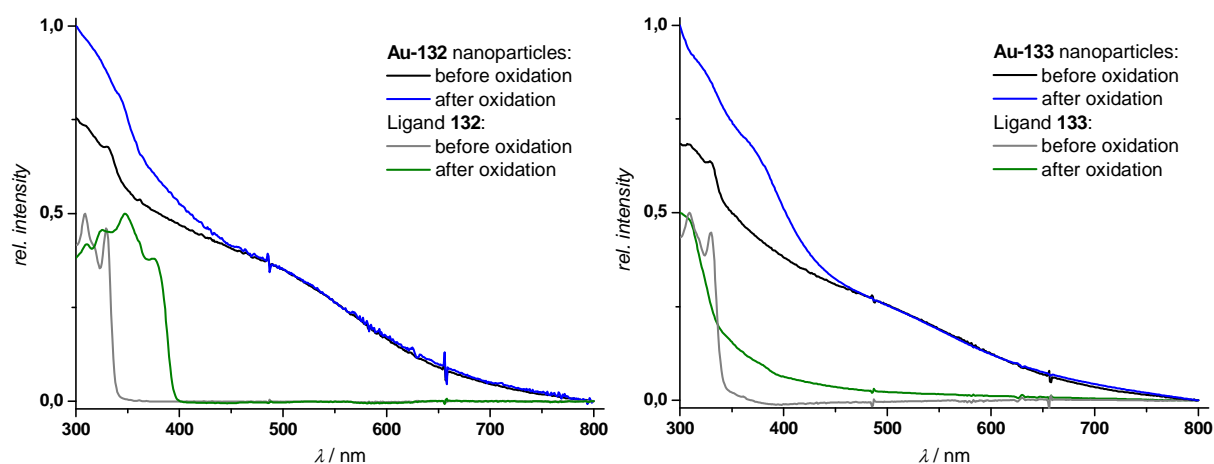


Figure 63. UV/vis absorption spectra (CH_2Cl_2) of **Au-132** and **Au-133** before and after the deprotection/Hay procedure.

TEM Investigations and Discussion

The reaction mixtures of the deprotection/Hay reaction conditions with **Au-132** and **Au-133** were directly investigated by TEM. Therefore, parts of the reaction mixtures were separated and highly diluted with CH_2Cl_2 . These barely colored dispersions were then applied to carbon

coated copper grids. In these cases, mainly smaller nanoparticle aggregates with up to *ca.* 10 particles were observed (Figure 64). However, some flat lying larger nanoparticle agglomerations were also found. As was already indicated by the UV/vis spectra, the nanoparticles retained their integrity and did not coagulate to larger particles.

For comparison, an aqueous work up with ammonium chloride was performed with the remaining reaction mixtures to remove the copper salts and TMEDA. The organic phases were then dried over magnesium sulfate and filtered. The dispersions were strongly brown colored after this procedure and were thus also diluted before application to the TEM grid. As expected, the purification procedure did remove very large nanoparticle aggregates, but otherwise, the TEM micrographs that were obtained before and after the purification procedure did not show great differences (Figure 64). In addition to some large aggregates, a large fraction of small nanoparticle superstructures was found in the micrographs that were taken from the diluted reaction mixture. However, due to the application of the reaction mixtures to the TEM grids in highly diluted form, these observations are only based on a low number of superstructures.

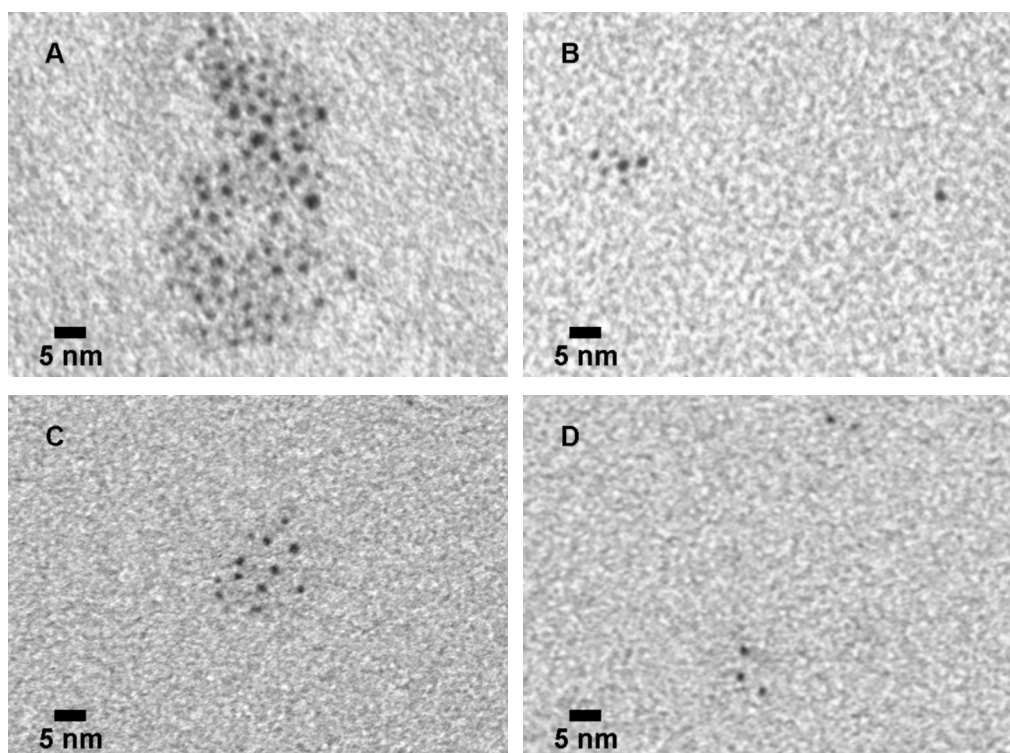


Figure 64. Representative TEM micrographs of $(\text{Au-132})_n$ (A), $(\text{Au-132})_{2-4}$ (B), $(\text{Au-133})_n$ (C) and $(\text{Au-133})_{2-4}$ (D). TEM micrographs of larger areas of the TEM grids can be found in the appendix.

The interparticle distances of the nanoparticle superstructures of **Au-132** and **Au-133** were measured similar to the investigations with OPE thioether heptamer stabilized nanoparticles (*vide supra*) by using only small structures **(Au-132)₂₋₄** and **(Au-133)₂₋₄** to minimize the influence of incidentally neighboring particles. Also, only particle-particle distances below 2.8 nm, the full stretched length of the diacetylene OPE spacer, were considered. The **(Au-132)₂₋₄** structures show a relatively broad interparticle distance distribution in a range between 0.5 and 2.5 nm with a maximum at about 1.2 nm (Figure 65). These results compare very well with the interparticle distance distribution that was found for the heptamer coated nanoparticles with the same OPE functional unit **(Au-66)₂₋₄**. The pyridine functionalized structures **(Au-133)₂₋₄** show an additional sharp maximum at about 2.7 nm, which is very close to the theoretical stretched length of the expected diacetylene OPE unit. This clearly shows that a perpendicular arrangement of the pyridine moiety relative to the nanoparticle surface is possible. Furthermore, the relatively narrow distance distribution between 2.3 and 2.8 nm indicates that such an arrangement is favored, which is probably due to the interaction between the pyridine and the gold surface. A closer investigation reveals that the first maximum of **(Au-133)₂₋₄** at about 1.4 nm is at longer distances than the maximum that is found for **(Au-132)₂₋₄**. This shift might be explained by the formation of direct bonds between the free acetylene and the gold surface, as was discussed before (section 3.3.4). For such structures, interparticle distances of 1.4 - 1.5 nm would be expected.

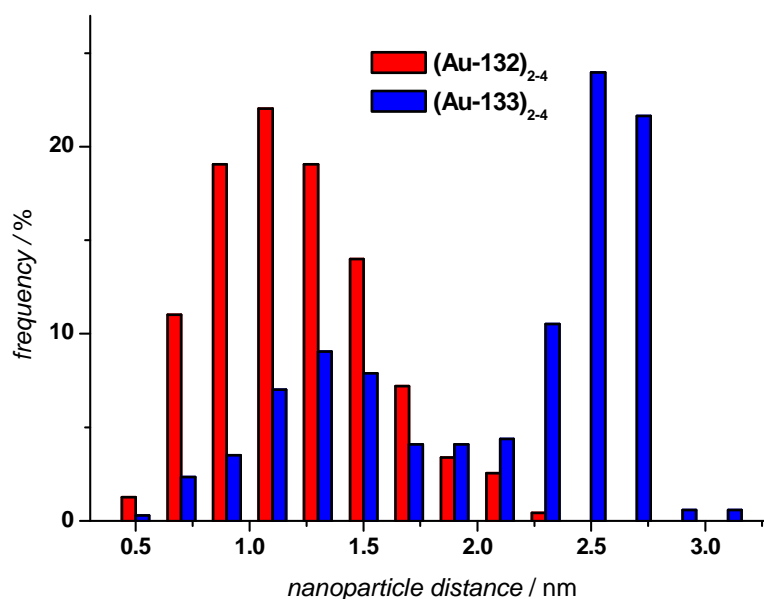


Figure 65. Interparticle distance distributions of nanoparticle superstructures **(Au-132)₂₋₄** and **(Au-133)₂₋₄**.

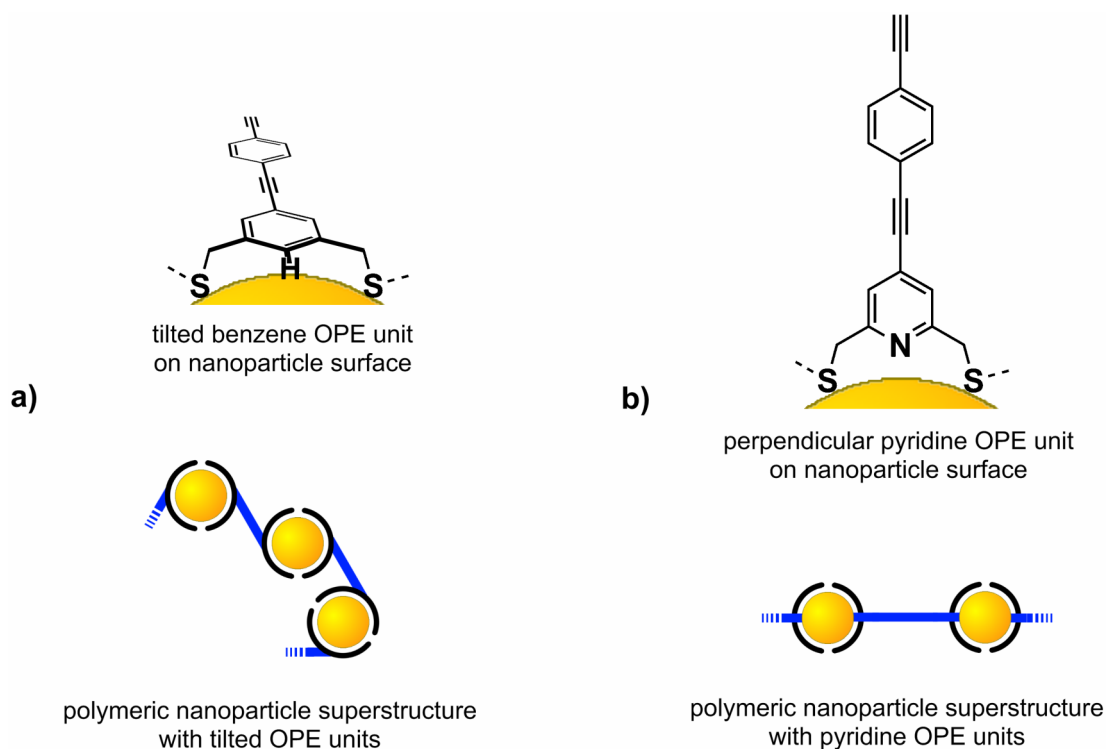


Figure 66. Schematic representation of the different arrangements of the functional OPE units of **Au-132** (a) and **Au-133** (b) relative to the nanoparticle surfaces and examples for the consequences of these arrangements on diacetylene interlinked nanoparticle superstructures. The thioether ligands are represented in black, while the functional OPE units are drawn as blue bars.

The formation of mainly smaller nanoparticle superstructures with the second generation dendrimers **132** and **133** can probably be attributed directly to the large surface area that can be covered by the ligands. Both, the dendrimer and the heptamer coated nanoparticles were found to be mainly difunctionalized. However, the calculated results that were obtained for the **Au-27** particles indicate that probably even particles smaller than 1.0 nm are stabilized by more than one heptameric ligand. On the other hand, spherical 1.0 nm particles that are found in the distributions of the dendrimer stabilized **Au-132** and **Au-133** have already approximately half of the surface than the average 1.35 nm particles and are therefore very likely stabilized by only one G2 dendrimer ligand **132** or **133**. The reaction with such monofunctionalized particles can stop the nanoparticle polymerization process and provides therefore smaller oligomeric superstructures that do not precipitate from the reaction mixture.

3.4.6 Summary and Conclusions

Large thioether dendrimers were synthesized and employed for the stabilization of gold nanoparticles by direct two-phase synthesis. The synthesis of the dendrons was developed such, that functionalized building blocks can be introduced in a final synthetic step to form monofunctionalized thioether dendrimers. Initially, dendrimers with ethylene dithiol bridges were synthesized with up to 92 thioether moieties. However, in gold nanoparticle formation experiments, these dendrimers did not provide an efficient stabilizing layer for the nanoparticles and the coagulation to larger particles or bulk gold was observed. The ethylene dithiol bridges were then exchanged with sterically demanding *t*-butyl benzene units. Nanoparticles stabilized by such sterically demanding second generation dendrimers were found to be stable and also more monodisperse than the particles stabilized by linear heptameric thioether ligands. Furthermore, the particles stabilized by the OPE functionalized G2 dendrimers **132** or **133** have average diameters around 1.3 nm, which is larger than the diameter of the heptameric thioether stabilized nanoparticles. This shows that the nanoparticle sizes can indeed be steered by the size and shape of the coating thioether ligand.

Similar to the OPE functionalized gold nanoparticles stabilized by linear ligands, nanoparticle superstructures were formed with **Au-132** and **Au-133** by oxidative diacetylene formation. In these cases, no precipitation of nanoparticle aggregates was observed upon application of the oxidative Hay conditions, showing that mainly smaller nanoparticle superstructures were obtained in these cases. Even more interestingly, the investigation of the interparticle distances in the nanoparticles superstructures of the pyridine functionalized **Au-133** particles shows that this functional unit allows the perpendicular arrangement of OPE unit relative to the nanoparticle surface. A high degree of control over the spatial arrangement of functional groups can thus be achieved with pyridine functionalized dendrimers.

The pyridine functionalized dendrimer **133** does not only provide more control over nanoparticle arrangements and nanoparticle sizes, but was also found to be more stable and easier to purify than the dendrimers that are based on benzene derivatives as central OPE building blocks. Larger dendrimers with pyridine central units can thus provide a versatile tool for the formation of selectively functionalized gold nanoparticles as 'artificial molecules'.

4 Mixed Thiol-Thioether Monolayers on Gold Surfaces

In this part, investigations on the film forming properties of linear mixed thiol/thioether compounds on gold surfaces will be presented.

Self-assembled monolayers (SAMs) of organic molecules provide a flexible and simple system to tailor the interfacial properties of metal or semiconductor surfaces.^[308] SAM forming molecules have a chemical functionality with a high affinity for the surface that allows the adsorption on the surface and also the spontaneous formation of crystalline structures. Due to the high affinity of thiols for the surfaces of coinage metals, the most extensively studied examples of SAMs are derived from the strong chemisorption of organic thiols on gold, silver and copper. Especially with *n*-alkanethiols on gold surfaces, highly ordered and stable SAMs were obtained.^[308] However, it was shown already in 1988 that the much weaker interaction between dialkylsulfides and gold surfaces can also provide ordered SAMs.^[309] In direct comparison with alkanethiol derived SAMs, dialkylsulfide SAMs on gold were found to be much less robust and also not as well ordered.^[284,310-313] Initial indications of C-S bond cleavage in dialkylsulfides on gold surfaces^[314] were later found to be due to minor (~0.1%) thiol impurities, which led to the displacement of weakly bound thioethers.^[315] More stable and better packed monolayers based on sulfides were obtained by using oligodentate thioether ligands such as the tetradentate calix(4)arene derived thioether ligand **18** from Reinhoudt *et al.*^[316-318] (see Figure 28, section 3.2) or other tridentate thioether ligands.^[319,320]

In this context, mixed thiol-thioether compounds are attractive substrates for the formation and investigation of SAMs on gold surfaces, as the behavior of such mixed compounds has not been studied so far. The linear thiol terminated oligomers **2**, **6**, **8** and **10** as well as the linear monothiols **36** and **39** (Figure 67) were thus investigated on their monolayer forming properties by the group of Michael Zharnikov in Heidelberg.

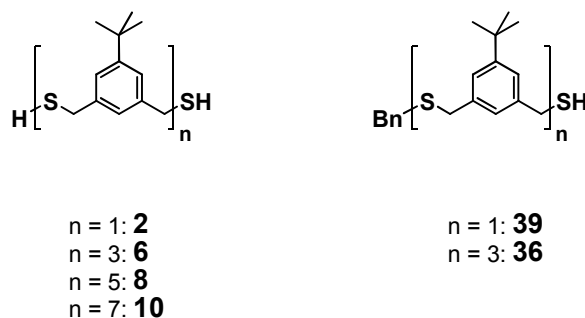


Figure 67. Molecular structures of the thiol/thioether compounds that were studied on gold surfaces.

4.1 Film Preparation and Investigation

Films of the different thiol compounds were prepared by immersion of gold substrates in 10 μM solutions of the thiols in ethanol for 24 hours at room temperature. After thorough rinsing with toluene, the so prepared organic films were characterized by synchrotron-based high resolution X-ray photoelectron spectroscopy (HRXPS) and in the cases of the dithiol oligomers also by near edge X-ray absorption fine structure spectroscopy (NEXAFS, also called X-ray absorption near edge spectroscopy, XANES).

NEXAFS can provide information on the molecular orientation on the surface. The orientation of the polarized X-ray photon beam can be changed with respect to the surface, whereby signals from particular orbitals can be enhanced or cancelled. In the particular cases of the linear oligothioethers, the relative orientation of the phenyl rings to the gold surfaces can be probed.^[321] The NEXAFS investigations of the films of the dithiol/oligothioether compounds **2**, **6**, **8** and **10** show very similar spectra in all four cases (Figure 68). Also the measured angle dependency is very small, showing that the orientation of the phenyl rings relative to the surface is not clearly defined. Predominantly, the phenyl rings have an upright orientation with a large inclination. From these data, it can also be concluded that the gold surfaces are passivated and protected from further contamination.

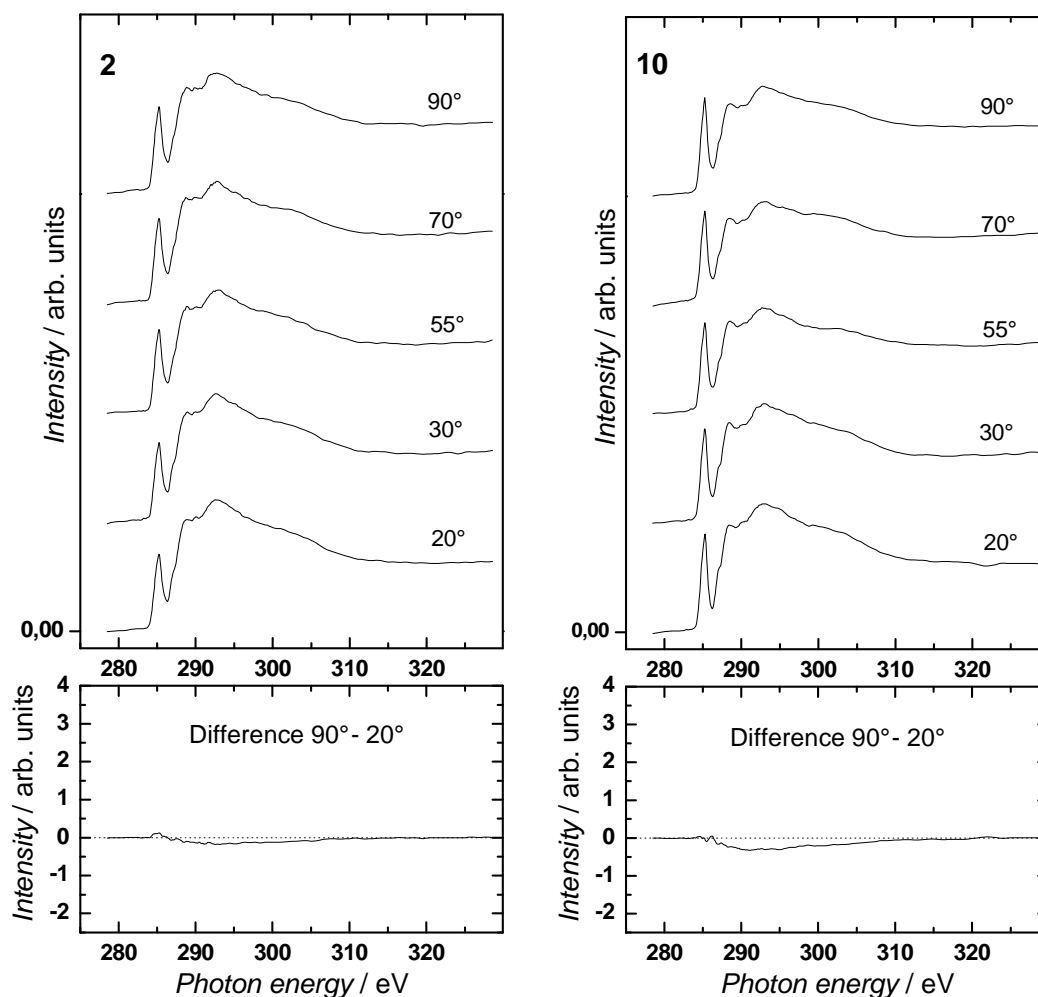


Figure 68. NEXAFS spectra of the monomer dithiol **2** and the heptamer dithiol **10** measured at different angles between 20° and 90°.

The HRXP spectra at the S 2p core level clearly show the presence of several S 2p_{3/2,1/2} doublets related to individual sulfur moieties in all cases (Figure 69). The doublets are found at S 2p_{3/2} binding energies of *ca.* 161.0 eV, 161.9 eV and 163.2 eV. A signal at *ca.* 162 eV is commonly assigned as a gold bound thiolate species.^[315,321,322] The prominent signal at about 163.2 eV can be due to different species: binding energies in this region have been assigned to unbound thiols, but were also found for physisorbed as well as for neat dialkylsulfides.^[315] Furthermore, doublets in this region were also attributed to disulfide species.^[323] The less prominent feature at *ca.* 161 eV can be ascribed either to atomic sulfur^[324] or to differently adsorbed sulfur species.^[325,326] Although this signal can be commonly found in thiolate monolayers on gold surfaces, the exact nature of this species remains unclear.^[320,321]

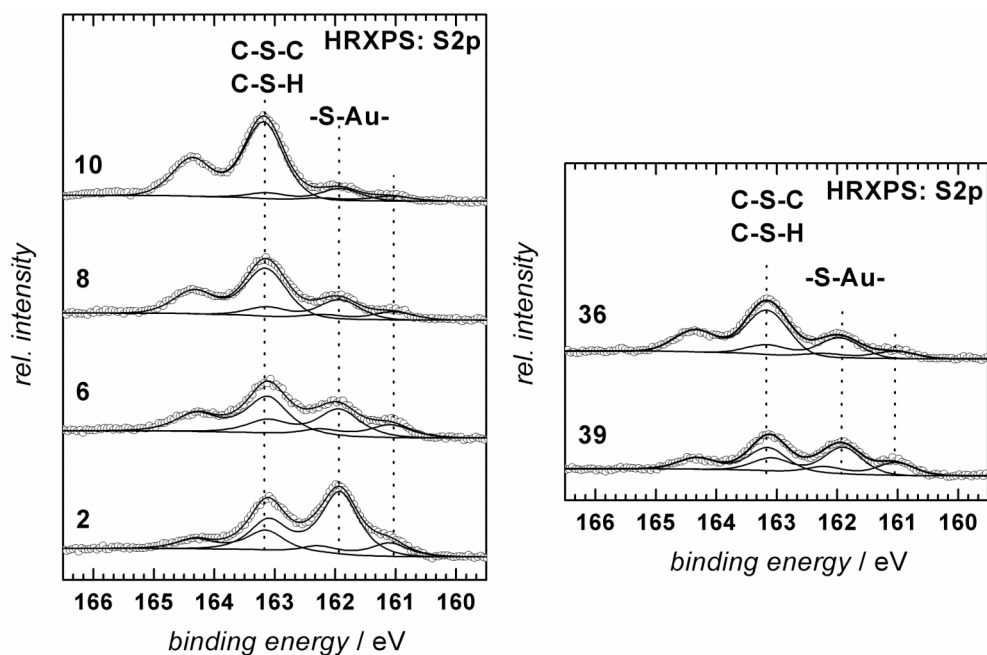


Figure 69. S 2p HRXP spectra of films of the dithiols **2**, **6**, **8** and **10** and of the monothiols **36** and **39**.

A signal at 161 eV is found in all cases with relative weights between 5% (for the dithiol heptamer **10**) and 20% (for the monothiol monomer **39**). Due to the unclear nature of this signal, only the relative proportions of the other two signals at *ca.* 162 eV and 163 eV were considered. The relative weights of these two signals are summarized in Table 1. With increasing thioether content, the proportion of the signal at 163.2 eV increases from 34% for the dithiol monomer **2** to 86% for the dithiol heptamer **10**. These results show that not all thiol moieties of the dithiols **2**, **6**, **8** and **10** are bound to the gold surface, as no signal in the 163 - 164 eV region would be expected for the dithiol monomer **2**. Also, the proportions of the signals in this region for the longer dithiol oligomers **6**, **8** and **10** are slightly larger than the thioether proportions in the molecules (**6**: 50%; **8**: 67%; **10**: 75%).

| Dithiol ligands | 162 eV signal / % | 163 eV signal / % |
|--------------------|-------------------|-------------------|
| Monomer 2 | 76 (65) | 34 (21) |
| Trimer 6 | 42 (35) | 58 (48) |
| Pentamer 8 | 28 (25) | 72 (64) |
| Heptamer 10 | 14 (13) | 86 (82) |
| Monothiol ligands | | |
| Monomer 39 | 52 (42) | 48 (38) |
| Trimer 36 | 30 (27) | 70 (63) |

Table 1. Relative weights of the HRXP signals at 162 eV and 163 eV. The signal proportions under consideration of the signals at 161 eV are given in parentheses.

For the two monothiol ligands **36** and **39**, the relative weights of the signals for thiolate bound sulfur and the signal at 163.2 eV fit very well with the thioether/thiol ratios of the molecules (1:1 for **39** and 3:1 for **36**). In these two cases, all thiol moieties are probably bound to the gold surface.

The thicknesses of the organic films on the gold substrates in comparison with films of known thickness were also determined by HRXPS, using the intensity ratios of the C 1s and Au 4f signals. For the dithiols **2**, **6**, **8** and **10** as well as for the monothiols **36** and **39**, the film thicknesses increase with increasing chain length (Table 2).

| Dithiol ligands | Film thickness / Å |
|--------------------|--------------------|
| Monomer 2 | 8.4 |
| Trimer 6 | 10.0 |
| Pentamer 8 | 12.5 |
| Heptamer 10 | 17.1 |
| Monothiol ligands | |
| Monomer 39 | 8.5 |
| Trimer 36 | 12.2 |

Table 2. Film thicknesses of the dithiol ligands **2**, **6**, **8** and **10** and of the monothiol ligands **36** and **39** on gold surfaces.

The two monomeric ligands **36** and **39** both provide films with a thickness of *ca.* 8.5 Å, while the longest dithiol oligomer **10** gives films with a thickness of around 17 Å. Very importantly, the film of the monothiol trimer **36** is significantly thicker than the film of the dithiol trimer **6** and is approximately the same height as the film of the dithiol pentamer **8**.

From these data it can be concluded that the dithiol oligomers **2**, **6**, **8** and **10** are predominantly bound to the surface by both thiol moieties, forming bridge-like structures with unbound thioether moieties (Figure 70). It seems however that a significant part of the molecules is bound by one of the two thiol groups only, leading to a low degree of order in the films as was found by NEXAFS. On the other hand, all thiol groups of the monothiols **36** and **39** that are present on the gold surface seem to be bound in a thiolate fashion, while the thioether groups are not bound to the surface (Figure 70).

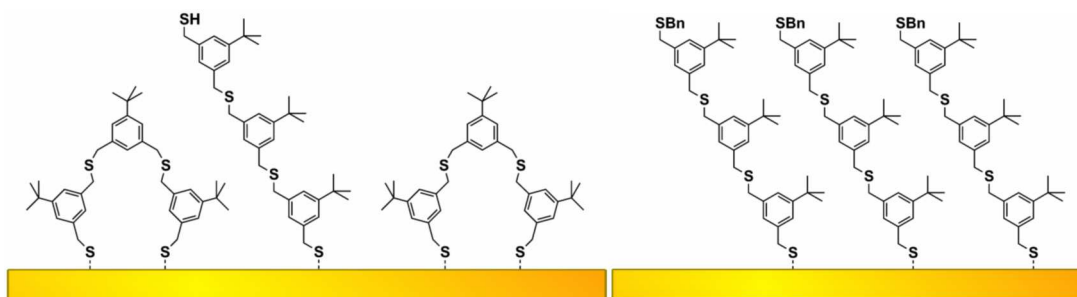


Figure 70. Schematic representation of the different possible binding modes to gold surfaces of the dithiol trimer **6** (left) and the monothiol trimer **36** (right).

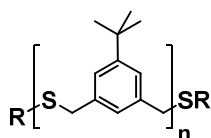
In accordance with previous results,^[315] the investigations concerning mixed thiol-thioether compounds suggest that free thiols bind much stronger to gold surfaces than thioethers. In the presented cases, the thiol moieties seem to account completely for the attachment of the mixed thiol-thioether molecules to the surfaces, while the thioethers remain unbound.

Based on these preliminary results concerning the arrangement and the binding modes of mixed thiol-thioether films on gold surfaces, further investigations will be done by scanning tunneling microscopy (STM). This technique should allow for the visualization of ordered film domains and thus give further insight to the surface passivation of thiol-thioether compounds.

5 Summary and Outlook

A set of linear and dendritic thioether ligands for the ligand controlled synthesis and surface functionalization of gold nanoparticles was developed. The properties of the thioether ligands concerning the sizes as well as the stability and dispersity of gold nanoparticles were investigated. It was shown that the size and surface functionalization of gold nanoparticles can be controlled by the thioether ligands. Furthermore, the functionalized nanoparticles can be employed as synthetic building blocks or 'artificial molecules' for the formation of nanoparticle superstructures by standard wet synthetic chemistry.

Initial experiments were geared towards the formation of thioether coated gold nanoparticles or clusters by exchange of the ligand shell of molecularly defined gold clusters. For the exchange of the eight phosphine ligands of $[\text{Au}_9(\text{PPh}_3)_8](\text{NO}_3)_3$, the linear octadentate ligand **1** based on benzylic thioethers was synthesized (Figure 71). Different attempts to introduce the thioether ligand and remove the phosphine ligands of the Au_9 cluster or water soluble derivatives thereof were not successful. It was then tried to introduce the heptamer **1** to gold nanoparticles that were only weakly stabilized by diglyme. The results of this study indicate firstly the coagulation of gold nanoparticles to larger particles and secondly the formation of nanoparticle aggregates by the octadentate thioether ligand. Based on these observations it was concluded that multidentate thioether ligands might not be ideally suited for the stabilization of gold nanoparticles by ligand exchange due to their weak binding properties and their multidentate nature that allows for the interlinkage of nanoparticles. Although conditions for the formation of thioether coated gold nanoparticles using ligand exchange reactions might be found, the general applicability of this method regarding the introduction of thioether ligands of different sizes seems to be limited.



- 1:** $n = 7$; $R = \text{Me}$ **24:** $n = 1$; $R = \text{Bn}$ **26:** $n = 5$; $R = \text{Bn}$
25: $n = 3$; $R = \text{Bn}$ **27:** $n = 7$; $R = \text{Bn}$

Figure 71. Molecular structures of unfunctionalized linear thioether ligands.

It was then shown that the heptamer **1** can be efficiently employed for the direct synthesis of gold nanoparticles with diameters smaller than 2 nm by reduction of a gold(III) precursor in the presence of the ligand in a two phase reaction system. Following this result, the requirements for the stabilization of gold nanoparticles by multidentate thioether ligands were investigated. For this, the mono- to heptameric thioether ligands **24** - **27** were synthesized (Figure 71). These ligands are based solely on dibenzyl sulfides and do not contain any other functional groups, allowing for a comprehensive study on the nanoparticle stabilizing and size steering properties of such thioether ligands. While the monomer stabilized **Au-24** particles were found to be only weakly stabilized by the dithioether ligand, the larger oligomers **25** - **27** with four to eight thioether moieties provided more stable gold nanoparticles. In particular the heptamer stabilized **Au-27** particles displayed a high long term stability in CH_2Cl_2 or toluene dispersion as well as in the solid phase even after removal of the phase transfer agent TOAB by precipitation of the nanoparticles and excess ligand by GPC. Analysis of the particle sizes by TEM revealed that mainly particles with diameters of 1.0 nm were obtained in the presence of the heptameric ligand **27**. It was found that only two heptameric thioether ligands **27** are required to stabilize one 1.0 nm particle.

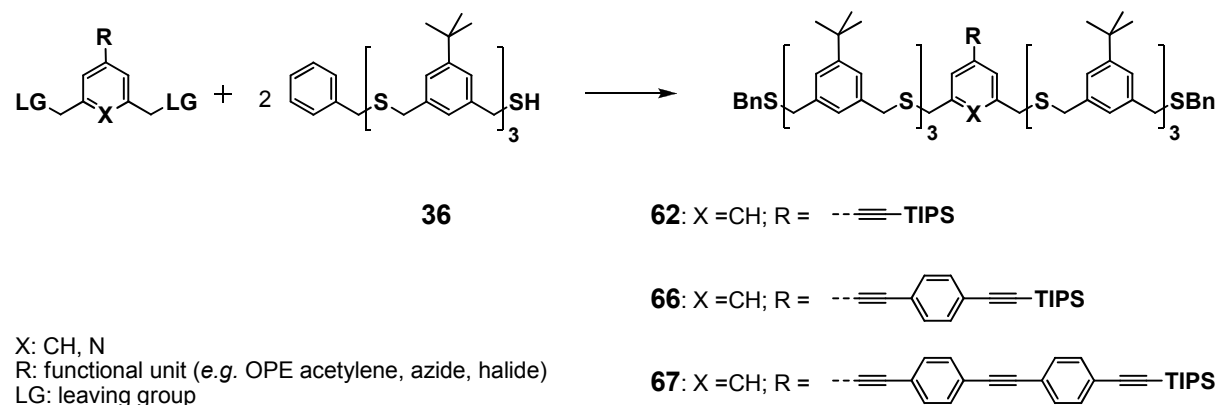


Figure 72. Modular synthetic strategy for the formation of monofunctionalized heptameric thioether ligands. Molecular structures of the trimer thioether building block **36** and the OPE functionalized ligands **62**, **66** and **67**.

On the basis of these results, building blocks for the modular synthesis of monofunctionalized thioether ligands for the formation of gold nanoparticles as 'artificial molecules' for nanoparticle superstructures were developed and synthesized (Figure 72). For the synthesis of functionalized ligands based on the structure of the linear heptameric ligand **27**, the monothiol trimer **36** was prepared. This thioether building block can be fused with different functional blocks carrying leaving groups in benzylic positions to form monofunctionalized heptamer

ligands. Functional building blocks were prepared with rigid rod type OPE structures of different length that carry TIPS protected acetylenes or with aryl azides for 'click' chemistry applications. In view of the application of thioether stabilized gold nanoparticles in single molecule electronic investigations, functional building blocks based on pyridine or thiophenol that allow for the electronic coupling of the ligand shell and the gold nanoparticle were developed. It was shown that both building blocks can be efficiently integrated to monofunctionalized thioether ligands.

To show the applicability of thioether coated gold nanoparticles as 'artificial molecules' for wet chemistry processing, acetylene functionalized gold nanoparticles were prepared in the presence of the ligands **62**, **66** and **67** (Figure 72), carrying rigid rod type OPE units of different length. The acetylene functionality on the nanoparticle surface allows - among *e.g.* Sonogashira coupling reactions or the formation of acetylene metal complexes - the covalent interlinkage of the nanoparticles by oxidative acetylene homocoupling. The length of the rigid rod interparticle spacer determines thereby the interparticle spacing in the linked nanoparticle superstructures.

As for the unfunctionalized heptamer coated **Au-27** particles, average diameters of *ca.* 1.0 nm with a deviation of 0.2 nm were found in the TEM micrographs of the OPE functionalized nanoparticles. Investigation by TGA revealed that the main fraction of particles is stabilized by two or three functionalized thioether ligands. Therefore also only a small number of functional acetylene groups is present per particle after removal of excess ligand molecules by GPC. The conjugated OPE units allowed thereby to monitor presence of the thioether ligands as stabilizer for the gold nanoparticles by UV/vis spectroscopy.

The TIPS-acetylene functionalized gold nanoparticles were covalently interlinked by oxidative diacetylene formation (Figure 73). A one-pot deprotection/oxidation procedure was developed and applied to the OPE functionalized gold nanoparticles. This led to the formation of nanoparticle aggregates, which was evident by the formation of precipitates and by aggregated nanoparticle structures and small nanoparticle superstructures in the TEM micrographs of the reaction mixtures. As such aggregates were not observed when the unfunctionalized **Au-27** particles were subjected to this procedure, these aggregates were due to the covalent interlinkage of nanoparticles by diacetylene formation. The formation of diacetylene linked gold nanoparticles was further corroborated by UV/vis, where a red shift of the OPE signals was observed, indicating the increased conjugation length of the diacetylene linked OPE spacers. After removal of large nanoparticle aggregates by an aqueous work-up

procedure and by filtration, mainly single particles and small superstructures of gold nanoparticles were found by TEM. Investigation of the interparticle distances in these structures revealed an increase of the particle-particle distances with increasing length of the OPE spacer of the acetylene functionalized ligand, showing the power of functionalized thioether ligands as building blocks or 'artificial molecules' that are processable by standard organic chemistry.

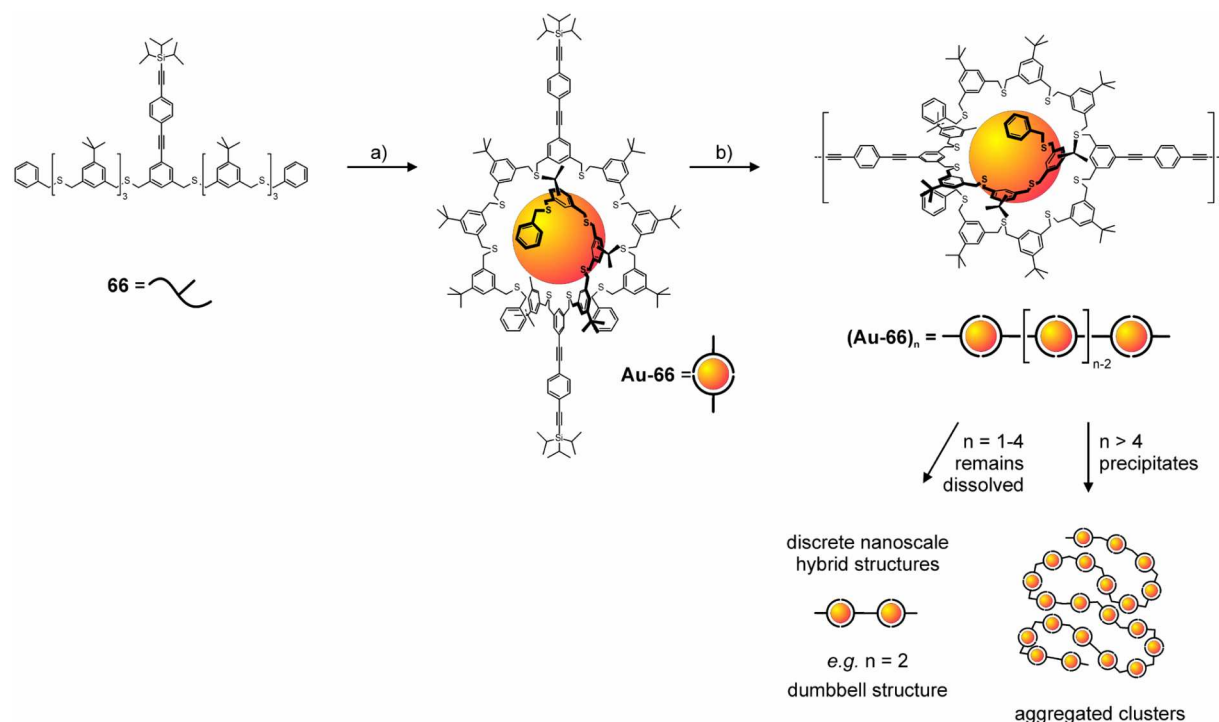


Figure 73. Increasing levels of structural complexity emerging from the ligand **66**. a) The thioether heptamer stabilizes gold particles of a given size and a low number of ligands at its surface (reaction conditions: HAuCl_4 , TOAB, NaBH_4 , $\text{CH}_2\text{Cl}_2/\text{H}_2\text{O}$; GPC.) b) Deprotection of the acetylene enables the formation of organic/inorganic hybrid chains by oxidative acetylene coupling (reaction conditions: 1. TBAF in CH_2Cl_2 , RT; 2. TMEDA, CuCl , RT). While longer chains aggregate and precipitate, short hybrid superstructures comprising up to approximately four interlinked particles remain in dispersion.

In order to be able to enwrap, stabilize and functionalize also gold nanoparticles with diameters larger than 1 nm and to investigate the nanoparticle size steering properties of multidentate thioether ligands, dendritic thioether ligands were developed. Initial gold nanoparticle formation experiments with thioether dendrimers based on mesitylene branching unit and ethylene dithiol bridges provided only very unstable particles. The basic dendrimer design was then developed further and the ethylene dithiol bridges were exchanged with the sterically more demanding monomer units of the linear thioether ligands (Figure 74).

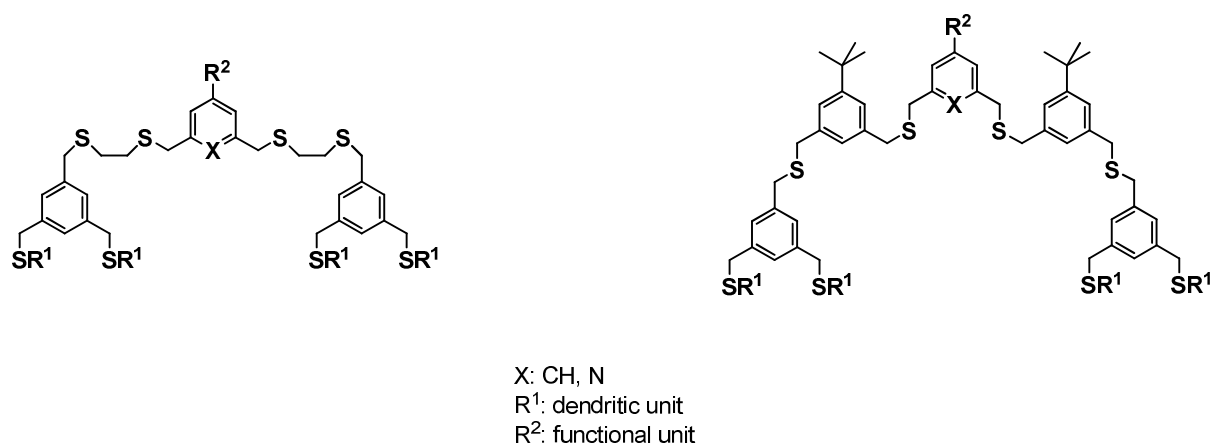


Figure 74. Initial thioether dendrimer design (left) and structure of sterically more demanding thioether dendrimers (right).

First and second generation thioether dendrimers were prepared efficiently. However, careful optimization of the reaction conditions was necessary, as hard to separate by-products often occurred. Furthermore, a limited long-term stability was found for the OPE functionalized G1 and G2 dendrimer ligands **131** and **132** (Figure 75), which might be attributed to the presence of minor amounts of the by-products. These problems were circumvented by using a pyridine functionalized building block as central unit for the dendrimer. The G2 dendrimer **133** was found to be more stable than **132** and also easier to separate from the by-products.

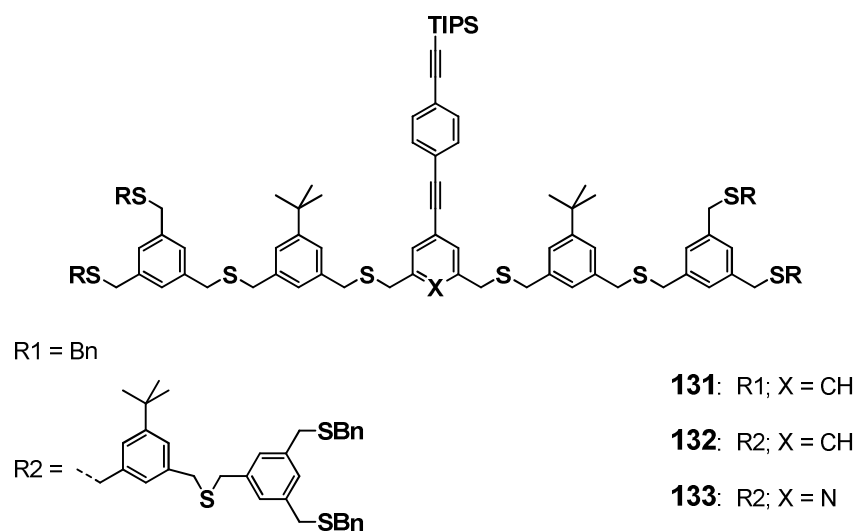


Figure 75. Molecular structures of the thioether dendrimers **131**, **132** and **133**.

First investigations on the nanoparticle stabilizing properties of the second generation dendrimer **133** showed the size steering properties of the multidentate thioether ligands. With the larger dendrimer ligand, nanoparticles with average diameters of *ca.* 1.3 ± 0.15 nm were

obtained. In addition the higher stability of the pyridine based ligand, the pyridine OPE functional moiety allows for a better control over the arrangement of gold nanoparticles. Similar to before, diacetylene-linked gold nanoparticle superstructures were prepared in a one-pot deprotection/ oxidation procedure. The investigation of the interparticle distances of the superstructures by TEM revealed larger distances with a less broad distance distribution compared to the nanoparticle superstructures that were obtained with benzene-OPE ligands such as **132**. The pyridine moiety allows thereby for a perpendicular arrangement of the rigid OPE rod relative to the nanoparticle surface, providing an even higher degree of control over the spatial arrangement of nanoparticles and the distances of functional moieties from the nanoparticle surface.

As these studies were geared mainly towards a proof of the concept of thioether coated nanoparticles as 'artificial molecules' for wet chemistry processing, some issues require further investigations. In particular the delicate synthesis of the dendritic thioether ligands should be revisited in order to have a reliable pathway towards higher dendrimer generations for the formation of larger nanoparticles. Also, factors concerning the monodispersity and the exact sizes of the thioether stabilized gold nanoparticles have not been varied systematically. The influence of thioether/gold ratio, concentration or temperature during nanoparticle synthesis should therefore be investigated in order to be able to fully control the outcome of the nanoparticle preparation.

Apart from that, the results obtained within this work open a wide playground for the preparation of selectively functionalized nanoparticles as building blocks for nanoparticle superstructures. The highly modular synthesis of the thioether ligands allows thereby for the easy exploration of ligands of variable sizes and with variable functionalities. The well developed acetylene functionalized thioether ligands as well as for instance the azide functionalized ones can provide versatile and selective tools for the formation of nanoparticle superstructures. Furthermore, the thiophenol building block can provide even more control on the degree of functionalization of nanoparticles, as thioether ligands with this central unit might be suitable for ligand exchange experiments with nanoparticles of predefined sizes. Also, single particle or single molecule electronic investigations become possible with thiophenol or pyridine derived functional thioether ligands.

The nanoparticle stabilizing properties of multidentate thioether ligands are probably not restricted to gold. Other metals such as silver, palladium or platinum are also interesting targets for the formation of thioether coated 'artificial molecules'.

6 Experimental Part

6.1 Materials and Methods

Solvents and Reagents

Reagents were used as received from *Fluka AG* (Buchs, Switzerland), *Acros AG* (Basel, Switzerland), *Merck* (Darmstadt, Germany) and *Aldrich* (Buchs, Switzerland) unless otherwise stated. Solvents for chromatography and extractions were of technical grade and were distilled prior to use. Dry solvents used for reactions corresponded to the quality *puriss p. a., abs., over Molecular Sieves* from *Fluka AG*. For an inert atmosphere *Argon 4.8* from *PanGas AG* (Dagmersellen, Switzerland) was used.

UV/vis spectroscopy

UV/vis spectra were recorded on an *Agilent 8453* diode array detector spectrophotometer using optical 114-QS *Hellma* cuvettes (10 mm light path).

NMR spectroscopy

Nuclear magnetic resonance (NMR) spectra were recorded using a *Bruker DPX-NMR* (400 MHz for ^1H and 100 MHz for ^{13}C) or a *Bruker DRX-500* (500 MHz for ^1H and 125 MHz for ^{13}C) spectrometer at ambient temperature in the solvents indicated. Solvents for NMR were obtained from *Cambridge Isotope Laboratories* (Andover, MA, USA). Chemical shifts are given in ppm relative to tetramethylsilane (TMS). The spectra are referenced to the residual proton signal of the deuterated solvent (CDCl_3 : 7.26 ppm, CD_2Cl_2 : 5.33 ppm, DMSO-d_6 : 2.49 ppm) for ^1H spectra or the carbon signal of the solvent (CDCl_3 : 77.0 ppm, CD_2Cl_2 : 55.8 ppm, DMSO-d_6 : 39.5 ppm) for ^{13}C spectra. The coupling constants (J) are given in Hertz (Hz), the multiplicities are denoted as: *s* (singlet), *d* (duplet), *t* (triplet), *q* (quartet), *m* (multiplet) and *br* (broad).

Mass spectrometry (MS)

Electron impact (EI) mass spectra and fast atom bombardment (FAB) mass spectra were recorded by *Dr. H. Nadig* on a *finnigan MAT 95Q* for EI-MS and on a *finnigan MAT 8400* for FAB-MS in the mass spectrometry laboratory of the institute. As matrix for FAB-MS *m*-nitro-benzyl alcohol or glycine was used. Electron spray ionization (ESI) mass spectra were recorded on a *Bruker Esquire 3000plus*. Matrix-assisted laser desorption/ionization-time of flight (MALDI-TOF) mass spectra were performed on a *Applied Bio Systems Voyager-De™*

Pro mass spectrometer using 1,8,9-anthracenetriol or α -cyano-4-hydroxycinnamic acid as matrix. Important signals are given in mass units per charge (m/z), the fragments and intensities are given in brackets.

Gel permeation chromatography (GPC)

Gel permeation chromatography for the purification of gold nanoparticles was performed using *Bio-Rad Bio-Beads S-X1 Beads* (operating range 600 – 14000 g/mol) with toluene as eluent.

Elemental analysis (EA)

Elemental analyses were carried out by W. Kirsch on a *Perkin-Elmer Analysator 240*. The values are given in mass percent.

Melting points (MP)

Melting points (MP) were determined in °C using a *Stuart SMP3* apparatus and are uncorrected.

Column Chromatography

For preparative separations by column chromatography, silica gel 60 from *Fluka* (0.043-0.06 mm) was used.

Thin layer chromatography (TLC)

Thin layer chromatography was performed on 0.25 mm precoated aluminium plates (silica gel 60 F₂₅₄, *Merck AG*, Darmstadt, Germany). Compounds were detected at 254 nm by fluorescence quenching or at 366 nm by self-fluorescence. If necessary, the plates were stained by dipping into a cerium(IV) reagent^[132] (molybdophosphoric acid and cerium(IV) sulfate dissolved in a mixture containing water and concentrated sulfuric acid) or Gibbs reagent^[132] (100 mg 2,6-dibromoquinone-4-chloroimide with sodium hydrogen carbonate in DMSO/chloroform).

Thermogravimetric Analysis (TGA)

TGA was performed on a *Mettler Toledo TGA/SDTA851^e* with a heating rate of 10°C/minute.

High Resolution Scanning Transmission Electron Microscopy (HRSTEM)

HRSTEM was performed by Alla Sologubenko on a *FEI Tecnai F20* operating at 200 kV and a *FEI Titan S* operating at 300 kV. For TEM studies, particles were brought on a conventional amorphous carbon TEM grid by carefully putting a drop of the nanoparticle dispersion on a grid and letting it dry in air.

Transmission Electron Microscopy (TEM)

TEM was performed by Philippe Ringler on a *Philips CM100* transmission electron microscope at 80 kV. The particles were deposited by carefully putting a drop of the nanoparticle dispersion on top of a thin carbon film that spanned a perforated carbon support film covering a gold-plated copper microscopy grid.

High Resolution X-ray Photoelectron Spectroscopy (HRXPS)

Synchrotron-based HRXP spectra were recorded and interpreted by Michael Zharnikov and coworkers. HRXPS experiments were performed at the MAX-lab synchrotron radiation facility in Lund, Sweden.

Near Edge X-ray Absorption Fine Structure Spectroscopy (NEXAFS)

NEXAFS was performed by Michael Zharnikov and coworkers at the synchrotron radiation facility BESSY II in Berlin, Germany.

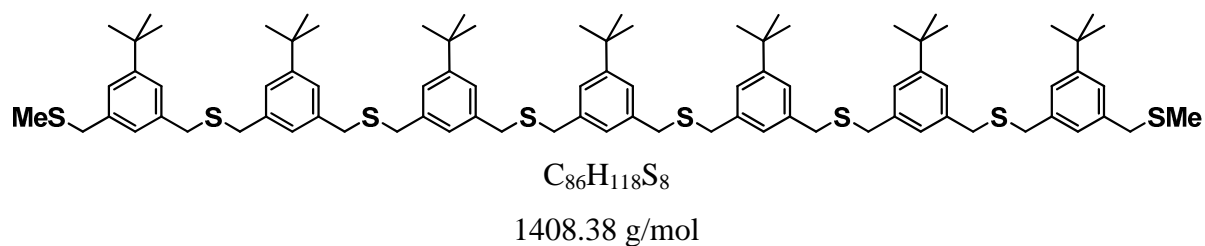
General remark

The synthetic procedures are ordered in the chapters *Unfunctionalized Thioether Ligands*, *Linear Monothiol Building Blocks*, *Acetylene Functionalized Thioether Ligands*, *Azide Functionalized Thioether Ligands*, *Pyridine Functionalized Thioether Ligands*, *Towards Thiophenol Building Blocks* and *Dendritic Thioether Ligands* according to the outline of the synthetic parts of section 3 (*Thioether Coated Nanoparticles*). Within these individual chapters, the respective compounds are arranged in numerical order.

6.2 Synthetic Procedures

6.2.1 Unfunctionalized Thioether Ligands

(5-*tert*-Butyl-1,3-phenylene)bis(methylene)bis((3-*tert*-butyl-5-((3-*tert*-butyl-5-((3-*tert*-butyl-5-(methylthiomethyl)benzylthio)methyl)benzylthio)methyl)benzyl)sulfane) (**1**)

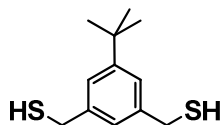


Sodium hydride (60% in mineral oil, 35 mg, 0.9 mmol, 10 eq) was added to a solution of the heptameric dithiol **10** (125.4 mg, 0.09 mmol, 1 eq) in dry tetrahydrofuran under an atmosphere of argon. After the gas formation had ceased, iodomethane (12.5 μ l, 28.4 mg, 0.20 mmol, 2.2 eq) was added and the mixture was left stirring for 2 hours at room temperature. The reaction was quenched with water and then extracted three times with MTBE. The combined organic fractions were washed with brine, dried over magnesium sulfate, filtered and evaporated to dryness. The crude was purified by column chromatography (hexane/dichloromethane 2:3) to give the desired methylated heptamer **1** as colorless solid. 112 mg, 0.08 mmol, 89%.

EA: found: C 73.34%, H 8.44%
 required: C 73.34%, H 8.44%

1H NMR (400 MHz, $CDCl_3$): δ = 7.20 – 7.17 (*m*, 14H, Aryl-*H*), 7.10 – 7.08 (*m*, 5H, Aryl-*H*), 7.07 – 7.05 (*m*, 2H, Aryl-*H*), 3.65 (*s*, 4H, CH_2), 3.61 – 3.58 (*m*, 24H, CH_2), 2.00 (*s*, 6H, CH_3), 1.33 – 1.29 (*m*, 63H, $C(CH_3)_3$).

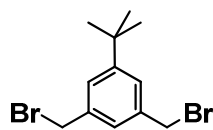
^{13}C NMR (100 MHz, $CDCl_3$): δ = 151.6 (3 \times), 138.0, 137.9, 126.8, 126.6, 124.7 (2 \times), 124.6, 38.6, 36.0, 35.9, 34.6 (2 \times), 31.4 (2 \times), 15.1.

(5-*tert*-Butyl-1,3-phenylene)dimethanethiol^[119] (**2**)

A solution of 1,3-bis(bromomethyl)-5-*tert*-butylbenzene (**3**) (3.00 g, 9.3 mmol, 1 eq) and thiourea (1.77 g, 23.3 mmol, 2.5 eq) in dry dimethyl sulfoxide (40 ml) under an atmosphere of argon was left stirring for 15 h at room temperature. The mixture was poured into an ice cold aqueous sodium hydroxide solution (1M, 50 ml), which was then acidified with 1M hydrochloric acid. The mixture was extracted with dichloromethane 3 times and the combined organic fractions were washed once with water. The crude product was obtained after drying over magnesium sulfate, filtration and evaporation to dryness. After purification by kugelrohr distillation (2×10^{-1} mbar, 195°C), the pure title compound **2** was obtained as colorless solid. 1.34 g, 6.0 mmol, 64%.

¹H NMR (400 MHz, CDCl₃): δ = 7.22 (*br*, 2H, Aryl-*H*), 7.14 (*br*, 1H, Aryl-*H*), 3.74 (*d*, J = 7.5 Hz, 4H, CH₂), 1.79 (*t*, J = 7.5 Hz, 2H, SH), 1.33 (*s*, 9H, C(CH₃)₃).

¹³C NMR (100 MHz, CDCl₃): δ = 152.1, 141.1, 124.8, 123.8, 34.7, 31.3, 29.1.

1,3-Bis(bromomethyl)-5-*tert*-butylbenzene^[120] (**3**)

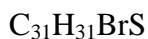
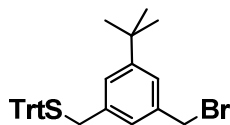
320.06 g/mol

N-Bromosuccinimide (30.17 g, 170 mmol, 2.1 eq) and 5-*tert*-butyl-*m*-xylene (15.0 ml, 12.98 g, 80 mmol, 1 eq) were dissolved in methyl formate (150 ml). 2,2'-Azobis(2-methylpropionitrile) (75 mg) was then added and the reaction mixture was illuminated by a 500 W halogen lamp for 3 hours. The solvent was evaporated by using a rotary evaporator and the residue was redissolved in dichloromethane. The organic solution was washed twice with a saturated aqueous solution of sodium hydrogen carbonate and then once with water. After drying with magnesium sulfate, the dichloromethane was removed by evaporation. The residue was recrystallized from dichloromethane/hexane twice to give 1,3,5-tris(bromomethyl)benzene (**3**) as colorless crystals.

18.02 g, 56.3 mmol, 70%.

¹H NMR (400 MHz, CDCl₃): δ = 7.34 (*br*, 2H, Aryl-*H*), 7.27 (*br*, 1H, Aryl-*H*), 4.49 (*s*, 4H, CH₂), 1.34 (*s*, 9H, C(CH₃)₃).

¹³C NMR (100 MHz, CDCl₃): δ = 153.0, 138.4, 127.3, 126.7, 35.2, 33.9, 31.6.

(3-(Bromomethyl)-5-*tert*-butylbenzyl)(trityl)sulfane (4)

515.55 g/mol

1,3-bis(bromomethyl)-5-*tert*-butylbenzene (**3**) (1.00 g, 3.1 mmol, 1 eq) and triphenylmethane-thiol (863 mg, 3.1 mmol, 1 eq) were dissolved in 20 ml dry tetrahydrofuran under an atmosphere of argon. Potassium carbonate (650 mg, 4.7 mmol, 1.5 eq) was added and the mixture was heated to reflux for 20 hours. After cooling to room temperature, 100 ml water was added and the mixture was extracted three times with 50 ml MTBE. The combined organic fractions were washed with brine, dried over magnesium sulfate and evaporated to dryness. After purification by column chromatography (hexane/dichloromethane 4:1), the product **4** was obtained as colorless solid.

818 mg, 1.6 mmol, 51%.

EA: found: C 71.92%, H 6.20%
required: C 72.22%, H 6.06%

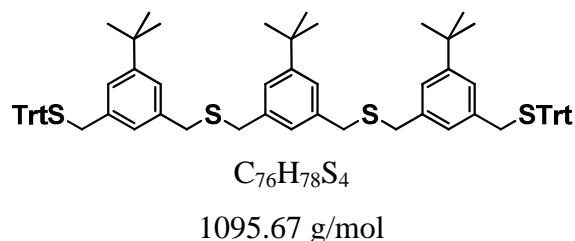
¹H NMR (400 MHz, CDCl₃): $\delta = 7.49 - 7.44$ (*m*, 6H, Aryl-*H*, Trt-*H*), $7.35 - 7.20$ (*m*, 10H, Trt-*H*), 7.03 (*s*, 1H, Aryl-*H*), 6.95 (*s*, 1H, Aryl-*H*), 4.43 (*s*, 2H, CH₂), 3.33 (*s*, 2H, CH₂), 1.27 (*s*, 9H, C(CH₃)₃).

¹³C NMR (100 MHz, CDCl₃): $\delta = 151.97, 144.65, 137.50, 137.46, 129.65, 127.94, 126.82, 126.72, 126.30, 124.81, 67.60, 36.95, 34.65, 33.95, 31.23$.

MS (MALDI-TOF, *m/z*): 537.0 [*M*+Na]⁺.

MP: 140.1°C.

(5-*tert*-Butyl-1,3-phenylene)bis(methylene)bis((3-*tert*-butyl-5-(tritylthiomethyl)benzyl)sulfane) (5)



(5-*tert*-Butyl-1,3-phenylene)dimethanethiol (**2**) (154 mg, 0.68 mmol, 1 eq) and (3-(Bromomethyl)-5-*tert*-butylbenzyl)(trityl)sulfane (**4**) (700 mg, 1.36 mmol, 2 eq) were dissolved in 40 ml dry tetrahydrofuran under an atmosphere of argon. Sodium hydride (60% in mineral oil, 135 mg, 3.3 mmol, 5 eq) was added and the mixture was stirred for 2 hours at room temperature. The reaction was quenched with water and extracted with MTBE three times. The combined organic fractions were washed with brine, dried over magnesium sulfate and evaporated to dryness. Purification of the crude product was achieved by column chromatography (hexane/dichloromethane 3:2) to yield the trityl protected trimer as colorless foam.

708 mg, 0.65 mmol, 96 %.

EA: found: C 81.10%, H 7.25%
required: C 81.12%, H 7.18%

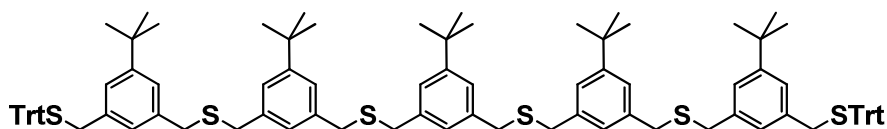
1H NMR (400 MHz, $CDCl_3$): δ = 7.49 – 7.44 (*m*, 12H, Trt-*H*), 7.32 – 7.27 (*m*, 12 H, Trt-*H*), 7.24 – 7.19 (*m*, 6H, Trt-*H*), 7.16 (*br*, 2H, Aryl-*H*), 7.13 (*br*, 2H, Aryl-*H*), 7.04 (*br*, 1H, Aryl-*H*), 6.98 (*br*, 2H, Aryl-*H*), 6.90 (*br*, 2H, Aryl-*H*), 3.55 (*s*, 4H, CH_2), 3.54 (*s*, 4H, CH_2), 3.30 (*s*, 4H, CH_2), 1.29 (*s*, 9H, $C(CH_3)_3$), 1.26 (*s*, 18H, $C(CH_3)_3$).

^{13}C NMR (100 MHz, $CDCl_3$): δ = 151.5, 144.7, 138.0, 137.9, 137.0, 129.7, 128.0, 126.8, 126.7, 124.8, 124.7, 67.5, 37.2, 35.9, 34.6 (2 \times), 31.4, 31.3.

MS (MALDI-TOF, *m/z*): 1033.3 [$M+K$] $^+$.

MP: 70.0°C.

(5-*tert*-Butyl-1,3-phenylene)bis(methylene)bis((3-*tert*-butyl-5-((3-*tert*-butyl-5-(tritylthiomethyl)benzylthio)methyl)benzyl)sulfane) (7)



1480.31 g/mol

The dithiol trimer **6** (227.0 mg, 0.37 mmol, 1 eq) and (3-(Bromomethyl)-5-*tert*-butylbenzyl)(trityl)sulfane (**4**) (421.4 mg, 0.82 mmol, 2.2 eq) were dissolved in 20 ml dry tetrahydrofuran under an atmosphere of argon. Sodium hydride (60% in mineral oil, 60 mg, 1.5 mmol, 4 eq) was added and the mixture was stirred for 1.5 hours at room temperature. The reaction was quenched with water and extracted with MTBE three times. The combined organic fractions were washed with brine, dried over magnesium sulfate and evaporated to dryness. Purification of the crude product was achieved by column chromatography (hexane/dichloromethane 3:2) to yield the trityl protected pentamer **7** as colorless foam. 525.5 mg, 0.36 mmol, 97 %.

EA: found: C 79.57%, H 7.64%
required: C 79.52%, H 7.49%

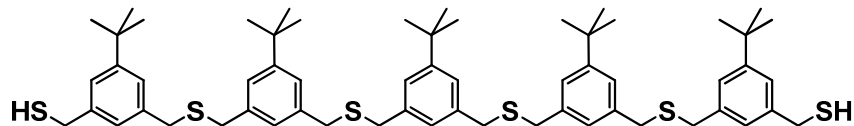
¹H NMR (400 MHz, CDCl₃): δ = 7.50 – 7.44 (*m*, 12H, Trt-*H*), 7.33 – 7.27 (*m*, 12H, Trt-*H*), 7.24 – 7.19 (*m*, 6H, Trt-*H*), 7.18 – 7.05 (*m*, 11H, Aryl-*H*), 6.98 (*br*, 2H, Aryl-*H*), 6.90 (*br*, 2H, Aryl-*H*), 3.60 – 3.54 (*m*, 16H, CH₂), 3.31 (*s*, 4H, CH₂), 1.32 – 1.24 (*m*, 45H, C(CH₃)₃).

¹³C NMR (100 MHz, CDCl₃): δ = 151.5, 144.7, 138.0, 137.9, 137.0, 129.7, 127.9, 126.8, 126.7, 126.6, 124.8, 124.7, 67.5, 37.2, 36.0, 35.9, 34.6 (2×), 31.3 (2×).

MS (MALDI-TOF, *m/z*): 1017.9 [*M* – (2×Trt) + Na]⁺, 1518.2 [*M*+K]⁺.

MP: 71.2°C.

5,5'-(5,5'-(5-*tert*-Butyl-1,3-phenylene)bis(methylene)bis(sulfanediyl)bis(methylene)bis(3-*tert*-butyl-5,1-phenylene)bis(methylene)bis(sulfanediyl)bis(methylene))bis(3-*tert*-butyl-5,1-phenylene)dimethanethiol (8)



995.68 g/mol

The trityl protected pentamer **7** (563.9 mg, 0.38 mmol, 1 eq) was dissolved in 6 ml dichloromethane. Triethylsilane (160 μl , 115.2 mg, 1.00 mmol, 2.6 eq) was added, followed by trifluoroacetic acid (240 μl , 4% of the dichloromethane volume). The mixture turned yellow and became colorless again after approx. 2 minutes. Stirring was continued for further 10 minutes, then the reaction was quenched with a saturated sodium bicarbonate solution. The two phases were separated and the aqueous phase was washed twice with dichloromethane. The combined organic fractions were dried over magnesium sulfate, filtrated and evaporated to dryness. The product was purified by column chromatography (hexane/dichloromethane 1:2), to give the dithiol pentamer **8** as colorless solid.

375.5 mg, 0.38 mmol, 99%.

EA: found: C 72.24%, H 8.34%
required: C 72.38%, H 8.30%

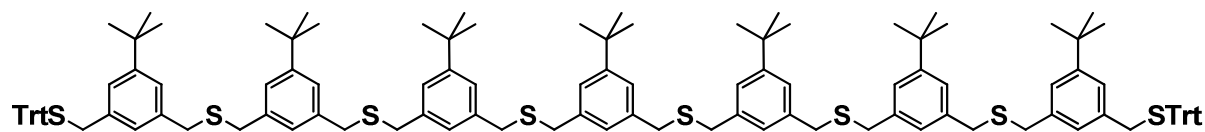
^1H NMR (400 MHz, CDCl_3): δ = 7.21 – 7.18 (*m*, 10H, Aryl-*H*), 7.11 – 7.06 (*m*, 5H, Aryl-*H*), 3.71 (*d*, J = 7.5 Hz, 4H, CH_2), 3.63 – 3.57 (*m*, 16H, CH_2), 1.76 (*t*, J = 7.5, 2H, *SH*), 1.33 – 1.29 (*m*, 45H, $\text{C}(\text{CH}_3)_3$).

^{13}C NMR (100 MHz, CDCl_3): δ = 151.8, 151.6, 140.9, 138.2, 138.0, 126.8, 125.8, 124.8, 124.7, 123.8, 36.0 (2 \times), 35.9, 34.7, 34.6, 31.4 (2 \times), 29.1.

MS (MALDI-TOF, m/z): 1017.9 [$M+\text{Na}$] $^+$.

MP: 107.5 $^\circ\text{C}$.

(5-*tert*-Butyl-1,3-phenylene)bis(methylene)bis((3-*tert*-butyl-5-((3-*tert*-butyl-5-((3-*tert*-butyl-5-(tritylthiomethyl)benzylthio)methyl)benzylthio)methyl)benzylthio)methyl)benzyl)sulfane) (9)



1864.95 g/mol

The dithiol pentamer **8** (365.0 mg, 0.37 mmol, 1 eq) and 1(3-(Bromomethyl)-5-*tert*-butylbenzyl)(trityl)sulfane (**4**) (416.1 mg, 0.81 mmol, 2.2 eq) were dissolved in 20 ml dry tetrahydrofuran under an atmosphere of argon. Sodium hydride (60% in mineral oil, 140 mg, 3.5 mmol, 9.5 eq) was added and the mixture was stirred for 2.5 hours at room temperature. The reaction was quenched with water and extracted with MTBE three times. The combined organic fractions were washed with brine, dried over magnesium sulfate and evaporated to dryness. Purification of the crude product was achieved by column chromatography (hexane/dichloromethane 2:3) to yield the trityl protected heptamer **9** as colorless solid. 624.3 mg, 0.34 mmol, 92 %.

EA: found: C 78.50%, H 7.80%
required: C 78.57%, H 7.67%

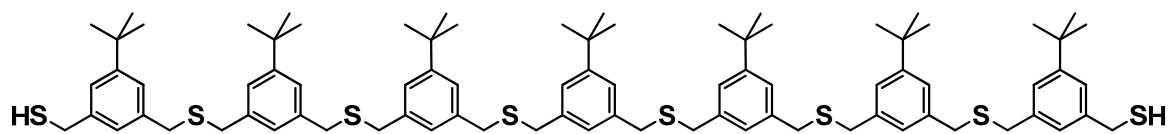
¹H NMR (400 MHz, CDCl₃): δ = 7.50 – 7.44 (*m*, 12H, Trt-*H*), 7.33 – 7.27 (*m*, 12H, Trt-*H*), 7.25 – 7.06 (*m*, 23 H, Aryl-*H*, Trt-*H*), 6.99 (*br*, 2H, Aryl-*H*), 6.91 (*br*, 2H, Aryl-*H*), 3.62 – 3.54 (*m*, 24H, CH₂), 3.31 (*s*, 4H, CH₂), 1.34 – 1.26 (*m*, 63H, C(CH₃)₃).

¹³C NMR (100 MHz, CDCl₃): δ = .151.5, 144.72, 138.0, 137.9, 137.0, 129.7, 127.9, 126.8, 126.7, 124.8, 124.7, 67.5, 37.2, 36.0, 35.9, 34.6 (2×), 31.4, 31.3.

MS (MALDI-TOF, *m/z*): 1901.8 [*M*+*K*]⁺.

MP: 71.5°C.

5,5'-(5,5'-(5,5'-(5-*tert*-Butyl-1,3-phenylene)bis(methylene)bis(sulfanediyl)bis(methylene)-bis(3-*tert*-butyl-5,1-phenylene)bis(methylene)bis(sulfanediyl)bis(methylene))bis(3-*tert*-butyl-5,1-phenylene)bis(methylene)bis(sulfanediyl)bis(methylene))bis(3-*tert*-butyl-5,1-phenylene)dimethanethiol (10**)**



1380.32 g/mol

The trityl protected heptamer **9** (295.7 mg, 0.16 mmol, 1 eq) was dissolved in 4 ml dichloromethane. Triethylsilane (101 μl , 73.5 mg, 0.63 mmol, 4 eq) was added, followed by trifluoroacetic acid (160 μl , 4% of the dichloromethane volume). The mixture turned yellow and became colorless again after approximately 2 minutes. Stirring was continued for further 10 min, before the reaction was quenched with a saturated sodium bicarbonate solution. The two phases were separated and the aqueous phase was washed twice with dichloromethane. The combined organic fractions were dried over magnesium sulfate, filtrated and evaporated to dryness. The product was purified by column chromatography (hexane/dichloromethane 1:1), to give the dithiol heptamer **10** as colorless solid.

215.9 mg, 0.16 mmol, 99%.

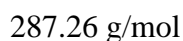
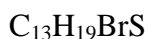
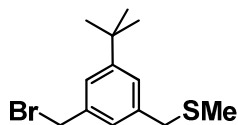
EA: found: C 73.00%, H 8.31%
required: C 73.09%, H 8.32%

^1H NMR (400 MHz, CDCl_3): $\delta = 7.21 - 7.17$ (*m*, 14H, Aryl-*H*), $7.11 - 7.06$ (*m*, 7H, Aryl-*H*), 3.71 (*d*, $J = 7.5$ Hz, 4H, CH_2), $3.62 - 3.57$ (*m*, 24H, CH_2), 1.76 (*t*, $J = 7.5$, 2H, *SH*), $1.33 - 1.29$ (*m*, 63H, $\text{C}(\text{CH}_3)_3$).

^{13}C NMR (100 MHz, CDCl_3): $\delta = 151.8, 151.6, 140.9, 138.2, 138.0, 126.8, 125.8, 124.8, 124.7, 123.8, 36.0, 35.9, 34.7, 34.6, 31.4$ (2 \times), 29.1.

MS (MALDI-TOF, m/z): 1401.1 [$M+\text{Na}$] $^+$.

MP: 131.0°C.

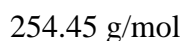
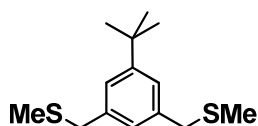
(3-(Bromomethyl)-5-*tert*-butylbenzyl)(methyl)sulfane (11)

To a solution of 1,3-Bis(Bromomethyl)-5-*tert*-butylbenzene (**3**) (500 mg, 1.56 mmol, 1 eq) in dry *N,N*-dimethylformamide (10 ml) under an atmosphere of argon was added sodium methanethiolate (110 mg, 1.56 mmol, 1 eq). The mixture was stirred for 3 hours at room temperature, before MTBE was added. The diluted reaction mixture was extracted with water four times, followed once by brine. The organic fraction was then dried over magnesium sulfate, filtered and evaporated to dryness. After purification by column chromatography (hexane/dichloromethane, 3:1) the title compound **11** was obtained as colorless liquid. The compound was not stable upon storage at 4°C (see section 3.1.1).

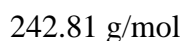
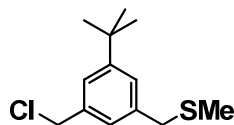
58.1 mg, 0.20 mmol, 13%.

The starting material 1,3-Bis(Bromomethyl)-5-*tert*-butylbenzene (**3**) (99.3 mg, 0.31 mmol, 20%) and the disubstituted compound **12** (44.3 mg, 0.17 mmol, 11.2%) were also isolated.

$^1\text{H NMR}$ (400 MHz, CDCl_3): $\delta = 7.28$ (*br*, 1H, Aryl-*H*), 7.24 (*br*, 1H, Aryl-*H*), 7.16 (*br*, 1H, Aryl-*H*), 4.49 (*s*, 2H, CH_2), 3.67 (*s*, 2H, CH_2), 2.01 (*s*, 3H, CH_3), 1.32 (*s*, 9H, $\text{C}(\text{CH}_3)_3$).

(5-*tert*-Butyl-1,3-phenylene)bis(methylene)bis(methylsulfane) (12)

$^1\text{H NMR}$ (400 MHz, CDCl_3): $\delta = 7.18$ (*br*, 2H, Aryl-*H*), 7.06 (*br*, 1H, Aryl-*H*), 7.16 (*br*, 1H, Aryl-*H*), 3.67 (*s*, 4H, CH_2), 2.01 (*s*, 6H, CH_3), 1.32 (*s*, 9H, $\text{C}(\text{CH}_3)_3$).

(3-*tert*-Butyl-5-(chloromethyl)benzyl)(methyl)sulfane (13)

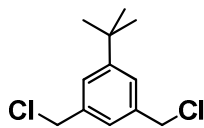
To a solution of 1,3-Bis(chloromethyl)-5-*tert*-butylbenzene (**14**) (737 mg, 3.19 mmol, 1 eq) in dry *N,N*-dimethylformamide (30 ml) under an atmosphere of argon was added sodium methanethiolate (221 mg, 3.19 mmol, 1 eq). The mixture was stirred for 2 hours at room temperature, before MTBE was added. The diluted reaction mixture was extracted with water four times, followed once by brine. The organic fraction was then dried over magnesium sulfate, filtered and evaporated to dryness. After purification by column chromatography (hexane/dichloromethane, 3:1, then 3:2, then 2:3) the title compound **13** was obtained as colorless liquid.

132 mg, 0.55 mmol, 18%.

The starting material 1,3-bis(chloromethyl)-5-*tert*-butylbenzene (**14**) (280 mg, 1.21 mmol, 38%) and the disubstituted compound **12** (207 mg, 0.81 mmol, 26%) were also isolated.

$^1\text{H NMR}$ (400 MHz, CDCl_3): $\delta = 7.28$ (*br*, 1H, Aryl-*H*), 7.27 (*br*, 1H, Aryl-*H*), 7.16 (*br*, 1H, Aryl-*H*), 4.59 (*s*, 2H, CH_2), 3.68 (*s*, 2H, CH_2), 2.02 (*s*, 3H, CH_3), 1.33 (*s*, 9H, $\text{C}(\text{CH}_3)_3$).

$^{13}\text{C NMR}$ (100 MHz, CDCl_3): $\delta = 152.0, 138.4, 137.3, 126.2, 126.1, 124.3, 46.5, 38.4, 34.7, 31.3, 15.1$.

1-*tert*-Butyl-3,5-bis(chloromethyl)benzene^[149] (**14**)

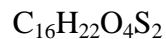
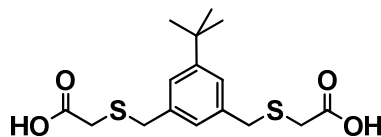
231.16 g/mol

1,3-Bis(bromomethyl)-5-*tert*-butylbenzene (**3**) (2.14 g, 6.7 mmol, 1 eq) was dissolved in dry *N,N*-dimethylformamide (40 ml) under an atmosphere of argon. Lithium chloride (3.80 g, 89.6 mmol, 13 eq) was added and the mixture was stirred at room temperature for 1 hour. MTBE was added and the organic phase was extracted three times with water and subsequently with brine. After drying with magnesium sulfate, filtration and evaporation of the solvent, the title compound **14** was obtained as colorless crystals in sufficient purity.

1.54 g, 6.6 mmol, 99 %.

¹H NMR (400 MHz, CDCl₃): δ = 7.35 (*br*, 2H, Aryl-*H*), 7.25 (*br*, 1H, Aryl-*H*), 4.59 (*s*, 4H, CH₂), 1.33 (*s*, 9H, C(CH₃)₃).

¹³C NMR (100 MHz, CDCl₃): δ = 152.4, 137.7, 125.9, 125.7, 46.2, 34.8, 31.2.

2,2'-(5-*tert*-Butyl-1,3-phenylene)bis(methylene)bis(sulfanediyl)diacetic acid (15)

To a solution of the diester **16** (187 mg, 0.47 mmol, 1 eq) in ethanol (15 ml) was added 1N aqueous sodium hydroxide solution and the mixture was left stirring for 1 hour. The ethanol was removed by rotary evaporation, before the solution was acidified with 1N hydrochloric acid. The resulting colorless solid was extracted with dichloromethane 3 times whereupon the combined organic fractions were dried over magnesium sulfate and filtered. After evaporation of the solvent, the diacid **15** was obtained as colorless solid.

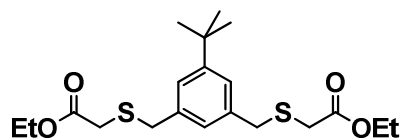
161 mg, 0.47 mmol, quant.

EA: found: C 56.22%, H 6.39%
required: C 56.11%, H 6.47%

¹H NMR (400 MHz, CDCl₃): δ = 10.62 (*br*, 2H, COOH), 7.32 (*m*, 2H, Aryl-*H*), 7.07 (*br*, 1H, Aryl-*H*), 3.85 (*s*, 4H, CH₂), 3.09 (*s*, 4H, CH₂), 1.32 (*s*, 9H, C(CH₃)₃).

¹³C NMR (100 MHz, CDCl₃): δ = 177.1, 152.7, 136.5, 127.9, 125.4, 36.3, 34.7, 31.8, 31.3.

MS (EI, *m/z* (%)): 342.1 (12) [*M*⁺], 324.1 (100) [*M*⁺-H₂O].

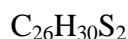
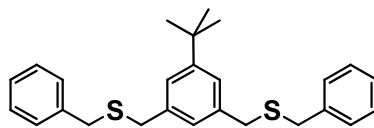
Diethyl 2,2'-(5-*tert*-butyl-1,3-phenylene)bis(methylene)bis(sulfaneyl)diacetate (16)

398.58 g/mol

To a solution of (5-*tert*-butyl-1,3-phenylene)dimethanethiol (**2**) (177.4 mg, 0.8 mmol, 1 eq) in dry dichloromethane (10 ml) under an atmosphere of argon was added ethyl bromoacetate (192 μl , 288 mg, 1.7 mmol, 2.2 eq) and triethylamine (1.20 ml, 870 mg, 8.6 mmol, 10 eq). The mixture was left stirring for 16 hours, before the organic phase was diluted and then washed with 1N hydrochloric acid, followed by water. The dichloromethane phase was dried over magnesium sulfate, filtered and evaporated to dryness. The crude was purified by column chromatography (dichloromethane) to give the pure title compound **16** as colorless oil.

192.6 mg, 0.5 mmol, 62%.

$^1\text{H NMR}$ (400 MHz, CDCl_3): δ = 7.23 (*m*, 2H, Aryl-*H*), 7.13 (*br*, 1H, Aryl-*H*), 4.20 (*q*, J = 7.13 Hz, 4H, CH_2), 3.81 (*s*, 4H, CH_2), 3.07 (*s*, 4H, CH_2), 1.32 (*s*, 9H, $\text{C}(\text{CH}_3)_3$), 1.30 (*t*, J = 7.12 Hz, 6H, CH_3).

(5-*tert*-Butyl-1,3-phenylene)bis(methylene)bis(benzylsulfane) (24)

406.65 g/mol

1,3-Bis(bromomethyl)-5-*tert*-butylbenzene (**3**) (2.645 g, 8.3 mmol, 1 eq) and benzyl mercaptan (2.04 ml, 2.155 g, 17.4 mmol, 2.1 eq) were dissolved in 50 ml dry tetrahydrofuran under an atmosphere of argon. Sodium hydride (60% in mineral oil, 900 mg, 22.5 mmol, 2.7 eq) was added slowly at 0°C. The mixture was then stirred for two hours at room temperature. Water was added to quench the reaction and the mixture was extracted three times with MTBE. The combined organic fractions were washed with brine, dried over magnesium sulfate and evaporated to dryness. After purification by column chromatography (hexane/dichloromethane 4:1), the product **24** was obtained as colorless oil.

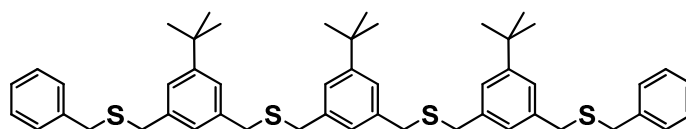
3.212 g, 7.9 mmol, 95%.

EA: found: C 76.74%, H 7.38%
required: C 76.80%, H 7.44%

¹H NMR (400 MHz, CDCl₃): δ = 7.35 – 7.31 (*m*, 10H, Aryl-*H*), 7.14 (*m*, 2H, Aryl-*H*), 7.05 (*m*, 1H, Aryl-*H*), 3.61 (*s*, 4H, CH₂), 3.58 (*s*, 4H, CH₂), 1.31 (*s*, 9H, C(CH₃)₃).

¹³C NMR (125 MHz, CDCl₃): δ = 151.4, 138.1, 137.8, 129.0, 128.4, 126.9, 126.8, 124.8, 35.8, 35.6, 34.6, 31.3.

MS (MALDI-TOF, *m/z*): 428.4 [*M*+Na]⁺, 445.6 [*M*+K]⁺.

(5-*tert*-Butyl-1,3-phenylene)bis(methylene)bis((3-(benzylthiomethyl)-5-*tert*-butylbenzyl)sulfane) (25)

791.29 g/mol

The dithiol trimer **6** (84.6 mg, 0.14 mmol, 1 eq) and benzyl chloride (35 μl , 38.6 mg, 0.30 mmol, 2.1 eq) were dissolved in 10 ml dry tetrahydrofuran under an atmosphere of argon. Sodium hydride (60% in mineral oil, 26 mg, 0.65 mmol, 4.6 eq) was added and the mixture was stirred for 1.5 hours at room temperature. The reaction was quenched with water and extracted with MTBE three times. The combined organic fractions were washed with brine, dried over magnesium sulfate and evaporated to dryness. Purification of the crude product was achieved by column chromatography (hexane/dichloromethane 3:2) to yield the dibenzyl trimer **25** as colorless oil, which slowly solidified at 4°C.

106.8 mg, 0.14 mmol, 98 %.

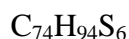
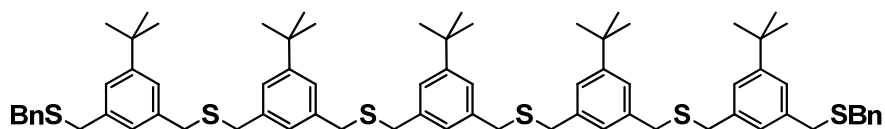
EA: found: C 75.80%, H 7.95%
required: C 75.90%, H 7.90%

^1H NMR (400 MHz, CDCl_3): $\delta = 7.35 - 7.05$ (*m*, 19H, Aryl-*H*), 3.60 (*br*, 12H, CH_2), 3.58 (*s*, 4H, CH_2), 1.31 (*m*, 27H, $\text{C}(\text{CH}_3)_3$).

^{13}C NMR (100 MHz, CDCl_3): $\delta = 151.6, 151.5, 138.2, 138.0, 137.8, 129.0, 128.4, 126.9, 126.8, 124.9, 124.7$ (2 \times), 36.0, 35.8, 35.7, 34.6, 31.4 (2 \times).

MS (MALDI-TOF, *m/z*): 813.3 [$M+\text{Na}$] $^+$, 829.2 [$M+\text{K}$] $^+$.

(5-*tert*-Butyl-1,3-phenylene)bis(methylene)bis((3-((3-(benzylthiomethyl)-5-*tert*-butylbenzylthio)methyl)-5-*tert*-butylbenzyl)sulfane) (26)



1175.93 g/mol

The dithiol pentamer **8** (101 mg, 0.10 mmol, 1 eq) and benzyl chloride (25.5 μl , 28 mg, 0.22 mmol, 2.2 eq) were dissolved in 8 ml dry tetrahydrofuran under an atmosphere of argon. Sodium hydride (60% in mineral oil, 23 mg, 0.58 mmol, 5.8 eq) was added and the mixture was stirred for 1.5 hours at room temperature. The reaction was quenched with water and extracted with MTBE three times. The combined organic fractions were washed with brine, dried over magnesium sulfate and evaporated to dryness. Purification of the crude product was achieved by column chromatography (hexane/dichloromethane 1:1) to yield the dibenzyl pentamer **26** as colorless solid.

115 mg, 0.10 mmol, quant.

EA: found: C 75.40%, H 8.06%
required: C 75.58%, H 8.06%

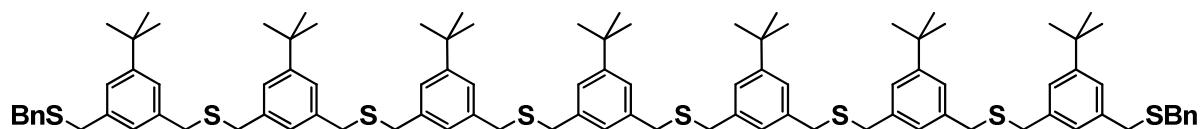
^1H NMR (400 MHz, CDCl_3): $\delta = 7.34 - 7.05$ (*m*, 25H, Aryl-*H*), 3.60 (*br*, 20H, CH_2), 3.57 (*s*, 4H, CH_2), 1.31 (*br*, 45H, $\text{C}(\text{CH}_3)_3$).

^{13}C NMR (125 MHz, CDCl_3): $\delta = 151.6, 151.5, 138.2, 138.0, 137.8, 129.0, 128.4, 127.0, 126.8, 124.9, 124.7$ (2 \times), 36.0, 35.9, 35.8, 35.7, 34.6, 31.4 (2 \times).

MS (MALDI-TOF, *m/z*): 1198.6 [$M+\text{Na}$] $^+$, 1214.9 [$M+\text{K}$] $^+$.

MP: 99.7 $^\circ\text{C}$.

(5-*tert*-Butyl-1,3-phenylene)bis(methylene)bis((3-((3-((3-(benzylthiomethyl)-5-*tert*-butylbenzylthio)methyl)-5-*tert*-butylbenzylthio)methyl)-5-*tert*-butylbenzyl)sulfane) (27)



1560.57 g/mol

The dithiol heptamer **10** (203.0 mg, 0.15 mmol, 1 eq) and benzyl chloride (37 μl , 41.1 mg, 0.32 mmol, 2.1 eq) were dissolved in 10 ml dry tetrahydrofuran under an atmosphere of argon. Sodium hydride (60% in mineral oil, 73 mg, 1.83 mmol, 12 eq) was added and the mixture was stirred for 1.5 hours at room temperature. The reaction was quenched with water and extracted with MTBE three times. The combined organic fractions were washed with brine, dried over magnesium sulfate and evaporated to dryness. Purification of the crude product was achieved by column chromatography (hexane/dichloromethane 2:3) to yield the dibenzyl heptamer **27** as colorless powder.

197.9 mg, 0.13 mmol, 87 %.

EA: found: C 75.38%, H 8.15%
required: C 75.43%, H 8.14%

^1H NMR (400 MHz, CD_2Cl_2): δ = 7.34 – 7.05 (*m*, 31H, Aryl-*H*), 3.61 (*br*, 28H, CH_2), 3.59 (*s*, 4H, CH_2), 1.31 (*m*, 63H, $\text{C}(\text{CH}_3)_3$).

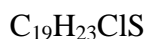
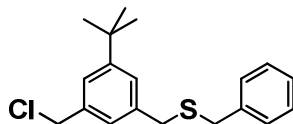
^{13}C NMR (125 MHz, CDCl_3): δ = 151.6, 151.5 (2 \times), 138.2, 138.0, 137.8, 129.0, 128.4, 126.9, 126.8, 124.9, 124.7 (2 \times), 36.0, 35.9, 35.8, 35.7, 34.6, 31.4 (2 \times).

MS (MALDI-TOF, *m/z*): 1582.7 [$M+\text{Na}$] $^+$.

MP: 125.5 $^\circ\text{C}$.

6.2.2 Linear Monothiol Building Blocks

Benzyl(3-*tert*-butyl-5-(chloromethyl)benzyl)sulfane (**28**)



1,3-Bis(chloromethyl)-5-*tert*-butylbenzene (**14**) (122 mg, 0.53 mmol, 1 eq) and benzyl mercaptan (62 μl , 0.53 mmol, 1 eq) were dissolved in 8 ml dry tetrahydrofuran under an atmosphere of argon. Potassium carbonate (110 mg, 0.80 mmol, 1.5 eq) was added and the mixture was heated to reflux for 30 hours. After cooling to room temperature, water was added and the reaction mixture was extracted three times with MTBE. The combined organic fractions were washed with brine, dried over magnesium sulfate and evaporated to dryness. After purification by column chromatography (hexane/dichloromethane 3:1, then 2:1), the title compound **28** was obtained as colorless oil.

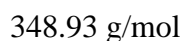
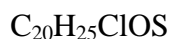
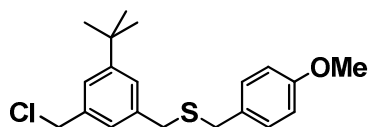
87 mg, 0.27 mmol, 52%.

The starting material 1,3-bis(chloromethyl)-5-*tert*-butylbenzene (**14**) (23.8 mg, 0.10 mmol, 19%) and the disubstituted compound **24** (39.0 mg, 0.10 mmol, 19%) were isolated as well.

EA: found: C 71.22%, H 7.24%
required: C 71.56%, H 7.27%

^1H NMR (400 MHz, CDCl_3): $\delta = 7.35 - 7.24$ (*m*, 6H, Aryl-*H*), 7.22 (*br*, 1H, Aryl-*H*), 7.14 (*br*, 1H, Aryl-*H*), 4.58 (*s*, 2H, CH_2), 3.61 (*s*, 2H, CH_2), 3.59 (*s*, 2H, CH_2), 1.32 (*s*, 9H, $\text{C}(\text{CH}_3)_3$).

^{13}C NMR (100 MHz, CDCl_3): $\delta = 152.0, 138.3, 138.0, 137.3, 129.0, 128.5, 127.0, 126.4, 126.3, 124.3, 46.6, 35.7, 35.6, 34.7, 31.3$.

(3-*tert*-Butyl-5-(chloromethyl)benzyl)(4-methoxybenzyl)sulfane (29)

1,3-Bis(chloromethyl)-5-*tert*-butylbenzene (**14**) (500 mg, 2.16 mmol, 1 eq) and 4-methoxybenzylmercaptan (301 μl , 2.16 mmol, 1 eq) were dissolved in 40 ml dry tetrahydrofuran under an atmosphere of argon. Potassium carbonate (700 mg, 5.06 mmol, 2.3 eq) was added and the mixture was heated to reflux for 30 hours. After cooling to room temperature, water was added and the reaction mixture was extracted three times with MTBE. The combined organic fractions were washed with brine, dried over magnesium sulfate and evaporated to dryness. After purification by column chromatography (hexane/dichloromethane 2:1, then 2:3), the product **29** was obtained as colorless oil.

314 mg, 0.90 mmol, 42%.

The starting material 1,3-bis(chloromethyl)-5-*tert*-butylbenzene (**14**) (164 mg, 0.71 mmol, 33%) was also isolated.

EA: found: C 68.61%, H 7.15%
required: C 68.84%, H 7.22%

^1H NMR (400 MHz, CDCl_3): δ = 7.27 (*br*, 1H, Aryl-*H*), 7.23 (*br*, 1H, Aryl-*H*), 7.20 (*d*, J = 8.6 Hz, 2H, Aryl-*H*), 7.14 (*br*, 1H, Aryl-*H*), 6.85 (*d*, J = 8.6 Hz, 2H, Aryl-*H*), 4.58 (*s*, 2H, CH_2), 3.81 (*s*, 3H, OCH_3), 3.59 (*s*, 2H, CH_2), 3.57 (*s*, 2H, CH_2), 1.33 (*s*, 9H, $\text{C}(\text{CH}_3)_3$).

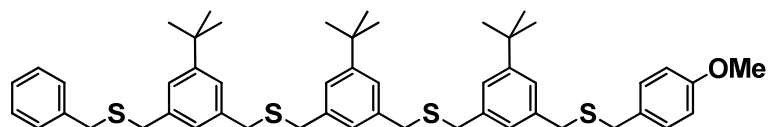
^{13}C NMR (100 MHz, CDCl_3): δ = 158.6, 151.9, 138.4, 137.2, 130.1, 130.0, 126.4, 126.3, 124.2, 113.8, 55.3, 46.6, 35.5, 35.0, 34.7, 31.3.

MS (EI, m/z (%)): 348.1 (11) [M^+], 121.1 (100) [$\text{C}_8\text{H}_9\text{O}^+$].

Formation of the Bn-PMB capped linear oligomers 30 - 32, general procedure

The linear dithiol oligomer (**2**, **6** or **8**, ~0.1 mmol, 1 eq), benzyl(3-*tert*-butyl-5-(chloromethyl)-benzyl)sulfane (**28**) (1.05 eq) and the PMB-capped monochloride **29** (1.05 eq) were dissolved in dry tetrahydrofuran (~10 ml). Sodium hydride (60% in mineral oil, 3 eq) was added and the mixture was stirred for 2 hours at room temperature. The reaction was then quenched with water and extracted with MTBE three times. The combined organic fractions were washed with brine, dried over magnesium sulfate, filtered and evaporated to dryness. The crude mixtures were purified by column chromatography (hexane/dichloromethane 1:1 → dichloromethane) to give the dibenzyl oligomers **25**, **26** or **27**, the Bn-PMB oligomers **30**, **31** or **32** and the di-PMB compounds **33**, **34** or **35**.

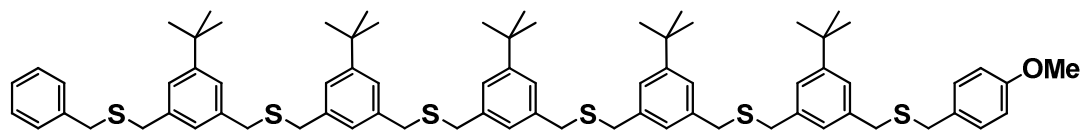
Bn-PMB Trimer 30



821.31 g/mol

Yield: 53%

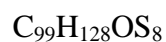
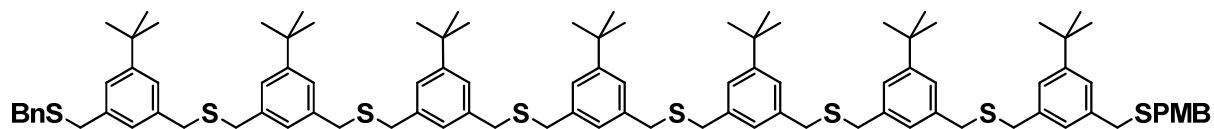
$^1\text{H NMR}$ (400 MHz, CDCl_3): $\delta = 7.31 - 7.25$ (*m*, 5H, Aryl-*H*), $7.21 - 7.16$ (*m*, 6H, Aryl-*H*), 7.14 (*br*, 2H, Aryl-*H*), 7.09 (*br*, 1H, Aryl-*H*), 7.07 (*br*, 2H, Aryl-*H*), 6.83 (*m*, 2H, Aryl-*H*), 3.79 (*s*, 3H, OCH_3), 3.60 (*br*, 10H, CH_2), 3.58 (*s*, 2H, CH_2), 3.57 (*s*, 2H, CH_2), 3.56 (*s*, 2H, CH_2), 1.31 (*m*, 27H, $\text{C}(\text{CH}_3)_3$).

Bn-PMB Pentamer 31

1205.95 g/mol

Yield: 39%

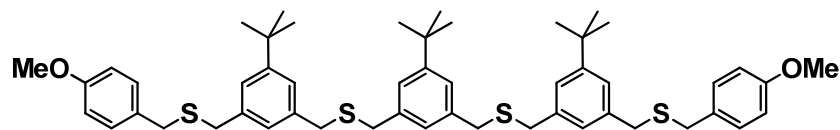
$^1\text{H NMR}$ (400 MHz, CDCl_3): $\delta = 7.31 - 7.25$ (*m*, 5H, Aryl-*H*), 7.21 – 7.16 (*m*, 10H, Aryl-*H*), 7.13 (*br*, 2H, Aryl-*H*), 7.09 (*br*, 3H, Aryl-*H*), 7.06 (*br*, 2H, Aryl-*H*), 6.83 (*m*, 2H, Aryl-*H*), 3.79 (*s*, 3H, OCH_3), 3.60 (*br*, 18H, CH_2), 3.58 (*s*, 2H, CH_2), 3.57 (*s*, 2H, CH_2), 3.56 (*s*, 2H, CH_2), 1.31 (*br*, 45H, $\text{C}(\text{CH}_3)_3$).

Bn-PMB Heptamer 32

1590.60 g/mol

Yield: 37%

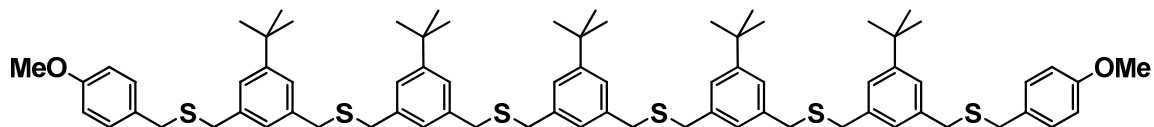
$^1\text{H NMR}$ (400 MHz, CDCl_3): $\delta = 7.31 - 7.25$ (*m*, 5H, Aryl-*H*), 7.21 – 7.16 (*m*, 14H, Aryl-*H*), 7.13 (*br*, 2H, Aryl-*H*), 7.09 (*br*, 5H, Aryl-*H*), 7.06 (*br*, 2H, Aryl-*H*), 6.83 (*m*, 2H, Aryl-*H*), 3.79 (*s*, 3H, OCH_3), 3.60 (*br*, 26H, CH_2), 3.58 (*s*, 2H, CH_2), 3.57 (*s*, 2H, CH_2), 3.56 (*s*, 2H, CH_2), 1.31 (*br*, 64H, $\text{C}(\text{CH}_3)_3$).

Di-PMB Trimer 33

851.34 g/mol

Yield: 18%

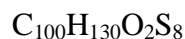
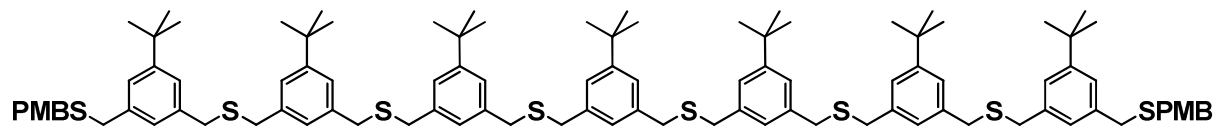
$^1\text{H NMR}$ (400 MHz, CDCl_3): $\delta = 7.21 - 7.16$ (*m*, 8H, Aryl-*H*), 7.14 (*br*, 2H, Aryl-*H*), 7.09 (*br*, 1H, Aryl-*H*), 7.07 (*br*, 2H, Aryl-*H*), 6.83 (*m*, 4H, Aryl-*H*), 3.79 (*s*, 6H, OCH_3), 3.60 (*br*, 8H, CH_2), 3.57 (*s*, 4H, CH_2), 3.56 (*s*, 4H, CH_2), 1.31 (*m*, 27H, $\text{C}(\text{CH}_3)_3$).

Di-PMB Pentamer 34

1235.98 g/mol

Yield: 20%

$^1\text{H NMR}$ (400 MHz, CDCl_3): $\delta = 7.21 - 7.16$ (*m*, 12H, Aryl-*H*), 7.13 (*br*, 2H, Aryl-*H*), 7.09 (*br*, 3H, Aryl-*H*), 7.06 (*br*, 2H, Aryl-*H*), 6.83 (*m*, 4H, Aryl-*H*), 3.79 (*s*, 6H, OCH_3), 3.60 (*br*, 16H, CH_2), 3.57 (*s*, 4H, CH_2), 3.56 (*s*, 4H, CH_2), 1.31 (*br*, 45H, $\text{C}(\text{CH}_3)_3$).

Di-PMB Heptamer 35

1620.62 g/mol

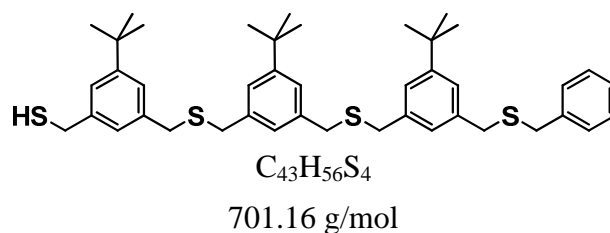
Yield: 11%

$^1\text{H NMR}$ (400 MHz, CDCl_3): $\delta = 7.21 - 7.16$ (*m*, 16H, Aryl-*H*), 7.13 (*br*, 2H, Aryl-*H*), 7.09 (*br*, 5H, Aryl-*H*), 7.06 (*br*, 2H, Aryl-*H*), 6.83 (*m*, 4H, Aryl-*H*), 3.79 (*s*, 6H, OCH_3), 3.60 (*br*, 24H, CH_2), 3.57 (*s*, 4H, CH_2), 3.56 (*s*, 4H, CH_2), 1.31 (*br*, 64H, $\text{C}(\text{CH}_3)_3$).

Deprotection of the PMB protecting group, general procedure

To a mixture of the Bn-PMB oligomer (**30**, **31** or **32**, ~0.03 mmol, 1 eq) and anisole (2 eq) in a 1:1 mixture of dichloromethane and trifluoroacetic acid (2 ml) was added mercury(II) trifluoroacetate (1.1 eq) at 0°C. After 1 hour stirring, the solvents were removed under vacuum at that temperature. The remains were dissolved in dichloromethane (10 ml) and water (10 ml). To this, excess of sodium hydrogen sulfide and trifluoroacetic acid (100 μl) were then added to precipitate the mercury out of the reaction mixture. The organic phase was separated and the aqueous phase was washed twice with dichloromethane. The combined organic fractions were then filtered through a pad of celites. Purification of the crude mixture was achieved by column chromatography (hexane/dichloromethane). However, only after several chromatographic purifications, an anisole derived side product could be removed from the desired monothiol trimer **36**. TLC of the reaction mixtures of the longer oligomers revealed overlapping spots of the products **37** or **38** and the side product.

(3-((3-((3-(Benzylthiomethyl)-5-*tert*-butylbenzylthio)methyl)-5-*tert*-butylbenzylthio)methyl)-5-*tert*-butylphenyl)methanethiol (36)



(3-(Bromomethyl)-5-*tert*-butylbenzyl)(trityl)sulfane (**4**) (934 mg, 1.81 mmol, 1 eq) and SH-SBn-dimer **40** (922 mg, 1.81 mmol, 1 eq) were dissolved in tetrahydrofuran (20 ml) under an atmosphere of argon. Sodium hydride (60% in mineral oil, 109 mg, 2.72 mmol, 1.5 eq) was added at 0°C and the mixture was left stirring for 1 hour. After quenching with water, the reaction mixture was extracted with MTBE three times. The combined organic fractions were washed with brine, dried over magnesium sulfate and evaporated to dryness. The crude STrt-SBn-trimer was dissolved in dichloromethane (15 ml) and triethylsilane (433 μ l, 2.72 mmol, 1.5 eq) was added. To this solution, trifluoroacetic acid (0.6 ml, 4% v/v of dichloromethane) was added dropwise. The mixture was stirred for 15 minutes, quenched with a saturated aqueous solution of sodium hydrogen carbonate and the organic phase was separated. The aqueous phase was washed twice with dichloromethane and the combined organic fractions were dried over magnesium sulfate. After filtration and evaporation of the solvent, the crude product was purified by column chromatography (hexane/dichloromethane 1:1) to yield the pure SH-SBn-trimer **36** as colorless oil, which solidified at 4°C.

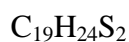
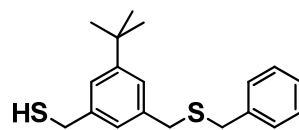
1.111 g, 1.59 mmol, 88 %.

EA: found: C 73.71%, H 8.01%
 required: C 73.66%, H 8.05%

¹H NMR (400 MHz, CDCl₃): δ = 7.35 – 7.18 (*m*, 10H, Aryl-*H*), 7.15 (*br*, 1H, Aryl-*H*), 7.08 (*m*, 3H, Aryl-*H*), 3.72 (*d*, *J* = 7.5 Hz, 2H, CH₂), 3.62 (*m*, 12H, CH₂), 1.77 (*t*, *J* = 7.5 Hz, 1H, SH), 1.33 (*s*, 9H, C(CH₃)₃), 1.32 (*s*, 18H, C(CH₃)₃).

¹³C NMR (100 MHz, CDCl₃): δ = 151.9, 151.6, 151.5, 140.9, 138.2 (2 \times), 138.0, 137.8, 129.0, 128.4, 126.9, 126.8, 125.8, 124.8, 124.7 (3 \times), 123.8, 36.0, 35.9, 35.8, 35.7, 34.7 (2 \times), 34.6, 31.4, 31.3 (2 \times), 29.1.

MS (MALDI-TOF): 724.0 [*M*+Na]⁺, 740.0 [*M*+K]⁺.

(3-(Benzylthiomethyl)-5-*tert*-butylphenyl)methanethiol (39)

316.52 g/mol

(3-(Bromomethyl)-5-*tert*-butylbenzyl)(trityl)sulfane (**4**) (2.059 g, 4.0 mmol, 1 eq) and benzyl mercaptan (492 μ l, 4.2 mmol, 1.05 eq) were dissolved in tetrahydrofuran (70 ml) under an atmosphere of argon. Sodium hydride (60% in mineral oil, 252 mg, 6.3 mmol, 1.6 eq) was added at 0°C and the mixture was left stirring for 1 hour. After quenching with water, the reaction mixture was extracted with MTBE three times. The combined organic fractions were washed with brine, dried over magnesium sulfate and evaporated to dryness. The crude intermediate was dissolved in dichloromethane (30 ml) and triethylsilane (954 μ l, 6.0 mmol, 1.5 eq) was added. To this solution, trifluoroacetic acid (1.2 ml, 4% v/v of dichloromethane) was added dropwise. The mixture was stirred for 15 minutes, quenched with a saturated aqueous solution of sodium hydrogen carbonate and the organic phase was separated. The aqueous phase was washed twice with dichloromethane and the combined organic fractions were dried over magnesium sulfate. After filtration and evaporation of the solvent, the crude product was purified by column chromatography (hexane/dichloromethane 2:1) to yield pure (3-(benzylthiomethyl)-5-*tert*-butylphenyl)methanethiol (**39**) as colorless liquid.

1.030 g, 3.26 mmol, 82%.

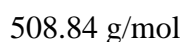
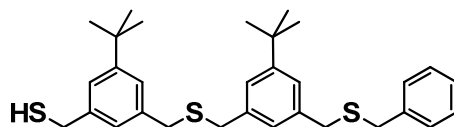
EA: found: C 72.14%, H 7.64%
required: C 72.10%, H 7.64%

¹H NMR (400 MHz, CD₂Cl₂): δ = 7.32 – 7.24 (*m*, 5H, Aryl-*H*), 7.21 (*br*, 1H, Aryl-*H*), 7.14 (*br*, 1H, Aryl-*H*), 7.08 (*br*, 1H, Aryl-*H*), 3.73 (*d*, *J* = 7.5 Hz, 2H, CH₂), 3.61 (*s*, 2H, CH₂), 3.58 (*s*, 2H, CH₂), 1.77 (*t*, *J* = 7.5, 1H, SH), 1.32 (*s*, 9H, C(CH₃)₃).

¹³C NMR (100 MHz, CDCl₃): δ = 151.8, 140.9, 138.1 (2 \times), 129.0, 128.4, 126.9, 125.8, 124.9, 123.7, 35.7 (2 \times), 34.7, 31.3, 29.1.

MS (MALDI-TOF, *m/z*): 339.2 [*M*+Na]⁺, 356.2 [*M*+K]⁺.

(3-((3-(Benzylthiomethyl)-5-*tert*-butylbenzylthio)methyl)-5-*tert*-butylphenyl)methanethiol (40)



(3-(Bromomethyl)-5-*tert*-butylbenzyl)(trityl)sulfane (**4**) (2.440 g, 4.73 mmol, 1 eq) and (3-(benzylthiomethyl)-5-*tert*-butylphenyl)methanethiol (**39**) (1.496 g, 4.73 mmol, 1 eq) were dissolved in tetrahydrofuran (30 ml) under an atmosphere of argon. Sodium hydride (60% in mineral oil, 300 mg, 7.50 mmol, 1.6 eq) was added at 0°C and the mixture was left stirring for 1 hour. After quenching with water, the reaction mixture was extracted with MTBE three times. The combined organic fractions were washed with brine, dried over magnesium sulfate and evaporated to dryness. The crude STrt-SBn-dimer was dissolved in dichloromethane (30 ml) and triethylsilane (1.130 ml, 825 mg, 7.10 mmol, 1.5 eq) was added. To this solution, trifluoroacetic acid (1.2 ml, 4% v/v of dichloromethane) was added dropwise. The mixture was stirred for 15 minutes, quenched with a saturated aqueous solution of sodium hydrogen carbonate and the organic phase was separated. The aqueous phase was washed twice with dichloromethane and the combined organic fractions were dried over magnesium sulfate. After filtration and evaporation of the solvent, the crude product was purified by column chromatography (hexane/dichloromethane 3:2) to yield the pure SH-SBn-dimer **40** as colorless oil. 1.986 g, 3.90 mmol, 83%.

EA: found: C 73.17%, H 7.95%
required: C 73.17%, H 7.92%

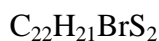
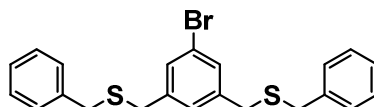
¹H NMR (400 MHz, CDCl₃): δ = 7.35 – 7.18 (*m*, 8H, Aryl-*H*), 7.15 (*br*, 1H, Aryl-*H*), 7.08 (*br*, 1H, Aryl-*H*), 7.07 (*br*, 1H, Aryl-*H*), 3.73 (*d*, *J* = 7.5 Hz, 2H, CH₂), 3.62 (*s*, 2H, CH₂), 3.61 (*s*, 2H, CH₂), 3.60 (*s*, 2H, CH₂), 3.59 (*s*, 2H, CH₂), 1.77 (*t*, *J* = 7.5 Hz, 1H, SH), 1.32 (2 × *s*, 2 × 9H, C(CH₃)₃).

¹³C NMR (100 MHz, CDCl₃): δ = 152.1, 151.8, 141.1, 138.4 (2×), 138.2, 138.1, 129.2, 128.7, 127.2, 127.0, 126.1, 125.1, 125.0, 124.9, 124.0, 36.2, 36.1 (2×), 35.9, 34.9 (2×), 31.6 (2×), 29.4.

MS (MALDI-TOF, *m/z*): 531.8 [*M*+Na]⁺, 547.8 [*M*+K]⁺.

6.2.3 Acetylene Functionalized Thioether Ligands

(5-Bromo-1,3-phenylene)bis(methylene)bis(benzylsulfane) (**43**)



To a solution of 1-bromo-3,5-bis(bromomethyl)benzene (**41**) (1.048 g, 3.1 mmol, 1 eq) and benzyl mercaptan (736 μl , 778 mg, 6.3 mmol, 2.05 eq) in dry tetrahydrofuran (40 ml) under an atmosphere of argon was added sodium hydride (60% in mineral oil, 378 mg, 9.5 mmol, 3.1 eq) at 0°C. After the gas formation had ceased, the mixture was left stirring at room temperature for 1.5 hours, before water was added to quench the reaction. The suspension was then extracted with MTBE three times. The combined organic fractions were washed with brine, dried over magnesium sulfate, filtered and evaporated to dryness. After purification by column chromatography (hexane/dichloromethane 2:1) the title compound **43** was obtained as colorless oil.

1.254 g, 2.92 mmol, 96%.

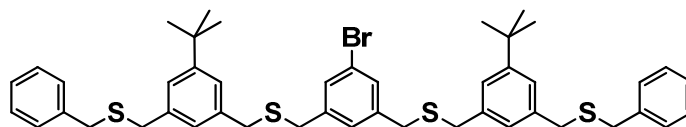
EA: found: C 61.50%, H 4.92%
required: C 61.53%, H 4.93%

$^1\text{H NMR}$ (400 MHz, CDCl_3): $\delta = 7.38 - 7.24$ (*m*, 12H, Aryl-*H*), 7.12 (*br*, 1H, Aryl-*H*), 3.64 (*s*, 4H, CH_2), 3.58 (*s*, 4H, CH_2).

$^{13}\text{C NMR}$ (100 MHz, CDCl_3): $\delta = 141.4, 138.6, 131.0, 129.5, 129.0, 128.9, 127.6, 122.7, 36.3, 35.6$.

MS (MALDI-TOF, m/z): 451.6 [$M+\text{Na}$] $^+$.

(5-Bromo-1,3-phenylene)bis(methylene)bis((3-(benzylthiomethyl)-5-*tert*-butylbenzyl)sulfane) (44)



814.08 g/mol

To a solution of 1-bromo-3,5-bis(bromomethyl)benzene (**41**) (137.9 mg, 0.40 mmol, 1 eq) and (3-(benzylthiomethyl)-5-*tert*-butylphenyl)methanethiol (**39**) (261.0 mg, 0.82 mmol, 2.05 eq) in dry tetrahydrofuran (15 ml) under an atmosphere of argon was added sodium hydride (60% in mineral oil, 50 mg, 1.24 mmol, 3.1 eq). After the gas formation had ceased, the mixture was left stirring at room temperature for 2 hours, before water was added to quench the reaction. The suspension was then extracted with MTBE three times. The combined organic fractions were washed with brine, dried over magnesium sulfate, filtered and evaporated to dryness. After purification by column chromatography (hexane/dichloromethane 1:1) the title compound **44** was obtained as colorless oil.

319.3 mg, 0.39 mmol, 97%.

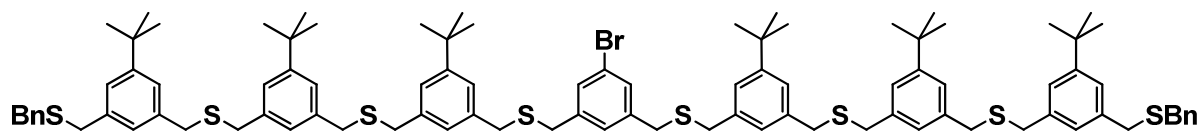
EA: found: C 66.81%, H 6.46%
required: C 67.87%, H 6.56%

¹H NMR (400 MHz, CDCl₃): δ = 7.39 – 7.24 (*m*, 12H, Aryl-*H*), 7.18 (*br*, 1H, Aryl-*H*), 7.14 (*br*, 4H, Aryl-*H*), 7.05 (*br*, 2H, Aryl-*H*), 3.61 (*s*, 4H, CH₂), 3.58 (*m*, 8H, CH₂), 3.52 (*s*, 4H, CH₂), 1.31 (*s*, 18H, C(CH₃)₃).

¹³C NMR (100 MHz, CDCl₃): δ = 151.6, 140.7, 138.1, 138.0, 137.5, 130.6, 129.0, 128.4, 128.3, 126.9, 126.8, 125.0, 124.7, 122.3, 35.8 (2 \times), 35.7, 34.9, 34.6, 31.4.

MS (MALDI-TOF, *m/z*): 837.1 [*M*+Na]⁺, 853.1 [*M*+K]⁺.

(5-Bromo-1,3-phenylene)bis(methylene)bis((3-((3-(3-(benzylthiomethyl)-5-tert-butylbenzylthio)methyl)-5-tert-butylbenzylthio)methyl)-5-tert-butylbenzyl)sulfane) (45)



1-Bromo-3,5-bis(bromomethyl)benzene (**41**) (47.7 mg, 0.14 mmol, 1 eq) and the SH-SBn-trimer **36** (200.1 mg, 0.29 mmol, 2.05 eq) were dissolved in dry tetrahydrofuran (10 ml) under an atmosphere of argon. The mixture was degassed by bubbling argon through the solution to avoid disulfide formation during the reaction. After that procedure, sodium hydride (60% in mineral oil, 17 mg, 0.42 mmol, 3 eq) was added and the mixture was left stirring at room temperature for 2 hours. The reaction was quenched with water and extracted with MTBE three times. The combined organic fractions were washed with brine, dried over magnesium sulfate and evaporated to dryness. Purification of the crude product was achieved by column chromatography (hexane/dichloromethane 1:1, then 2:3) to yield the Br-heptamer **45** as colorless solid.

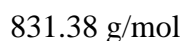
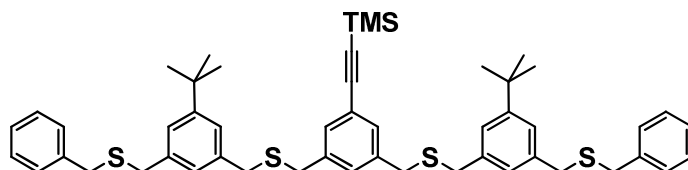
204.2 mg, 0.13 mmol, 93%.

EA: found: C 71.22%, H 7.42%
required: C 71.30%, H 7.45%

¹H NMR (400 MHz, CD₂Cl₂): δ = 7.33 – 7.05 (*m*, 31H, Aryl-*H*), 3.61 – 3.55 (*m*, 28H, CH₂), 3.51 (*s*, 4H, CH₂), 1.31 (*m*, 54H, C(CH₃)₃).

¹³C NMR (125 MHz, CD₂Cl₂): δ = 151.5 (2×), 151.5, 140.7, 138.2, 138.1, 138.0, 137.8, 137.5, 130.6, 129.0, 128.4, 128.3, 127.0, 126.8, 124.9, 124.8, 124.7 (2×), 122.3, 36.0, 35.9, 35.8 (2×), 35.7, 34.9, 34.6, 31.4 (2×).

((3,5-Bis((3-(benzylthiomethyl)-5-*tert*-butylbenzylthio)-methyl)phenyl)ethynyl)trimethylsilane (46)



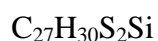
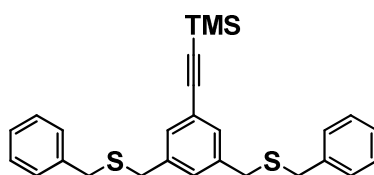
The bromo functionalized trimer **44** (100.9 mg, 0.12 mmol, 1 eq) was dissolved in triethylamine (3 ml) under an atmosphere of argon. The solution was degassed by bubbling argon through the solution for 10 minutes. (Trimethylsilyl)acetylene (90 μl , 63.8 mg, 0.62 mmol, 5 eq) and bis(triphenylphosphine)palladium(II) chloride (8.4 mg, 0.012 mmol, 10 mol%) were added and the mixture was degassed again for 2 minutes, before copper(I) iodide (2.3 mg, 0.012 mmol, 10 mol%) was added. The suspension was then heated to 45°C and was stirred at that temperature for 15 hours. After cooling to room temperature, a saturated aqueous solution of ammonium chloride was added and the resulting mixture was extracted with dichloromethane three times. The combined organic fractions were dried over magnesium sulfate and evaporated to dryness after filtration. Purification of the crude product by column chromatography (hexane/dichloromethane 3:2) gave the desired TMS-acetylated product **46** as slightly yellow colored oil.

91.0 mg, 0.11 mmol, 92%.

EA: found: C 73.46%, H 7.57%
required: C 73.68%, H 7.52%

^1H NMR (400 MHz, CDCl_3): $\delta = 7.39 - 7.24$ (*m*, 13H, Aryl-*H*), 7.14 (*br*, 4H, Aryl-*H*), 7.07 (*br*, 2H, Aryl-*H*), 3.61 (*s*, 4H, CH_2), 3.59 (*s*, 4H, CH_2), 3.57 (*s*, 4H, CH_2), 3.53 (*s*, 4H, CH_2), 1.33 (*s*, 18H, $\text{C}(\text{CH}_3)_3$), 0.26 (*s*, 9H, SiCH_3).

^{13}C NMR (100 MHz, CDCl_3): $\delta = 151.5, 138.7, 138.2, 138.0, 137.6, 131.1, 129.9, 129.0, 128.4, 126.9, 126.8, 124.9, 124.8, 123.3, 104.7, 94.4, 35.8, 35.7, 35.0, 34.6, 31.4, 0.2$.

((3,5-Bis(benzylthiomethyl)phenyl)ethynyl)trimethylsilane (47)

(5-Bromo-1,3-phenylene)bis(methylene)bis(benzylsulfane) (**43**) (506.1 mg, 1.18 mmol, 1 eq) was dissolved in triethylamine (7 ml) under an atmosphere of argon. The solution was degassed by bubbling argon through the solution for 10 minutes. (Trimethylsilyl)acetylene (816 μl , 578.8 mg, 5.9 mmol, 5 eq) and bis(triphenylphosphine)palladium(II) chloride (82.7 mg, 0.12 mmol, 10 mol%) were added and the mixture was degassed again for 2 minutes, before copper(I) iodide (11.3 mg, 0.06 mmol, 5 mol%) was added. The dark brown suspension was then heated to 45°C and was stirred at that temperature for 15 hours. After cooling to room temperature, a saturated aqueous solution of ammonium chloride was added and the resulting mixture was extracted with dichloromethane three times. The combined organic fractions were dried over magnesium sulfate and evaporated to dryness after filtration. Purification of the crude product by column chromatography (hexane/dichloromethane 2:1) gave the desired TMS-acetylated product **47** as colorless oil.

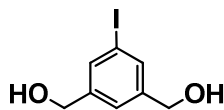
495.7 mg, 1.11 mmol, 94%.

EA: found: C 72.30%, H 6.78%

required: C 72.59%, H 6.77%

^1H NMR (400 MHz, CD_2Cl_2): $\delta = 7.39 - 7.24$ (*m*, 12H, Aryl-*H*), 7.15 (*br*, 1H, Aryl-*H*), 3.60 (*s*, 4H, CH_2), 3.54 (*s*, 4H, CH_2), 0.26 (*s*, 9H, SiCH_3).

^{13}C NMR (100 MHz, CD_2Cl_2): $\delta = 139.5, 138.7, 131.4, 130.5, 129.5, 129.0, 127.5, 123.9, 105.1, 94.9, 36.3, 35.8, 0.15$.

(5-Iodo-1,3-phenylene)dimethanol^[238] (**49**)

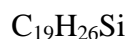
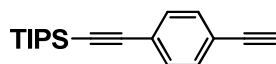
To a solution of dimethyl 5-iodoisophthalate (**50**) (2.999 g, 9.37 mmol, 1 eq) in dry tetrahydrofuran (100 ml) under an atmosphere of argon was slowly added a diisobutylaluminium hydride solution (1M in hexane, 60 ml, 60 mmol, 6.4 eq) at -40°C . After the addition was complete, the mixture was left stirring for three hours at that temperature. The reaction was then quenched with ice, followed by the addition of 1M hydrochloric acid. This mixture was extracted with MTBE three times. The combined organic fractions were washed with brine, dried over magnesium sulfate, filtered and evaporated to dryness to yield the title compound **49** as colorless crystalline solid.

2.305 g, 9.37 mmol, quant.

$^1\text{H NMR}$ (400 MHz, acetone- d_6): $\delta = 7.62$ (*s*, 2H, Aryl-*H*), 7.34 (*s*, 1H, Aryl-*H*), 4.60 (*d*, $J = 5.83$ Hz, 4H, CH_2), 4.32 (*t*, $J = 5.83$ Hz, 2H, *OH*).

$^{13}\text{C NMR}$ (100 MHz, acetone- d_6): $\delta = 146.0, 134.6, 124.9, 94.6, 63.8$.

MS (EI, m/z (%)): 264.0 (100) [M^+].

((4-Ethynylphenyl)ethynyl)triisopropylsilane^[240] (51)

starting from **53**

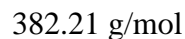
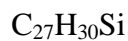
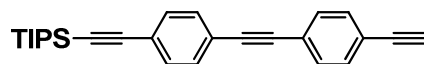
3-(4-((Triisopropylsilyl)ethynyl)phenyl)prop-2-yn-1-ol (**53**) (206.9 mg, 0.66 mmol, 1 eq) was dissolved in dry diethyl ether (9 ml) under an atmosphere of argon. A mixture of ground potassium hydroxide (74.1 mg, 1.32 mmol, 2 eq) and activated manganese(IV) oxide (229.5 mg, 2.64 mmol, 4 eq) was added and the mixture was stirred for 3 hours at room temperature. Most of the solvent was removed by a stream of argon and the crude was directly transferred to a silica gel column (hexane) to give the title compound **51** as colorless liquid. 154.4 mg, 0.55 mmol, 83%.

starting from **54**

2-Methyl-4-(4-((triisopropylsilyl)ethynyl)phenyl)but-3-yn-2-ol (**54**) (1.736 g, 5.10 mmol, 1 eq) was dissolved in degassed toluene (20 ml) under an atmosphere of argon, ground sodium hydroxide (1.02 g, 25.5 mmol, 5.6 eq) was added and the mixture heated to reflux. After 5 hours at that temperature, the mixture was filtered to remove solid sodium hydroxide. The solvent was evaporated and the crude was subjected to column chromatography (hexane) to yield pure ((4-ethynylphenyl)ethynyl)triisopropylsilane **51** as colorless liquid. 1.336 g, 4.73 mmol, 93%.

¹H NMR (400 MHz, CDCl₃): δ = 7.42 (s, 4H, Aryl-H), 3.16 (s, 1H, CH), 1.13 (s, 21H, iPr-H).

¹³C NMR (100 MHz, CDCl₃): δ = 131.9, 124.0, 121.9, 106.4, 93.0, 83.3, 78.8, 18.6, 11.3.

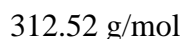
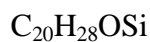
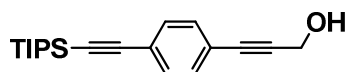
((4-((4-Ethynylphenyl)ethynyl)phenyl)ethynyl)triisopropylsilane^[240] (52)

The OPE rod **56** (565 mg, 1.28 mmol, 1 eq) was dissolved in degassed toluene (15 ml) under an atmosphere of argon. Ground sodium hydroxide (260 mg, 6.40 mmol, 5 eq) was then added and the mixture heated to reflux. After 3 hours, the solvent was evaporated and the crude was subjected to column chromatography (hexane/dichloromethane 4:1) to yield the title compound **52** as colorless oil.

486 mg, 1.27 mmol, 99%.

¹H NMR (400 MHz, CDCl₃): δ = 7.47 (s, 4H, Aryl-*H*), 7.45 (s, 4H, Aryl-*H*), 3.18 (s, 1H, *CH*), 1.13 (m, 21H, *iPr-H*).

¹³C NMR (100 MHz, CDCl₃): δ = 132.1, 132.0, 131.5, 131.4, 123.6, 123.5, 122.7, 122.0, 106.5, 93.0, 91.1, 90.6, 83.2, 79.0, 18.7, 11.3.

3-(4-((Triisopropylsilyl)ethynyl)phenyl)prop-2-yn-1-ol^[241] (53)

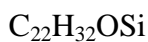
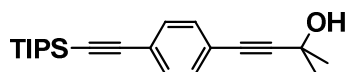
To a solution 1-bromo-4-iodobenzene (344.0 mg, 1.22 mmol, 1 eq) and (triisopropylsilyl)-acetylene (300 μl , 244 mg, 1.34 mmol, 1.1 eq) in degassed triethylamine (6 ml) under an atmosphere of argon was added bis(triphenylphosphine)palladium(II) chloride (85.6 mg, 0.12 mmol, 10 mol%) and copper(I) iodide (23.5 mg, 0.12 mmol, 10 mol%). After stirring at 45°C for 2 hours, propargyl alcohol (283 μl , 272.7 mg, 4.86 mmol, 4 eq) was added and the mixture was heated to reflux for 2 hours. After cooling to room temperature, a saturated aqueous solution of ammonium chloride was added and the resulting mixture was extracted with dichloromethane three times. The combined organic fractions were dried over magnesium sulfate and evaporated to dryness after filtration. Purification of the crude product by column chromatography (hexane/dichloromethane 1:1, then dichloromethane) yielded 3-(4-((triisopropylsilyl)ethynyl)phenyl)prop-2-yn-1-ol (**53**) as yellow oil.

285.2 mg, 0.91 mmol, 75%.

¹H NMR (400 MHz, CDCl_3): $\delta = 7.43 - 7.33$ (*m*, 4H, Aryl-*H*), 4.50 (*d*, $J = 5.93$ Hz, 4H, CH_2), 1.69 (*br t*, 1H, *OH*), 1.12 (*s*, 21H, *iPr-H*).

¹³C NMR (100 MHz, CDCl_3): $\delta = 131.9, 131.4, 123.7, 122.3, 106.4, 92.8, 88.9, 85.4, 51.7, 18.6, 11.3$.

MS (EI, m/z (%)): 312.2 (12) [M^+], 269.2 (100) [$M^+ - \text{C}_3\text{H}_7$].

2-Methyl-4-(4-((triisopropylsilyl)ethynyl)phenyl)but-3-yn-2-ol^[242] (**54**)

340.57 g/mol

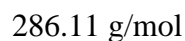
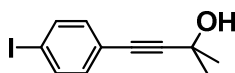
To a solution 1-bromo-4-iodobenzene (1.600 g, 5.66 mmol, 1 eq) and (triisopropylsilyl)-acetylene (1.33 ml, 5.94 mmol, 1.05 eq) in degassed triethylamine (20 ml) under an atmosphere of argon was added bis(triphenylphosphine)palladium(II) chloride (397 mg, 0.57 mmol, 10 mol%) and copper(I) iodide (109 mg, 0.57 mmol, 10 mol%). After stirring at 45°C for 2 hours, 2-methyl-3-butyn-2-ol (2.2 ml, 22.62 mmol, 4 eq) was added and the mixture was heated to reflux for 2 hours. After cooling to room temperature, a saturated aqueous solution of ammonium chloride was added and the resulting mixture was extracted with dichloromethane three times. The combined organic fractions were dried over magnesium sulfate and evaporated to dryness after filtration. Purification of the crude product by column chromatography (hexane/dichloromethane 1:4) yielded 2-methyl-4-(4-((triisopropylsilyl)ethynyl)phenyl)but-3-yn-2-ol (**54**) as colorless oil.

1.753 g, 5.15 mmol, 91%.

¹H NMR (400 MHz, CDCl₃): δ = 7.42 – 7.32 (*m*, 4H, Aryl-*H*), 2.00 (*s*, 1H, OH), 1.62 (*s*, 6H, CH₃), 1.12 (*s*, 21H, *i*Pr-*H*).

¹³C NMR (100 MHz, CDCl₃): δ = 132.3, 131.8, 123.8, 123.0, 106.9, 95.8, 93.0, 82.3, 66.1, 31.8, 19.1, 11.7.

MS (EI, *m/z* (%)): 340.2 (12) [*M*⁺], 297.1 (100) [*M*⁺-C₃H₇].

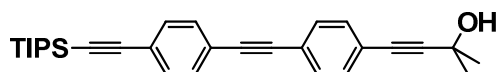
4-(4-Iodophenyl)-2-methylbut-3-yn-2-ol^[243] (55)

To a solution 1,4-diiodobenzene (1.00 g, 3.03 mmol, 1 eq) and 2-methyl-3-butyn-2-ol (296 μl , 3.03 mmol, 1 eq) in degassed triethylamine (50 ml) under an atmosphere of argon was added bis(triphenylphosphine)palladium(II) chloride (110 mg, 0.16 mmol, 5 mol%) and copper(I) iodide (31 mg, 0.16 mmol, 5 mol%). The mixture was stirred at 45°C for 2 hours and then quenched with a saturated aqueous solution of ammonium chloride. The aqueous phase was extracted three times with dichloromethane, the combined organic fractions were dried over magnesium sulfate and evaporated to dryness after filtration. After column chromatography (hexane/dichloromethane 1:4), the pure title compound **55** was obtained as colorless solid.

414 mg, 1.45 mmol, 48%.

¹H NMR (400 MHz, CDCl₃): δ = 7.64 (*d*, *J* = 8.3 Hz, 2H, Aryl-*H*), 7.13 (*d*, *J* = 8.3 Hz, 2H, Aryl-*H*), 2.00 (*s*, 1H, OH), 1.61 (*s*, 6H, CH₃).

¹³C NMR (100 MHz, CDCl₃): δ = 137.4, 133.2, 122.2, 94.1, 65.6, 31.4.

2-Methyl-4-(4-((4-((triisopropylsilyl)ethynyl)phenyl)ethynyl)phenyl)but-3-yn-2-ol (56)

440.69 g/mol

((4-Ethynylphenyl)ethynyl)triisopropylsilane (**51**) (523 mg, 1.85 mmol, 1.3 eq), 4-(4-iodophenyl)-2-methylbut-3-yn-2-ol (411 mg, 1.44 mmol, 1 eq), bis(triphenylphosphine)-palladium(II) chloride (50 mg, 0.14 mmol, 10 mol%) and copper(I) iodide (13 mg, 0.14 mmol, 10 mol%) were added to degassed triethylamine (10 ml). The mixture was left stirring for 1.5 hours at 45°C. After cooling to room temperature, a saturated aqueous solution of ammonium chloride was added and the resulting mixture was extracted with dichloromethane three times. The combined organic fractions were dried over magnesium sulfate and evaporated to dryness. Purification of the crude product by column chromatography (dichloromethane) yielded the desired product **56** as colorless oil.

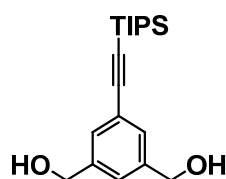
626 mg, 1.43 mmol, 99%.

EA: found: C 81.64%, H 8.32%
required: C 81.76%, H 8.23%

¹H NMR (400 MHz, CDCl₃): δ = 7.48 – 7.36 (*m*, 8H, Aryl-*H*), 2.00 (*s*, 1H, OH), 1.63 (*s*, 6H, CH₃), 1.13 (*m*, 21H, *iPr-H*).

¹³C NMR (100 MHz, CDCl₃): δ = 132.0, 131.6, 131.4 (2×), 123.5, 122.9, 122.8, 122.7, 106.6, 95.7, 93.0, 90.8, 90.7, 81.8, 65.7, 31.4, 18.7, 11.3.

MS (EI, *m/z* (%)): 440.3 (37) [*M*⁺], 397.2 (66) ([*M*⁺ – C₃H₇]⁺), 339.0 (100) ([*M*⁺ – C₃H₇ – C₂H₆O]⁺).

(5-((Triisopropylsilyl)ethynyl)-1,3-phenylene)dimethanol (57) $C_{19}H_{30}O_2Si$

318.53 g/mol

(5-Iodo-1,3-phenylene)dimethanol (**49**) (198 mg, 0.75 mmol, 1 eq) was dissolved in degassed triethylamine (5 ml) under an atmosphere of argon. (Triisopropylsilyl)acetylene (507 μ l, 412 mg, 2.26 mmol, 3 eq), bis(triphenylphosphine)palladium(II) chloride (53 mg, 0.08 mmol, 10 mol%) and copper(I) iodide (15 mg, 0.08 mmol, 10 mol%) were added and the mixture was stirred at 45°C for 2 hours. After cooling to room temperature, a saturated aqueous solution of ammonium chloride was added and the resulting mixture was extracted with dichloromethane three times. The combined organic fractions were dried over magnesium sulfate and evaporated to dryness after filtration. Purification of the crude product by column chromatography (ethyl acetate/dichloromethane 4:1) yielded the desired product **57** as colorless solid.

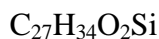
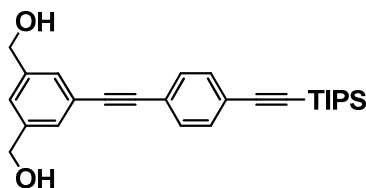
237 mg, 0.75 mmol, quant.

EA: found: C 71.35%, H 9.22%
required: C 71.64%, H 9.49%

1H NMR (400 MHz, $CDCl_3$): δ = 7.40 (*m*, 2H, Aryl-*H*), 7.31 (*s*, 1H, Aryl-*H*), 4.69 (*d*, J = 5.94 Hz, 4H, CH_2), 1.67 (*t*, J = 5.97 Hz, 2H, *OH*), 1.13 (*m*, 21H, *iPr-H*).

^{13}C NMR (100 MHz, $CDCl_3$): δ = 141.3, 129.6, 125.3, 124.0, 106.6, 90.9, 64.7, 18.7, 11.3.

MS (EI, m/z (%)): 318.2 (4) [M^+], 275.2 (100) [$M^+ - C_3H_7$].

(5-((4-((Triisopropylsilyl)ethynyl)phenyl)ethynyl)phenyl)ethynyl)-1,3-phenylene)dimethanol (58)

(5-Iodo-1,3-phenylene)dimethanol (**49**) (115 mg, 0.44 mmol, 1 eq), ((4-ethynylphenyl)-ethynyl)triisopropylsilane (**51**) (149 mg, 0.53 mmol, 1.2 eq), bis(triphenylphosphine)-palladium(II) chloride (31 mg, 0.04 mmol, 10 mol%) and copper(I) iodide (8 mg, 0.04 mmol, 10 mol%) were added to degassed triethylamine (5 ml). The mixture was left stirring for 1 hour at 45°C. After cooling to room temperature, a saturated aqueous solution of ammonium chloride was added and the resulting mixture was extracted with dichloromethane three times. The combined organic fractions were dried over magnesium sulfate and evaporated to dryness. Purification of the crude product by column chromatography (ethylacetate/dichloromethane 1:1) yielded the desired product **58** as slightly yellow oil.

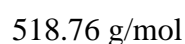
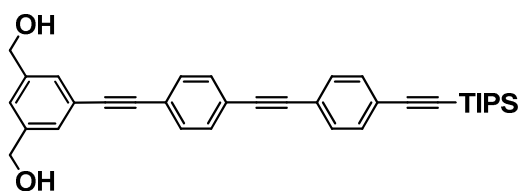
181 mg, 0.43 mmol, 98%.

EA: found: C 77.05%, H 8.07%
required: C 77.46%, H 8.19%

¹H NMR (400 MHz, CDCl₃): δ = 7.45 (*m*, 6H, Aryl-*H*), 7.35 (*br*, 1H, Aryl-*H*), 4.70 (*d*, *J* = 5.6 Hz, 4H, CH₂), 1.91 (*t*, *J* = 5.8 Hz, 2H, OH), 1.13 (*s*, 21H, *iPr-H*).

¹³C NMR (100 MHz, CDCl₃): δ = 141.5, 132.0, 131.4, 129.1, 125.4, 123.5 (2 \times), 122.9, 106.6, 92.9, 90.8, 89.3, 64.7, 18.6, 11.3.

MS (EI, *m/z* (%)): 418.2 (30) [*M*⁺], 375.2 (100) [*M*⁺-C₃H₇].

(5-((4-((4-(Triisopropylsilyl)ethynyl)phenyl)ethynyl)phenyl)ethynyl)-1,3-phenylene)dimethanol (59)

(5-Iodo-1,3-phenylene)dimethanol (**49**) (111 mg, 0.41 mmol, 1 eq), ((4-((4-ethynylphenyl)ethynyl)phenyl)ethynyl)triisopropylsilane (**52**) (218 mg, 0.57 mmol, 1.4 eq), bis(triphenylphosphine)palladium(II) chloride (28 mg, 0.04 mmol, 10 mol%) and copper(I) iodide (8 mg, 0.04 mmol, 10 mol%) were added to degassed triethylamine (8 ml). The mixture was left stirring overnight at 45°C. After cooling to room temperature, a saturated aqueous solution of ammonium chloride was added and the resulting mixture was extracted with dichloromethane three times. The combined organic fractions were dried over magnesium sulfate and evaporated to dryness. Purification of the crude product by column chromatography (ethylacetate/dichloromethane 1:1) yielded the desired product **59** as slightly yellow oil.

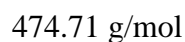
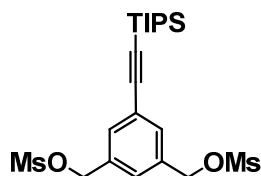
208 mg, 0.40 mmol, 98%.

EA: found: C 80.45%, H 7.42%
required: C 81.04%, H 7.38%

¹H NMR (400 MHz, CDCl₃): δ = 7.50 (*s*, 4H, Aryl-*H*), 7.48 (*br*, 2H, Aryl-*H*), 7.46 (*s*, 4H, Aryl-*H*), 7.37 (*br*, 1H, Aryl-*H*), 4.72 (*d*, $J = 5.3$ Hz, 4H, CH₂), 1.78 (*t*, $J = 5.7$ Hz, 2H, OH), 1.13 (*s*, 21H, *iPr-H*).

¹³C NMR (100 MHz, CDCl₃): δ = 141.5, 132.0, 131.6 (2×), 131.4, 129.2, 125.4, 123.6, 123.5, 123.1, 123.0, 122.8, 106.6, 93.0, 91.0 (2×), 90.8, 89.3, 64.8, 18.7, 11.3.

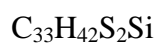
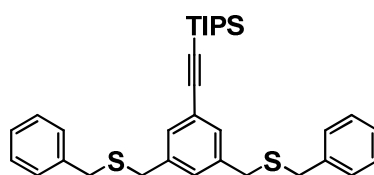
MS (EI, *m/z* (%)): 518.3 (91) [*M*⁺], 475.3 (100) [*M*⁺-C₃H₇].

(5-((Triisopropylsilyl)ethynyl)-1,3-phenylene)bis(methylene) dimethanesulfonate (60)

To a solution of (5-((triisopropylsilyl)ethynyl)-1,3-phenylene)dimethanol (**57**) (9.5 mg, 0.03 mmol, 1 eq) in dry dichloromethane (2 ml) under an atmosphere of argon was added methanesulfonyl chloride (6.9 μl , 10.2 mg, 0.09 mmol, 3 eq) and triethylamine (12.4 μl , 9.0 mg, 0.09 mmol, 3 eq) at room temperature. The mixture was stirred for 1 hour at that temperature before water was added and the dichloromethane phase was separated. The aqueous phase was then washed twice with dichloromethane. The combined organic fractions were dried over magnesium sulfate, filtered and evaporated to dryness, yielding the title compound **60** as colorless oil.

14.3 mg, 0.03 mmol, quant.

$^1\text{H NMR}$ (400 MHz, CDCl_3): $\delta = 7.52$ (*br*, 2H, Aryl-*H*), 7.42 (*s*, 1H, Aryl-*H*), 5.21 (*s*, 4H, CH_2), 3.01 (*s*, 6H, CH_3), 1.13 (*m*, 21H, *iPr-H*).

((3,5-Bis(benzylthiomethyl)phenyl)ethynyl)triisopropylsilane (61)

530.90 g/mol

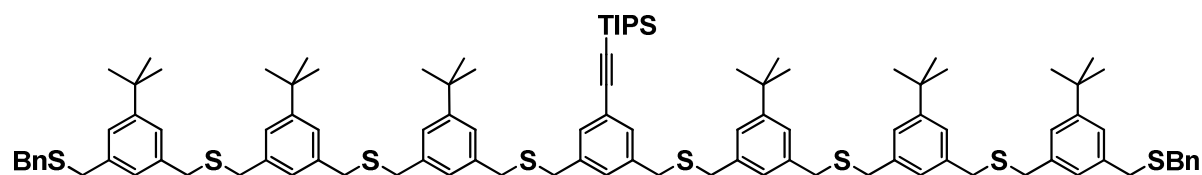
To a solution of (5-((triisopropylsilyl)ethynyl)-1,3-phenylene)bis(methylene) dimethanesulfonate (**60**) (13.5 mg, 0.03 mmol, 1 eq) and benzyl mercaptan (10.2 μl , 10.8 mg, 0.09 mmol, 3 eq) in dry tetrahydrofuran (4 ml) under an atmosphere of argon was added sodium hydride (60% in mineral oil, 10 mg, 0.25 mmol, 8.3 eq). The mixture was stirred for 1 hour at room temperature before water was added to quench the reaction. The suspension was extracted three times with MTBE. The combined organic fractions were then washed with brine, dried over magnesium sulfate, filtered and evaporated to dryness. The crude was purified by column chromatography (hexane/dichloromethane 4:1, then 3:1) to give the title compound **61** as colorless oil.

13.2 mg, 0.03 mmol, 88%.

$^1\text{H NMR}$ (400 MHz, CD_2Cl_2): δ = 7.37 – 7.22 (*m*, 12H, Aryl-*H*), 7.17 (*br*, 1H, Aryl-*H*), 3.63 (*s*, 4H, CH_2), 3.57 (*s*, 4H, CH_2), 1.17 (*m*, 21H, *iPr-H*).

$^{13}\text{C NMR}$ (100 MHz, CD_2Cl_2): δ = 139.4, 138.7, 131.6, 130.4, 129.5, 129.0, 127.5, 124.1, 107.2, 91.2, 36.3, 35.7, 19.0, 11.9.

((3,5-Bis((3-((3-((3-(benzylthiomethyl)-5-*tert*-butylbenzylthio)methyl)-5-*tert*-butylbenzylthio)methyl)-5-*tert*-butylbenzylthio)methyl)phenyl)ethynyl)triisopropylsilane (62)



Starting from 60:

To a solution of the dimesyl acetylene **60** (78.3 mg, 0.17 mmol, 1 eq) and the monothiol trimer **36** (231.6 mg, 0.33 mmol, 2 eq) in dry tetrahydrofuran (15 ml) under an atmosphere of argon was added sodium hydride (60% in mineral oil, 30 mg, 0.75 mmol, 4.5 eq). The mixture was left stirring at room temperature for 1.5 hours. TLC analysis revealed that the starting materials were not consumed after this time. The mixture was then heated to reflux temperature for 36 hours. The reaction was quenched with water and extracted with MTBE three times. The combined organic fractions were washed with brine, dried over magnesium sulfate and evaporated to dryness. The crude mixture was purified by column chromatography (hexane/dichloromethane 2:3) to yield the target compound as colorless **62** oil.

213.1 mg, 0.13 mmol, 77%.

Starting from 63:

((3,5-Bis(bromomethyl)phenyl)ethynyl)triisopropylsilane (**63**) (19 mg, 0.04 mmol, 1 eq) and the trimer **36** (62 mg, 0.09 mmol, 2.2 eq) were dissolved in dry tetrahydrofuran (5 ml) under an atmosphere of argon. The mixture was degassed by bubbling argon through the solution to avoid disulfide formation during the reaction. After this procedure, sodium hydride (60% in mineral oil, 10 mg, 0.25 mmol, 6.3 eq) was added and the mixture was left stirring at room temperature for 1.5 hours. The reaction was quenched with water and extracted with MTBE three times. The combined organic fractions were washed with brine, dried over magnesium sulfate and evaporated to dryness. Purification of the crude product was achieved by column chromatography (hexane/dichloromethane 2:3) to yield the TIPS-acetylene heptamer **62** as colorless oil.

67 mg, 0.04 mmol, 97%.

EA: found: C 74.89%, H 8.28%

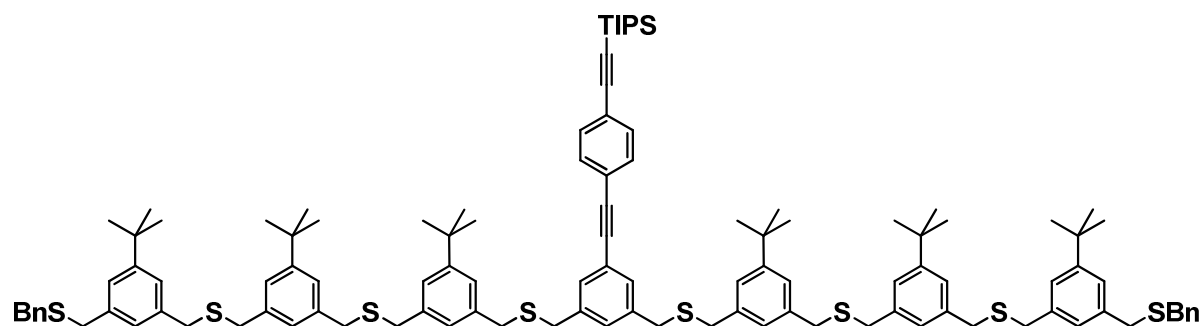
required: C 74.85%, H 8.26%

^1H NMR (400 MHz, CDCl_3): $\delta = 7.33 - 7.04$ (*m*, 31H, Aryl-*H*), 3.62 – 3.55 (*m*, 28H, CH_2), 3.53 (*s*, 4H, CH_2), 1.31 (*m*, 54H, $\text{C}(\text{CH}_3)_3$), 1.13 (*m*, 21H, *iPr-H*).

^{13}C NMR (125 MHz, CDCl_3): $\delta = 151.5$ (3 \times), 138.7, 138.2, 138.1, 138.0, 137.8, 137.6, 131.2, 129.7, 129.0, 128.4, 126.9, 126.8, 124.9, 124.8, 124.7, 124.6, 123.8, 106.6, 90.7, 35.9, 35.8 (2 \times), 35.7, 35.2, 34.6, 31.4 (3 \times), 18.7, 11.3.

MS (MALDI-TOF, *m/z*): 1706.4 [$M+\text{Na}$] $^+$, 1722.4 [$M+\text{K}$] $^+$.

((4-((3,5-Bis((3-((3-(benzylthiomethyl)-5-*tert*-butylbenzylthio)methyl)-5-*tert*-butylbenzylthio)methyl)-5-*tert*-butylbenzylthio)methyl)phenyl)ethynyl)phenyl)ethynyl)-triisopropylsilane (66)



A mixture of the dihydroxy OPE unit **58** (77.0 mg, 0.18 mmol, 1 eq), triphenylphosphine (144.8 mg, 0.55 mmol, 3 eq) and carbon tetrabromide (183.1 mg, 0.55 mmol, 3 eq) was stirred at room temperature for 1 hour in dry tetrahydrofuran (10 ml) under an atmosphere of argon. Water was added and the mixture was extracted with dichloromethane three times. The combined organic extracts were dried over magnesium sulfate and evaporated to dryness. Filtration over silica gel (hexane/dichloromethane 9:1) yielded the dibromide **64**. After evaporation of the solvents, the crude was dissolved in dry tetrahydrofuran (10 ml) and the SH-SBn-trimer **36** (265.0 mg, 0.38 mmol, 2.1 eq) was added. The mixture was degassed by bubbling argon through the solution for 15 minutes to avoid disulfide formation during the reaction. After that procedure, sodium hydride (60% in mineral oil, 22.0 mg, 0.55 mmol, 3 eq) was added and the mixture was left stirring at room temperature for 1.5 hours. The reaction was then quenched with water and extracted with MTBE three times. The combined organic fractions were washed with brine, dried over magnesium sulfate and evaporated to dryness. Purification of the crude product was achieved by column chromatography (hexane/dichloromethane 2:3) to yield the TIPS-acetylene heptamer **66** as colorless oil. 283 mg, 0.16 mmol, 87%.

EA: found: C 75.96%, H 8.00%

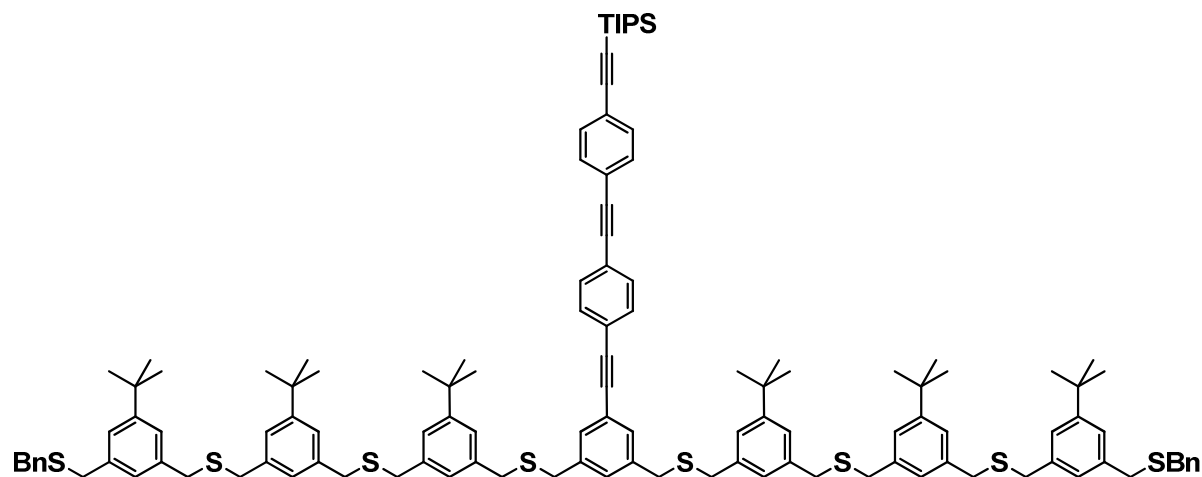
required: C 76.04%, H 8.02%

¹H NMR (400 MHz, CDCl₃): $\delta = 7.47 - 7.40$ (*m*, 4H, Aryl-*H*), $7.33 - 7.05$ (*m*, 31H, Aryl-*H*), 3.60 (*br*, 20H, CH₂), 3.59 (*s*, 4H, CH₂), 3.58 (*s*, 4H, CH₂), 3.56 (*s*, 4H, CH₂), 1.31 (*m*, 54H, C(CH₃)₃), 1.14 (*m*, 21H, *iPr-H*).

¹³C NMR (100 MHz, CDCl₃): $\delta = 151.6$ (2 \times), 151.5, 140.4, 138.9, 138.2, 138.1, 138.0, 138.0, 137.8, 137.6, 132.0, 131.3 130.8, 129.9, 129.0, 128.4, 126.9, 126.8, 124.9, 124.8, 124.7 (2 \times), 123.4, 123.1, 123.0, 106.6, 92.8, 90.9 (2 \times), 89.3, 35.9, 35.8, 35.7 (2 \times), 35.1, 34.6, 31.4 (2 \times), 18.7, 11.3.

MS (MALDI-TOF, *m/z*): 1806.4 [*M*+Na]⁺, 1822.8 [*M*+K]⁺.

((4-((4-((3,5-bis((3-((3-((3-(Benzylthiomethyl)-5-*tert*-butylbenzylthio)methyl)-5-*tert*-butylbenzylthio)methyl)-5-*tert*-butylbenzylthio)methyl)phenyl)ethynyl)phenyl)ethynyl)phenyl)ethynyl)triisopropylsilane (67)



1885.06 g/mol

A mixture of the dihydroxy OPE unit **59** (154.3 mg, 0.24 mmol, 1 eq), triphenylphosphine (188.9 mg, 0.72 mmol, 3 eq) and carbon tetrabromide (238.8 mg, 0.72 mmol, 3 eq) was stirred at room temperature for 2 hours in dry tetrahydrofuran (10 ml) under an atmosphere of argon. Water was added and the mixture was extracted with dichloromethane three times. The combined organic extracts were dried over magnesium sulfate and evaporated to dryness. Filtration over silica gel (hexane/dichloromethane 9:1) yielded the dibromide **65**. After evaporation of the solvents, the crude was dissolved in dry tetrahydrofuran (10 ml) and the SH-SBn-trimer **36** (353.4 mg, 0.5 mmol, 2.1 eq) was added. The mixture was degassed by bubbling argon through the solution for 15 minutes to avoid disulfide formation during the reaction. After that procedure, sodium hydride (60% in mineral oil, 29.0 mg, 0.72 mmol, 3 eq) was added and the mixture was left stirring at room temperature for 1.5 hours. The reaction was then quenched with water and extracted with MTBE three times. The combined organic fractions were washed with brine, dried over magnesium sulfate and evaporated to dryness. Purification of the crude product was achieved by column chromatography (hexane/dichloromethane 2:3) to yield the TIPS-acetylene heptamer **67** as colorless oil.

321 mg, 0.17 mmol, 71%.

EA: found: C 76.96%, H 7.85%

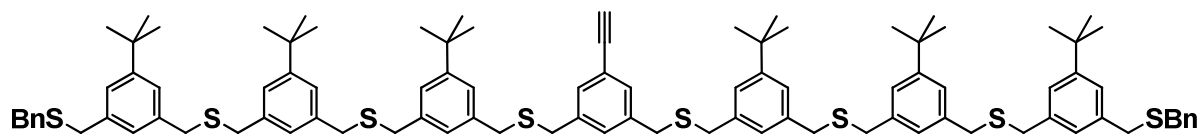
required: C 77.10%, H 7.81%

¹H NMR (400 MHz, CDCl₃): $\delta = 7.57 - 7.45$ (*m*, 8H, Aryl-*H*), $7.36 - 7.05$ (*m*, 31H, Aryl-*H*), $3.63 - 3.55$ (*m*, 32H, CH₂), 1.32 (*m*, 54H, C(CH₃)₃), 1.15 (*s*, 21H, *iPr-H*).

¹³C NMR (100 MHz, CDCl₃): $\delta = 151.6, 151.5, 141.0, 139.0, 138.2, 138.1, 138.0, 137.8, 137.6, 132.0, 131.5, 131.4, 130.8, 130.1, 129.9, 129.0, 128.4, 126.9, 126.8, 125.0, 124.9, 124.8, 124.7$ (2 \times), $123.5, 123.1$ (2 \times), $122.9, 122.8, 122.2, 106.6, 92.7, 91.1, 91.0, 90.9, 89.3, 35.9, 35.8, 35.7, 35.1, 34.6, 31.4$ (2 \times), $18.7, 11.3$.

MS (MALDI-TOF, *m/z*): 1906.7 [M+Na]⁺, 1922.8 [M+K]⁺.

(5-Ethynyl-1,3-phenylene)bis(methylene)bis((3-((3-((3-(benzylthiomethyl)-5-tert-butylbenzylthio)methyl)-5-tert-butylbenzylthio)methyl)-5-tert-butylbenzylthio)sulfane) (68)



1528.48 g/mol

The TIPS-protected heptamer **62** (46.8 mg, 0.03 mmol, 1 eq) was dissolved in dry tetrahydrofuran (6 ml) under an atmosphere of argon. Tetrabutylammonium fluoride (1M in tetrahydrofuran, 120 μl , 0.12 mmol, 4 eq) was added and the mixture was left stirring at room temperature. Thin layer chromatography after 1 hour revealed one new spot and the complete consumption of the starting material **62**. Water was added and the aqueous fraction was extracted with MTBE three times. The combined organic fractions were washed with brine, dried over magnesium sulfate and evaporated to dryness. The crude was purified by column chromatography (hexane/dichloromethane 2:3) to yield the acetylene heptamer **68** as colorless solid.

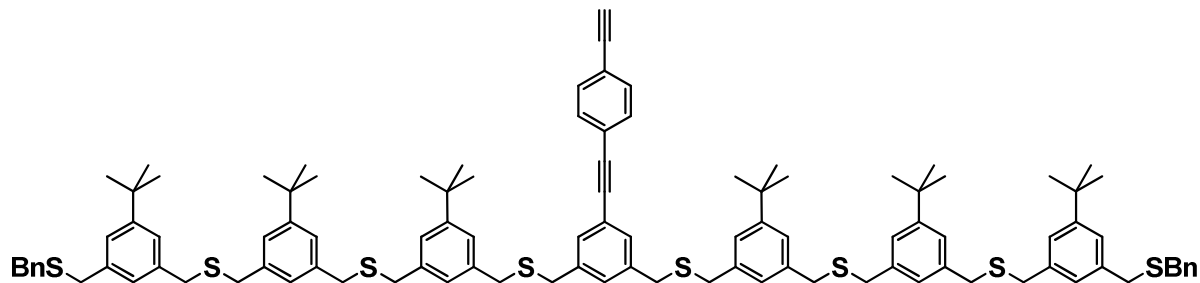
40.4 mg, 0.03 mmol, 98%.

EA: found: C 74.82%, H 7.67%
required: C 75.44%, H 7.78%

^1H NMR (400 MHz, CDCl_3): δ = 7.33 – 7.04 (*m*, 31H, Aryl-*H*), 3.60 (*br*, 20H, CH_2), 3.58 (*s*, 4H, CH_2), 3.57 (*s*, 4H, CH_2), 3.54 (*s*, 4H, CH_2), 3.03 (*s*, 1H, *CH*), 1.32 (*m*, 54H, $\text{C}(\text{CH}_3)_3$).

^{13}C NMR (125 MHz, CDCl_3): δ = 151.6 (2 \times), 151.5, 138.9, 138.2, 138.1, 138.0, 137.8, 137.6, 131.3, 130.2, 129.0, 128.4, 126.9, 126.8, 124.9, 124.7 (3 \times), 122.2, 83.3, 35.9, 35.8, 35.7, 35.1, 34.6, 31.4 (2 \times), 29.4.

(5-((4-Ethynylphenyl)ethynyl)-1,3-phenylene)bis(methylene)bis((3-((3-(3-(benzylthiomethyl)-5-*tert*-butylbenzylthio)methyl)-5-*tert*-butylbenzylthio)methyl)-5-*tert*-butylbenzyl)sulfane) (69)



1628.60 g/mol

The TIPS-protected heptamer **66** (52.3 mg, 0.03 mmol, 1 eq) was dissolved in dry tetrahydrofuran (5 ml) under an atmosphere of argon. Tetrabutylammonium fluoride (1M in tetrahydrofuran, 120 μl , 0.12 mmol, 4 eq) was added and the mixture was left stirring at room temperature for 2.5 hours. Water was added and the mixture was extracted with MTBE three times. The combined organic fractions were washed with brine, dried over magnesium sulfate and evaporated to dryness. The crude was purified by column chromatography (hexane/dichloromethane 2:3) to yield the acetylene heptamer **69** as colorless solid.

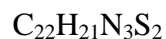
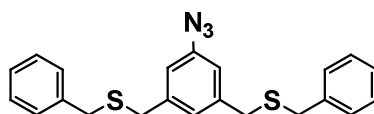
47.0 mg, 0.03 mmol, quant.

$^1\text{H NMR}$ (500 MHz, CDCl_3): $\delta = 7.47 - 7.40$ (*m*, 4H, Aryl-*H*), 7.33 - 7.05 (*m*, 31H, Aryl-*H*), 3.59 (*br*, 20H, CH_2), 3.58 (*s*, 4H, CH_2), 3.57 (*s*, 4H, CH_2), 3.56 (*s*, 4H, CH_2), 3.18 (*s*, 4H, *CH*), 1.31 (*m*, 54H, $\text{C}(\text{CH}_3)_3$).

$^{13}\text{C NMR}$ (125 MHz, CDCl_3): $\delta = 151.6$ (2 \times), 151.5, 139.0, 138.2, 138.1, 138.0, 137.8, 137.6, 132.1, 131.4, 130.8, 130.0, 129.0, 128.4, 126.9, 126.8, 124.9, 124.8, 124.7 (2 \times), 123.6, 123.0, 121.9, 96.0, 91.1, 83.2, 77.2, 35.9 (2 \times), 35.8, 35.7, 35.1, 34.6, 31.4 (2 \times).

6.2.4 Azide Functionalized Thioether Ligands

(5-Azido-1,3-phenylene)bis(methylene)bis(benzylsulfane) (**70**)



391.55 g/mol

Method a), starting from **73**

To a solution of (5-azido-1,3-phenylene)bis(methylene) dimethanesulfonate **73** (26.8 mg, 0.08 mmol, 1 eq) and benzyl mercaptan (28.0 μl , 30.0 mg, 0.24 mmol, 3 eq) in dry tetrahydrofuran (5 ml) under an atmosphere of argon was added sodium hydride (60% in mineral oil, 19 mg, 0.48 mmol, 6 eq). The mixture was stirred for 1 hour at room temperature before water was added to quench the reaction. The suspension was extracted three times with MTBE. The combined organic fractions were washed with brine, dried over magnesium sulfate, filtered and evaporated to dryness. The crude was purified by column chromatography (hexane/dichloromethane 3:1, then 3:2) to give the title compound **70** as colorless oil.

28.4 mg, 0.07 mmol, 91%.

Method b), starting from **43**

A mixture of ethanol (2.8 ml), tetrahydrofuran (2 ml), water (1.2 ml), (5-bromo-1,3-phenylene)bis(methylene)bis(benzylsulfane) **43** (105.3 mg, 0.25 mmol, 1 eq), sodium azide (36.0 mg, 0.55 mmol, 2.3 eq), sodium ascorbate (2.4 mg, 0.01 mmol, 5 mol%) and *N,N'*-methylethylenediamine (4.0 μl , 3.2 mg, 0.04 mmol, 15 mol%) was degassed for 10 minutes by bubbling argon through the solution. Copper(I) iodide (4.7 mg, 0.02 mmol, 10 mol%) was added and the mixture was heated to reflux for 1 hour. After cooling to room temperature, water was added and the diluted mixture was extracted 3 times with MTBE. The combined organic fractions were washed with brine, dried over magnesium sulfate, filtered and evaporated to dryness. The crude product was purified by column chromatography (hexane/dichloromethane 2:1, then 3:2) to give the desired product **70** as colorless oil.

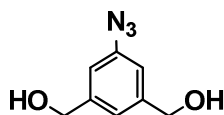
82.4 mg, 0.21 mmol, 86%.

^1H NMR (400 MHz, CDCl_3): $\delta = 7.35 - 7.24$ (*m*, 10H, Aryl-*H*), 6.95 (*br*, 1H, Aryl-*H*), 6.81 (*br*, 2H, Aryl-*H*), 3.62 (*s*, 4H, CH_2), 3.54 (*s*, 4H, CH_2).

^{13}C NMR (100 MHz, CDCl_3): $\delta = 140.4, 140.3, 137.8, 129.0, 128.5, 127.1, 126.3, 118.2, 35.8, 35.2$.

MS (MALDI-TOF, m/z): 414.2 [$M+\text{Na}$] $^+$, 430.2 [$M+\text{Na}$] $^+$.

(5-Azido-1,3-phenylene)dimethanol^[255] (**71**)



179.18 g/mol

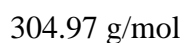
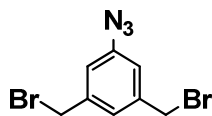
A mixture of ethanol (5 ml) and water (2 ml) was degassed for 20 minutes by bubbling argon through the mixture. To this was added (5-iodo-1,3-phenylene)dimethanol (**49**) (150.1 mg, 0.57 mmol, 1 eq), sodium azide (73.9 mg, 1.14 mmol, 2 eq), sodium ascorbate (5.7 mg, 0.03 mmol, 5 mol%), copper(I) iodide (11.0 mg, 0.06 mmol, 10 mol%) and *N,N'*-methyl-ethylenediamine (9.2 μl , 7.5 mg, 0.09 mmol, 15 mol%). The mixture was heated to reflux for 1 hour, before the solvents were removed with a rotary evaporator. The crude mixture was purified by column chromatography (ethyl acetate) to give the desired product **71** as colorless crystals.

97.5 mg, 0.54 mmol, 96%.

^1H NMR (400 MHz, acetone- d_6): $\delta = 7.15$ (*s*, 1H, Aryl-*H*), 6.97 (*s*, 2H, Aryl-*H*), 4.64 (*d*, $J = 5.82$ Hz, 4H, CH_2), 4.32 (*t*, $J = 5.82$ Hz, 2H, OH).

^{13}C NMR (100 MHz, acetone- d_6): $\delta = 175.7, 140.7, 122.1, 116.1, 64.2$.

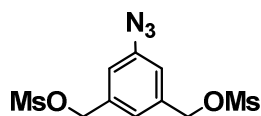
MS (EI, m/z (%)): 179.1 (9) [M^+], 151.1 (100) [$M^+-\text{N}_2$].

1-Azido-3,5-bis(bromomethyl)benzene (72)

(5-Azido-1,3-phenylene)dimethanol (**71**) (38.3 mg, 0.21 mmol, 1 eq), triphenylphosphine (151.3 mg, 0.58 mmol, 2.7 eq) and carbon tetrabromide (212.6 mg, 0.64 mmol, 3 eq) were stirred at 0°C for 1.5 hours in dry *N,N*-dimethylformamide (3 ml) under an atmosphere of argon. The solvent was evaporated under high vacuum and the residue was transferred to a silica gel column (hexane/dichloromethane 4:1, then 2:1). After the chromatography, the title compound **72** was obtained as colorless solid. After 3 days at 4°C, the material was dark brown and TLC revealed a partial decomposition of the product.

52.9 mg, 0.17 mmol, 82%.

¹H NMR (400 MHz, CDCl₃): δ = 7.18 (*m*, 1H, Aryl-*H*), 6.98 (*m*, 2H, Aryl-*H*), 4.43 (*s*, 4H, CH₂).

(5-Azido-1,3-phenylene)bis(methylene) dimethanesulfonate (73) $C_{10}H_{13}N_3O_6S_2$

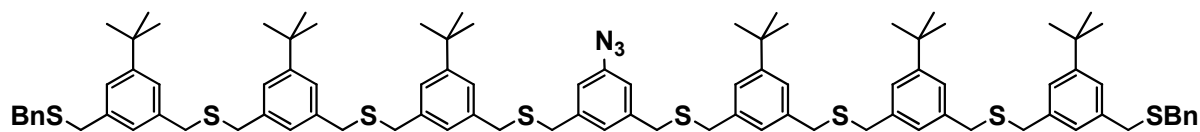
335.36 g/mol

To a solution of (5-azido-1,3-phenylene)dimethanol (**71**) (15.9 mg, 0.09 mmol, 1 eq) in dry tetrahydrofuran (3 ml) under an atmosphere of argon was added methanesulfonyl chloride (20.6 μ l, 30.5 mg, 0.27 mmol, 3 eq) and triethylamine (37.0 μ l, 26.9 mg, 0.27 mmol, 3 eq) at room temperature. The mixture was stirred for 45 minutes at that temperature before water and MTBE were added and the organic phase was separated. The aqueous phase was then washed twice with MTBE. The combined organic fractions were dried over magnesium sulfate, filtered and evaporated to dryness, yielding the title compound **73** as colorless oil.

32.7 mg, 0.09 mmol, quant.

$^1\text{H NMR}$ (400 MHz, CD_2Cl_2): δ = 7.26 (*br*, 1H, Aryl-*H*), 7.12 (*br*, 2H, Aryl-*H*), 5.22 (*s*, 4H, CH_2), 3.02 (*s*, 6H, CH_3).

(5-Azido-1,3-phenylene)bis(methylene)bis((3-((3-((3-(benzylthiomethyl)-5-tert-butylbenzylthio)methyl)-5-tert-butylbenzylthio)methyl)-5-tert-butylbenzylthio)methyl)-5-tert-butylbenzylthio)sulfane) (74)



To a solution of the SH-SBn-trimer **36** (199.1 mg, 0.28 mmol, 2 eq) and (5-azido-1,3-phenylene)bis(methylene) dimethanesulfonate (**73**) (47.0 mg, 0.14 mmol, 1 eq) in dry *N,N*-dimethylformamide (5 ml) under an atmosphere of argon was added potassium carbonate (77.3 mg, 0.56 mmol, 4 eq). After stirring for 1.5 hours at room temperature, MTBE was added and the suspension was extracted with water three times, followed once by brine. The organic extracts were dried over magnesium sulfate, filtered and evaporated to dryness. The pure product **74** was obtained as colorless solid after purification by column chromatography (hexane/dichloromethane 2:3).

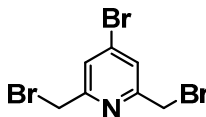
98.9 mg, 0.06 mmol, 45%.

$^1\text{H NMR}$ (400 MHz, CD_2Cl_2): $\delta = 7.33 - 7.05$ (*m*, 28H, Aryl-*H*), 7.04 (*br*, 1H, Aryl-*H*), 6.85 (*br*, 2H, Aryl-*H*), 3.62 – 3.59 (*m*, 28H, CH_2), 3.57 (*s*, 4H, CH_2), 1.31 (*m*, 54H, $\text{C}(\text{CH}_3)_3$).

MS (MALDI-TOF, *m/z*): 1545.4 [M] $^+$, 1567.4 [$M+\text{Na}$] $^+$, 1584.4 [$M+\text{K}$] $^+$.

6.2.5 Pyridine Functionalized Thioether Ligands

4-Bromo-2,6-bis(bromomethyl)pyridine^[256] (**75**)



343.84 g/mol

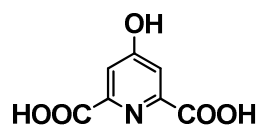
To (4-bromopyridine-2,6-diyl)dimethanol (**80**) (598 mg, 2.7 mmol, 1 eq) was added 48% aqueous hydrobromic acid (10 ml) and concentrated sulfuric acid (2 ml). The mixture was heated to reflux for 5 hours. After cooling to room temperature, the mixture was basified with concentrated aqueous sodium hydrogen carbonate solution and then extracted three times with dichloromethane. The combined organic fractions were dried over magnesium sulfate, filtered and evaporated to dryness, giving the title compound **75** as colorless solid.

906 mg, 2.6 mmol, 96%.

$^1\text{H NMR}$ (400 MHz, CDCl_3): $\delta = 7.55$ (s, 2H, Aryl-H), 4.47 (s, 4H, CH_2).

$^{13}\text{C NMR}$ (100 MHz, CDCl_3): $\delta = 157.9, 134.2, 126.1, 32.3$.

MS (EI, m/z (%)): 342.8 (16) [M^+], 263.9 (100) [$M^+ - \text{Br}$].

Chelidamic Acid^[259] (**76**)

183.12 g/mol

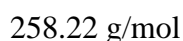
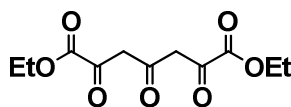
Chelidonic acid (**78**) (1.60 g, 8.8 mmol, 1 eq) was dissolved in an aqueous ammonium hydroxide solution (10%, 10 ml) and heated to reflux for 6 hours. During the reaction period, additional ammonium hydroxide solution (28%, 2 ml, overall 10 ml) was added each hour. The volatiles were removed *in vacuo* and the residue was dissolved in water (7.5 ml). Concentrated hydrochloric acid (2.5 ml) was slowly added at 0°C and the resulting solid was filtered off and washed with cold water. Chelidamic acid (**76**) was obtained as a slight brown powder.

1.54 g, 7.7 mmol, 87 %.

¹H NMR (400 MHz, DMSO-d₆): δ = 7.56 (s, 2H, CH).

¹³C NMR (100 MHz, DMSO-d₆): δ = 166.5, 165.2, 149.2, 114.7.

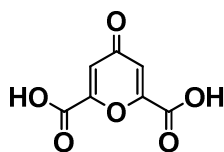
MS (EI, *m/z* (%)): 183.0 (3) [*M*⁺], 139.0 (100) [*M*⁺-CO₂].

Diethyl 2,4,6-trioxoheptanedioate^[258] (**77**)

In a three necked flask equipped with a reflux condenser, sodium (1.62 g, 70.45 mmol, 2.07 eq) was added in portions to dry ethanol (20 ml) under an atmosphere of argon. When the reaction had slowed down, the mixture was heated to reflux until all of the sodium had disappeared. The mixture was allowed to cool before diethyl oxalate (10.0 g, 9.35 ml, 68.4 mmol, 2.01 eq) was added, followed by acetone (1.98 g, 2.5 ml, 34 mmol, 1 eq). This mixture was stirred for 1 hour, after which excess ethanol was distilled off at ambient pressure. The resulting brownish yellow solid was dried under high vacuum and then added to a mixture of concentrated hydrochloric acid (10 ml) and crushed ice (35 g). The resulting solid was filtered off and washed thoroughly with water. After drying under high vacuum, the title compound **77** was obtained as yellow powder.

4.91 g, 19 mmol, 56%.

¹H NMR (400 MHz, CDCl₃): δ = 6.37 (*s*, 4H, CH₂), 4.37 (*q*, 7.13 Hz, 4H, CH₂) 1.39 (*t*, 7.13 Hz, 6H, CH₃).

Chelidonic Acid^[258] (**78**)

184.10 g/mol

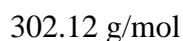
Diethyl 2,4,6-trioxoheptanedioate (**77**) (4.9 g, 19 mmol, 1 eq) was suspended in concentrated hydrochloric acid (20 ml) and heated to reflux for 20 hours. After cooling to room temperature, the mixture was poured onto crushed ice (10 g). The resulting solid was collected by filtration, washed with ice cold water and dried under high vacuum. Chelidonic acid (**78**) was obtained as brown powder.

1.61 g, 8.8 mmol, 46%.

¹H NMR (400 MHz, DMSO-d₆): $\delta = 6.85$ (s, 2H, CH).

¹³C NMR (100 MHz, DMSO-d₆): $\delta = 179.6, 160.8, 155.5, 117.8$.

MS (EI, *m/z* (%)): 184.0 (100) [*M*⁺].

Diethyl 4-bromopyridine-2,6-dicarboxylate^[2571] (**79**)

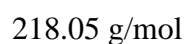
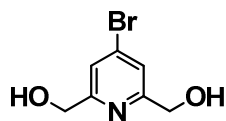
To a solution of bromine (2.7 ml, 8.34 g, 52 mmol, 3.2 eq) in hexane under argon was added slowly phosphorus tribromide (5.9 ml, 17.96 g, 63 mmol, 3.9 eq) with a syringe. Phosphorus pentabromide precipitated as yellow solid, which was washed four times with hexane (10 ml) and then dried under high vacuum. To the powder was added chelidamic acid (**76**) (3.4 g, 16.9 mmol, 1 eq) and the mixture was heated to 90°C for 1.5 hours. After cooling to room temperature, dry chloroform (17 ml) was added to the black solid and the slurry was filtered under argon. To the slight red filtrate was added absolute ethanol (50 ml) at 0°C, resulting in a blue solution. The solvent was evaporated and the residue was taken up in dichloromethane and extracted with a saturated aqueous solution of sodium hydrogen carbonate. The organic fraction was dried over magnesium sulfate, filtered and evaporated to dryness, leaving some colorless solid material in some highly boiling liquid (together 5.5 g). The crude was purified by recrystallization from ethanol, giving the title compound **79** as fluffy, colorless crystals.

4.03 g, 13.3 mmol, 79%

¹H NMR (400 MHz, CDCl₃): δ = 8.41 (*s*, 2H, Aryl-*H*), 4.48 (*q*, *J* = 7.05 Hz, 4H, CH₂) 1.44 (*t*, *J* = 7.08 Hz, 6H, CH₃).

¹³C-NMR (100 MHz, CDCl₃): δ = 163.5, 149.4, 134.9, 131.0, 62.7, 14.1.

MS (FAB, *m/z*): 301.9 [*M*+*H*]⁺.

4-Bromopyridine-2,6-dimethanol^[256] (**80**)

To a solution of diethyl 4-bromopyridine-2,6-dicarboxylate (**79**) (3.75 g, 12.4 mmol, 1 eq) in absolute ethanol (150 ml) was added sodium borohydride (3.29 g, 86.9 mmol, 7 eq). The mixture was heated to reflux for 20 hours, before the solvent was removed by evaporation. A saturated aqueous solution of sodium hydrogen carbonate (23 ml) was added to the residue and the mixture was heated to reflux until all solid material was dissolved. Water (28 ml) was then added and the mixture was left for 14 hours at 4°C. The formed oily solid was collected by decantation and the dried under vacuum. The white powder was extracted 5 times with acetone (100 ml) and the combined acetone fractions were evaporated to dryness, giving 4-bromopyridine-2,6-dimethanol (**80**) as colorless solid.

1.49 g, 6.8 mmol, 55 %.

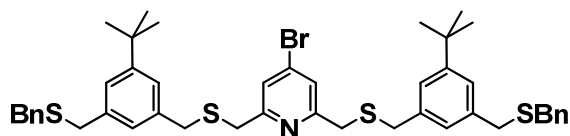
TLC revealed the presence of the desired product **80** in the extracted solid. Therefore this residue was dissolved in water (800 ml) and this solution was extracted 4 times with ethyl acetate (200 ml). The combined organic fractions were dried over magnesium sulfate, filtered and evaporated to dryness, giving more of the desired product **80** (1.01 g, 4.6 mmol, 38%).

2.50 g, 11.5 mmol, 93%

¹H NMR (400 MHz, DMSO-d₆): δ = 7.51 (*s*, 2H, Aryl-*H*), 5.54 (*t*, *J* = 5.91 Hz, 2H, *OH*) 4.52 (*d*, *J* = 5.87 Hz, 4H, *CH*₂).

¹³C NMR (100 MHz, DMSO-d₆): δ = 163.2, 133.3, 121.1, 63.7.

MS (EI, *m/z* (%)): 216.0 (100) [*M*⁺].

2,6-Bis((3-(benzylthiomethyl)-5-*tert*-butylbenzylthio)methyl)-4-bromopyridine (81)

To a solution of (3-(benzylthiomethyl)-5-*tert*-butylphenyl)methanethiol (**39**) (98 mg, 0.31 mmol, 2.1 eq) and 4-bromo-2,6-bis(bromomethyl)pyridine (**75**) (51 mg, 0.15 mmol, 1 eq) in dry *N,N*-dimethylformamide (8 ml) under an atmosphere of argon was added potassium carbonate (86 mg, 0.62 mmol, 4.2 eq). After stirring for 2 hours at room temperature, MTBE was added and the suspension was extracted with water three times, followed once by brine. The organic extracts were dried over magnesium sulfate, filtered and evaporated to dryness. The pure product **81** was obtained as colorless oil after purification by column chromatography (hexane/dichloromethane 1:4, then pure dichloromethane).

98 mg, 0.12 mmol, 81%.

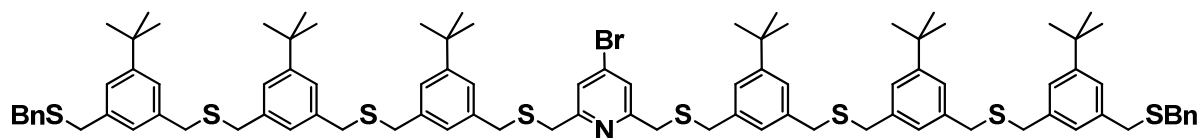
EA: found: C 66.17%, H 6.43%, N 1.57%

required: C 66.31%, H 6.43%, N 1.72%

¹H NMR (400 MHz, CD₂Cl₂): δ = 7.37 – 7.22 (*m*, 14H, Aryl-*H*), 7.16 (*br*, 2H, Aryl-*H*), 7.09 (*br*, 2H, Aryl-*H*), 3.70 (*s*, 4H, CH₂), 3.69 (*s*, 4H, CH₂), 3.62 (*s*, 4H, CH₂), 3.59 (*s*, 4H, CH₂), 1.31 (*s*, 18H, C(CH₃)₃).

¹³C NMR (100 MHz, CD₂Cl₂): δ = 160.5, 152.2, 139.1, 138.8, 138.5, 134.0, 129.0, 127.5, 127.3, 125.5 (2x), 124.9, 119.2, 37.7, 36.7, 36.5, 36.4, 35.1, 31.7.

2,6-Bis((3-((3-((3-(benzylthiomethyl)-5-*tert*-butylbenzylthio)methyl)-5-*tert*-butylbenzylthio)methyl)-5-*tert*-butylbenzylthio)methyl)-4-bromopyridine (82)



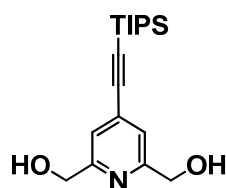
To a solution of SH-SBn-trimer **36** (119.8 mg, 0.17 mmol, 2 eq) and 4-bromo-2,6-bis(bromomethyl)pyridine (**75**) (29.4 mg, 0.085 mmol, 1 eq) in dry *N,N*-dimethylformamide (10 ml) under an atmosphere of argon was added potassium carbonate (47 mg, 0.34 mmol, 4 eq). After stirring for 2 hours at room temperature, MTBE was added and the suspension was extracted with water three times, followed once by brine. The organic extracts were dried over magnesium sulfate, filtered and evaporated to dryness. The pure product **82** was obtained as colorless oil after purification by column chromatography (hexane/dichloromethane 1:3, then pure dichloromethane).

114.5 mg, 0.072 mmol, 85%.

EA: found: C 70.30%, H 7.34%
required: C 70.50%, H 7.38%

¹H NMR (400 MHz, CDCl₃): δ = 7.37 – 7.15 (*m*, 22H, Aryl-*H*), 7.14 (*br*, 2H, Aryl-*H*), 7.10 (*br*, 2H, Aryl-*H*), 7.09 (*br*, 2H, Aryl-*H*), 7.07 (*br*, 2H, Aryl-*H*), 3.68 (*br*, 8H, CH₂), 3.62 – 3.56 (*m*, 24H, CH₂), 1.31 (*m*, 54H, C(CH₃)₃).

¹³C NMR (100 MHz, CDCl₃): δ = 159.8, 151.6 (2×), 151.5, 138.2, 138.1, 138.0, 137.8, 137.5, 133.6, 129.0, 128.4, 126.9, 126.8, 125.0, 124.9, 124.7 (2×), 124.4, 37.1, 36.2, 36.0, 35.9, 35.7, 34.6, 31.4 (2×).

(4-((Triisopropylsilyl)ethynyl)pyridine-2,6-diyl)dimethanol (83) $C_{18}H_{29}NO_2Si$

319.51 g/mol

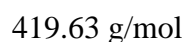
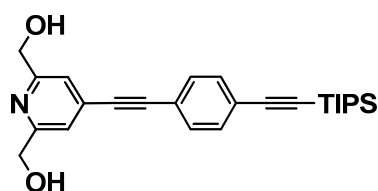
(4-Bromopyridine-2,6-diyl)dimethanol (**80**) (86.5 mg, 0.40 mmol, 1 eq) was dissolved in degassed triethylamine (10 ml) under an atmosphere of argon. (Triisopropylsilyl)acetylene (240 μ l, 217 mg, 1.19 mmol, 3 eq), bis(triphenylphosphine)palladium(II) chloride (28 mg, 0.04 mmol, 10 mol%) and copper(I) iodide (7.6 mg, 0.04 mmol, 10 mol%) were added and the mixture was heated to 80°C for 15 hours. After cooling to room temperature, the solvent was evaporated under vacuum. Dichloromethane was added and the resulting mixture was extracted with water. The aqueous phase was then extracted two more times with dichloromethane. The combined organic fractions were dried over magnesium sulfate and evaporated to dryness after filtration. Purification of the crude product by column chromatography (ethyl acetate, then ethyl acetate/acetone 1:1) yielded the desired product **83** as colorless solid.

113.5 mg, 0.32 mmol, 81%

EA: found: C 67.97%, H 8.66%, N 3.95%

required: C 67.66%, H 9.15%, N 4.38%

 1H NMR (400 MHz, $CDCl_3$): δ = 7.24 (*s*, 2H, Aryl-*H*), 4.76 (*s*, 4H, CH_2), 3.16 (*br*, 2H, *OH*), 1.13 (*m*, 21H, *iPr-H*). **^{13}C NMR** (100 MHz, $CDCl_3$): δ = 158.6, 132.9, 121.4, 104.0, 97.1, 64.2, 18.6, 11.1.**MS** (EI, *m/z* (%)): 319.2 (2) [M^+], 276.2 (100) [$M^+ - C_3H_7$].

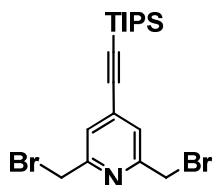
(4-((4-((Triisopropylsilyl)ethynyl)phenyl)ethynyl)pyridine-2,6-diyl)dimethanol (84)

(4-Bromopyridine-2,6-diyl)dimethanol (**80**) (201.8 mg, 0.93 mmol, 1 eq) and ((4-ethynylphenyl)ethynyl)triisopropylsilane (**51**) (313.8 mg, 1.11 mmol, 1.2 eq) were dissolved in degassed triethylamine (7 ml) under an atmosphere of argon. Argon was then bubbled through the solution for 10 minutes, before bis(triphenylphosphine)palladium(II) chloride (65 mg, 0.09 mmol, 10 mol%) and copper(I) iodide (17.8 mg, 0.09 mmol, 10 mol%) were added. The dark brown mixture was heated under stirring to 80°C for 1.5 hours. Dichloromethane and a saturated aqueous solution of ammonium chloride were added and the two phases were separated. The aqueous phase was washed twice with dichloromethane and the combined organic fractions were dried over magnesium sulfate. After filtration, the solvent was removed by rotary evaporation. The crude mixture was purified by column chromatography (ethyl acetate, then ethyl acetate/acetone 2:1) to give the desired product **84** as colorless solid. 315.3 mg, 0.75 mmol, 81%.

$^1\text{H NMR}$ (400 MHz, CDCl_3): $\delta = 7.47$ (*br*, 4H, Aryl-*H*), 7.31 (*br*, 2H, Aryl-*H*), 4.78 (*s*, 4H, CH_2), 3.20 (*br*, 2H, *OH*), 1.13 (*m*, 21H, *iPr-H*).

$^{13}\text{C NMR}$ (100 MHz, CDCl_3): $\delta = 158.8, 132.6, 132.1, 131.7, 124.5, 121.6, 121.0, 106.3, 93.7, 91.1, 88.3, 64.3, 18.6, 11.3$.

MS (EI, m/z (%)): 419.2 (11) [M^+], 376.3 (100) [$M^+ - \text{C}_3\text{H}_7$].

2,6-Bis(bromomethyl)-4-((triisopropylsilyl)ethynyl)pyridine (85) $C_{18}H_{27}Br_2NSi$

445.31 g/mol

(4-((Triisopropylsilyl)ethynyl)pyridine-2,6-diyl)dimethanol (**83**) (86.4 mg, 0.27 mmol, 1 eq) was dissolved in dry tetrahydrofuran (12 ml) under an atmosphere of argon. To this solution was added triphenylphosphine (213 mg, 0.81 mmol, 3 eq), followed by carbon tetrabromide (269 mg, 0.81 mmol, 3 eq). The solution was stirred at room temperature for 2 hours, during which a white precipitate formed. A saturated aqueous solution of sodium hydrogen carbonate was added and the mixture was extracted three times with MTBE. The combined organic fractions were washed with brine, dried over magnesium sulfate, filtered and then evaporated to dryness. Purification of the crude by column chromatography (hexane/dichloromethane 2:1, then 1:2) gave the title compound **85** as colorless solid.

83.0 mg, 0.19 mmol, 69%.

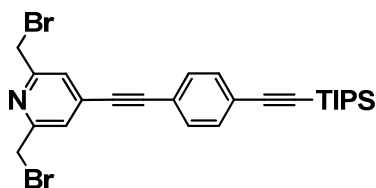
EA: found: C 48.76%, H 6.15%, N 3.06%

required: C 48.55%, H 6.11%, N 3.15%

¹H NMR (400 MHz, CDCl₃): δ = 7.38 (*s*, 2H, Aryl-*H*), 4.50 (*s*, 4H, CH₂), 1.13 (*m*, 21H, *i*Pr-*H*).

¹³C NMR (100 MHz, CDCl₃): δ = 156.9, 133.7, 125.0, 103.2, 98.0, 33.0, 18.6, 11.1.

MS (EI, *m/z* (%)): 545.1 (9) [*M*⁺], 502.0 (100) [*M*⁺-C₃H₇].

2,6-Bis(bromomethyl)-4-((4-((triisopropylsilyl)ethynyl)phenyl)ethynyl)pyridine (86) $C_{26}H_{31}Br_2NSi$

545.42 g/mol

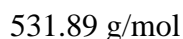
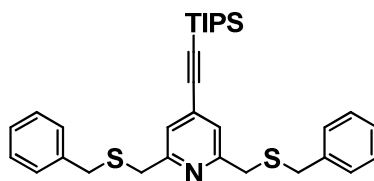
The OPE dihydroxide **84** (278.1 mg, 0.66 mmol, 1 eq) was dissolved in dry tetrahydrofuran (20 ml) under an atmosphere of argon. To this solution was added triphenylphosphine (521.9 mg, 1.99 mmol, 3 eq), followed by carbon tetrabromide (660.0 mg, 1.99 mmol, 3 eq). The solution was stirred at room temperature for 1 hour, during which a white precipitate formed. A saturated aqueous solution of sodium hydrogen carbonate was added and the mixture was extracted three times with MTBE. The combined organic fractions were washed with brine, dried over magnesium sulfate, filtered and then evaporated to dryness. Purification of the crude by column chromatography (hexane/dichloromethane 2:1, then 1:1) gave the title compound **86** as slightly yellow oil, which slowly solidified.

228.9 mg, 0.42 mmol, 63%.

$^1\text{H NMR}$ (400 MHz, CDCl_3): $\delta = 7.48$ (*br*, 4H, Aryl-*H*), 7.47 (*br*, 2H, Aryl-*H*), 4.53 (*s*, 4H, CH_2), 1.13 (*m*, 21H, *iPr-H*).

$^{13}\text{C NMR}$ (100 MHz, CDCl_3): $\delta = 157.0, 133.4, 132.1, 131.7, 124.6, 124.5, 121.4, 106.2, 94.4, 93.8, 87.7, 33.0, 18.6, 11.3$.

MS (EI, m/z (%)): 545.1 (9) [M^+], 502.0 (100) [$M^+ - \text{C}_3\text{H}_7$].

2,6-Bis(benzylthiomethyl)-4-((triisopropylsilyl)ethynyl)pyridine (87)

To a solution of 2,6-Bis(bromomethyl)-4-((triisopropylsilyl)ethynyl)pyridine (**85**) (7.1 mg, 0.016 mmol, 1 eq) in dry *N,N*-dimethylformamide (3 ml) under an atmosphere of argon was added benzyl mercaptan (5.7 μl , 6.0 mg, 0.05 mmol, 3 eq), followed by potassium carbonate (8.3 mg, 0.06 mmol, 3.75 eq). The mixture was stirred for 1 hour at room temperature before MTBE was added. The suspension was extracted three times with water in order to remove *N,N*-dimethylformamide. The organic fraction was then washed with brine, dried over magnesium sulfate, filtered and evaporated to dryness. The crude was purified by column chromatography (hexane/dichloromethane 1:1, then dichloromethane) to give the title compound **87** as colorless oil.

7.1 mg, 0.013 mmol, 83%.

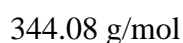
$^1\text{H NMR}$ (400 MHz, CD_2Cl_2): $\delta = 7.39 - 7.21$ (*m*, 10H, Aryl-*H*), 7.19 (*s*, 2H, Aryl-*H*), 3.73 (*s*, 4H, CH_2), 3.69 (*s*, 4H, CH_2), 1.16 (*m*, 21H, *iPr-H*).

$^{13}\text{C NMR}$ (100 MHz, CD_2Cl_2): $\delta = 158.4, 138.0, 129.1, 128.5, 127.2, 127.0, 123.5, 104.5, 98.0, 37.1, 35.9, 18.6, 11.2$.

MS (EI, *m/z* (%)): 488.3 (0.5) [$M^+ - \text{C}_3\text{H}_7$], 409.2 (100) [$M^+ - \text{C}_7\text{H}_6\text{S}$].

6.2.6 Towards Thiophenol Building Blocks

2,5-Dibromo-1,3-di(but-3-enyl)benzene (**88**)

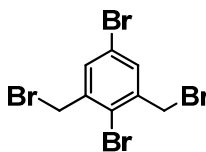


To a solution of 2,5-dibromo-1,3-bis(bromomethyl)benzene (**89**) (1.00 g, 2.4 mmol, 1 eq) in dry tetrahydrofuran (20 ml) under an atmosphere of argon was slowly added allyl magnesium bromide (1M in diethyl ether, 14.22 ml, 14.2 mmol, 6 eq) at 0°C. After the addition of allyl magnesium bromide was complete, the mixture was allowed to warm to room temperature and was stirred for 4 hours. A saturated aqueous solution of ammonium chloride was then added to quench the reaction and the suspension was extracted three times with MTBE. The combined organic fractions were washed once with brine, dried over magnesium sulfate, filtered and evaporated to dryness. After purification of the crude by column chromatography (hexane/dichloromethane 9:1) the desired product **88** was obtained as colorless liquid.

454 mg, 1.3 mmol, 56%.

$^1\text{H NMR}$ (400 MHz, CDCl_3): $\delta = 7.20$ (*s*, 2H, Aryl-*H*), 5.86 (*m*, 2H, $J = 6.8$ Hz, *CH*), 5.05 (*m*, 4H, *CH*₂), 2.82 (*t*, 4H, $J = 6.8$ Hz, *CH*₂), 2.36 (*m*, 4H, *m*, *CH*₂).

$^{13}\text{C NMR}$ (100 MHz, CDCl_3): $\delta = 144.1, 137.7, 131.1, 125.7, 121.1, 115.9, 36.7, 34.0$.

2,5-Dibromo-1,3-bis(bromomethyl)benzene^[266] (89)

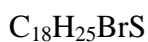
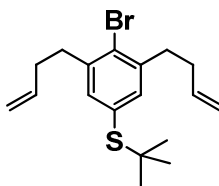
421.75 g/mol

To a solution of 2,5-dibromo-*m*-xylene (**90**) (2.50 g, 9.5 mmol, 1 eq) in carbon tetrachloride (70 ml) were added *N*-bromosuccinimide (4.21 g, 23.7 mmol, 2.5 eq.) and 2,2'-azobis(2-methylpropionitrile) (60 mg, 0.38 mmol, 4 mol%). The resulting mixture was heated to reflux and illuminated with light (500 W halogen lamp) for 24 hours. After cooling to room temperature, the solvent was evaporated under reduced pressure and the remains were dissolved in dichloromethane. The solution was washed two times with a saturated aqueous solution of sodium hydrogen carbonate, followed once by water. The organic layer was dried over magnesium sulfate, filtered off and concentrated to dryness. After two recrystallization steps (dichloromethane/hexane), the title compound **89** was obtained as colorless crystals.

2.86 g, 6.8 mmol, 72%.

$^1\text{H NMR}$ (400 MHz, CDCl_3): $\delta = 7.55$ (*s*, 2H, Aryl-*H*), 4.57 (*s*, 4H, CH_2).

$^{13}\text{C NMR}$ (100 MHz, CDCl_3): $\delta = 140.6, 134.4, 125.6, 121.7, 33.0$.

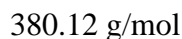
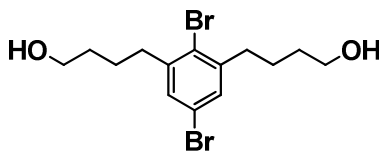
(4-Bromo-3,5-di(but-3-enyl)phenyl)tert-butylsulfane (91)

353.36 g/mol

A solution of 2,5-Dibromo-1,3-di(but-3-enyl)benzene (**88**) (500 mg, 1.45 mmol, 1 eq) in *n*-butanol (15 ml) was degassed by bubbling argon through the solution for 30 minutes. Sodium 2-methyl-2-propanethiolate (162 mg, 1.45 mmol, 1 eq) and tetrakis(triphenylphosphine)-palladium(0) (162 mg, 0.14 mmol, 10 mol%) were added and the mixture was degassed again for 10 minutes before it was heated to reflux for 24 hours. Water was added and the reaction was extracted with MTBE three times. The combined organic fractions were washed with brine, dried over magnesium sulfate, filtered and evaporated to dryness. The title compound **91** was obtained as colorless oil after purification by column chromatography (hexane/dichloromethane/9:1). Even after repetitive purification by column chromatography, some side products were present.

238.2 mg, 0.67 mmol, 46%.

$^1\text{H NMR}$ (400 MHz, CDCl_3): $\delta = 7.22$ (*s*, 2H, Aryl-*H*), 5.86 – 5.88 (*m*, 2H, *CH*), 4.98 – 5.07 (*m*, 4H, *CH}_2*), 2.86 (*t*, 4H, *CH}_2*), 2.38-2.41 (*m*, 4H, *CH}_2*), 1.27 (*s*, 9H, $\text{C}(\text{CH}_3)_3$).

4,4'-(2,5-Dibromo-1,3-phenylene)dibutan-1-ol (92)

To a solution of 2,5-dibromo-1,3-di(but-3-enyl)benzene (**88**) (626 mg, 1.8 mmol, 1 eq) in dry tetrahydrofuran (7 ml) under an atmosphere of argon was slowly added a borane tetrahydrofuran complex (1M in tetrahydrofuran, 3.64 ml, 3.6 mmol, 2 eq). The mixture was left for 1 hour at room temperature, stirring was not possible due to the formation of a precipitate. An aqueous sodium hydroxide solution (3M, 1.83 ml, 5.4 mmol, 3 eq) and an aqueous hydrogen peroxide solution (35%, 1.56 ml, 18 mmol, 10 eq) were carefully added. The resulting mixture was left stirring for 45 minutes. After dilution with water, the reaction was extracted with MTBE three times. The combined organic fractions were washed with brine, dried over magnesium sulfate, filtered and evaporated to dryness. After purification by column chromatography (dichloromethane/ethyl acetate 2:1, then 1:1) the title compound **92** was obtained as colorless oil.

418.1 mg, 1.1 mmol, 61%.

EA: found: C 44.06%, H 5.27%
required: C 44.24%, H 5.30%

¹H NMR (400 MHz, CDCl₃): δ = 7.20 (*s*, 2H, Aryl-*H*), 3.69 (*t*, *J* = 6.05 Hz, 4H, CH₂), 2.76 (*t*, *J* = 7.41 Hz, 4H, CH₂), 1.73 – 1.62 (*m*, 8H, CH₂), 1.37 (*br*, 2H, OH).

¹³C NMR (100 MHz, CDCl₃): δ = 144.2, 130.6, 125.3, 120.8, 62.6, 36.5, 32.3, 25.9.

MS (EI, *m/z* (%)): 301.1 (100) [*M*⁺-Br].

MS (FAB, *m/z* (%)): 419 (38) [*M*+K]⁺, 381 (100) [*M*+H]⁺.

4,4'-(2-Bromo-5-(*tert*-butylthio)-1,3-phenylene)dibutan-1-ol (93) $C_{18}H_{29}BrO_2S$

389.39 g/mol

A solution of 4,4'-(2,5-dibromo-1,3-phenylene)dibutan-1-ol (**92**) (265.3 mg, 0.70 mmol, 1 eq) in *n*-butanol (15 ml) was degassed by bubbling argon through the solution for 30 minutes. Sodium 2-methyl-2-propanethiolate (86.1 mg, 0.77 mmol, 1.1 eq) and tetrakis(triphenylphosphine)palladium(0) (80.6 mg, 0.07 mmol, 10 mol%) were added and the mixture was degassed again for 10 minutes before it was heated to reflux for 15 hours. Water was added and the reaction was extracted with MTBE three times. The combined organic fractions were washed with brine, dried over magnesium sulfate, filtered and evaporated to dryness. The title compound **93** was obtained as colorless oil after purification by column chromatography (dichloromethane/ethyl acetate 4:1, then 2:1).

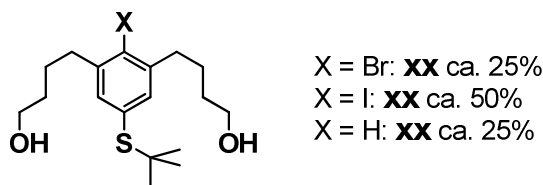
178.0 mg, 0.46 mmol, 66%.

EA: found: C 55.57%, H 7.33%
required: C 55.52%, H 7.51%

¹H NMR (400 MHz, CDCl₃): δ = 7.22 (*s*, 2H, Aryl-*H*), 3.69 (*m*, 4H, CH₂), 2.79 (*m*, 4H, CH₂), 1.73 – 1.62 (*m*, 8H, CH₂), 1.28 (*m*, 11H, C(CH₃)₃, OH).

¹³C NMR (100 MHz, CDCl₃): δ = 142.3, 136.5, 131.2, 127.6, 62.7, 45.9, 36.5, 32.3, 30.9, 26.0.

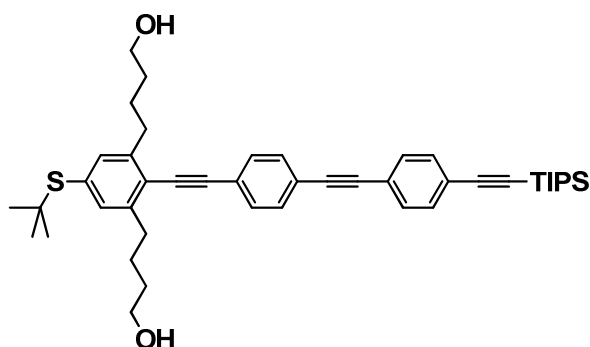
MS (EI, *m/z* (%)): 390.1 (100) [*M*⁺], 334.1 (78) [*M*⁺-C₄H₈].

Attempt to form the iodide 94

To a solution of the monobromide **93** (32.3 mg, 0.08 mmol, 1 eq) in dry tetrahydrofuran (5 ml) was slowly added *n*-butyl lithium (1.6M in hexane, 187 μ l, 0.3 mmol, 3.5 eq) at -78°C . The mixture was left stirring at that temperature for 10 minutes, before iodine (35 mg, 0.28 mmol, 3.4 eq) was added. The mixture was allowed to warm to room temperature and was left stirring at that temperature for 30 minutes. The reaction was quenched with a saturated aqueous solution of sodium thiosulfate and then extracted with MTBE three times. The combined organic fractions were washed with brine, dried over magnesium sulfate, filtered and evaporated to dryness to give 34 mg of a colorless oil. ^1H NMR analysis reveals the presence of the starting material **93** (ca. 25%), the desired product **94** (ca. 50%) and the dehalogenated benzene derivative **95** (ca. 25%).

^1H NMR (400 MHz, CDCl_3): δ = 7.22 (*s*, 0.5H, Bromo Aryl-*H*), 7.18 (*m*, 1.5H, Iodo Aryl-*H*), 7.00 (*br*, 0.25H, Aryl-*H*), 3.69 (*m*, 4H, CH_2), 2.79 (*m*, 4H, CH_2), 1.73 – 1.62 (*m*, 8H, CH_2), 1.28 (*m*, 11H, $\text{C}(\text{CH}_3)_3$, OH).

4,4'-(5-(*tert*-Butylthio)-2-((4-((4-(triisopropylsilyl)ethynyl)phenyl)ethynyl)-phenyl)ethynyl)-1,3-phenylene)dibutan-1-ol (96**)**



$C_{45}H_{58}O_2SSi$

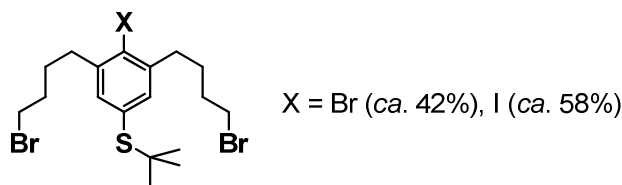
691.09 g/mol

The crude mixture of the iodination attempt (from 0.08 mmol **93**), ((4-((4-ethynylphenyl)ethynyl)phenyl)ethynyl)triisopropylsilane (**52**) (47.6 mg, 0.12 mmol, 1.5 eq), bis(triphenylphosphine)palladium(II) chloride (7 mg, 0.01 mmol, 10 mol%) and copper(I) iodide (2 mg, 0.01 mmol, 10 mol%) were added to degassed triethylamine (3 ml). The mixture was heated to 50°C and was maintained at that temperature for 1.5 hours. After cooling to room temperature, a saturated aqueous solution of ammonium chloride was added and the resulting mixture was extracted with dichloromethane three times. The combined organic fractions were dried over magnesium sulfate and evaporated to dryness. Purification of the crude product by column chromatography (ethyl acetate/dichloromethane 1:4) yielded the desired product **96** as slightly yellow oil. A mixture of the bromide **93** (*ca.* 42%) and the iodide **94** (*ca.* 58%) was also isolated (14.7 mg, average molecular weight 416.7 g/mol, 0.035 mmol, 44% for the two steps).

10.8 mg, 0.016 mmol, 20% for two steps.

$^1\text{H NMR}$ (400 MHz, CDCl_3): $\delta = 7.53 - 7.45$ (*m*, 8H, 7.22, Aryl-*H*), 7.26 (*s*, 2H, Aryl-*H*), 3.69 (*br t*, 4H, CH_2), 2.90 (*t*, 7.54 Hz, 4H, CH_2), 1.84 – 1.63 (*m*, 8H, CH_2), 1.32 – 1.25 (*m*, 11H, $\text{C}(\text{CH}_3)_3$, *OH*), 1.14 (*m*, 21H, *iPrH*).

$^{13}\text{C NMR}$ (100 MHz, CDCl_3): $\delta = 144.8, 135.2, 135.1, 132.8, 132.0, 131.7, 131.4, 131.2, 123.6, 123.5, 123.4, 106.6, 97.8, 93.0, 90.8, 88.5, 88.4, 62.8, 46.4, 34.5, 32.5, 31.1, 26.7, 18.7, 11.3$.

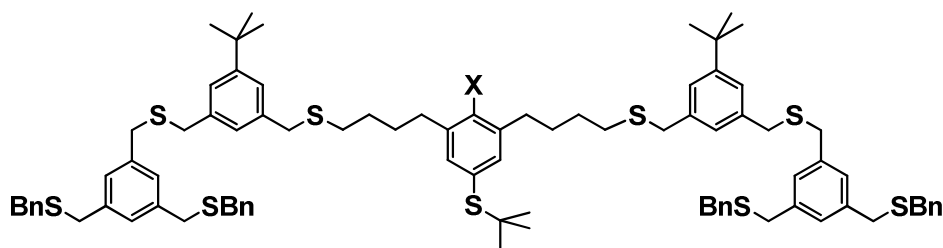
Introduction of bromide leaving groups to the mixture of 93 and 94 to form 97

542.44 g/mol (average with X = 42% Br and 58% I)

The purified 42/58 mixture of **93** and **94** (14.7 mg, 0.03 mmol, 1 eq), triphenylphosphine (39.4 mg, 0.15 mmol, 5 eq) and carbon tetrabromide (49.8 mg, 0.15 mmol, 5 eq) were stirred at room temperature for 1.5 hours in dry tetrahydrofuran (2 ml) under an atmosphere of argon. A saturated aqueous solution of ammonium chloride and dichloromethane were added to the reaction mixture. After separation of the organic phase, the aqueous phase was extracted two more times with dichloromethane. The combined organic fractions were dried over magnesium sulfate, filtered and evaporated to dryness. The crude was purified by column chromatography (hexane/dichloromethane 4:1) to give a 42/58 mixture of the bromo/iodo compounds **97**.

15.5 mg, 0.028 mmol, 95%.

$^1\text{H NMR}$ (400 MHz, CDCl_3): $\delta = 7.22$ (s, 0.85H, Bromo Aryl-*H*), 7.18 (s, 1.15H, Iodo Aryl-*H*), 3.45 (m, 4H, CH_2), 2.79 (m, 4H, CH_2), 2.01 – 1.72 (m, 8H, CH_2), 1.28 (s, 9H, $\text{C}(\text{CH}_3)_3$).

Formation of the G1 *t*-butyl protected monothiol dendrimer 99

X = Br (ca. 42%), I (ca. 58%)



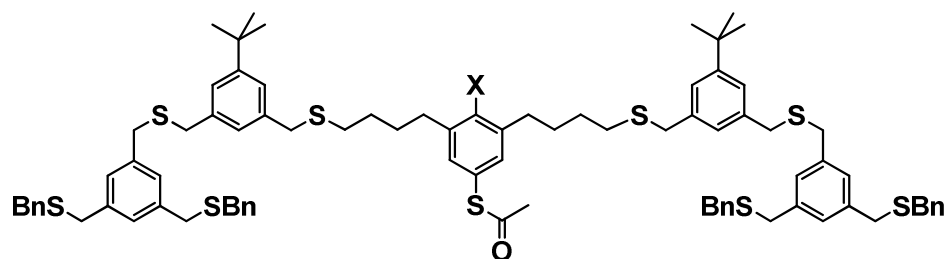
1558.52 g/mol (average with X = 42% Br and 58% I)

The bromo/iodo mixture of the dibromo thiol building block **97** (15.5 mg, 0.028 mmol, 1 eq) and the free thiol G0 dendron **98** (54.7 mg, 0.09 mmol, 3.2 eq) were dissolved in degassed tetrahydrofuran (4 ml) under an atmosphere of argon. Sodium hydride (60% in mineral oil, 12 mg, 0.3 mmol, 10 eq) was added and the mixture was left stirring at room temperature for 3 hours. As the reaction performed very slow under these conditions (TLC), the reaction mixture was heated to reflux for 2 hours. Water was then added after cooling to room temperature and the mixture was extracted three times with MTBE. The combined organic fractions were washed with brine, dried over magnesium sulfate, filtered and evaporated to dryness. The crude was purified by column chromatography (hexane/dichloromethane 1:2, then 1:3), to give the G1 bromo/iodo mixture **99** as colorless oil.

44.8 mg, 0.028 mmol, quant.

¹H NMR (400 MHz, CDCl₃): δ = 7.33 – 7.21 (*m*, 20H, Aryl-*H*), 7.19 (*br*, 4.85H, Aryl-*H*), 7.14 (*s*, 1.15H, Iodo Aryl-*H*), 7.11 – 7.05 (*m*, 8H, Aryl-*H*), 3.69 (*m*, 4H, CH₂), 3.63 – 3.55 (*m*, 24H, CH₂), 2.72 (*br*, 4H, CH₂), 2.46 (*br*, 4H, CH₂), 1.65 (*m*, 8H, CH₂), 1.31 (*m*, 18H, C(CH₃)₃), 1.26 (*s*, 9H, C(CH₃)₃).

Transprotection of **99** with the acetyl protecting group to form **100**



X = Br (ca. 42%), I (ca. 58%)



1544.46 g/mol (average with X = 42% Br and 58% I)

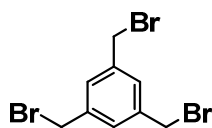
The *t*-butyl protected G1 dendrimer **99** (10.0 mg, 0.006 mmol, 1 eq) was dissolved in a degassed mixture of toluene (2 ml) and acetyl chloride (300 μ l) under an atmosphere of argon. Boron tribromide (1M in dichloromethane, 50 μ l, 0.05 mmol, 8.3 eq) was slowly added and the mixture was left stirring for 1 hour. After this time, TLC showed a new spot in addition to the spot of the starting material. The reaction was then directly quenched with water and extracted two times with dichloromethane. The combined organic fractions were dried over magnesium sulfate, filtered and evaporated to dryness. The crude mixture was purified by column chromatography (hexane/dichloromethane 1:2, then dichloromethane) to give the starting material (3.7 mg, 2.3 μ mol, 40%) and the acetyl protected first generation **100** as colorless oils.

5.8 mg, 3.7 mmol, 60%.

$^1\text{H NMR}$ (400 MHz, CDCl_3): δ = 7.33 – 7.21 (*m*, 20H, Aryl-*H*), 7.19 – 7.16 (*m*, 4H, Aryl-*H*), 7.11 – 7.04 (*m*, 8.85H, Aryl-*H*), 7.01 (*s*, 1.15H, Iodo Aryl-*H*), 3.69 (*m*, 4H, CH_2), 3.61 (*s*, 8H, CH_2), 3.58 (*s*, 4H, CH_2), 3.57 (*s*, 8H, CH_2), 3.55 (*s*, 4H, CH_2), 2.72 (*br*, 4H, CH_2), 2.46 (*br*, 4H, CH_2), 2.39 (*s*, 3H, CH_3), 1.65 (*br*, 8H, CH_2), 1.30 (*s*, 18H, $\text{C}(\text{CH}_3)_3$).

6.2.7 Dendritic Thioether Ligands

1,3,5-Tris(bromomethyl)benzene^[299] (**102**)



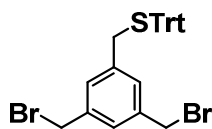
356.88 g/mol

N-Bromosuccinimide (60.34 g, 770 mmol, 3.3 eq) and mesitylene (32.4 ml, 28.00 g, 233 mmol, 1 eq) were dissolved in methyl formate (600 ml). 2,2'-Azobis(2-methylpropionitrile) (700 mg, 4.3 mmol, 0.02 eq) was then added and the reaction mixture was illuminated by a 500 W halogen lamp for 6 hours. The solvent was evaporated by using a rotary evaporator and the residue was redissolved in dichloromethane. The organic solution was washed twice with a saturated aqueous solution of sodium hydrogen carbonate and then once with water. After drying with magnesium sulfate, the dichloromethane was removed by evaporation. The residue was recrystallized from dichloromethane/hexane five times to give 1,3,5-tris(bromomethyl)benzene (**102**) (24.14 g, 68 mmol) as colorless crystals. The filtrates of the crystallization 3 – 5 were put together, evaporated to dryness and crystallized again to yield the title compound **102** (12.56 g, 35 mmol).

36.70 g, 104 mmol, 45%.

¹H NMR (400 MHz, CDCl₃): δ = 7.36 (*s*, 3H, Aryl-*H*), 4.46 (*s*, 6H, CH₂).

¹³C NMR (100 MHz, CDCl₃): δ = 139.0, 129.6, 32.2.

3,5-Bis(bromomethyl)benzyl(trityl)sulfane (103)

552.36 g/mol

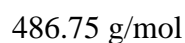
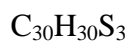
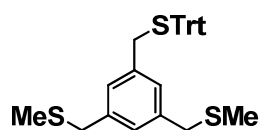
1,3,5-Tris(bromomethyl)benzene (**102**) (2.50 g, 7.0 mmol, 1 eq) and triphenylmethanethiol (1.94 g, 7.0 mmol, 1 eq) were dissolved in dry tetrahydrofuran (20 ml) under an atmosphere of argon. Potassium carbonate (1.45 g, 10.5 mmol, 1.5 eq) was added and the mixture was heated to reflux for 20 hours. After cooling to room temperature, water was added and the mixture was extracted three times with MTBE. The combined organic fractions were washed with brine, dried over magnesium sulfate and evaporated to dryness. After purification by column chromatography (hexane/dichloromethane 3:1), the product **103** was obtained as colorless solid.

1.82 g, 3.3 mmol, 47 %.

EA: found: C 60.75%, H 4.41%
required: C 60.89%, H 4.38%

¹H NMR (400 MHz, CDCl₃): $\delta = 7.48 - 7.42$ (*m*, 6H, Aryl-*H*), $7.35 - 7.20$ (*m*, 10H, Aryl-*H*), 7.01 (*s*, 2H, Aryl-*H*), 4.39 (*s*, 4H, CH₂), 3.32 (*s*, 2H, CH₂).

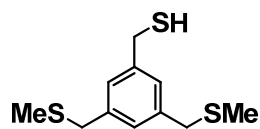
¹³C NMR (100 MHz, CDCl₃): $\delta = 144.5, 138.7, 138.4, 129.7, 129.6, 128.2, 128.0, 126.8, 67.3, 36.4, 32.6$.

(5-(Tritylthiomethyl)-1,3-phenylene)bis(methylene)bis(methylsulfane) (104)

3,5-Bis(bromomethyl)benzyl(trityl)sulfane (**103**) (500 mg, 0.90 mmol, 1 eq), was dissolved in dry *N,N*-dimethylformamide (10 ml) under an atmosphere of argon. Sodium methanethiolate (140 mg, 1.99 mmol, 2.2 eq) was added and the mixture was left stirring for 1 hour. MTBE was added and the organic solution was extracted four times with water, followed once by brine. The MTBE fraction was dried over magnesium sulfate, filtered and evaporated to dryness. After purification by column chromatography (hexane/dichloromethane 1:1, the 1:3), the title compound **104** was obtained as colorless oil. 395 mg, 0.81 mmol, 90 %.

$^1\text{H NMR}$ (400 MHz, CDCl_3): $\delta = 7.48 - 7.42$ (*m*, 6H, Aryl-*H*), $7.34 - 7.20$ (*m*, 9H, Aryl-*H*), 7.07 (*br*, 1H, Aryl-*H*), 6.93 (*br*, 2H, Aryl-*H*), 3.59 (*s*, 4H, CH_2), 3.30 (*s*, 2H, CH_2), 1.96 (*s*, 6H, CH_3).

$^{13}\text{C NMR}$ (100 MHz, CDCl_3): $\delta = 144.6, 138.6, 137.6, 129.6, 128.2, 128.1, 128.0, 126.7, 67.5, 38.04, 36.8, 15.0$.

(3,5-bis(methylthiomethyl)phenyl)methanethiol (105)

244.44 g/mol

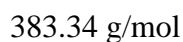
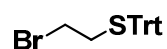
104 (370 mg, 0.76 mmol, 1 eq) and triethylsilane (182 μl , 132 mg, 1.14 mmol, 1.5 eq) were dissolved in dichloromethane (8 ml). Trifluoroacetic acid (420 μl , 4% v/v) was slowly added under stirring, which was maintained for further 15 minutes after the addition. A saturated aqueous solution of sodium hydrogen carbonate was then added to quench the reaction. After completion of the gas formation, the two phases were separated and the aqueous phase was washed twice with dichloromethane. The combined organic fractions were dried over magnesium sulfate, filtered and evaporated to dryness. After purification by column chromatography (hexane/dichloromethane 2:3, then dichloromethane) the title compound **105** was obtained as colorless oil.

152 mg, 0.62 mmol, 82%.

EA: found: C 53.99%, H 6.60%
required: C 54.05%, H 6.60%

^1H NMR (400 MHz, CDCl_3): δ = 7.16 (*br*, 2H, Aryl-*H*), 7.12 (*br*, 1H, Aryl-*H*), 3.72 (*d*, J = 7.60 Hz, 2H, CH_2), 3.65 (*s*, 4H, CH_2), 2.01 (*s*, 6H, CH_3), 1.77 (*t*, J = 7.60 Hz, 1H, *SH*).

^{13}C NMR (100 MHz, CDCl_3): δ = 141.6, 139.0, 128.1, 127.2, 38.1, 28.7, 15.1.

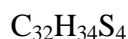
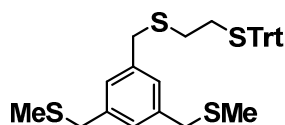
(2-bromoethyl)(trityl)sulfane^[124] (**106**)

Triphenylmethanethiol (494 mg, 1.79 mmol, 1 eq) was dissolved in dry tetrahydrofuran (6 ml) under an atmosphere of argon and sodium hydride (60% in mineral oil, 160 mg, 4.0 mmol, 2.2 eq) was added. In a separate flask, dibromoethane (156 μl , 340.1 mg, 1.81 mmol, 1.1 eq) was dissolved in dry tetrahydrofuran under argon. The solution of the triphenylmethanethiolate was added dropwise at 0°C to the dibromoethane solution, the reaction mixture was then allowed to warm to room temperature and stirred for 1 hour. Water was added to quench the reaction and the mixture was extracted with MTBE. The organic fraction was then washed with brine, dried over magnesium sulfate, filtered and evaporated to dryness. The title compound **106** was obtained as colorless solid, which was used in the subsequent steps without further purification.

694 mg, 1.81 mmol, quant.

¹H NMR (400 MHz, CDCl₃): δ = 7.48 – 7.28 (*m*, 15H, Aryl-*H*), 2.89 – 2.70 (*m*, 4H, CH₂).

(5-((2-(Tritylthio)ethylthio)methyl)-1,3-phenylene)bis(methylene)bis(methylsulfane)
(107)



546.87 g/mol

a) starting from **105**

(3,5-Bis(methylthiomethyl)phenyl)methanethiol (**105**) (248 mg, 1.02 mmol, 1 eq) was dissolved in dry tetrahydrofuran (15 ml) under an atmosphere of argon. Sodium hydride (60% in mineral oil, 80 mg, 2.00 mmol, 2 eq) was added and the mixture was left stirring for 5 minutes, after which (2-bromoethyl)(trityl)sulfane (**106**) (467 mg, 1.22 mmol, 1.2 eq) was added. After 2 hours stirring at room temperature, water was slowly added to quench the reaction. The mixture was extracted three times with MTBE. After washing with brine, drying with magnesium sulfate and filtration, the combined organic fractions were evaporated to dryness. Purification by column chromatography (hexane/dichloromethane 2:3, then 1:2) gave the title compound **107** as colorless oil, which slowly solidifies at 4°C.

473 mg, 0.87 mmol, 85%.

b) starting from **110**

(3,5-Bis(chloromethyl)benzyl)(2-(tritylthio)ethyl)sulfane (**110**) (2.26 g, 4.3 mmol, 1 eq) was dissolved in dry *N,N*-dimethylformamide (30 ml) under an atmosphere of argon. Sodium methanethiolate (666 mg, 9.5 mmol, 2.2 eq) was added and the mixture was left stirring for 2 hours at room temperature. MTBE was added and the solution was extracted 4 times with water. After washing with brine and drying with magnesium sulfate, the solvent was removed. Purification by column chromatography (hexane/dichloromethane 2:3, then 1:2) gave the title compound **107** as colorless oil, which slowly solidifies at 4°C.

2.06 g, 3.8 mmol, 88%.

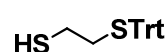
EA: found: C 70.22%, H 6.23%

required: C 70.28%, H 6.27%

$^1\text{H NMR}$ (400 MHz, CDCl_3): $\delta = 7.44 - 7.18$ (*m*, 15H, Aryl-*H*), 7.11 (*br*, 1H, Aryl-*H*), 7.02 (*br*, 2H, Aryl-*H*), 3.61 (*s*, 4H, CH_2H), 3.50 (*s*, 2H, CH_2), 2.42 – 2.25 (*m*, 4H, CH_2), 1.97(*s*, 6H, CH_3).

$^{13}\text{C NMR}$ (100 MHz, CDCl_3): $\delta = 145.1, 139.2, 138.9, 130.0, 128.6, 128.4, 128.3, 127.1, 67.4, 38.5, 36.4, 32.2, 30.9, 15.4$.

2-(Tritylthio)ethanethiol^[304] (**108**)



336.51 g/mol

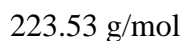
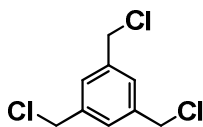
Triphenylmethanethiol (4.56 g, 16 mmol, 2 eq) and triethylamine (280 μl , 2 mmol, 25 mol%) were dissolved in dry *N,N*-dimethylformamide (50 ml) under an atmosphere of argon. Ethylenesulfide (475 μl , 480 mg, 8 mmol, 1 eq) was added and the mixture was left stirring overnight. MTBE was added and the solution was extracted three times with water in order to remove the *N,N*-dimethylformamide, followed once by brine. The organic fraction was dried over magnesium sulfate, filtered and evaporated to dryness. The pure title compound **108** was obtained after column chromatography (hexane/dichloromethane 4:1, then 3:1, then 2:1) as colorless crystals. The excess of the starting material triphenylmethanethiol was also separated by this procedure and could be reused.

2.47 g, 7.3 mmol, 92%.

EA: found: C 74.49%, H 6.02%
required: C 74.96%, H 5.99%

$^1\text{H NMR}$ (400 MHz, CDCl_3): $\delta = 7.46 - 7.41$ (*m*, 6H, Aryl-*H*), 7.33 – 7.20 (*m*, 9H, Aryl-*H*), 2.52 – 2.46 (*m*, 2H, CH_2), 2.32 – 2.24 (*m*, 2H, CH_2), 1.44 (*t*, $J = 8.3$ Hz, 1H, *SH*).

$^{13}\text{C NMR}$ (100 MHz, CDCl_3): $\delta = 144.7, 129.6, 127.9, 126.7, 67.0, 36.0, 23.8$.

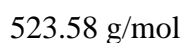
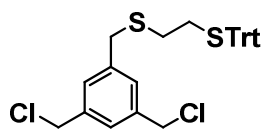
1,3,5-tris(chloromethyl)benzene^[303] (109)

1,3,5-Tris(bromomethyl)benzene (**102**) (9.92 g, 28 mmol, 1 eq) was dissolved in dry *N,N*-dimethylformamide (50 ml) under an atmosphere of argon. Lithium chloride (17 g, 410 mmol, 14.7 eq) was slowly added at 0°C. The reaction mixture was left stirring for 30 minutes at that temperature and was then allowed to warm to room temperature. After two hours stirring at room temperature, MTBE was added and the mixture was extracted four times with water followed once by brine. The organic fraction was dried over magnesium sulfate and evaporated to dryness. Recrystallization from dichloromethane/hexane gave 1,3,5-tris(chloromethyl)benzene (**109**) as colorless crystals.

5.57 g, 25 mmol, 90%.

¹H NMR (400 MHz, CDCl₃): δ = 7.38 (s, 3H, Aryl-H), 4.59 (s, 6H, CH₂).

¹³C NMR (100 MHz, CDCl₃): δ = 138.6, 128.6, 45.3.

(3,5-Bis(chloromethyl)benzyl)(2-(tritylthio)ethyl)sulfane (110)

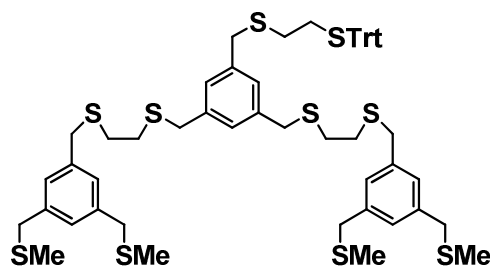
1,3,5-tris(chloromethyl)benzene (**109**) (3.81 g, 17.0 mmol, 1 eq), 2-(tritylthio)ethanethiol (**108**) (5.73 g, 17.0 mmol, 1 eq) and potassium carbonate (4.70 g, 34.0 mmol, 2 eq) were added to dry tetrahydrofuran (250 ml) under an atmosphere of argon. The mixture was heated to reflux and left at that temperature for 36 hours. After cooling to room temperature, water was added and the mixture was extracted three times with MTBE. The combined organic fractions were washed with brine, dried over magnesium sulfate and evaporated to dryness. After purification by column chromatography (hexane/dichloromethane 2:1, then 3:2), the title compound **110** was obtained as colorless solid.

4.09 g, 7.8 mmol, 46%.

EA: found: C 67.67%, H 5.41%
required: C 68.82%, H 5.39%

¹H NMR (400 MHz, CDCl₃): $\delta = 7.42 - 7.15$ (*m*, 18H, Aryl-*H*), 4.53 (*s*, 4H, CH₂), 3.51 (*s*, 2H, CH₂), 2.42 - 2.25 (*m*, 4H, CH₂).

¹³C NMR (100 MHz, CDCl₃): $\delta = 144.7, 139.4, 138.3, 129.6, 128.9, 127.9, 129.4, 126.7, 67.0, 45.6, 35.7, 31.7, 30.6$

G1 ethylene dendron 111

The G0 dendron **107** (1.416 g, 2.6 mmol, 2.05 eq) and triethylsilane (619 μl , 451.6 mg, 3.9 mmol, 3.08 eq) were dissolved in dichloromethane (15 ml). Trifluoroacetic acid (600 μl , 4% v/v) was slowly added under stirring, which was maintained for further 15 minutes after the addition. A saturated aqueous solution of sodium hydrogen carbonate was then added to quench the reaction. After the gas formation had ceased, the two phases were separated and the aqueous phase was washed twice with dichloromethane. The combined organic fractions were dried over magnesium sulfate, filtered and evaporated to dryness.

The crude thiol was then dissolved in dry tetrahydrofuran (10 ml) under an atmosphere of argon together with (3,5-bis(chloromethyl)benzyl)(2-(tritylthio)ethyl)sulfane (**110**) (657 mg, 1.25 mmol, 1 eq) and sodium hydride (60% in mineral oil, 210 mg, 5.2 mmol, 4.1 eq) was added. The mixture was left stirring for 2 hours at room temperature. Water was then added to quench the reaction and the mixture was extracted 3 times with MTBE. The combined organic fractions were washed with brine, dried over magnesium sulfate, filtered and evaporated to dryness. After purification by column chromatography (dichloromethane, then hexane/dichloromethane 2:3 with 2 % ethyl acetate), the first generation dendron **111** was obtained as colorless oil.

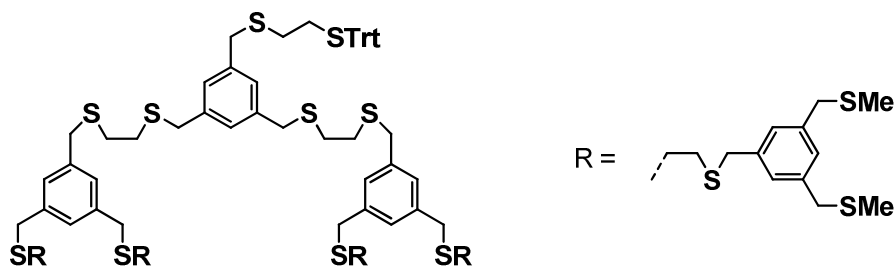
1.162 g, 1.10 mmol, 88%.

EA: found: C 62.68%, H 6.29%

required: C 63.47%, H 6.28%

¹H NMR (400 MHz, CDCl₃): $\delta = 7.42 - 7.20$ (*m*, 15H, Aryl-*H*), $7.13 - 7.08$ (*m*, 7H, Aryl-*H*), 7.00 (*br*, 2H, Aryl-*H*), 3.67 (*s*, 4H, CH₂), 3.63 (*br*, 12H, CH₂), 3.47 (*s*, 2H, CH₂), 2.56 (*br*, 8H, CH₂), $2.42 - 2.23$ (*m*, 4H, CH₂), 1.98 (*s*, 12H, CH₃).

¹³C NMR (100 MHz, CDCl₃): $\delta = 145.1, 139.3, 139.2$ (2 \times), $139.0, 130.0, 128.6, 128.5, 128.4$ (2 \times), $128.3, 127.1, 68.9, 38.5, 36.6, 36.5, 36.3, 32.2, 31.7, 31.6, 31.0, 15.5$.

G2 ethylene dendron 112

The trityl protected first generation dendron **111** (452.5 mg, 0.43 mmol, 2.2 eq) and triethylsilane (103 μl , 75 mg, 0.65 mmol, 3.3 eq) were dissolved in dichloromethane (8 ml). Trifluoroacetic acid (320 μl , 4% v/v) was slowly added under stirring, which was maintained for further 15 minutes after the addition. A saturated aqueous solution of sodium hydrogen carbonate was then added to quench the reaction. After the gas formation had ceased, the two phases were separated and the aqueous phase was washed twice with dichloromethane. The combined organic fractions were dried over magnesium sulfate, filtered and evaporated to dryness.

The crude thiol was then dissolved in dry tetrahydrofuran (20 ml) under an atmosphere of argon together with (3,5-bis(chloromethyl)benzyl)(2-(tritylthio)ethyl)sulfane (**110**) (101.6 mg, 0.19 mmol, 1 eq) and sodium hydride (60% in mineral oil, 35 mg, 0.86 mmol, 4.4 eq) was added. The mixture was left stirring for 2 hours at room temperature. Water was then added to quench the reaction and the mixture was extracted 3 times with MTBE. The combined organic fractions were washed with brine, dried over magnesium sulfate, filtered and evaporated to dryness. After purification by column chromatography (hexane/dichloromethane 2:3 with 4 % ethyl acetate), the second generation dendron **112** was obtained as colorless oil.

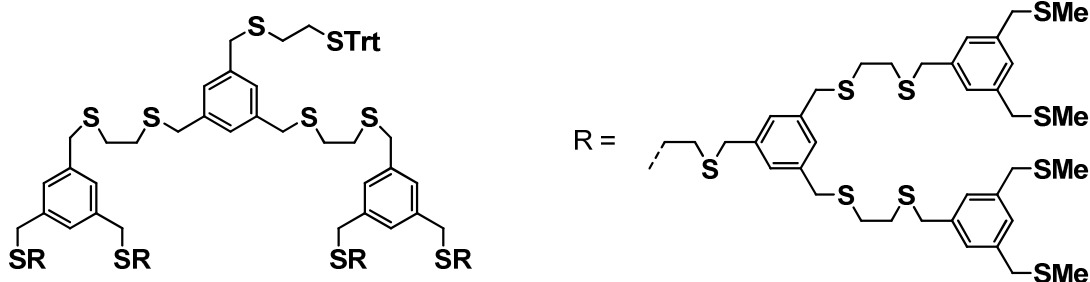
305.0 mg, 0.15 mmol, 79%.

EA: found: C 59.19%, H 6.20%
 required: C 59.89%, H 6.28%

¹H NMR (400 MHz, CDCl₃): δ = 7.44 – 7.15 (*m*, 15H, Aryl-*H*), 7.13 – 7.08 (*m*, 19H, Aryl-*H*), 7.00 (*br*, 2H, Aryl-*H*), 3.69 – 3.61 (*m*, 40H, CH₂), 3.46 (*s*, 2H, CH₂), 2.59 – 2.54 (*m*, 24H, CH₂), 2.42 – 2.23 (*m*, 4H, CH₂), 1.97 (*s*, 24H, CH₃).

¹³C NMR (100 MHz, CDCl₃): δ = 144.6, 138.7 (2 \times), 138.6, 138.5, 129.4, 128.1, 128.0 (2 \times), 127.9, 127.8, 126.6, 66.9, 38.0, 35.8, 31.7, 31.2, 31.1, 30.5, 15.0.

G3 ethylene dendron 113



4137.18 g/mol

The trityl protected second generation **112** (182.0 mg, 0.09 mmol, 2.2 eq) and triethylsilane (21 μ l, 15.2 mg, 0.13 mmol, 3.3 eq) were dissolved in dichloromethane (5 ml). Trifluoroacetic acid (200 μ l, 4% v/v) was slowly added under stirring, which was maintained for further 15 minutes after the addition. A saturated aqueous solution of sodium hydrogen carbonate was then added to quench the reaction. After the gas formation had ceased, the two phases were separated and the aqueous phase was washed twice with dichloromethane. The combined organic fractions were dried over magnesium sulfate, filtered and evaporated to dryness.

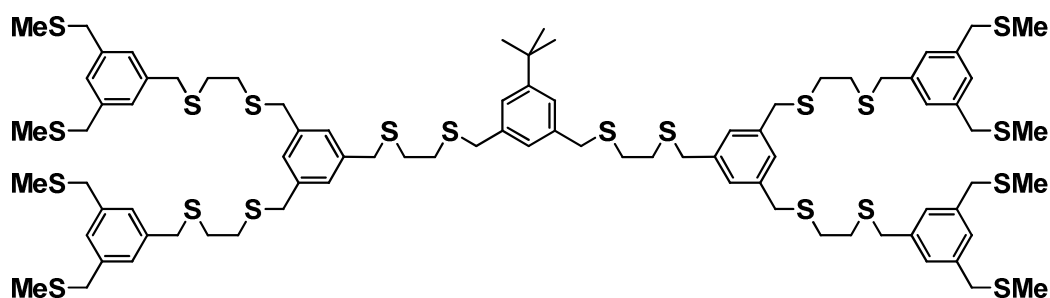
The crude thiol was then dissolved in dry tetrahydrofuran (20 ml) under an atmosphere of argon together with (3,5-bis(chloromethyl)benzyl)(2-(tritylthio)ethyl)sulfane (**110**) (20.7 mg, 0.04 mmol, 1 eq) and sodium hydride (60% in mineral oil, 7.2 mg, 0.18 mmol, 4.4 eq) was added. The mixture was left stirring for 1 hour at room temperature. Water was then added to quench the reaction and the mixture was extracted 3 times with ethyl acetate. The combined

organic fractions were washed with brine, dried over magnesium sulfate, filtered and evaporated to dryness. After purification by column chromatography (hexane/dichloromethane 1:4 with 4 % ethyl acetate), the third generation **113** was obtained as colorless oil.

121.6 mg, 0.03 mmol, 75%.

$^1\text{H NMR}$ (400 MHz, CDCl_3): $\delta = 7.43 - 7.15$ (*m*, 15H, Aryl-*H*), $7.13 - 7.08$ (*m*, 43H, Aryl-*H*), 7.00 (*br*, 2H, Aryl-*H*), $3.69 - 3.61$ (*m*, 88H, CH_2), 3.46 (*s*, 2H, CH_2), $2.59 - 2.54$ (*m*, 56H, CH_2), $2.42 - 2.23$ (*m*, 4H, CH_2), 1.97 (*s*, 48H, CH_3).

G2 *tert*-butyl terminated dendrimer **114**



1793.16 g/mol

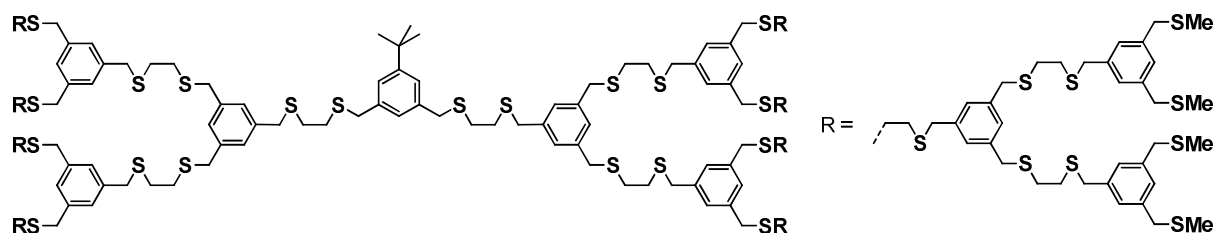
The trityl protected first generation dendron **111** (174.0 mg, 0.16 mmol, 2.1 eq) and triethylsilane (65.5 μl , 47.8 mg, 0.41 mmol, 5.4 eq) were dissolved in dichloromethane (4 ml). Trifluoroacetic acid (160 μl , 4% v/v) was slowly added under stirring, which was maintained for further 15 minutes after the addition. A saturated aqueous solution of sodium hydrogen carbonate was then added to quench the reaction. After the gas formation had ceased, the two phases were separated and the aqueous phase was washed twice with dichloromethane. The combined organic fractions were dried over magnesium sulfate, filtered and evaporated to dryness.

The crude thiol was then dissolved in dry tetrahydrofuran (10 ml) under an atmosphere of argon together with 1,3-bis(bromomethyl)-5-*tert*-butylbenzene (**3**) (24.7 mg, 0.08 mmol, 1 eq) and sodium hydride (60% in mineral oil, 13 mg, 0.32 mmol, 4.2 eq) was added. The mixture was left stirring for 1.5 hours at room temperature. Water was then added to quench the reaction and the mixture was extracted 3 times with MTBE. The combined organic fractions were washed with brine, dried over magnesium sulfate, filtered and evaporated to dryness. After purification by column chromatography (hexane/dichloromethane 2:3 with 4 % ethyl acetate), the *tert*-butyl terminated second generation **114** was obtained as colorless oil. 117.1 mg, 0.07 mmol, 88%.

EA: found: C 57.42%, H 6.53%
required: C 57.60%, H 6.63%

¹H NMR (400 MHz, CDCl₃): δ = 7.17 (*m*, 2H, Aryl-*H*), 7.12 – 7.08 (*m*, 18H, Aryl-*H*), 7.05 (*br*, 1H, Aryl-*H*), 3.69 – 3.61 (*m*, 40H, CH₂), 2.59 – 2.54 (*m*, 24H, CH₂), 1.97 (*s*, 24H, CH₃), 1.29 (*s*, 9H, C(CH₃)₃).

¹³C NMR (100 MHz, CDCl₃): δ = 151.7, 138.7, 138.5, 137.9, 128.1, 128.0, 127.9, 126.4, 124.7, 38.0, 36.5, 36.1, 36.0, 34.6, 31.3, 31.2, 31.1, 15.0.

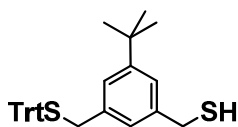
G4 *tert*-butyl terminated dendrimer 115

The trityl protected third generation dendron **113** (34.1 mg, 8.2 μmol , 2.1 eq) and triethylsilane (3.3 μl , 2.4 mg, 20.6 μmol , 5.3 eq) were dissolved in dichloromethane (1.5 ml). Trifluoroacetic acid (60 μl , 4% v/v) was slowly added under stirring, which was maintained for further 25 minutes after the addition. A saturated aqueous solution of sodium hydrogen carbonate was then added to quench the reaction. After the gas formation had ceased, the two phases were separated and the aqueous phase was washed twice with dichloromethane. The combined organic fractions were dried over magnesium sulfate, filtered and evaporated to dryness.

The crude thiol was then dissolved in dry tetrahydrofuran (20 ml) under an atmosphere of argon together with 1,3-bis(bromomethyl)-5-*tert*-butylbenzene (**3**) (1.2 mg, 3.7 μmol , 1 eq) and sodium hydride (60% in mineral oil, 1.3 mg, 33 μmol , 8.4 eq) was added. The mixture was left stirring for 2 hours at room temperature. Water was then added to quench the reaction and the mixture was extracted 3 times with ethyl acetate. The combined organic fractions were washed with brine, dried over magnesium sulfate, filtered and evaporated to dryness. After purification by column chromatography (hexane/dichloromethane 1:4 with 5 % ethyl acetate), the *tert*-butyl terminated fourth generation dendrimer **115** was obtained as colorless oil.

16.24 mg, 2.1 μmol , 57%.

$^1\text{H NMR}$ (400 MHz, CDCl_3): δ = 7.19 – 7.05 (*m*, 93H, Aryl-*H*), 3.69 – 3.61 (*m*, 184H, CH_2), 2.59 – 2.54 (*m*, 120H, CH_2), 1.97 (*s*, 96H, CH_3), 1.29 (*s*, 9H, $\text{C}(\text{CH}_3)_3$).

(3-*tert*-Butyl-5-(tritylthiomethyl)phenyl)methanethiol (116)

468.72 g/mol

To a solution of (3-(bromomethyl)-5-*tert*-butylbenzyl)(trityl)sulfane (**4**) (1.184 g, 2.3 mmol, 1 eq) in dry tetrahydrofuran (15 ml) under an atmosphere of argon was added potassium thioacetate (525 mg, 4.6 mmol, 2 eq). After 1 hour stirring at room temperature, dry methanol (15 ml) and potassium carbonate (950 mg, 6.9 mmol, 3 eq) were added and the mixture was left stirring for 1 hour. Water was added and the solution was extracted three times with MTBE. The combined organic fractions were washed with brine, dried over magnesium sulfate, filtered and evaporated to dryness. After purification by column chromatography (hexane/dichloromethane 4:1, then 3:1), the title compound **116** was obtained as colorless oily solid.

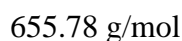
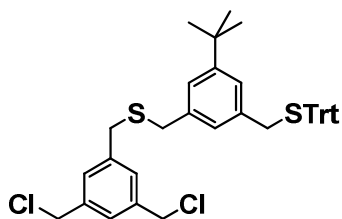
855 mg, 1.8 mmol, 80%.

EA: found: C 78.89%, H 6.96%
required: C 79.44%, H 6.88%

¹H NMR (400 MHz, CDCl₃): δ = 7.50 – 7.44 (*m*, 6H, Aryl-*H*), 7.34 – 7.29 (*m*, 6H, Aryl-*H*), 7.26 – 7.20 (*m*, 3H, Aryl-*H*), 7.16 (*br*, 1H, Aryl-*H*), 6.99 (*br*, 1H, Aryl-*H*), 6.90 (*br*, 1H, Aryl-*H*), 3.68 (*d*, *J* = 7.5 Hz, 2H, CH₂), 3.32 (*s*, 2H, CH₂), 1.71 (*t*, *J* = 7.5 Hz, 1H, SH), 1.27 (*s*, 9H, C(CH₃)₃).

¹³C NMR (100 MHz, CDCl₃): δ = 152.1, 144.9, 141.1, 137.5, 129.7, 128.2, 126.9, 126.0, 125.1, 124.1, 67.8, 37.3, 34.7, 31.5, 29.3.

MS (MALDI-TOF, *m/z*): 491.5 [*M*+Na]⁺, 507.4 [*M*+K]⁺.

(3,5-Bis(chloromethyl)benzyl)(3-*tert*-butyl-5-(tritylthiomethyl)benzyl)sulfane (118)

To a solution of 1,3,5-tris(chloromethyl)benzene (**109**) (1.376 g, 6.2 mmol, 1.25 eq) and (3-*tert*-butyl-5-(tritylthiomethyl)phenyl)methanethiol (**116**) (2.322 g, 4.9 mmol, 1 eq) in dry tetrahydrofuran (50 ml) under an atmosphere of argon was added sodium hydride (60% in mineral oil, 400 mg, 10.0 mmol, 2 eq) at 0°C. After the gas formation had ceased, the mixture was allowed to come to room temperature and stirred at that temperature for 2 hours. Water was then added to quench the reaction and the mixture was extracted 3 times with MTBE. The combined organic fractions were washed with brine, dried over magnesium sulfate, filtered and evaporated to dryness. After purification by column chromatography (hexane/dichloromethane 3:1, then 2:1), the title compound **118** was obtained as colorless solid.

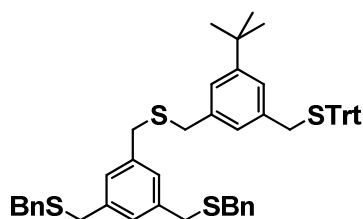
1.578 g, 2.4 mmol, 49%.

EA: found: C 73.24%, H 6.24%
required: C 73.26%, H 6.15%

¹H NMR (400 MHz, CDCl₃): $\delta = 7.50 - 7.44$ (*m*, 6H, Aryl-*H*), $7.35 - 7.27$ (*m*, 7H, Aryl-*H*), $7.26 - 7.20$ (*m*, 5H, Aryl-*H*), 7.13 (*br*, 1H, Aryl-*H*), 7.00 (*br*, 1H, Aryl-*H*), 6.88 (*br*, 1H, Aryl-*H*), 4.53 (*s*, 4H, CH₂), 3.55 (*s*, 2H, CH₂), 3.54 (*s*, 2H, CH₂), 3.32 (*s*, 2H, CH₂), 1.28 (*s*, 9H, C(CH₃)₃).

¹³C NMR (100 MHz, CDCl₃): $\delta = 151.7, 144.7, 139.6, 138.2, 137.5, 137.1, 129.7, 129.1, 127.9, 127.3, 126.8, 126.7, 124.9, 124.8, 67.6, 45.6, 37.2, 35.8, 34.9, 34.6, 31.3$.

(5-((3-*tert*-Butyl-5-(tritylthiomethyl)benzylthio)methyl)-1,3-phenylene)bis(methylene)bis(benzylsulfane) (119)



831.27 g/mol

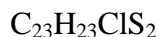
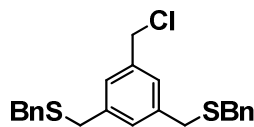
To a solution of the monochloride **120** (1.263 g, 3.2 mmol, 1 eq) and (3-*tert*-butyl-5-(tritylthiomethyl)phenyl)methanethiol (**116**) (1.514 g, 3.2 mmol, 1.05 eq) in dry tetrahydrofuran (30 ml) under an atmosphere of argon was added sodium hydride (60% in mineral oil, 260 mg, 6.5 mmol, 2.1 eq) at 0°C. After the gas formation had ceased, the mixture was allowed to come to room temperature and stirred at that temperature for 2 hours. Water was then added to quench the reaction and the mixture was extracted 3 times with MTBE. The combined organic fractions were washed with brine, dried over magnesium sulfate, filtered and evaporated to dryness. After purification by column chromatography (hexane/dichloromethane 3:2, then 1:1), the title compound **119** was obtained as colorless oil. 2.649 g, 3.2 mmol, quant.

EA: found: C 77.65%, H 6.51%
required: C 78.03%, H 6.55%

¹H NMR (400 MHz, CDCl₃): δ = 7.50 – 7.44 (*m*, 6H, Aryl-*H*), 7.35 – 7.20 (*m*, 19H, Aryl-*H*), 7.15 (*br*, 1H, Aryl-*H*), 7.08 (*br*, 3H, Aryl-*H*), 7.00 (*br*, 1H, Aryl-*H*), 6.91 (*br*, 1H, Aryl-*H*), 3.60 (*s*, 4H, CH₂), 3.58 – 3.52 (*m*, 8H, CH₂), 3.33 (*s*, 2H, CH₂), 1.28 (*s*, 9H, C(CH₃)₃).

¹³C NMR (100 MHz, CDCl₃): δ = 151.6, 144.7, 138.6, 138.0, 137.7, 137.1, 129.7, 127.9, 127.0, 126.8, 126.7, 124.8, 67.5, 37.1, 35.9, 35.7, 35.4, 34.6, 31.3.

MS (MALDI-TOF, *m/z*): 854.1 [*M*+Na]⁺, 871.1 [*M*+K]⁺.

(5-(Chloromethyl)-1,3-phenylene)bis(methylene)bis(benzylsulfane) (120)

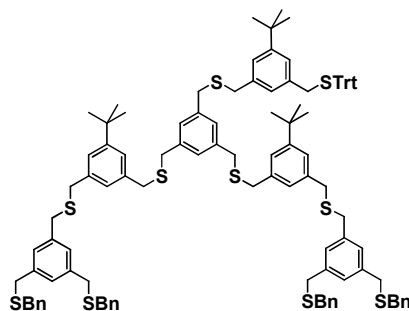
To a solution of 1,3,5-tris(chloromethyl)benzene (**109**) (1.980 g, 8.9 mmol, 1 eq) and benzyl mercaptan (1.87 ml, 1.98 g, 15.9 mmol, 1.8 eq) in dry tetrahydrofuran (40 ml) under an atmosphere of argon was added sodium hydride (60% in mineral oil, 1.28 g, 32.0 mmol, 3.6 eq) at 0°C. After the gas formation had ceased, the mixture was allowed to come to room temperature and stirred at that temperature for 1 hour. Water was then added to quench the reaction and the mixture was extracted 3 times with MTBE. The combined organic fractions were washed with brine, dried over magnesium sulfate, filtered and evaporated to dryness. After purification by column chromatography (hexane/dichloromethane 3:2, then 1:1), the title compound **120** was obtained as colorless liquid. The dichloride **121** was also isolated (0.776 g, 2.5 mmol, 28%) and was reused in further attempts to synthesize **120**.

1.562 g, 3.9 mmol, 44%.

EA: found: C 68.89%, H 5.85%
required: C 69.24%, H 5.81%

¹H NMR (400 MHz, CDCl₃): $\delta = 7.36 - 7.20$ (*m*, 10H, Aryl-*H*), 7.16 (*s*, 2H, Aryl-*H*), 7.14 (*s*, 1H, Aryl-*H*), 4.55 (*s*, 2H, CH₂), 3.61 (*s*, 4H, CH₂), 3.57 (*s*, 4H, CH₂).

¹³C NMR (100 MHz, CDCl₃): $\delta = 139.0, 137.9, 137.8, 129.7, 129.0, 128.5, 127.9, 127.1, 46.0, 35.7, 35.2$.

G1 dendron 122

The G0 dendron **119** (1.616 g, 1.94 mmol, 1 eq) was dissolved in a mixture of dichloromethane (20 ml) and triethylsilane (470 μl , 339.2 mg, 2.92 mmol, 1.5 eq). Trifluoroacetic acid (800 μl , 4% v/v of dichloromethane) was added dropwise to this solution. The mixture was stirred for 15 minutes, quenched with a saturated aqueous solution of sodium hydrogen carbonate and the organic phase was separated. The aqueous phase was washed twice with dichloromethane and the combined organic fractions were dried over magnesium sulfate. After filtration and evaporation of the solvent, the crude product was purified by column chromatography (hexane/dichloromethane 3:2) to yield the free thiol **98**, which was directly used in the next step.

1.104 g, 1.88 mmol, 97 %.

$^1\text{H NMR}$ (400 MHz, CDCl_3): $\delta = 7.32 - 7.15$ (*m*, 12H, Aryl-*H*), 7.08 (*br*, 2H, Aryl-*H*), 7.06 (*br*, 2H, Aryl-*H*), 3.70 (*d*, $J = 7.5$ Hz, 2H, CH_2), 3.60 (*s*, 4H, CH_2), 3.57 (*s*, 2H, CH_2), 3.56 (*s*, 4H, CH_2), 3.55 (*s*, 2H, CH_2), 1.75 (*t*, $J = 7.5$ Hz, 1H, *SH*), 1.29 (*s*, 9H, $\text{C}(\text{CH}_3)_3$).

The free thiol **98** (1.104 g, 1.88 mmol, 2.2 eq) and (3,5-bis(chloromethyl)benzyl)(3-*tert*-butyl-5-(tritylthiomethyl)benzyl)sulfane (**118**) (560 mg, 0.85 mmol, 1 eq) were dissolved in dry tetrahydrofuran (20 ml) under an atmosphere of argon. The mixture was degassed by bubbling argon through the solution to avoid disulfide formation during the reaction. After this procedure, sodium hydride (60 % in mineral oil, 150 mg, 3.76 mmol, 4.4 eq) was added and the mixture was left stirring at room temperature for 45 minutes. The reaction was quenched with water and extracted with MTBE three times. The combined organic fractions were

washed with brine, dried over magnesium sulfate and evaporated to dryness. Purification of the crude product was achieved by column chromatography (hexane/dichloromethane 2:3, then 1:2, then 1:3) to yield the first generation dendron **122** as colorless oil.

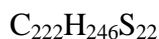
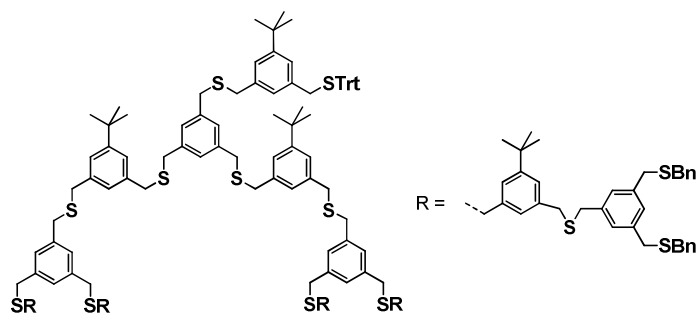
1.353 g, 0.77 mmol, 90%.

EA: found: C 75.12%, H 6.69%
required: C 75.04%, H 6.75%

$^1\text{H NMR}$ (400 MHz, CDCl_3): $\delta = 7.47 - 7.43$ (*m*, 6H, Aryl-*H*), $7.32 - 7.04$ (*m*, 45H, Aryl-*H*), 6.97 (*br*, 1H, Aryl-*H*), 6.90 (*br*, 1H, Aryl-*H*), $3.61 - 3.51$ (*m*, 36H, CH_2), 3.30 (*s*, 2H, CH_2), 1.29 (*s*, 18H, $\text{C}(\text{CH}_3)_3$), 1.25 (*s*, 9H, $\text{C}(\text{CH}_3)_3$).

$^{13}\text{C NMR}$ (100 MHz, CDCl_3): $\delta = 151.7, 144.7, 138.7, 138.6, 138.0, 137.9, 137.7, 137.1, 129.7, 129.0, 128.5, 128.4, 127.9, 127.3, 127.0, 126.9, 126.8, 126.7, 124.8, 67.5, 37.2, 35.9, 35.8, 35.6, 35.5, 34.6$ (2 \times), 31.4, 31.3.

G2 dendron **124**



3619.76 g/mol

The first generation dendron **122** (1.325 g, 0.75 mmol, 1 eq) was dissolved in a mixture of dichloromethane (20 ml) and triethylsilane (180 μl , 131.4 mg, 1.13 mmol, 1.5 eq). Trifluoroacetic acid (800 μl , 4% v/v of dichloromethane) was added dropwise to this solution. The mixture was stirred for 15 minutes, quenched with a saturated aqueous solution of sodium hydrogen carbonate and the organic phase was separated. The aqueous phase was washed

twice with dichloromethane and the combined organic fractions were dried over magnesium sulfate. After filtration and evaporation of the solvent, the crude product was purified by column chromatography (hexane/dichloromethane 1:2) to yield the free thiol **127**, which was directly used in the next step.

1.013 g, 0.67 mmol, 89 %

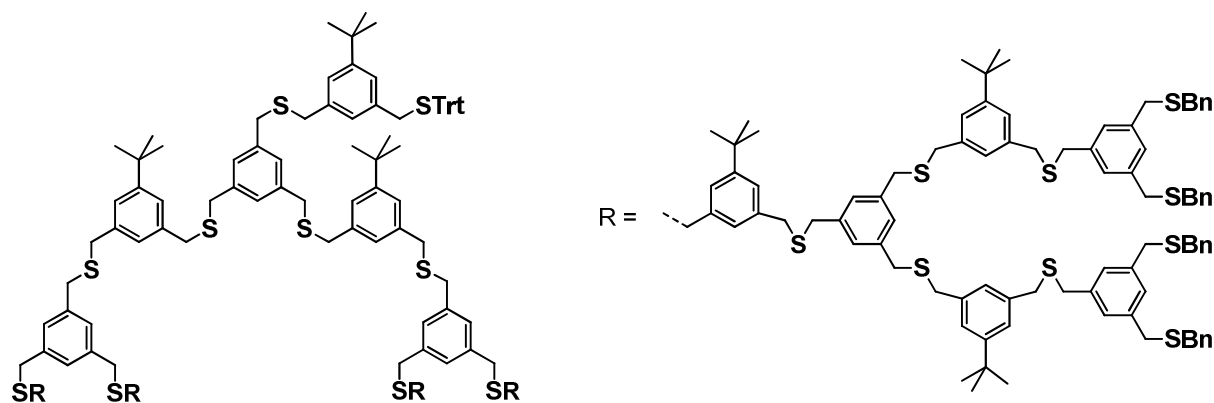
¹H NMR (400 MHz, CDCl₃): δ = 7.32 – 7.04 (*m*, 38H, Aryl-*H*), 3.69 (*d*, *J* = 7.5 Hz, 2H, CH₂), 3.61 – 3.53 (*m*, 36H, CH₂), 1.75 (*t*, *J* = 7.5 Hz, 1H, SH), 1.29 (*s*, 27H, C(CH₃)₃).

The deprotected dendron **127** (474.1 mg, 0.31 mmol, 2.3 eq) and (3,5-bis(chloromethyl)-benzyl)(3-*tert*-butyl-5-(tritylthiomethyl)benzyl)sulfane (**118**) (88.8 mg, 0.14 mmol, 1 eq) were dissolved in dry tetrahydrofuran (15 ml) under an atmosphere of argon. The mixture was degassed by bubbling argon through the solution to avoid disulfide formation during the reaction. After this procedure, sodium hydride (60 % in mineral oil, 25 mg, 0.62 mmol, 4.6 eq) was added and the mixture was left stirring at room temperature for 45 minutes. The reaction was quenched with water and extracted with MTBE three times. The combined organic fractions were washed with brine, dried over magnesium sulfate and evaporated to dryness. Purification of the crude product was achieved by column chromatography (hexane/dichloromethane 1:3, then 1:4, then dichloromethane) to give the second generation dendron **124** as colorless oil.

444.3 mg, 0.13 mmol, 90%,

¹H NMR (400 MHz, CD₂Cl₂): δ = 7.47 – 7.43 (*m*, 6H, Aryl-*H*), 7.32 – 7.03 (*m*, 90H, Aryl-*H*), 6.96 (*br*, 1H, Aryl-*H*), 6.90 (*br*, 1H, Aryl-*H*), 3.62 – 3.51 (*m*, 84H, CH₂), 3.30 (*s*, 2H, CH₂), 1.29 (*s*, 36H, C(CH₃)₃), 1.27 (*s*, 18H, C(CH₃)₃), 1.24 (*s*, 9H, C(CH₃)₃).

¹³C NMR (100 MHz, CD₂Cl₂): δ = 152.2, 145.3, 139.4 (3×), 139.3, 138.8, 138.6 (2×), 130.2, 129.5, 129.0, 128.8, 128.5, 127.5, 127.4 (2×), 127.3, 125.3 (2×), 68.0, 37.5, 36.5 (3×), 36.3, 36.2, 36.1 (2×), 35.1 (2×), 31.7, 31.6.

G3 dendron 128

7337.75 g/mol

The second generation dendron **124** (154.5 mg, 0.042 mmol, 1 eq) was dissolved in a mixture of dichloromethane (5 ml) and triethylsilane (17 μ l, 12.4 mg, 0.107 mmol, 2.5 eq). Trifluoroacetic acid (200 μ l, 4% v/v of dichloromethane) was added to this solution. The mixture was stirred for 15 minutes, quenched with a saturated aqueous solution of sodium hydrogen carbonate and the organic phase was separated. The aqueous phase was washed twice with dichloromethane and the combined organic fractions were dried over magnesium sulfate. After filtration and evaporation of the solvent, the crude product was purified by column chromatography (dichloromethane) to yield the free thiol **130**, which was directly used in the next step.

120.2 mg, 0.036 mmol, 84 %

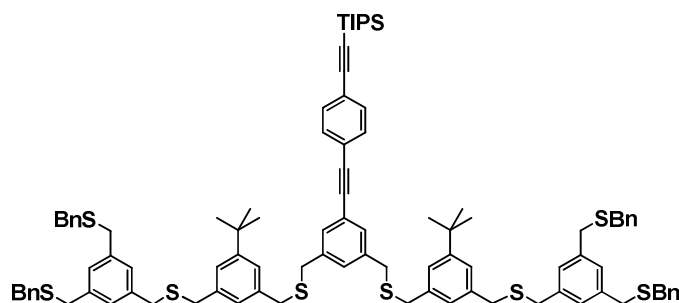
The deprotected dendron **130** (82.0 mg, 0.024 mmol, 2.1 eq) and (3,5-bis(chloromethyl)-benzyl)(3-*tert*-butyl-5-(tritylthiomethyl)benzyl)sulfane (**118**) (7.46 mg, 0.011 mmol, 1 eq) were dissolved in dry tetrahydrofuran (7 ml) under an atmosphere of argon. Sodium hydride (60 % in mineral oil, 15 mg, 0.37 mmol, 34 eq) was added and the mixture was left stirring at room temperature for 45 minutes. The reaction was quenched with water and extracted with MTBE three times. The combined organic fractions were washed with brine, dried over magnesium sulfate and evaporated to dryness. Purification of the crude product was achieved by column chromatography (dichloromethane, then dichloromethane/2.5% ethyl acetate) to give the third generation dendron **128** as colorless oil.

24.2 mg, 0.003 mmol, 29%,

¹H NMR (400 MHz, CDCl₃): δ = 7.47 – 7.43 (*m*, 6H, Aryl-*H*), 7.32 – 7.03 (*m*, 177H, Aryl-*H*), 6.95 (*br*, 1H, Aryl-*H*), 6.89 (*br*, 1H, Aryl-*H*), 3.62 – 3.51 (*m*, 180H, CH₂), 3.29 (*s*, 2H, CH₂), 1.30 – 1.25 (*m*, 135H, C(CH₃)₃).

Reduction of the Disulfide By-products 123, 126 and 129, General Procedure

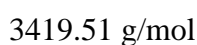
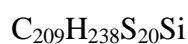
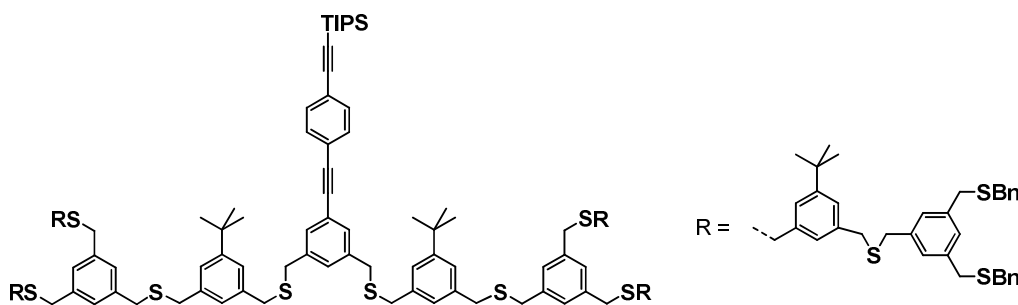
The respective dendrimer disulfide (1 eq) was dissolved in dry tetrahydrofuran under an atmosphere of argon and methanol (10% v/v) and tri-*n*-butyl phosphine (3 eq) were added. The resulting mixture was stirred at room temperature for two hours. Subsequently, the solvents were removed by rotary evaporation and the crude was subjected to column chromatography.

G1 OPE dendrimer 131

The freshly prepared starting generation thiol dendron **98** (170.2 mg, 0.29 mmol, 2.5 eq) and the OPE dibromide **64** (62.9 mg, 0.12 mmol, 1 eq) were dissolved in dry tetrahydrofuran (5 ml) under an atmosphere of argon. The mixture was degassed by bubbling argon through the solution to avoid disulfide formation during the reaction. After this procedure, sodium hydride (60 % in mineral oil, 24.0 mg, 0.60 mmol, 5 eq) was added and the mixture was left stirring at room temperature for 1.5 hours. The reaction was quenched with water and extracted with MTBE three times. The combined organic fractions were washed with brine, dried over magnesium sulfate and evaporated to dryness. Purification of the crude product was achieved by column chromatography (hexane/dichloromethane 2:3, then 1:2) to yield the G1 dendrimer **131** as colorless oil. Traces of the disulfide **123** were observed by NMR. This compound was removed in a second purification step by column chromatography.

177.4 mg, 0.11 mmol, 98%.

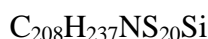
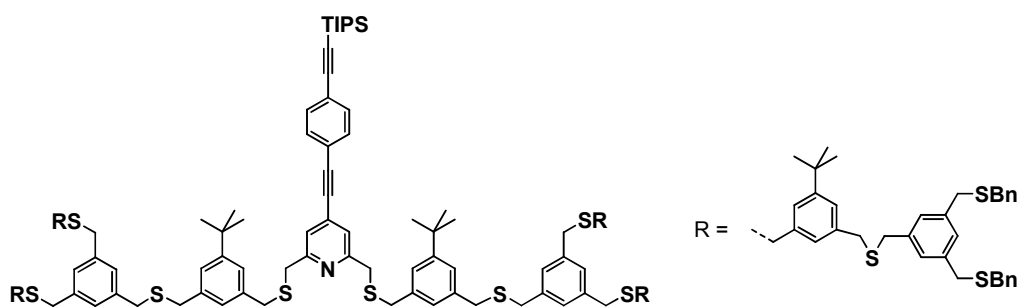
¹H-NMR (400 MHz, CDCl₃): $\delta = 7.47 - 7.39$ (*m*, 4H, Aryl-*H*), $7.32 - 7.19$ (*m*, 23H, Aryl-*H*), 7.18 (*br*, 2H, Aryl-*H*), 7.14 (*br*, 2H, Aryl-*H*), 7.10 (*br*, 2H, Aryl-*H*), 7.08 (*br*, 4H, Aryl-*H*), 7.05 (*br*, 2H, Aryl-*H*), 3.60 (*s*, 8H, CH₂), 3.58 (*s*, 4H, CH₂), 3.57 (*s*, 4H, CH₂), 3.55 (*m*, 16H, CH₂), 1.30 (*s*, 18H, C(CH₃)₃), 1.14 (*m*, 21H, *iPr-H*).

G2 OPE dendrimer **132**

The freshly prepared G1 free thiol dendron **127** (195.7 mg, 0.13 mmol, 2.2 eq) and the OPE dibromide **64** (31.2 mg, 0.06 mmol, 1 eq) were dissolved in dry tetrahydrofuran (7 ml) under an atmosphere of argon. The mixture was degassed by bubbling argon through the solution to avoid disulfide formation during the reaction. After this procedure, sodium hydride (60 % in mineral oil, 10.4 mg, 0.26 mmol, 4.4 eq) was added and the mixture was left stirring at room temperature for 1 hour. The reaction was quenched with water and extracted with MTBE three times. The combined organic fractions were washed with brine, dried over magnesium sulfate and evaporated to dryness. Purification of the crude product was achieved by column chromatography (hexane/dichloromethane 1:4, then dichloromethane) to yield the G2 dendrimer **132** as colorless oil. However, traces of the disulfide **126** were observed by NMR. This compound was removed in a second purification step by column chromatography. 199.5 mg, 0.06 mmol, 99%.

¹H-NMR (500 MHz, CDCl₃): $\delta = 7.47 - 7.39$ (*m*, 4H, Aryl-*H*), $7.32 - 7.19$ (*m*, 43H, Aryl-*H*), 7.15 (*br*, 10H, Aryl-*H*), 7.12 (*br*, 10H, Aryl-*H*), 7.08 (*br*, 12H, Aryl-*H*), 7.05 (*br*, 4H, Aryl-*H*), $3.61 - 3.52$ (*m*, 72H, CH₂), 1.28 (*s*, 54H, C(CH₃)₃), 1.27 (*s*, 36H, C(CH₃)₃), 1.13 (*m*, 21H, *iPr-H*).

¹³C NMR (125 MHz, CDCl₃): $\delta = 151.6, 151.5, 139.0, 138.7, 138.6, 138.0$ (2×), $137.8, 137.7, 132.0, 131.3, 130.8, 129.9, 129.0, 128.5, 128.4, 128.3, 127.0, 126.9, 126.8, 124.9$ (2×), $124.8, 123.4, 123.1, 123.0, 106.6, 92.8, 90.9, 89.4, 35.9$ (2×), $35.7, 35.6, 35.4, 35.1, 34.6, 34.5, 31.4$ (2×), $18.7, 11.3$.

G2 pyridine OPE dendrimer 133

The freshly prepared G1 free thiol dendron **127** (284.2 mg, 0.19 mmol, 2.4 eq) and the pyridine OPE dibromide **86** (43.2 mg, 0.08 mmol, 1 eq) were dissolved in dry tetrahydrofuran (8 ml) under an atmosphere of argon. The mixture was degassed by bubbling argon through the solution to avoid disulfide formation during the reaction. After this procedure, sodium hydride (60 % in mineral oil, 16 mg, 0.4 mmol, 5 eq) was added and the mixture was left stirring at room temperature for 1 hour. The reaction was quenched with water and extracted with MTBE three times. The combined organic fractions were washed with brine, dried over magnesium sulfate and evaporated to dryness. Purification of the crude product was achieved by column chromatography (hexane/dichloromethane 1:4 with 2 % triethylamine) to yield **133** as colorless oil.

272.5 mg, 0.08 mmol, quant.

EA: found: C 72.09%, H 6.90%, N 0.36%
required: C 73.04%, H 6.98%, N 0.41%

¹H NMR (400 MHz, CD₂Cl₂): δ = 7.48 (*br*, 4H, Aryl-*H*), 7.32 – 7.05 (*m*, 78H, Aryl-*H*), 3.71 (*s*, 4H, CH₂), 3.68 (*s*, 4H, CH₂), 3.61 – 3.52 (*m*, 80H, CH₂), 1.29 (*s*, 18H, C(CH₃)₃), 1.28 (*s*, 36H, C(CH₃)₃), 1.13 (*m*, 21H, *i*Pr-*H*).

¹³C-NMR (125 MHz, CDCl₃): δ = 158.6, 151.6, 151.5, 138.7, 138.4, 138.0, 137.9, 137.8, 137.7, 132.1 (2×), 131.7, 131.6, 129.0, 128.5, 128.3, 127.0, 126.9, 126.8, 125.1, 124.9, 124.8, 124.3, 123.0, 121.9, 93.6, 93.3, 88.6, 37.3, 36.1, 35.9, 35.7, 35.6, 35.4, 34.6, 31.4, 16.7, 11.3.

MS (MALDI-TOF, *m/z*): broad peak starting at 3440 [*M*+Na]⁺.

6.3 Gold Nanoparticle Experiments

6.3.1 Gold Cluster Ligand Exchange Experiments

NMR Titration Experiment

A solution of the heptameric ligand **1** (1.4 mg, 1 μmol , 1 eq) in deuterated dichloromethane (CD_2Cl_2) (1 ml) was prepared in an NMR tube. $[\text{Au}_9(\text{PPh}_3)_8](\text{NO}_3)_3$ (total 2 μmol , 2 eq) was then added in 0.2 μmol portions. After each addition of gold cluster, the ^1H and the ^{31}P NMR spectra of the mixture were recorded.

Long Term NMR Studies

A mixture of the heptameric ligand **1** (1.4 mg, 1 μmol , 1 eq), $[\text{Au}_9(\text{PPh}_3)_8](\text{NO}_3)_3$ (4.05 mg, 1 μmol , 1 eq) and ferrocene (0.2 mg, 1 μmol , 1 eq) was dissolved in deuterated dichloromethane under an atmosphere of argon. The NMR tube was then directly sealed and was investigated regularly by ^1H and the ^{31}P NMR over a period of 10 weeks.

Similarly, a mixture of $[\text{Au}_9(\text{PPh}_3)_8](\text{NO}_3)_3$ (4.05 mg, 1 μmol , 1 eq) and ferrocene (0.2 mg, 1 μmol , 1 eq) was prepared and investigated for comparison.

Ligand Exchange Experiments Using Excess Ligand **1**

a) in dichloromethane

A mixture of $[\text{Au}_9(\text{PPh}_3)_8](\text{NO}_3)_3$ (7.0 mg, 1.7 μmol , 1 eq) and the thioether heptamer **1** (40.0 mg, 25.5 μmol , 15 eq) in dry dichloromethane (10 ml) was stirred at room temperature under an atmosphere of argon. The mixture was investigated by ^{31}P NMR and UV/vis spectroscopy after 48 hours. As no changes were observed, the solution was warmed to 35°C and further investigated by ^{31}P NMR (see Figure 25, section 3.1.2.2) and UV/vis spectroscopy (see Figure 26, section 3.1.2.2).

b) in biphasic methanol/hexane or ethylene glycol/toluene mixtures

A solution of $[\text{Au}_9(\text{PPh}_3)_8](\text{NO}_3)_3$ (7.0 mg, 1.7 μmol , 1 eq) in methanol or ethylene glycol (5 ml) was added to a solution of the thioether heptamer **1** (40.0 mg, 25.5 μmol , 15 eq) in hexane or toluene (5 ml) under an atmosphere of argon. The to some extent biphasic mixtures

were stirred at room temperature for 72 hours and the cluster containing phases were regularly investigated by ^{31}P NMR and UV/vis spectroscopy.

Ligand Exchange Experiments Using Water Soluble Gold Clusters

a) with heptamer **1**

Solutions of freshly prepared gold clusters stabilized by triphenylphosphine monosulfonate or trisulfonate (from 2.5 μmol $[\text{Au}_9(\text{PPh}_3)_8](\text{NO}_3)_3$) in water (3 ml) were added to solutions of the heptameric thioether ligand **1** (52.8 mg, 37.5 μmol , 15 eq) in dichloromethane (5 ml). The biphasic mixtures were stirred vigorously at room temperature for 4 days.

b) with the diacid ligand **15**

A solution of freshly prepared gold clusters stabilized by triphenylphosphine monosulfonate (from 2.5 μmol $[\text{Au}_9(\text{PPh}_3)_8](\text{NO}_3)_3$) in water (3 ml) was added to a solution of the diacid **15** (42.8 mg, 0.13 mmol, 50 eq) in dichloromethane (5 ml). The biphasic mixture was stirred vigorously at room temperature for 15 days.

Ligand Exchange Experiments with Diglyme Stabilized Gold Nanoparticles

The diglyme stabilized gold nanoparticles were prepared by addition of the preformed reducing agent sodium naphthalenide (400 μl , 0.04 mmol, 2.5 eq of a solution prepared from 4.3 mmol sodium and 3.2 mmol naphthalene in 35 ml diglyme, 0.04 mmol, 2.5 eq) to a solution of tetrachloroauric acid (9 mg, 0.015 mmol, 1 eq) in dry diglyme (5 ml) under an atmosphere of argon. The mixture turned brown immediately after the addition of the reducing agent. After two minutes, 500 μl portions of the reaction mixture were added to solutions of the heptamer **1** (2.1 mg - 21 mg, 1, 3, 6 or 10 eq concerning the amount of HAuCl_4 in the 500 μl aliquot) in toluene (500 μl). The resulting precipitates were centrifuged and the supernatant was taken off. It was then attempted to redisperse the residues in dichloromethane, which was only partially possible and led to very slightly purple dispersions in all cases.

6.3.2 Gold Nanoparticle Formation and Purification, General Procedure

Gold nanoparticle syntheses were carried out on a 20 – 28 μmol scale with respect to the number n of thioether moieties present in the respective ligand. Tetrachloroauric acid (n eq) was dissolved in deionized water (2.5 ml). A solution of tetraoctylammonium bromide ($2n$ eq) in dichloromethane (2.5 ml) was added and the two-phase mixture stirred until the aqueous phase became colorless. The respective thioether ligand (1 eq) was dissolved in dichloromethane (2.5 ml) and then added to the reaction mixture, followed by a freshly prepared solution of sodium borohydride ($8n$ eq) in water (2.5 ml). After 10 minutes stirring, the resulting strongly colored dichloromethane phase was separated and the aqueous phase was washed twice with dichloromethane. The combined organic fractions were dried over magnesium sulfate, filtered and concentrated to a volume of *ca.* 1 ml. Ethanol (approx. 15 ml) was added to precipitate the particles, which were then centrifuged. The supernatant was discarded and the procedure was repeated two times. After this procedure, the nanoparticles were subjected to Gel Permeation Chromatography (*Bio-Rad Bio-Beads S-X1 Beads*) using toluene as eluent. The colored, nanoparticle containing fractions were collected and the solvent was removed using a rotary evaporator.

6.3.3 Gold Nanoparticle Superstructures

Diacetylene formation of the free acetylene OPE heptamer **68**

The acetylene heptamer **68** (6.4 mg, 0.004 mmol) was dissolved in dichloromethane (2 ml), *N,N,N',N'*-tetramethylethylenediamine (50 μl) and copper(I) chloride (1.0 mg, 0.01 mmol) were added. The mixture was stirred vigorously in an open reaction vessel. After 15 minutes, thin layer chromatography revealed the complete consumption of the starting material **68** and the formation of one new spot. The reaction mixture was extracted with a saturated aqueous solution of ammonium chloride, dried over magnesium sulfate and evaporated to dryness to give a slightly yellow oil (6.4 mg). The ^1H NMR spectrum shows the disappearance of the acetylene proton and indicates therefore the formation of the diacetylene **101**.

6.4 mg, 0.002 mmol, quant.

^1H NMR (400 MHz, CDCl_3): 7.33 – 7.04 (*m*, 62H, Aryl-*H*), 3.60 (*m*, 40H, CH_2), 3.58 (*s*, 8H, CH_2), 3.57 (*s*, 8H, CH_2), 3.54 (*s*, 8H, CH_2), 1.32 (*m*, 108H, $\text{C}(\text{CH}_3)_3$).

One-pot deprotection/diacetylene formation, general procedure

To a solution of the respective TIPS acetylene thioether ligand (0.9 – 1.1 μmol) in dichloromethane (400 μl) was added tetra-*n*-butylammonium fluoride (1M in tetrahydrofuran, 5 μl). The mixture was left stirring until the deprotection of the acetylene moiety was completed by thin layer chromatography (approx. 30 minutes). *N,N,N',N'*-tetramethylethylenediamine (10 μl) and copper(I) chloride (0.5 mg, 0.005 mmol) were then added and the resulting mixture was stirred in an open reaction vessel, until the reaction was complete by thin layer chromatography (approx. 15 minutes). After dilution of the solution with dichloromethane, the reaction mixture was extracted with a saturated aqueous solution of ammonium chloride. The aqueous phase was washed with dichloromethane (2 \times 5 ml) and the combined organic fractions were dried over magnesium sulfate. After filtration, the respective diacetylene was investigated by UV/vis.

Formation of gold nanoparticle aggregates and superstructures, general procedure

The formation of gold nanoparticle aggregates and superstructures (**Au-X**)_{*n*} was done on a 0.9 – 1.1 mg scale regarding **Au-X**. The acetylene functionalized gold nanoparticles were dispersed in dichloromethane (200 μl) and tetra-*n*-butylammonium fluoride (1M in tetrahydrofuran, 5 μl) was added. The mixture was left stirring for 1 hour, after which *N,N,N',N'*-tetramethylethylenediamine (5 μl) and copper(I) chloride (0.5 mg) were added. After 15 minutes, approximately half of the reaction mixture was removed, diluted with dichloromethane (*ca.* 20 ml) and investigated by UV/vis spectroscopy and TEM. The other half was diluted with dichloromethane (*ca.* 5 ml) extracted with a saturated aqueous solution of ammonium chloride. The aqueous phase was washed with dichloromethane (2 \times 5 ml) and the combined organic fractions were dried over magnesium sulfate. After filtration, this dispersion was also analyzed by UV/vis and TEM.

7 Appendix: TEM Micrographs

7.1 OPE Functionalized Linear Thioether Ligands

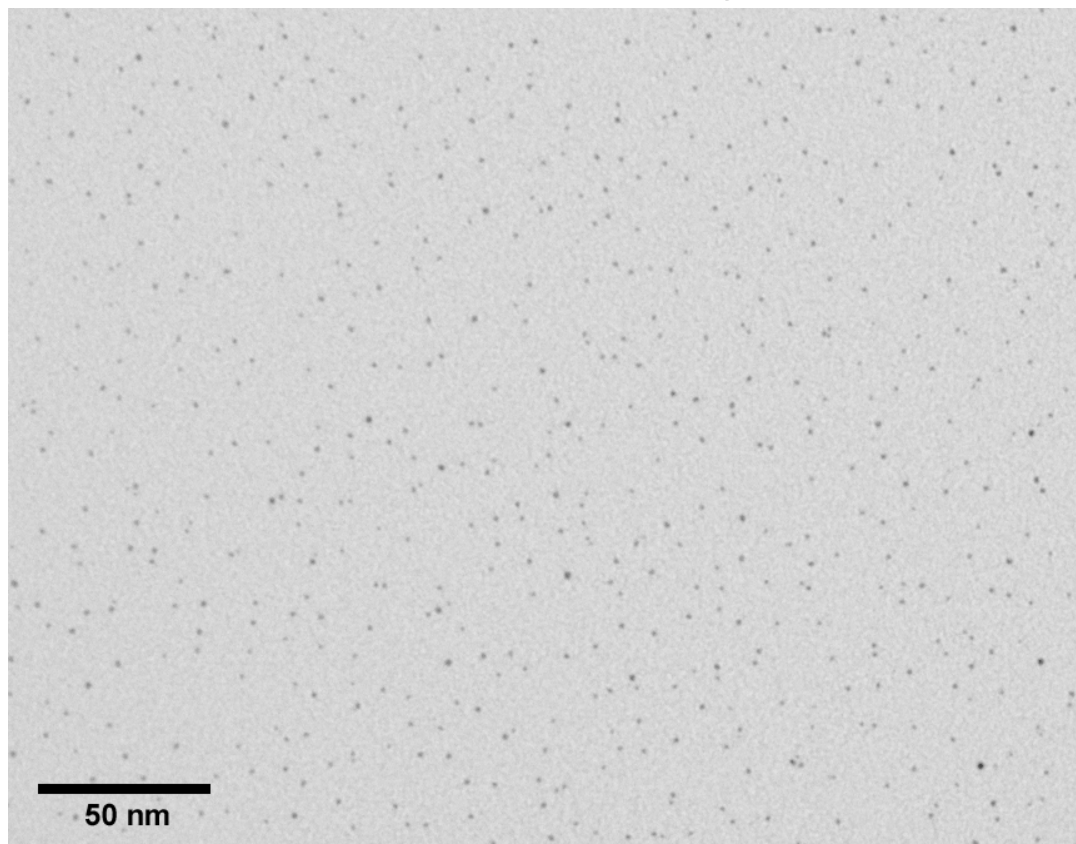


Figure 76. Representative TEM micrograph of **Au-62**.

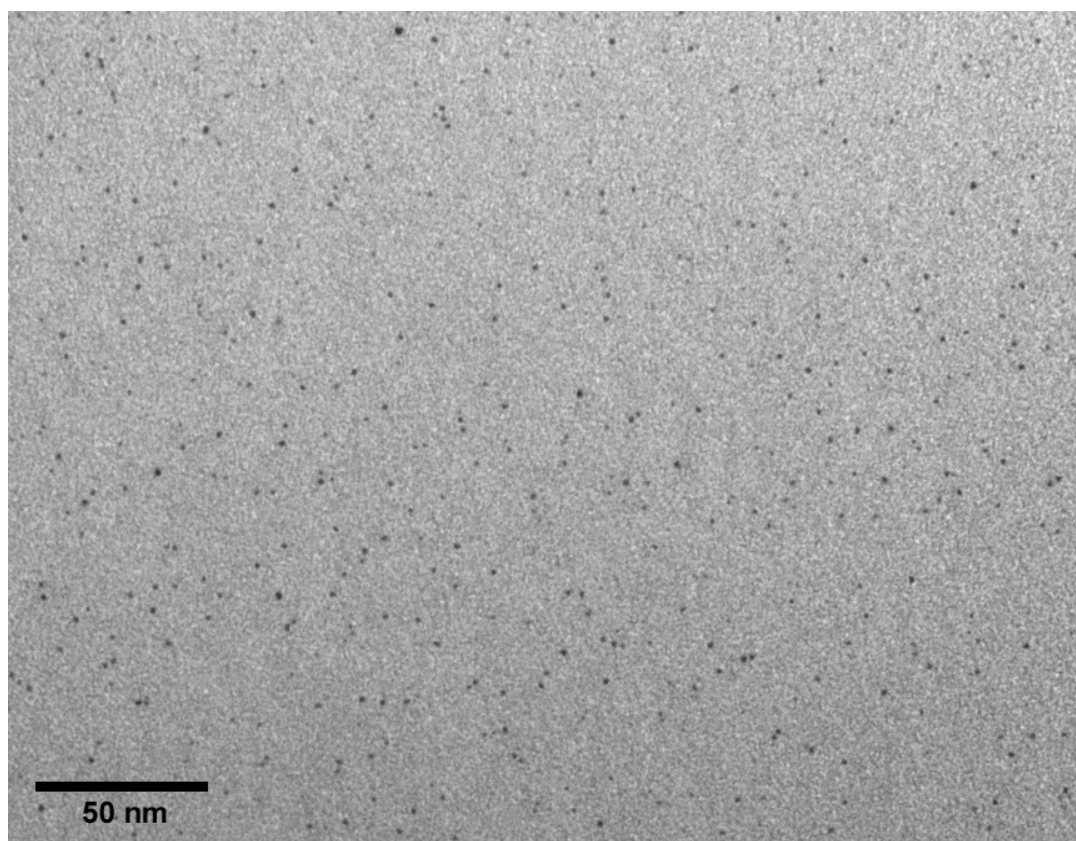


Figure 77. Representative TEM micrograph of **Au-66**.

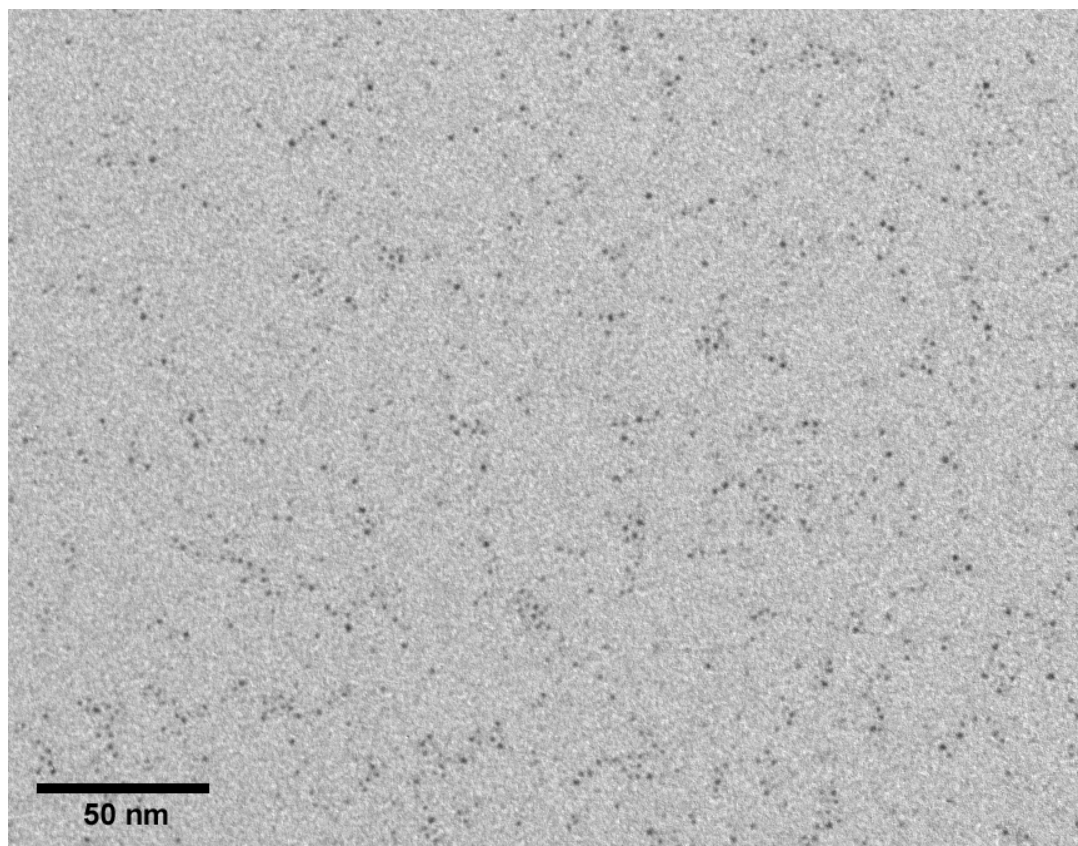


Figure 78. Representative TEM micrograph of **Au-67**.

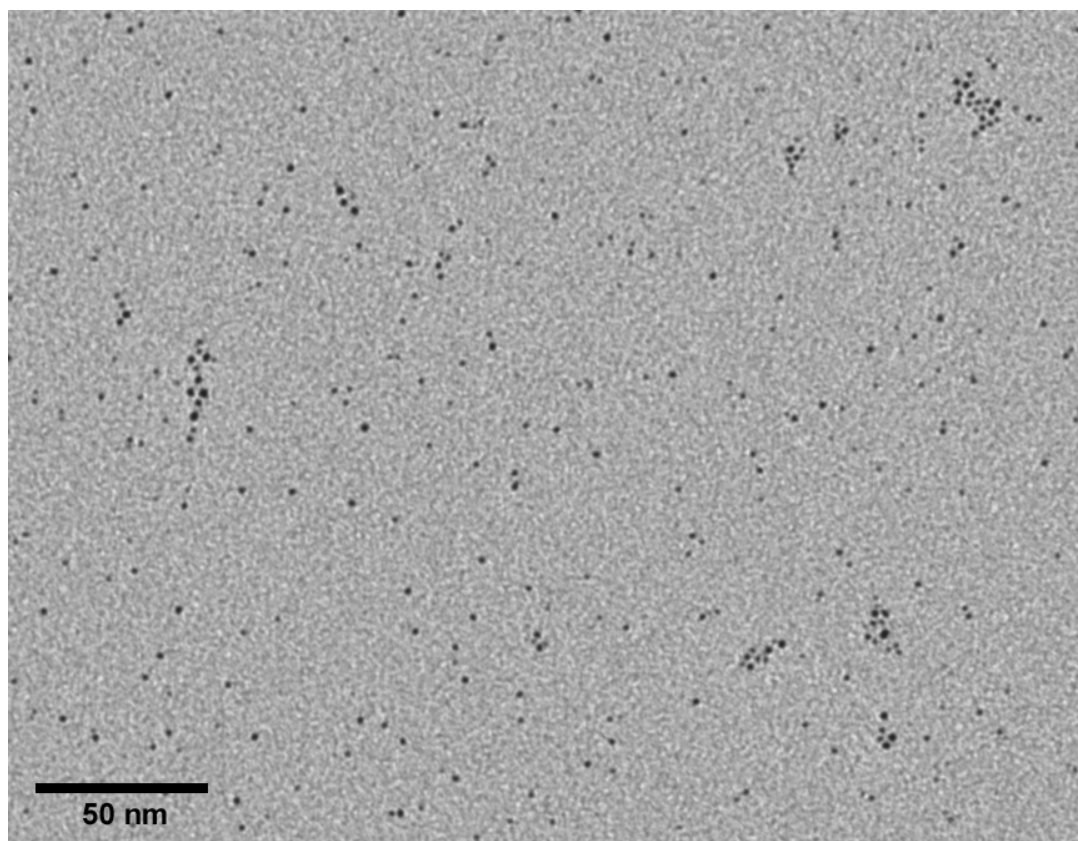


Figure 79. Representative TEM micrograph of **Au-69**.

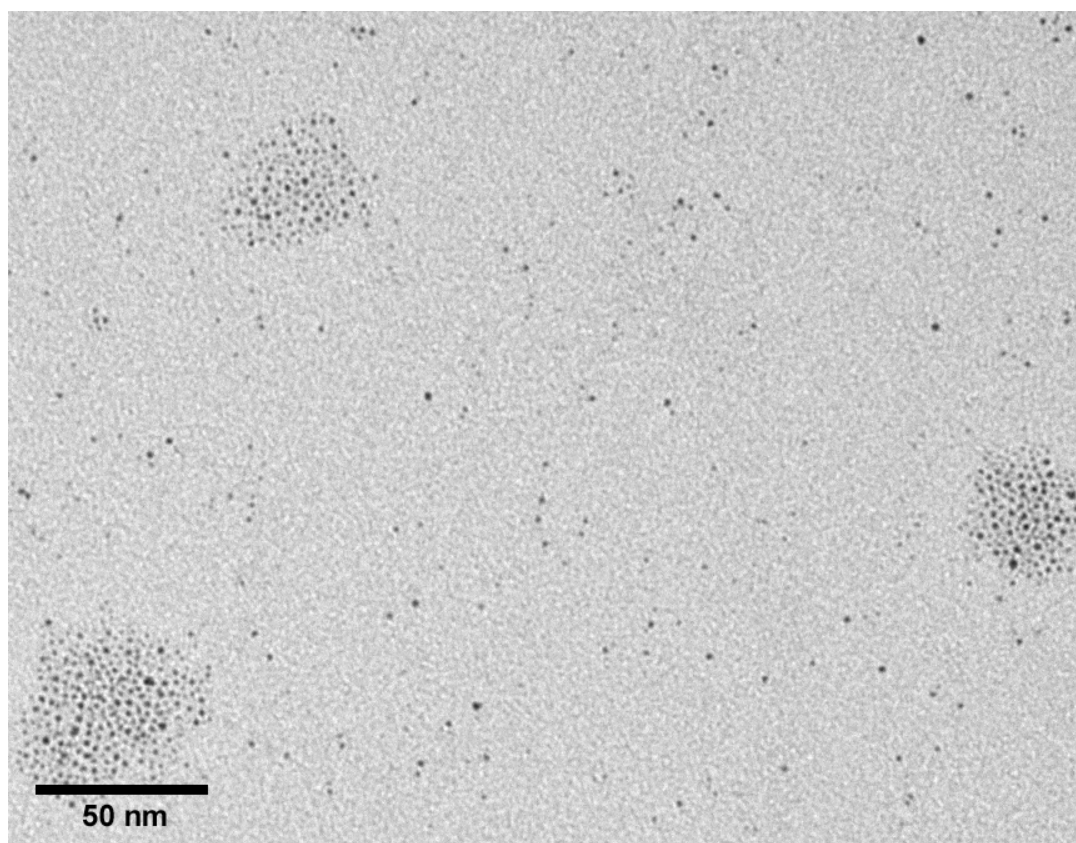


Figure 80. Representative TEM micrograph of $(\text{Au-62})_n$.

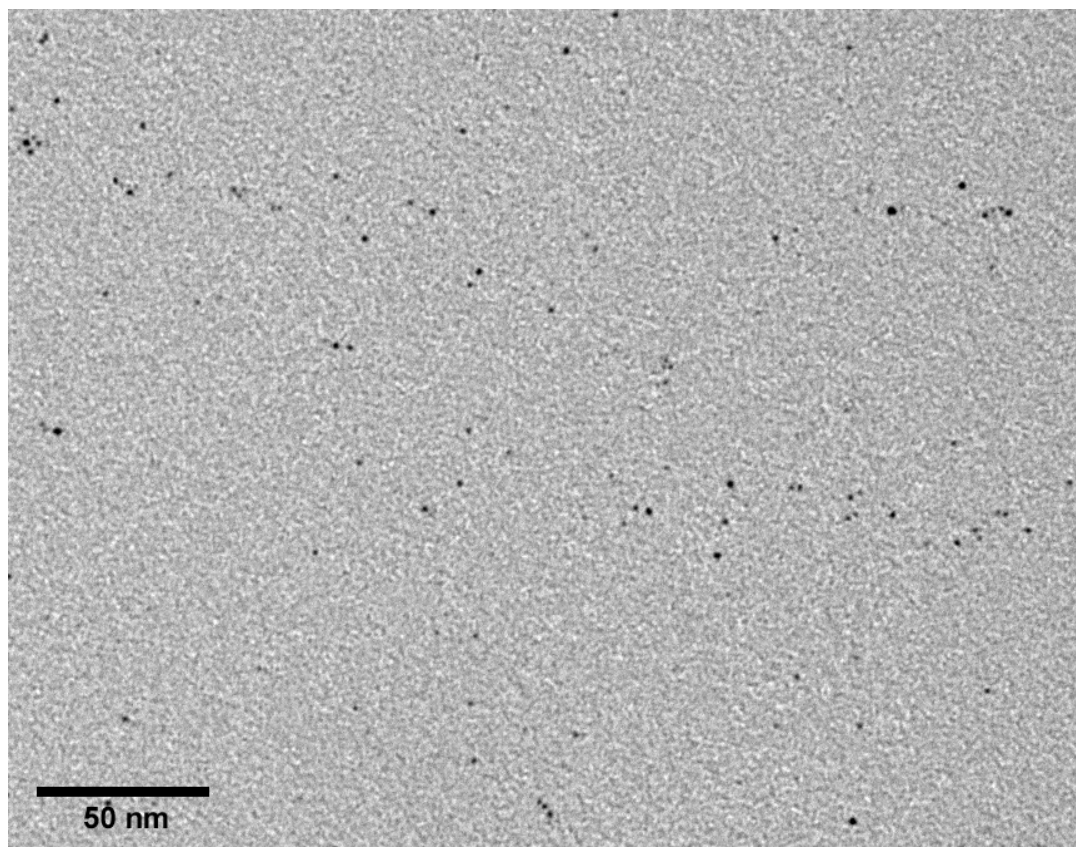


Figure 81. Representative TEM micrograph of $(\text{Au-62})_{2-4}$.

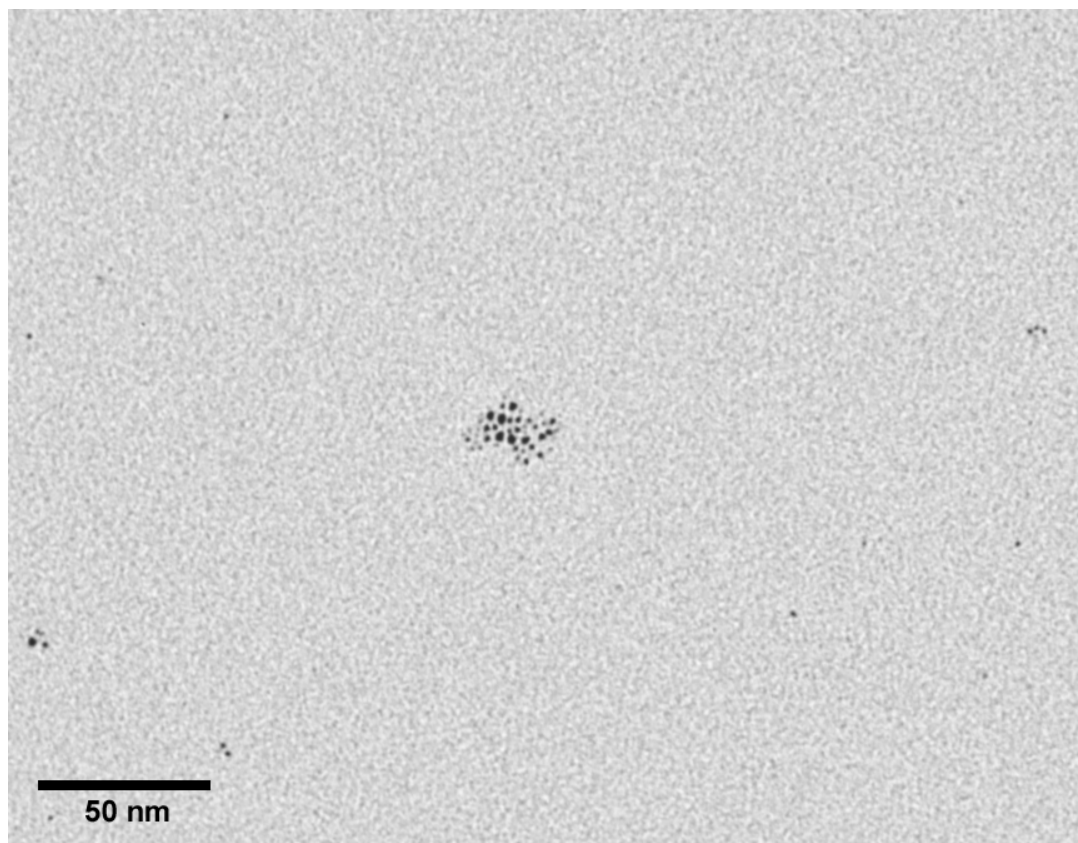


Figure 82. Representative TEM micrograph of $(\text{Au-66})_n$.

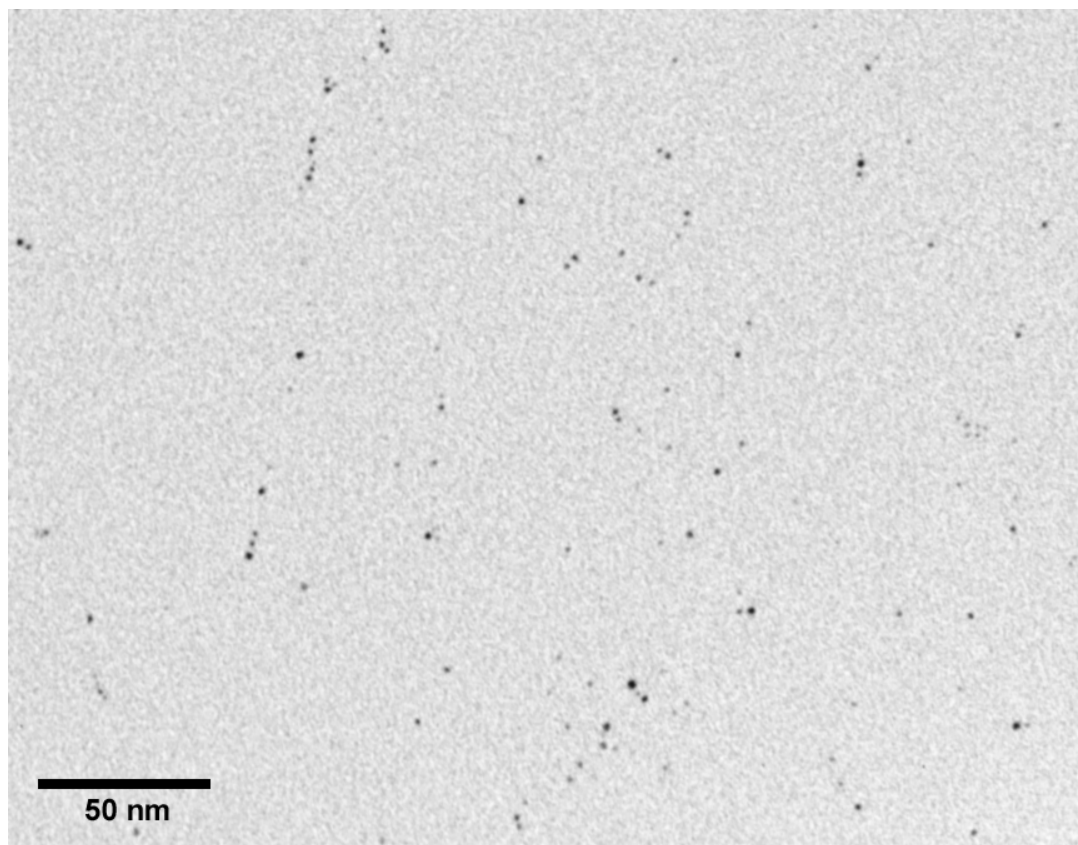


Figure 83. Representative TEM micrograph of $(\text{Au-66})_{2.4}$.

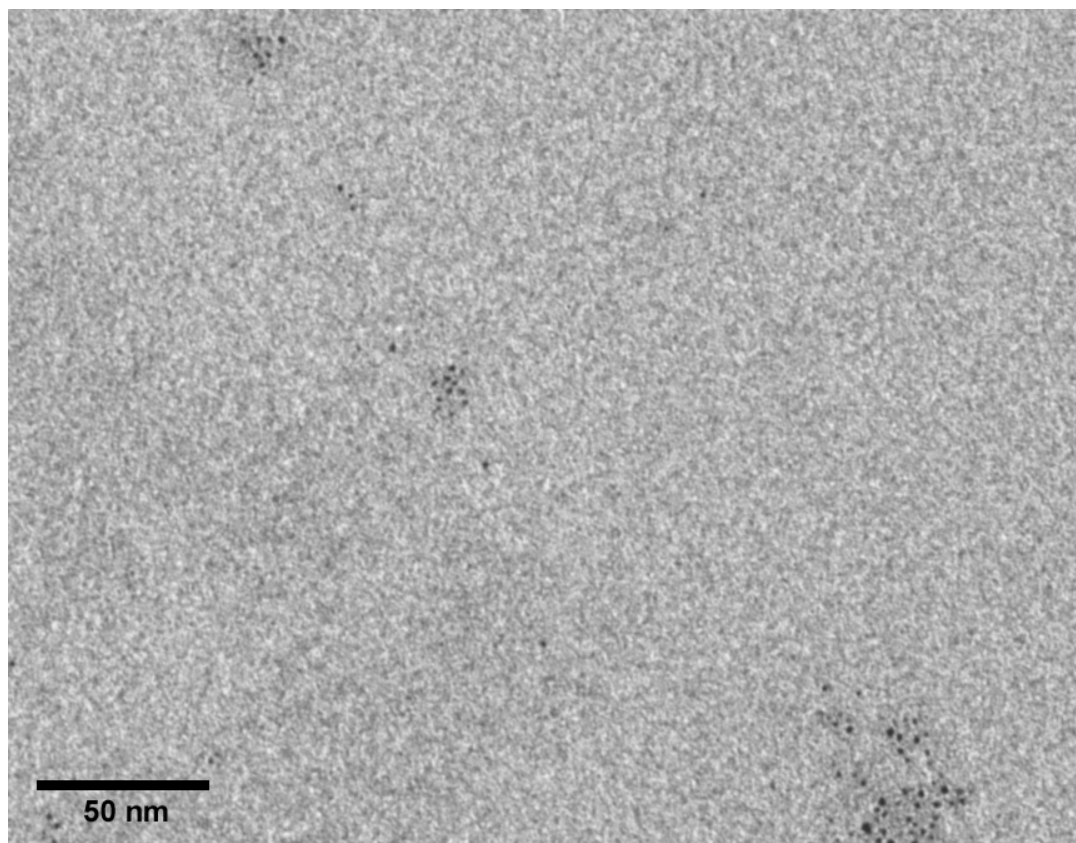


Figure 84. Representative TEM micrograph of $(\text{Au-67})_n$.

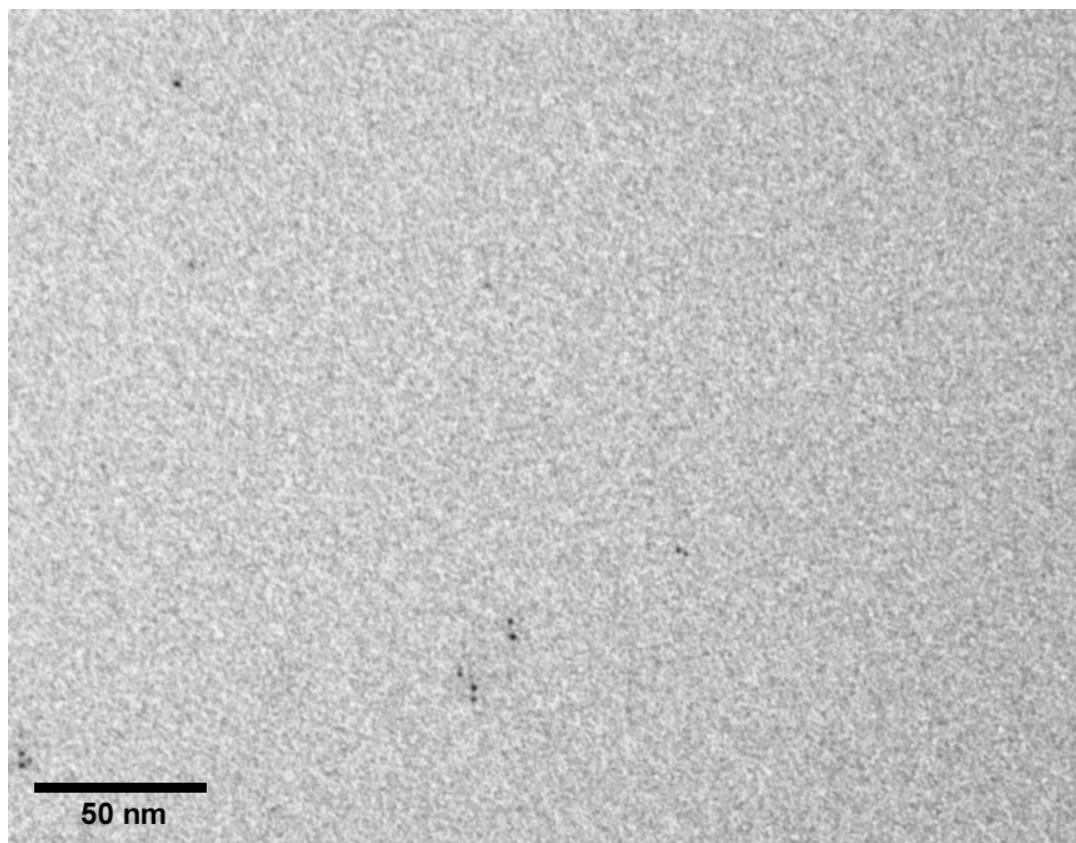


Figure 85. Representative TEM micrograph of $(\text{Au-67})_{2.4}$.

7.2 Dendritic Thioether Ligands

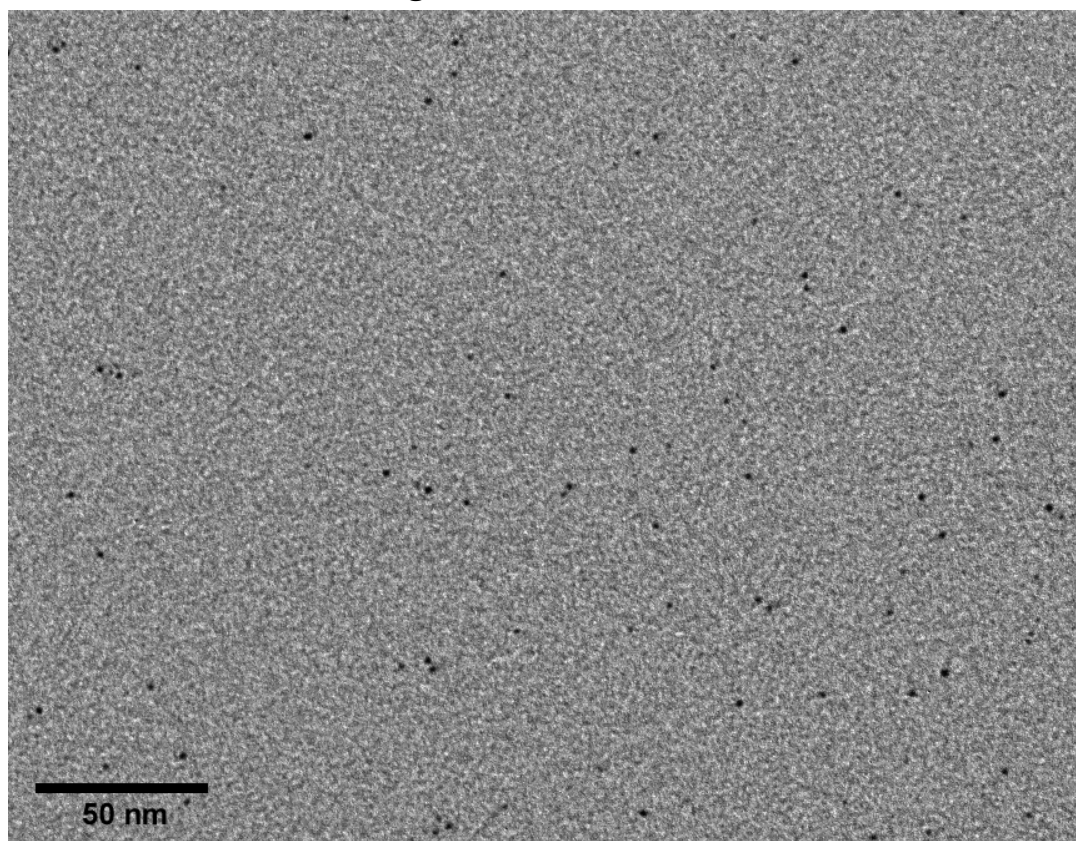


Figure 86. Representative TEM micrograph of **Au-132**.

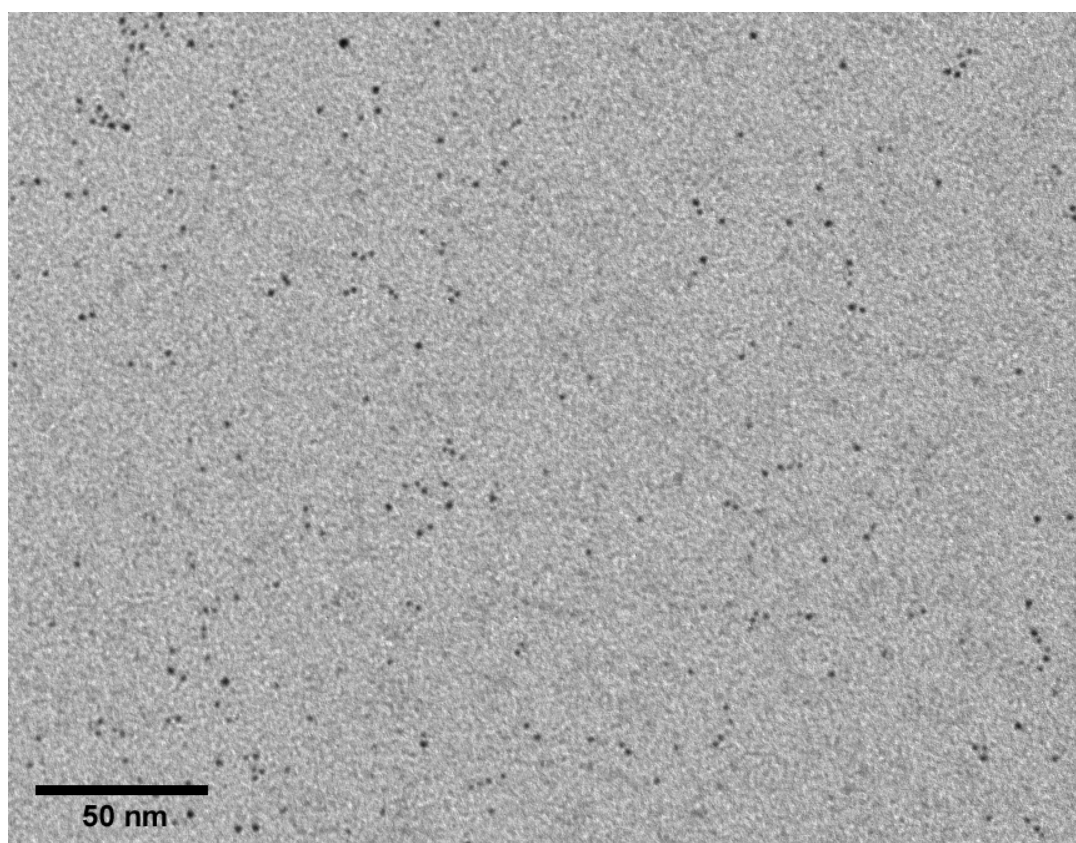


Figure 87. Representative TEM micrograph of **Au-133**.

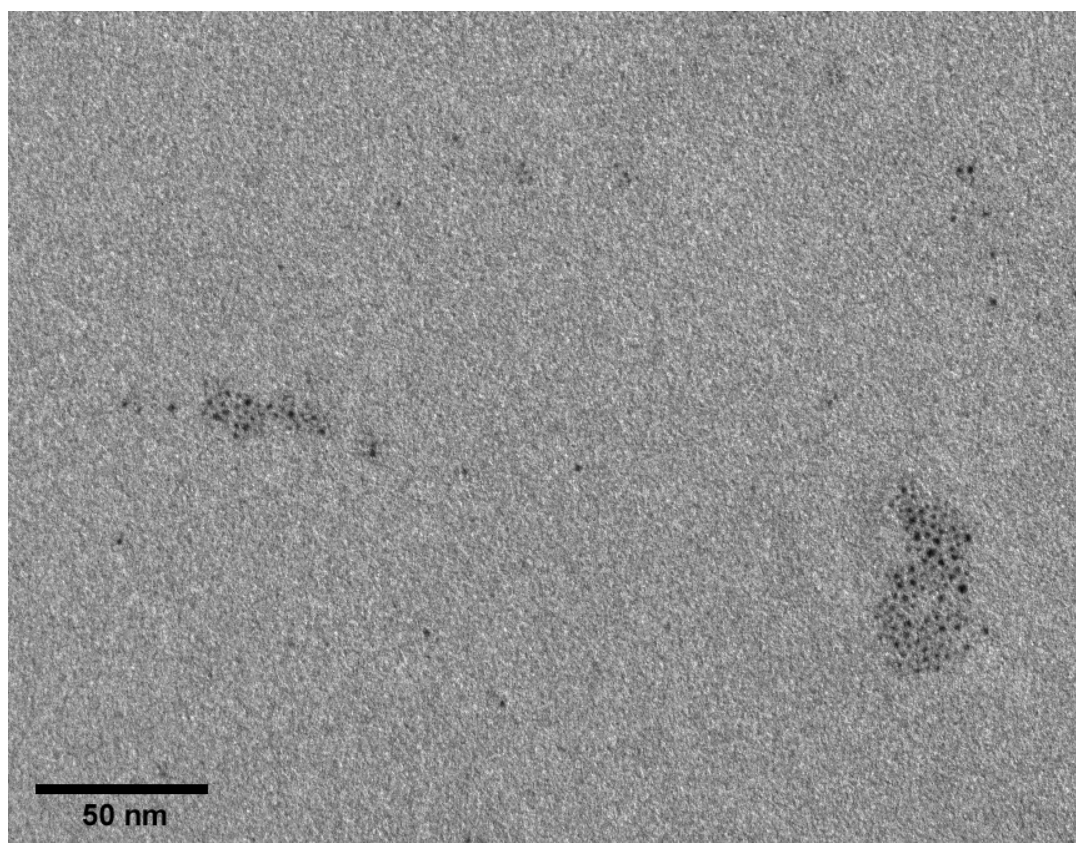


Figure 88. Representative TEM micrograph of $(\text{Au-132})_n$.

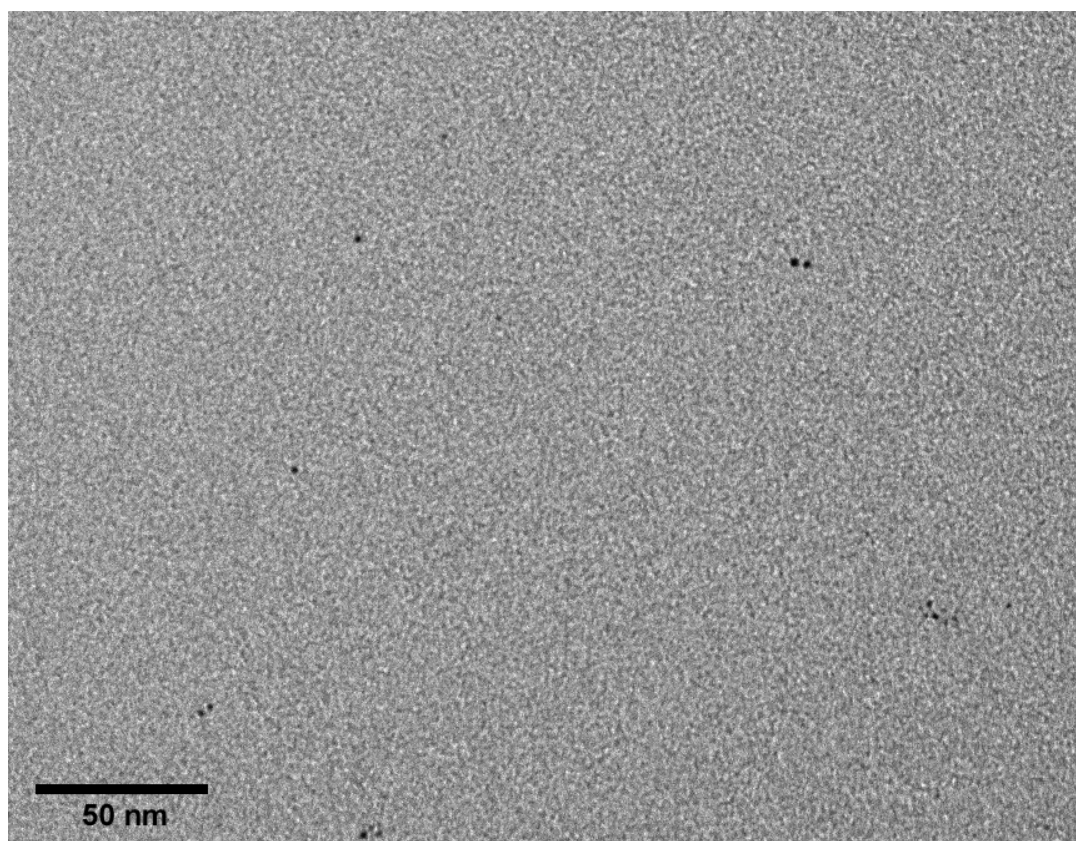


Figure 89. Representative TEM micrograph of $(\text{Au-132})_{2.4}$.

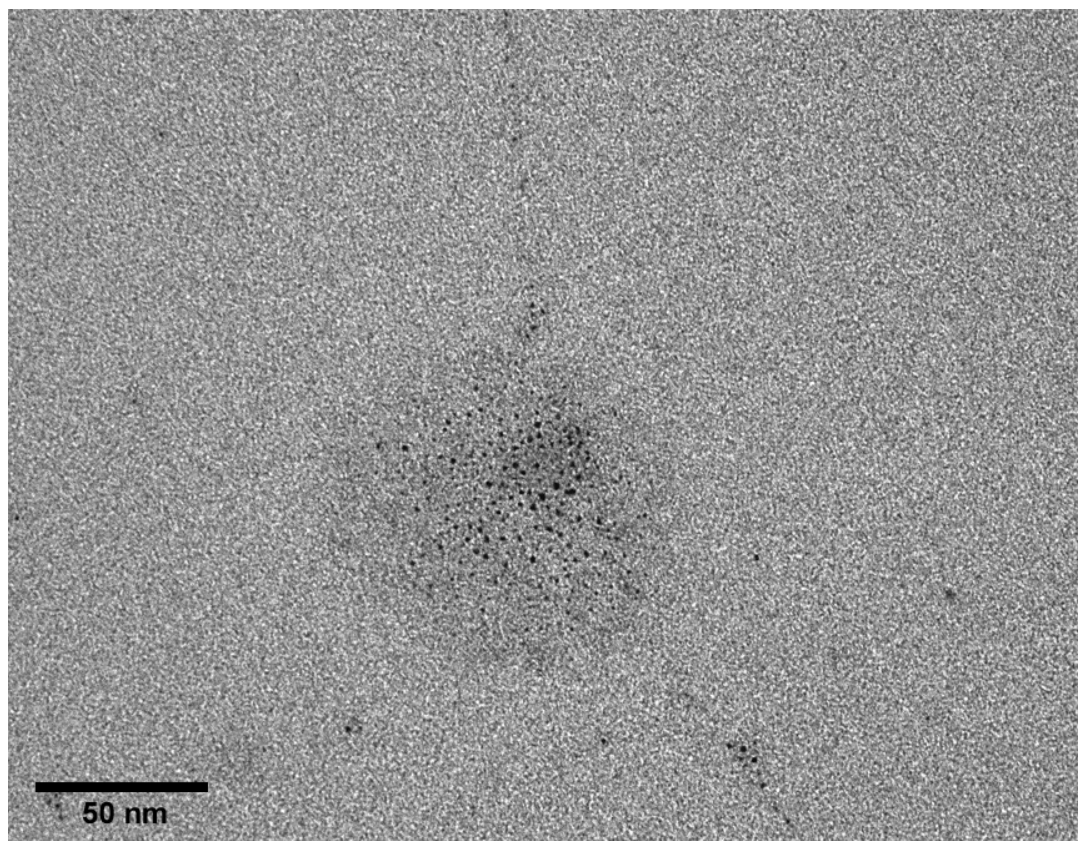


Figure 90. Representative TEM micrograph of $(\text{Au-133})_n$.

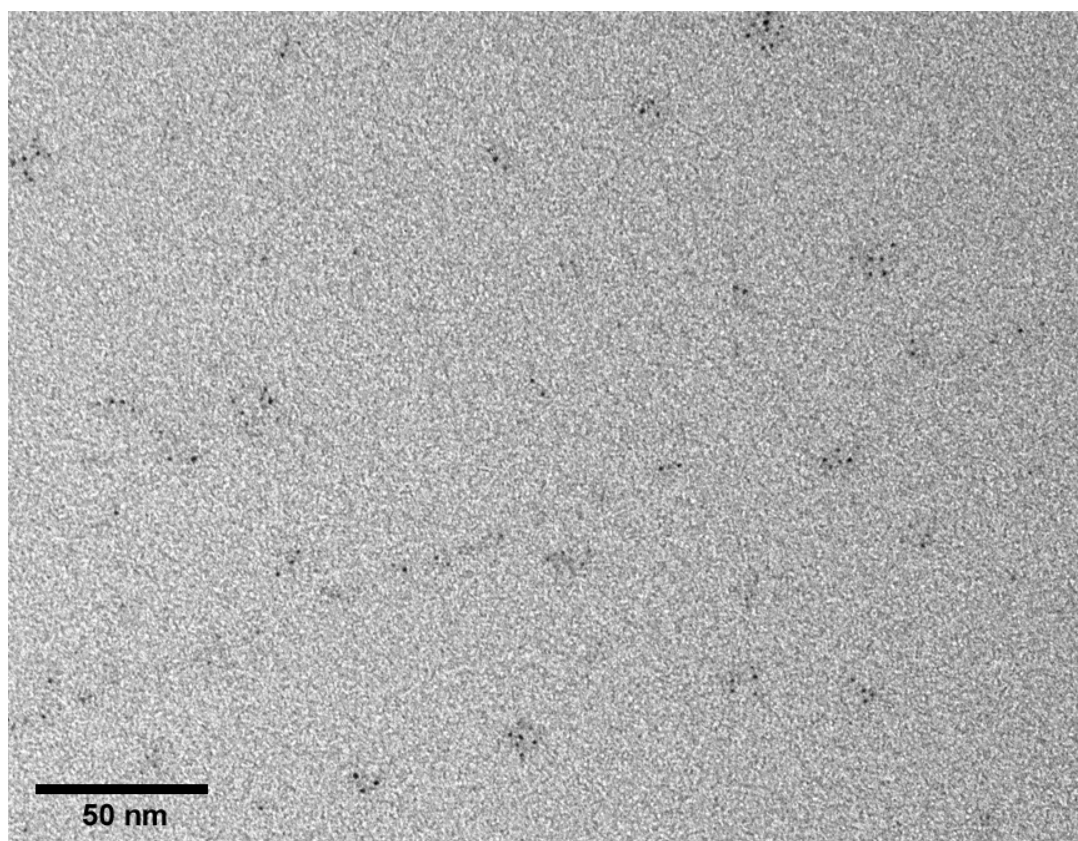


Figure 91. Representative TEM micrograph of $(\text{Au-133})_{2.4}$.

8 Abbreviations

| | |
|----------------------|---|
| Ac | acetyl |
| AIBN | 2,2'-azobis(2-methylpropionitrile) |
| aq. | aqueous |
| Bn | benzyl |
| <i>br</i> | broad |
| Bu | butyl |
| <i>d</i> | duplet |
| DIBAL-H | diisobutylaluminium hydride |
| diglyme | diethylene glycol dimethyl ether |
| DIPA | diisopropylamine |
| DMF | <i>N,N</i> -dimethylformamide |
| DMSO | dimethylsulfoxide |
| DNA | 2'-deoxyribonucleic acid |
| EA | elemental analysis |
| EI | Electron Impact |
| eq. | equivalent |
| ESI | Electron Spray Ionization |
| Et | ethyl |
| FAB | Fast Atom Bombardment |
| FG | functional group |
| <i>G_n</i> | generation <i>n</i> (with <i>n</i> being an integer number) |
| GPC | Gel Permeation Chromatography |
| HRSTEM | High Resolution Scanning Transmission Electron Microscopy |
| HRXPS | High Resolution X-ray Photoelectron Spectroscopy |
| <i>hν</i> | light |
| <i>m</i> | multiplet |
| <i>m/z</i> | mass per charge |
| MALDI | Matrix-Assisted Laser Desorption/Ionization |
| Me | methyl |
| MP | melting point |
| MS | Mass Spectrometry |
| Ms | mesyl |
| MTBE | <i>t</i> -butyl methyl ether |
| NBS | <i>N</i> -Bromosuccinimide |
| NEXAFS | Near Edge X-ray Absorption Fine Structure Spectroscopy |
| NMR | Nuclear Magnetic Resonance |

| | |
|----------|--|
| NOESY | Nuclear Overhauser Effect Spectroscopy |
| OPE | oligophenyleneethynyl |
| PAMAM | poly(amidoamine) |
| PEI | poly(ethylene imine) |
| PG | protecting group |
| Ph | phenyl |
| PMB | <i>p</i> -methoxybenzyl |
| ppm | parts per million |
| <i>q</i> | quartet |
| quant. | quantitative |
| R_f | retention factor |
| RT | room temperature |
| <i>s</i> | singlet |
| STM | Scanning Tunneling Microscopy |
| <i>t</i> | triplet |
| TBAF | tetra- <i>n</i> -butylammonium fluoride |
| TEA | triethylamine |
| TEM | Transmission Electron Microscopy |
| TFA | trifluoroacetic acid |
| TGA | Thermogravimetric Analysis |
| THF | tetrahydrofuran |
| TIPS | tri- <i>iso</i> -propylsilyl |
| TLC | thin layer chromatography |
| TMEDA | <i>N,N,N',N'</i> -tetramethylethylenediamine |
| TMS | trimethylsilyl |
| TMS | tetramethylsilane |
| TOAB | tetra- <i>n</i> -octylammonium bromide |
| TOF | Time of Flight |
| Trt | trityl |
| UV/vis | ultraviolet and visible |
| v/v | volume per volume |
| XANES | X-ray Absorption Near Edge Spectroscopy |

9 Literature

- [1] M. Faraday, *Philos. Trans. R. Soc. London* **1857**, 147, 145.
- [2] P. P. Edwards, J. M. Thomas, *Angew. Chem. Int. Ed.* **2007**, 46, 5480.
- [3] J. M. Thomas, *Pure Appl. Chem.* **1988**, 60, 1517.
- [4] T. H. Graham, *Philos. Trans. R. Soc. London* **1861**, 151, 183.
- [5] G. Schmid, B. Corain, *Eur. J. Inorg. Chem.* **2003**, 3081.
- [6] G. Schmid, *Angew. Chem. Int. Ed.* **2008**, 47, 3496.
- [7] P. Mulvaney, *MRS Bull.* **2001**, 26, 1009.
- [8] M.-C. Daniel, D. Astruc, *Chem. Rev.* **2004**, 104, 293.
- [9] U. Kreibig, M. Vollmer, *Optical Properties of Metal Clusters*, Vol. 25, Springer, Berlin **1995**.
- [10] L. M. Liz-Marzán, *Langmuir* **2006**, 22, 32.
- [11] R. P. Andres, T. Bein, M. Dorogi, S. Feng, J. I. Henderson, C. P. Kubiak, W. Mahoney, R. G. Osifchin, R. Reifenberger, *Science* **1996**, 272, 1323.
- [12] S. Chen, R. S. Ingram, M. J. Hostetler, J. J. Pietron, R. W. Murray, T. G. Schaaff, J. T. Khoury, M. M. Alvarez, R. L. Whetten, *Science* **1998**, 280, 2098.
- [13] F. Remacle, R. D. Levine, *ChemPhysChem* **2001**, 2, 20.
- [14] T. Laaksonen, V. Ruiz, P. Liljeroth, B. M. Quinn, *Chem. Soc. Rev.* **2008**, 37, 1836.
- [15] G. Schmid, *Adv. Eng. Mater.* **2001**, 3, 737.
- [16] U. Simon, in *Nanoparticles* (Ed.: G. Schmid), Wiley-VCH, Weinheim, **2004**, p. 328.
- [17] G. Schmid, U. Simon, *Chem. Commun.* **2005**, 697.
- [18] J. F. Hainfeld, R. D. Powell, *J. Histochem. Cytochem.* **2000**, 48, 471.
- [19] W. P. Faulk, G. M. Taylor, *Immunochemistry* **1971**, 8, 1081.
- [20] D. A. Schultz, *Curr. Opin. Biotechnol.* **2003**, 14, 13.
- [21] R. A. Sperling, P. Rivera Gil, F. Zhang, M. Zanella, W. J. Parak, *Chem. Soc. Rev.* **2008**, 37, 1896.
- [22] S. Eustis, M. A. El-Sayed, *Chem. Soc. Rev.* **2006**, 35, 209.
- [23] J. H. W. Leuvers, P. J. H. M. Thal, M. van der Waart, A. H. W. M. Schuurs, *Fresenius' Z. Anal. Chem.* **1980**, 301, 132.
- [24] C. A. Mirkin, R. L. Letsinger, R. C. Mucic, J. J. Storhoff, *Nature* **1996**, 382, 607.
- [25] R. Elghanian, J. J. Storhoff, R. C. Mucic, R. L. Letsinger, C. A. Mirkin, *Science* **1997**, 277, 1078.
- [26] R. Wilson, *Chem. Soc. Rev.* **2008**, 37, 2028.
- [27] D. Li, A. Wieckowska, I. Willner, *Angew. Chem. Int. Ed.* **2008**, 47, 3927.
- [28] J. Liu, Y. Lu, *J. Am. Chem. Soc.* **2003**, 125, 6642.
- [29] A. B. Descalzo, R. Martínez-Mañez, F. Sancenón, K. Hoffmann, K. Rurack, *Angew. Chem. Int. Ed.* **2006**, 45, 5924.
- [30] A. S. K. Hashmi, *Chem. Rev.* **2007**, 107, 3180.
- [31] A. Corma, H. Garcia, *Chem. Soc. Rev.* **2008**, 37, 2096.
- [32] M. Haruta, T. Kobayashi, H. Sano, N. Yamada, *Chem. Lett.* **1987**, 405.
- [33] C. Della Pina, E. Falletta, L. Prati, M. Rossi, *Chem. Soc. Rev.* **2008**, 37, 2077.
- [34] T. Ishida, M. Haruta, *Angew. Chem. Int. Ed.* **2007**, 46, 7154.

- [35] J. Turkevich, P. C. Stevenson, J. Hillier, *Discuss. Faraday Soc.* **1951**, *11*, 55.
- [36] G. Frens, *Nature (London), Phys. Sci.* **1973**, *241*, 20.
- [37] X. Ji, X. Song, J. Li, Y. Bai, W. Yang, X. Peng, *J. Am. Chem. Soc.* **2007**, *129*, 13939.
- [38] L. Naldini, F. Cariati, G. Simonetta, L. Malatesta, *Chem. Commun. (London)* **1966**, 647.
- [39] L. Malatesta, L. Naldini, G. Simonetta, F. Cariati, *Coord. Chem. Rev.* **1966**, *1*, 255.
- [40] M. McPartlin, L. Malatesta, R. Mason, *J. Chem. Soc. D, Chem. Commun.* **1969**, 334.
- [41] B. K. Teo, X. Shi, H. Zhang, *J. Am. Chem. Soc.* **1992**, *114*, 2743.
- [42] G. Schmid, *Chem. Rev.* **1992**, *92*, 1709.
- [43] G. Schmid, *Chem. Soc. Rev.* **2008**, *37*, 1909.
- [44] G. Schmid, R. Pfeil, R. Boese, F. Brandermann, S. Meyer, G. H. M. Calis, J. W. A. van der Velden, *Chem. Ber.* **1981**, *114*, 3634.
- [45] D. H. Rapoport, W. Vogel, H. Cölfen, R. Schlögl, *J. Phys. Chem. B* **1997**, *101*, 4175.
- [46] M. Brust, M. Walker, D. Bethell, D. J. Schiffrin, R. Whyman, *J. Chem. Soc., Chem. Commun.* **1994**, 801.
- [47] M. J. Hostetler, J. E. Wingate, C.-J. Zhong, J. E. Harris, R. W. Vachet, M. R. Clark, J. D. Londono, S. J. Green, J. J. Stokes, G. D. Wignall, G. L. Glish, M. D. Porter, N. D. Evans, R. W. Murray, *Langmuir* **1998**, *14*, 17.
- [48] A. C. Templeton, W. P. Wuelving, R. W. Murray, *Acc. Chem. Res.* **2000**, *33*, 27.
- [49] A. C. Templeton, M. J. Hostetler, C. T. Kraft, R. W. Murray, *J. Am. Chem. Soc.* **1998**, *120*, 1906.
- [50] A. C. Templeton, M. J. Hostetler, E. K. Warmoth, S. Chen, C. M. Hartshorn, V. M. Krishnamurthy, M. D. E. Forbes, R. W. Murray, *J. Am. Chem. Soc.* **1998**, *120*, 4845.
- [51] T. G. Schaaff, G. Knight, M. N. Shafiqullin, R. F. Borkman, R. L. Whetten, *J. Phys. Chem. B* **1998**, *102*, 10643.
- [52] T. G. Schaaff, R. L. Whetten, *J. Phys. Chem. B* **2000**, *104*, 2630.
- [53] Y. Negishi, Y. Takasugi, S. Sato, H. Yao, K. Kimura, T. Tsukuda, *J. Am. Chem. Soc.* **2004**, *126*, 6518.
- [54] Y. Negishi, K. Nobusada, T. Tsukuda, *J. Am. Chem. Soc.* **2005**, *127*, 5261.
- [55] P. D. Jadzinsky, G. Calero, C. J. Ackerson, D. A. Bushnell, R. D. Kornberg, *Science* **2007**, *318*, 430.
- [56] M. W. Heaven, A. Dass, P. S. White, K. M. Holt, R. W. Murray, *J. Am. Chem. Soc.* **2008**, *130*, 3754.
- [57] R. L. Whetten, R. C. Price, *Science* **2007**, *318*, 407.
- [58] C. E. Briant, B. R. C. Theobald, J. W. White, L. K. Bell, D. M. P. Mingos, A. J. Welch, *J. Chem. Soc., Chem. Commun.* **1981**, 201.
- [59] G. J. Hutchings, M. Brust, H. Schmidbaur, *Chem. Soc. Rev.* **2008**, *37*, 1759.
- [60] B. L. V. Prasad, S. I. Stoeva, C. M. Sorensen, K. J. Klabunde, *Langmuir* **2002**, *18*, 7515.
- [61] J. E. Martin, J. P. Wilcoxon, J. Odinek, P. Provencio, *J. Phys. Chem. B* **2000**, *104*, 9475.
- [62] J. Fink, C. J. Kiely, D. Bethell, D. J. Schiffrin, *Chem. Mater.* **1998**, *10*, 922.
- [63] B. L. Frankamp, A. K. Boal, V. M. Rotello, *J. Am. Chem. Soc.* **2002**, *124*, 15146.
- [64] S. Srivastava, B. L. Frankamp, V. M. Rotello, *Chem. Mater.* **2005**, *17*, 487.

- [65] A. K. Boal, F. Ilhan, J. E. DeRouchey, T. Thurn-Albrecht, T. P. Russell, V. M. Rotello, *Nature* **2000**, *404*, 746.
- [66] G. Schmid, M. Bäuml, N. Beyer, *Angew. Chem. Int. Ed.* **2000**, *39*, 181.
- [67] B. L. Frankamp, O. Uzun, F. Ilhan, A. K. Boal, V. M. Rotello, *J. Am. Chem. Soc.* **2002**, *124*, 892.
- [68] H. Cui, Z. Chen, S. Zhong, K. L. Wooley, D. J. Pochan, *Science* **2007**, *317*, 647.
- [69] C. M. Niemeyer, *Angew. Chem. Int. Ed.* **2003**, *42*, 5796.
- [70] A. Szuchmacher Blum, C. M. Soto, C. D. Wilson, J. D. Cole, M. Kim, B. Gnade, A. Chatterji, W. F. Ochoa, T. Lin, J. E. Johnson, B. R. Ratna, *Nano Lett.* **2004**, *4*, 867.
- [71] A. Szuchmacher Blum, C. M. Soto, C. D. Wilson, T. L. Brower, S. K. Pollack, T. L. Schull, A. Chatterji, T. Lin, J. E. Johnson, C. Amsinck, P. Franzon, R. Shashidhar, B. R. Ratna, *Small* **2005**, *1*, 702.
- [72] M. Hu, L. Qian, R. P. Brinas, E. S. Lyman, J. F. Hainfeld, *Angew. Chem. Int. Ed.* **2007**, *46*, 5111.
- [73] C. M. Niemeyer, U. Simon, *Eur. J. Inorg. Chem.* **2005**, 3641.
- [74] A. P. Alivisatos, K. P. Johnsson, X. Peng, T. E. Wilson, C. J. Loweth, M. P. Bruchez, Jr., P. G. Schultz, *Nature* **1996**, *382*, 609.
- [75] C. J. Loweth, W. B. Caldwell, X. Peng, A. P. Alivisatos, P. G. Schultz, *Angew. Chem. Int. Ed.* **1999**, *38*, 1808.
- [76] Z. Deng, Y. Tian, S.-H. Lee, A. E. Ribbe, C. Mao, *Angew. Chem. Int. Ed.* **2005**, *44*, 3582.
- [77] F. A. Aldaye, H. F. Sleiman, *Angew. Chem. Int. Ed.* **2006**, *45*, 2204.
- [78] F. A. Aldaye, H. F. Sleiman, *J. Am. Chem. Soc.* **2007**, *129*, 4130.
- [79] S. Y. Park, A. K. R. Lytton-Jean, B. Lee, S. Weigand, G. C. Schatz, C. A. Mirkin, *Nature* **2008**, *451*, 553.
- [80] D. Nykypanchuk, M. M. Maye, D. van der Lelie, O. Gang, *Nature* **2008**, *451*, 549.
- [81] A. J. Mastroianni, S. A. Claridge, A. P. Alivisatos, *J. Am. Chem. Soc.* **2009**, DOI: 10.1021/ja808570g.
- [82] J. H. Lee, D. P. Wernette, M. V. Yigit, J. Liu, Z. Wang, Y. Lu, *Angew. Chem. Int. Ed.* **2007**, *46*, 9006.
- [83] M. Fischler, A. Sologubenko, J. Mayer, G. Clever, G. Burley, J. Gierlich, T. Carell, U. Simon, *Chem. Commun.* **2008**, 169.
- [84] M. Noyong, K. Gloddek, J. Mayer, T. Weirich, U. Simon, *J. Cluster Sci.* **2007**, *18*, 193.
- [85] F. Patolsky, Y. Weizmann, O. Lioubashevski, I. Willner, *Angew. Chem. Int. Ed.* **2002**, *41*, 2323.
- [86] C. M. Niemeyer, W. Bürger, J. Peplies, *Angew. Chem. Int. Ed.* **1998**, *37*, 2265.
- [87] H. Li, S. H. Park, J. H. Reif, T. H. LaBean, H. Yan, *J. Am. Chem. Soc.* **2004**, *126*, 418.
- [88] M. Brust, D. Bethell, D. J. Schiffrin, C. J. Kiely, *Adv. Mater.* **1995**, *7*, 795.
- [89] B. L. V. Prasad, C. M. Sorensen, K. J. Klabunde, *Chem. Soc. Rev.* **2008**, *37*, 1871.
- [90] R. P. Andres, J. D. Bielefeld, J. I. Henderson, D. B. Janes, V. R. Kolagunta, C. P. Kubiak, W. J. Mahoney, R. G. Osifchin, *Science* **1996**, *273*, 1690.
- [91] J. Liao, L. Bernard, M. Langer, C. Schönenberger, M. Calame, *Adv. Mater.* **2006**, *18*, 2444.

- [92] G. Zotti, B. Vercelli, A. Berlin, *Chem. Mater.* **2008**, *20*, 397.
- [93] T. Dadosh, Y. Gordin, R. Krahn, I. Khivrich, D. Mahalu, V. Frydman, J. Sperling, A. Yacoby, I. Bar-Joseph, *Nature* **2005**, *436*, 677.
- [94] D. Zanchet, C. M. Micheel, W. J. Parak, D. Gerion, A. P. Alivisatos, *Nano Lett.* **2001**, *1*, 32.
- [95] R. Lévy, Z. Wang, L. Duchesne, R. C. Doty, A. I. Cooper, M. Brust, D. G. Fernig, *ChemBioChem* **2006**, *7*, 592.
- [96] J. G. Worden, A. W. Shaffer, Q. Huo, *Chem. Commun.* **2004**, 518.
- [97] K.-M. Sung, D. W. Mosley, B. R. Pelle, S. Zhang, J. M. Jacobson, *J. Am. Chem. Soc.* **2004**, *126*, 5064.
- [98] C. Krüger, S. Agarwal, A. Greiner, *J. Am. Chem. Soc.* **2008**, *130*, 2710.
- [99] W. M. Pankau, K. Verbist, G. von Kiedrowski, *Chem. Commun.* **2001**, 519.
- [100] W. M. Pankau, S. Mönninghoff, G. von Kiedrowski, *Angew. Chem. Int. Ed.* **2006**, *45*, 1889.
- [101] D. F. Perepichka, F. Rosei, *Angew. Chem. Int. Ed.* **2007**, *46*, 6006.
- [102] A. M. Jackson, J. W. Myerson, F. Stellacci, *Nature Materials* **2004**, *3*, 330.
- [103] A. M. Jackson, Y. Hu, P. J. Silva, F. Stellacci, *J. Am. Chem. Soc.* **2006**, *128*, 11135.
- [104] G. A. DeVries, M. Brunnbauer, Y. Hu, A. M. Jackson, B. Long, B. T. Neltner, O. Uzun, B. H. Wunsch, F. Stellacci, *Science* **2007**, *315*, 358.
- [105] F. A. Vollenbroek, W. P. Bosman, J. J. Bour, J. H. Noordik, P. T. Beurskens, *J. Chem. Soc., Chem. Commun.* **1979**, 387.
- [106] M. Manassero, L. Naldini, M. Sansoni, *J. Chem. Soc., Chem. Commun.* **1979**, 385.
- [107] P. L. Bellon, F. Cariati, M. Manassero, L. Naldini, M. Sansoni, *J. Chem. Soc. D, Chem. Commun.* **1971**, 1423.
- [108] V. Albano, P. L. Bellon, M. Manassero, M. Sansoni, *J. Chem. Soc. D, Chem. Commun.* **1970**, 1210.
- [109] W. W. Weare, S. M. Reed, M. G. Warner, J. E. Hutchison, *J. Am. Chem. Soc.* **2000**, *122*, 12890.
- [110] C. E. Briant, K. P. Hall, D. M. P. Mingos, *J. Chem. Soc., Chem. Commun.* **1984**, 290.
- [111] F. Wen, U. Englert, M. Homberger, U. Simon, *Z. Anorg. Allg. Chem.* **2006**, *632*, 2159.
- [112] F. Wen, U. Englert, B. Gutrath, U. Simon, *Eur. J. Inorg. Chem.* **2008**, 106.
- [113] M. Schulz-Dobrick, M. Jansen, *Eur. J. Inorg. Chem.* **2006**, 4498.
- [114] K. P. Hall, B. R. C. Theobald, D. I. Gilmour, D. M. P. Mingos, A. J. Welch, *J. Chem. Soc., Chem. Commun.* **1982**, 528.
- [115] F. A. Vollenbroek, J. P. van den Berg, J. W. A. van der Velden, J. J. Bour, *Inorg. Chem.* **1980**, *19*, 2685.
- [116] D. M. P. Mingos, *Polyhedron* **1984**, *3*, 1289.
- [117] H. R. C. Jaw, W. R. Mason, *Inorg. Chem.* **1991**, *30*, 275.
- [118] C.-C. Han, R. Balakumar, *Tetrahedron Lett.* **2006**, *47*, 8255.
- [119] M. Tashiro, T. Yamato, *J. Org. Chem.* **1981**, *46*, 1543.
- [120] R. C. Fuson, B. Freedman, *J. Org. Chem.* **1958**, *23*, 1161.
- [121] W. Offermann, F. Vögtle, *Synthesis* **1977**, 272.
- [122] E. Weber, H. P. Josel, H. Puff, S. Franken, *J. Org. Chem.* **1985**, *50*, 3125.

- [123] A. Tsuge, Y. Ueda, T. Araki, T. Moriguchi, K. Sakata, K. Koya, S. Mataka, M. Tashiro, *J. Chem. Research (S)* **1997**, 168.
- [124] T. G. M. Dhar, L. A. Borden, S. Tyagarajan, K. E. Smith, T. A. Brancheck, R. L. Weinshank, C. Gluchowski, *J. Med. Chem.* **1994**, 37, 2334.
- [125] S.-W. Tam-Chang, J. C. Mason, *Tetrahedron* **1999**, 55, 13333.
- [126] T. W. Greene, P. G. M. Wuts, *Protective Groups in Organic Synthesis*, Wiley & Sons, Hoboken, New Jersey **2006**.
- [127] A. Bugaut, K. Jantos, J.-L. Wietor, R. Rodriguez, J. K. M. Sanders, S. Balasubramanian, *Angew. Chem. Int. Ed.* **2008**, 47, 2677.
- [128] H. B. Lee, M. C. Zaccaro, M. Pattarawarapan, S. Roy, H. U. Saragovi, K. Burgess, *J. Org. Chem.* **2004**, 69, 701.
- [129] J. Nam, S.-K. Lee, K. Y. Kim, Y. S. Park, *Tetrahedron Lett.* **2002**, 43, 8253.
- [130] D. A. Pearson, M. Blanchette, M. L. Baker, C. A. Guindon, *Tetrahedron Lett.* **1989**, 30, 2739.
- [131] X. Moreau, J.-M. Campagne, *J. Org. Chem.* **2003**, 68, 5346.
- [132] E. Hahn-Deinstrop, *Dünnschicht-Chromatographie*, Wiley-VCH, Weinheim **1998**.
- [133] F. A. L. Anet, S. S. Miura, J. Siegel, K. Mislow, *J. Am. Chem. Soc.* **1983**, 105, 1419.
- [134] R. J. M. Klein Gebbink, S. I. Klink, M. C. Feiters, R. J. M. Nolte, *Eur. J. Inorg. Chem.* **2000**, 253.
- [135] Y. Hosokawa, S. Maki, T. Nagata, *Bull. Chem. Soc. Jpn.* **2005**, 78, 1773.
- [136] J. Lee, J. Kim, J. S. Koh, H.-H. Chung, K.-H. Kim, *Bioorg. Med. Chem. Lett.* **2006**, 16, 1954.
- [137] F. D. Mango, W. A. Bonner, *J. Org. Chem.* **1964**, 29, 1367.
- [138] T. M. Brown, W. Carruthers, M. G. Pellatt, *J. Chem. Soc., Perkin Trans. 1* **1982**, 483.
- [139] V. Cere, C. Paolucci, S. Pollicino, E. Sandri, A. Fava, *J. Org. Chem.* **1978**, 43, 4826.
- [140] I. Stahl, S. Schomburg, H. O. Kalinowski, *Chem. Ber.* **1984**, 117, 2247.
- [141] Y. Le Stanc, M. Le Corre, *Can. J. Chem.* **1985**, 63, 2958.
- [142] M. E. Borredon, M. Delmas, A. Gaset, *Tetrahedron* **1987**, 43, 3945.
- [143] Y. Okazaki, F. Ando, J. Koketsu, *Bull. Chem. Soc. Jpn.* **2003**, 76, 2155.
- [144] J. T. Doi, G. W. Luehr, *Tetrahedron Lett.* **1985**, 26, 6143.
- [145] J. Srogl, G. D. Allred, L. S. Liebeskind, *J. Am. Chem. Soc.* **1997**, 119, 12376.
- [146] T. Nakata, M. Nakatani, M. Takahashi, J. Okai, Y. Kawaoka, K. Kouge, H. Okai, *Bull. Chem. Soc. Jpn.* **1996**, 69, 1099.
- [147] S. Antoun, *Collect. Czech. Chem. Commun.* **1987**, 52, 162.
- [148] R. Breslow, K. Groves, M. U. Mayer, *J. Am. Chem. Soc.* **2002**, 124, 3622.
- [149] D. J. Cram, J. Weiss, R. C. Helgeson, C. B. Knobler, A. E. Dorigo, K. N. Houk, *J. Chem. Soc., Chem. Commun.* **1988**, 407.
- [150] S. Harvey, P. C. Junk, C. L. Raston, G. Salem, *J. Org. Chem.* **1988**, 53, 3134.
- [151] G. A. Olah, C. W. McFarland, *J. Org. Chem.* **1969**, 34, 1832.
- [152] F. Wen, U. Simon, personal communication, **2007**.
- [153] K. P. Hall, D. M. P. Mingos, *Prog. Inorg. Chem.* **1984**, 32, 237.
- [154] G. Schmid, *Inorg. Synth.* **1990**, 27, 214.
- [155] J. Petroski, M. H. Chou, C. Creutz, *Inorg. Chem.* **2004**, 43, 1597.
- [156] G. Schmid, *Struct. Bonding (Berlin)* **1985**, 62, 51.

- [157] L. O. Brown, J. E. Hutchison, *J. Am. Chem. Soc.* **1997**, *119*, 12384.
- [158] R. C. B. Copley, D. M. P. Mingos, *J. Chem. Soc., Dalton Trans.* **1996**, 479.
- [159] X. M. Lin, C. M. Sorensen, K. J. Klabunde, *Chem. Mater.* **1999**, *11*, 198.
- [160] M. Schulz-Dobrick, K. V. Sarathy, M. Jansen, *J. Am. Chem. Soc.* **2005**, *127*, 12816.
- [161] M. M. Maye, S. C. Chun, L. Han, D. Rabinovich, C.-J. Zhong, *J. Am. Chem. Soc.* **2002**, *124*, 4958.
- [162] M. M. Maye, I. I. S. Lim, J. Luo, Z. Rab, D. Rabinovich, T. Liu, C.-J. Zhong, *J. Am. Chem. Soc.* **2005**, *127*, 1519.
- [163] M. M. Maye, J. Luo, I. I. S. Lim, L. Han, N. N. Kariuki, D. Rabinovich, T. Liu, C.-J. Zhong, *J. Am. Chem. Soc.* **2003**, *125*, 9906.
- [164] X.-M. Li, M. R. de Jong, K. Inoue, S. Shinkai, J. Huskens, D. N. Reinhoudt, *J. Mater. Chem.* **2001**, *11*, 1919.
- [165] E. J. Shelley, D. Ryan, S. R. Johnson, M. Couillard, D. Fitzmaurice, P. D. Nellist, Y. Chen, R. E. Palmer, J. A. Preece, *Langmuir* **2002**, *18*, 1791.
- [166] A. Taubert, U.-M. Wiesler, K. Müllen, *J. Mater. Chem.* **2003**, *13*, 1090.
- [167] A. D'Aléo, R. M. Williams, F. Osswald, P. Edamana, U. Hahn, J. van Heyst, F. D. Tichelaar, F. Vögtle, L. De Cola, *Adv. Funct. Mater.* **2004**, *14*, 1167.
- [168] H.-M. Huang, C.-Y. Chang, I. C. Liu, H.-C. Tsai, M.-K. Lai, R. C.-C. Tsiang, *J. Polym. Sci., Part A: Polym. Chem.* **2005**, *43*, 4710.
- [169] D. Wan, Q. Fu, J. Huang, *J. Appl. Polym. Sci.* **2006**, *101*, 509.
- [170] Z. Wang, B. Tan, I. Hussain, N. Schaeffer, M. F. Wyatt, M. Brust, A. I. Cooper, *Langmuir* **2007**, *23*, 885.
- [171] I. Hussain, S. Graham, Z. Wang, B. Tan, D. C. Sherrington, S. P. Rannard, A. I. Cooper, M. Brust, *J. Am. Chem. Soc.* **2005**, *127*, 16398.
- [172] R. C. Price, R. L. Whetten, *J. Am. Chem. Soc.* **2005**, *127*, 13750.
- [173] L. Fabris, S. Antonello, L. Armelao, R. L. Donkers, F. Polo, C. Toniolo, F. Maran, *J. Am. Chem. Soc.* **2006**, *128*, 326.
- [174] C. Gentilini, F. Evangelista, P. Rudolf, P. Franchi, M. Lucarini, L. Pasquato, *J. Am. Chem. Soc.* **2008**, *130*, 15678.
- [175] V. Chechik, R. M. Crooks, *Langmuir* **1999**, *15*, 6364.
- [176] M.-K. Kim, Y.-M. Jeon, W. S. Jeon, H.-J. Kim, K. Kim, S. G. Hong, C. G. Park, *Chem. Commun.* **2001**, 667.
- [177] M.-C. Daniel, J. Ruiz, S. Nlate, J.-C. Blais, D. Astruc, *J. Am. Chem. Soc.* **2003**, *125*, 2617.
- [178] C. S. Love, V. Chechik, D. K. Smith, C. Brennan, *J. Mater. Chem.* **2004**, *14*, 919.
- [179] K. R. Gopidas, J. K. Whitesell, M. A. Fox, *J. Am. Chem. Soc.* **2003**, *125*, 6491.
- [180] Y. Komine, I. Ueda, T. Goto, H. Fujihara, *Chem. Commun.* **2006**, 302.
- [181] M. M. Alvarez, J. T. Khoury, T. G. Schaaff, M. N. Shafiqullin, I. Vezmar, R. L. Whetten, *J. Phys. Chem. B* **1997**, *101*, 3706.
- [182] K. G. Thomas, J. Zajicek, P. V. Kamat, *Langmuir* **2002**, *18*, 3722.
- [183] R. B. Wyrwas, M. M. Alvarez, J. T. Khoury, R. C. Price, T. G. Schaaff, R. L. Whetten, *Eur. Phys. J. D* **2007**, *43*, 91.
- [184] O. Kohlmann, W. E. Steinmetz, X.-A. Mao, W. P. Wuelfing, A. C. Templeton, R. W. Murray, C. S. Johnson, Jr., *J. Phys. Chem. B* **2001**, *105*, 8801.

- [185] R. L. Donkers, Y. Song, R. W. Murray, *Langmuir* **2004**, *20*, 4703.
- [186] R. H. Terrill, T. A. Postlethwaite, C.-h. Chen, C.-D. Poon, A. Terzis, A. Chen, J. E. Hutchison, M. R. Clark, G. Wignall, J. D. Londono, R. Superfine, M. Falvo, C. S. Johnson, Jr., E. T. Samulski, R. W. Murray, *J. Am. Chem. Soc.* **1995**, *117*, 12537.
- [187] S. Chen, K. Kimura, *Langmuir* **1999**, *15*, 1075.
- [188] G. Ramakrishna, O. Varnavski, J. Kim, D. Lee, T. Goodson, *J. Am. Chem. Soc.* **2008**, *130*, 5032.
- [189] G. H. Woehrle, M. G. Warner, J. E. Hutchison, *J. Phys. Chem. B* **2002**, *106*, 9979.
- [190] R. Huisgen, *Angew. Chem. Int. Ed. Eng.* **1963**, *2*, 565.
- [191] R. Huisgen, *Angew. Chem. Int. Ed. Eng.* **1963**, *2*, 633.
- [192] H. C. Kolb, M. G. Finn, K. B. Sharpless, *Angew. Chem. Int. Ed.* **2001**, *40*, 2004.
- [193] V. V. Rostovtsev, L. G. Green, V. V. Fokin, K. B. Sharpless, *Angew. Chem. Int. Ed.* **2002**, *41*, 2596.
- [194] D. A. Fleming, C. J. Thode, M. E. Williams, *Chem. Mater.* **2006**, *18*, 2327.
- [195] E. Boisselier, L. Salmon, J. Ruiz, D. Astruc, *Chem. Commun.* **2008**, 5788.
- [196] W. J. Sommer, M. Weck, *Langmuir* **2007**, *23*, 11991.
- [197] J. L. Brennan, N. S. Hatzakis, T. R. Tshikhudo, N. Dirvianskyte, V. Razumas, S. Patkar, J. Vind, A. Svendsen, R. J. M. Nolte, A. E. Rowan, M. Brust, *Bioconjugate Chem.* **2006**, *17*, 1373.
- [198] J. M. Spruell, B. A. Sheriff, D. I. Rozkiewicz, W. R. Dichtel, R. D. Rohde, D. N. Reinhoudt, J. F. Stoddart, J. R. Heath, *Angew. Chem. Int. Ed.* **2008**, *47*, 9927.
- [199] Y. Zhou, S. Wang, K. Zhang, X. Jiang, *Angew. Chem. Int. Ed.* **2008**, *47*, 7454.
- [200] J. Zhu, M. D. Ganton, M. A. Kerr, M. S. Workentin, *J. Am. Chem. Soc.* **2007**, *129*, 4904.
- [201] J. Zhu, B. M. Lines, M. D. Ganton, M. A. Kerr, M. S. Workentin, *J. Org. Chem.* **2008**, *73*, 1099.
- [202] X. Liu, M. Zhu, S. Chen, M. Yuan, Y. Guo, Y. Song, H. Liu, Y. Li, *Langmuir* **2008**, *24*, 11967.
- [203] P. J. Costanzo, F. L. Beyer, *Macromolecules* **2007**, *40*, 3996.
- [204] P. J. Costanzo, J. D. Demaree, F. L. Beyer, *Langmuir* **2006**, *22*, 10251.
- [205] J. Zhu, A. J. Kell, M. S. Workentin, *Org. Lett.* **2006**, *8*, 4993.
- [206] M. Proupín-Pérez, R. Cosstick, L. M. Liz-Marzán, V. Salgueiriño-Maceira, M. Brust, *Nucleosides, Nucleotides Nucleic Acids* **2005**, *24*, 1075.
- [207] K. J. Watson, J. Zhu, S. T. Nguyen, C. A. Mirkin, *J. Am. Chem. Soc.* **1999**, *121*, 462.
- [208] M. Wu, S. A. O'Neill, L. C. Brousseau, W. P. McConnell, D. A. Shultz, R. J. Linderman, D. L. Feldheim, *Chem. Commun.* **2000**, 775.
- [209] T. Inomata, K. Konishi, *Chem. Commun.* **2003**, 1282.
- [210] C. S. Love, I. Ashworth, C. Brennan, V. Chechik, D. K. Smith, *Langmuir* **2007**, *23*, 5787.
- [211] C. Ornelas, D. Méry, E. Cloutet, J. Ruiz Aranzaes, D. Astruc, *J. Am. Chem. Soc.* **2008**, *130*, 1495.
- [212] M. Brust, J. Fink, D. Bethell, D. J. Schiffrin, C. Kiely, *J. Chem. Soc., Chem. Commun.* **1995**, 1655.
- [213] C. J. Thode, M. E. Williams, *Langmuir* **2008**, *24*, 5988.

- [214] N. Shibata, J. E. Baldwin, A. Jacobs, M. E. Wood, *Tetrahedron* **1996**, *52*, 12839.
- [215] P. Siemsen, R. C. Livingston, F. Diederich, *Angew. Chem. Int. Ed.* **2000**, *39*, 2632.
- [216] K. Sonogashira, Y. Tohda, N. Hagihara, *Tetrahedron Lett.* **1975**, 4467.
- [217] L. Cassar, *J. Organomet. Chem.* **1975**, *93*, 253.
- [218] H. A. Dieck, F. R. Heck, *J. Organomet. Chem.* **1975**, *93*, 259.
- [219] K. Sonogashira, Y. Fujikura, T. Yatake, N. Toyoshima, S. Takahashi, N. Hagihara, *J. Organomet. Chem.* **1978**, *145*, 101.
- [220] U. H. F. Bunz, Y. Rubin, Y. Tobe, *Chem. Soc. Rev.* **1999**, *28*, 107.
- [221] F. Diederich, *Chem. Commun.* **2001**, 219.
- [222] S. Zhang, K. L. Chandra, C. B. Gorman, *J. Am. Chem. Soc.* **2007**, *129*, 4876.
- [223] K. Sonogashira, in *Metal-Catalyzed Cross-Coupling Reactions* (Eds.: F. Diederich, P. J. Stang), Wiley-VCH, Weinheim, **1998**, pp. 203.
- [224] S. A. Sherrod, R. L. Da Costa, R. A. Barnes, V. Boekelheide, *J. Am. Chem. Soc.* **1974**, *96*, 1565.
- [225] P. Steenwinkel, L. S. James, D. M. Grove, N. Veldman, A. L. Spek, G. van Koten, *Chem. Eur. J.* **1996**, *2*, 1440.
- [226] C. H. M. Amijs, G. P. M. van Klink, G. van Koten, *Green Chemistry* **2003**, *5*, 470.
- [227] Y. Shirai, L. Cheng, B. Chen, J. M. Tour, *J. Am. Chem. Soc.* **2006**, *128*, 13479.
- [228] J. P. Genet, E. Blart, M. Savignac, *Synlett* **1992**, 715.
- [229] Y. Morisaki, T. Ishida, Y. Chujo, *Org. Lett.* **2006**, *8*, 1029.
- [230] M. R. an der Heiden, H. Plenio, S. Immel, E. Burello, G. Rothenberg, H. C. J. Hoefsloot, *Chem. Eur. J.* **2008**, *14*, 2857.
- [231] F. A. Carey, R. J. Sundberg, *Advanced Organic Chemistry. Part B: Reaction and Synthesis*, Springer Netherlands, Dordrecht **2007**.
- [232] G. T. Crisp, P. D. Turner, *Tetrahedron* **2000**, *56*, 407.
- [233] S. S. Bhagwat, D. M. Roland, A. J. Main, C. Gude, K. Grim, R. Goldstein, D. S. Cohen, R. Dotson, J. Mathis, W. Lee, *Bioorg. Med. Chem. Lett.* **1992**, *2*, 1623.
- [234] H. Galan, A. Fragosó, J. de Mendoza, P. Prados, *J. Org. Chem.* **2008**, *73*, 7124.
- [235] J. D. Butler, D. M. Solano, L. I. Robins, M. J. Haddadin, M. J. Kurth, *J. Org. Chem.* **2008**, *73*, 234.
- [236] I. Aujard, C. Benbrahim, M. Gouget, O. Ruel, J.-B. Baudin, P. Neveu, L. Jullien, *Chem. Eur. J.* **2006**, *12*, 6865.
- [237] B. Felber, F. Diederich, *Helv. Chim. Acta* **2005**, *88*, 120.
- [238] F. Zeng, S. C. Zimmerman, *J. Am. Chem. Soc.* **1996**, *118*, 5326.
- [239] Y. Liu, P. M. Lahti, *Molecules* **2004**, *9*, 725.
- [240] O. Lavastre, L. Ollivier, P. Dixneuf, S. Sibandhit, *Tetrahedron* **1996**, *52*, 5495.
- [241] T. Cardolaccia, A. M. Funston, M. E. Kose, J. M. Keller, J. R. Miller, K. S. Schanze, *J. Phys. Chem. B* **2007**, *111*, 10871.
- [242] Y. Nakano, K. Ishizuka, K. Muraoka, H. Ohtani, Y. Takayama, F. Sato, *Org. Lett.* **2004**, *6*, 2373.
- [243] E. Hänninen, H. Takalo, J. Kankare, *Acta Chem. Scand., Ser. B* **1988**, *B42*, 614.
- [244] J. G. Rodríguez, J. L. Tejedor, T. La Parra, C. Díaz, *Tetrahedron* **2006**, *62*, 3355.
- [245] M. V. Gil, M. J. Arévalo, O. López, *Synthesis* **2007**, 1589.
- [246] H. Bretschneider, H. Rager, *Monatsh. Chem.* **1950**, *81*, 970.

- [247] A. S. Bailey, J. R. Case, *Tetrahedron* **1958**, 3, 113.
- [248] P. A. S. Smith, G. F. Budde, S. S. P. Chou, *J. Org. Chem.* **1985**, 50, 2062.
- [249] R. S. Gairns, C. J. Moody, C. W. Rees, *J. Chem. Soc., Perkin Trans. 1* **1986**, 501.
- [250] A. Hansson, T. Wixe, K.-E. Bergquist, K. Wärnmark, *Org. Lett.* **2005**, 7, 2019.
- [251] H. Suzuki, K. Miyoshi, M. Shinoda, *Bull. Chem. Soc. Jpn.* **1980**, 53, 1765.
- [252] W. Zhu, D. Ma, *Chem. Commun.* **2004**, 888.
- [253] Q. Cai, W. Zhu, H. Zhang, Y. Zhang, D. Ma, *Synthesis* **2005**, 496.
- [254] J. Andersen, U. Madsen, F. Björkling, X. Liang, *Synlett* **2005**, 2209.
- [255] T. Hosoya, T. Hiramatsu, T. Ikemoto, M. Nakanishi, H. Aoyama, A. Hosoya, T. Iwata, K. Maruyama, M. Endo, M. Suzuki, *Org. Biomol. Chem.* **2004**, 2, 637.
- [256] H. Takalo, P. Pasanen, J. Kankare, *Acta Chem. Scand., Ser. B* **1988**, B42, 373.
- [257] H. Takalo, J. Kankare, *Acta Chem. Scand., Ser. B* **1987**, B41, 219.
- [258] E. R. Riegel, F. Zwiilmeyer, *Org. Synth. Coll.* **1943**, 2, 126.
- [259] L. Huang, K. Wu, J. Meng, M. Zhang, J. Cheng, J. Yang, L. Li, *Huaxue Shiji* **1982**, 4, 193.
- [260] X.-M. Gan, R. T. Paine, E. N. Duesler, H. Nöth, *Dalton Trans.* **2003**, 153.
- [261] M. Loï, E. Graf, M. W. Hosseini, A. De Cian, J. Fischer, *Chem. Commun.* **1999**, 603.
- [262] T. Posner, *Ber. Dtsch. Chem. Ges.* **1905**, 38, 646.
- [263] A. Dondoni, *Angew. Chem. Int. Ed.* **2008**, 47, 8995.
- [264] J. Ham, I. Yang, H. Kang, *J. Org. Chem.* **2004**, 69, 3236.
- [265] T. Migita, T. Shimizu, Y. Asami, J. Shiobara, Y. Kato, M. Kosugi, *Bull. Chem. Soc. Jpn.* **1980**, 53, 1385.
- [266] K. Toyota, S. Kawasaki, M. Yoshifuji, *J. Org. Chem.* **2004**, 69, 5065.
- [267] M. Newcomb, R. S. Vieta, *J. Org. Chem.* **1980**, 45, 4793.
- [268] A. B. Smith, III, B. S. Freeze, M. J. LaMarche, T. Hirose, I. Brouard, M. Xian, K. F. Sundermann, S. J. Shaw, M. A. Burlingame, S. B. Horwitz, D. C. Myles, *Org. Lett.* **2005**, 7, 315.
- [269] P. Noy, project thesis, University of Basel **2007**.
- [270] A. G. Guex, project thesis, University of Basel **2007**.
- [271] M. Hornstein, project thesis, University of Basel **2009**.
- [272] H. Doucet, J.-C. Hierso, *Angew. Chem. Int. Ed.* **2007**, 46, 834.
- [273] J.-C. Hierso, J. Boudon, M. Picquet, P. Meunier, *Eur. J. Org. Chem.* **2007**, 583.
- [274] A. Köllhofer, H. Plenio, *Adv. Synth. Catal.* **2005**, 347, 1295.
- [275] B. H. Lipshutz, D. W. Chung, B. Rich, *Org. Lett.* **2008**, 10, 3793.
- [276] I. J. S. Fairlamb, P. S. Bäuerlein, L. R. Marrison, J. M. Dickinson, *Chem. Commun.* **2003**, 632.
- [277] J.-H. Li, Y. Liang, Y.-X. Xie, *J. Org. Chem.* **2005**, 70, 4393.
- [278] A. S. Batsanov, J. C. Collings, I. J. S. Fairlamb, J. P. Holland, J. A. K. Howard, Z. Lin, T. B. Marder, A. C. Parsons, R. M. Ward, J. Zhu, *J. Org. Chem.* **2005**, 70, 703.
- [279] J. Yan, F. Lin, Z. Yang, *Synthesis* **2007**, 1301.
- [280] C. Glaser, *Ber. Dtsch. Chem. Ges.* **1869**, 2, 422.
- [281] C. Glaser, *Ann. Chem. Pharm.* **1870**, 154, 137.
- [282] G. Eglinton, A. R. Galbraith, *Chem. Ind. (London)* **1956**, 737.

- [283] R. Klajn, T. P. Gray, P. J. Wesson, B. D. Myers, V. P. Dravid, S. K. Smoukov, B. A. Grzybowski, *Adv. Funct. Mater.* **2008**, *18*, 2763.
- [284] D. J. Lavrich, S. M. Wetterer, S. L. Bernasek, G. Scoles, *J. Phys. Chem. B* **1998**, *102*, 3456.
- [285] F. Schreiber, *Prog. Surf. Sci.* **2000**, *65*, 151.
- [286] H. Takiguchi, K. Sato, T. Ishida, K. Abe, K. Yase, K. Tamada, *Langmuir* **2000**, *16*, 1703.
- [287] M. W. J. Beulen, M. I. Kastenbergh, F. C. J. M. van Veggel, D. N. Reinhoudt, *Langmuir* **1998**, *14*, 7463.
- [288] A. S. Hay, *J. Org. Chem.* **1962**, *27*, 3320.
- [289] M. Pittelkow, T. Brock-Nannestad, K. Moth-Poulsen, J. B. Christensen, *Chem. Commun.* **2008**, 2358.
- [290] J. D. Gilbertson, G. Vijayaraghavan, K. J. Stevenson, B. D. Chandler, *Langmuir* **2007**, *23*, 11239.
- [291] K. Esumi, A. Kameo, A. Suzuki, K. Torigoe, *Colloids Surf., A* **2001**, *189*, 155.
- [292] R. M. Crooks, M. Zhao, L. Sun, V. Chechik, L. K. Yeung, *Acc. Chem. Res.* **2001**, *34*, 181.
- [293] J. J. Michels, J. Huskens, D. N. Reinhoudt, *J. Chem. Soc., Perkin Trans. 2* **2002**, 102.
- [294] A. Dahan, A. Weissberg, M. Portnoy, *Chem. Commun.* **2003**, 1206.
- [295] A. Dahan, M. Portnoy, *J. Am. Chem. Soc.* **2007**, *129*, 5860.
- [296] A. van Bierbeek, M. Gingras, *Tetrahedron Lett.* **1998**, *39*, 6283.
- [297] H.-F. Chow, M.-K. Ng, C.-W. Leung, G.-X. Wang, *J. Am. Chem. Soc.* **2004**, *126*, 12907.
- [298] T. Nagata, *J. Organomet. Chem.* **2007**, *692*, 225.
- [299] W. Reppe, W. J. Schweckendiek, *Liebigs Ann. Chem.* **1948**, *560*, 104.
- [300] M. Komiyama, S. Kina, K. Matsumura, J. Sumaoka, S. Tobey, V. M. Lynch, E. Anslyn, *J. Am. Chem. Soc.* **2002**, *124*, 13731.
- [301] G. Mehta, P. V. V. S. Sarma, *Tetrahedron Lett.* **2002**, *43*, 9343.
- [302] M. J. Plater, T. Jackson, *Tetrahedron* **2003**, *59*, 4673.
- [303] W. P. Cochrane, P. L. Pauson, T. S. Stevens, *J. Chem. Soc. C* **1968**, 630.
- [304] W. R. Chan, D. R. Taylor, C. R. Willis, R. L. Bodden, H. W. Fehlhaber, *Tetrahedron* **1971**, *27*, 5081.
- [305] R. Sato, M. Okanuma, S.-i. Chida, S. Ogawa, *Tetrahedron Lett.* **1994**, *35*, 891.
- [306] H. Takeuchi, Y. Nakajima, *J. Chem. Soc., Perkin Trans. 2* **1998**, 2441.
- [307] T. Hotchkiss, H. B. Kramer, K. J. Doores, D. P. Gamblin, N. J. Oldham, B. G. Davis, *Chem. Commun.* **2005**, 4264.
- [308] J. C. Love, L. A. Estroff, J. K. Kriebel, R. G. Nuzzo, G. M. Whitesides, *Chem. Rev.* **2005**, *105*, 1103.
- [309] E. B. Troughton, C. D. Bain, G. M. Whitesides, R. G. Nuzzo, D. L. Allara, M. D. Porter, *Langmuir* **1988**, *4*, 365.
- [310] C. Jung, O. Dannenberger, Y. Xu, M. Buck, M. Grunze, *Langmuir* **1998**, *14*, 1103.
- [311] J. Noh, T. Murase, K. Nakajima, H. Lee, M. Hara, *J. Phys. Chem. B* **2000**, *104*, 7411.
- [312] J. Noh, H. S. Kato, M. Kawai, M. Hara, *J. Phys. Chem. B* **2002**, *106*, 13268.
- [313] J. Noh, F. Nakamura, J. Kim, H. Lee, M. Hara, *Mol. Cryst. Liq. Cryst.* **2002**, *377*, 165.

- [314] C.-J. Zhong, M. D. Porter, *J. Am. Chem. Soc.* **1994**, *116*, 11616.
- [315] C.-J. Zhong, R. C. Brush, J. Anderegg, M. D. Porter, *Langmuir* **1999**, *15*, 518.
- [316] E. U. Thoden van Velzen, J. F. J. Engbersen, D. N. Reinhoudt, *J. Am. Chem. Soc.* **1994**, *116*, 3597.
- [317] B.-H. Huisman, D. M. Rudkevich, F. C. J. M. van Veggel, D. N. Reinhoudt, *J. Am. Chem. Soc.* **1996**, *118*, 3523.
- [318] H. Schönherr, G. J. Vancso, B.-H. Huisman, F. C. J. M. van Veggel, D. N. Reinhoudt, *Langmuir* **1999**, *15*, 5541.
- [319] K. W. Kittredge, M. A. Minton, M. A. Fox, J. K. Whitesell, *Helv. Chim. Acta* **2002**, *85*, 788.
- [320] T. Weidner, A. Krämer, C. Bruhn, M. Zharnikov, A. Shaporenko, U. Siemeling, F. Träger, *Dalton Trans.* **2006**, 2767.
- [321] C. Vericat, M. E. Vela, G. A. Benitez, J. A. M. Gago, X. Torrelles, R. C. Salvarezza, *J. Phys.: Condens. Matter* **2006**, *18*, R867.
- [322] C. Vericat, M. E. Vela, G. Andreasen, R. C. Salvarezza, L. Vázquez, J. A. Martín-Gago, *Langmuir* **2001**, *17*, 4919.
- [323] D. G. Castner, K. Hinds, D. W. Grainger, *Langmuir* **1996**, *12*, 5083.
- [324] Y. W. Yang, L. J. Fan, *Langmuir* **2002**, *18*, 1157.
- [325] M. Himmelhaus, I. Gauss, M. Buck, F. Eisert, C. Wöll, M. Grunze, *J. Electron Spectrosc. Relat. Phenom.* **1998**, *92*, 139.
- [326] T. Ishida, N. Choi, W. Mizutani, H. Tokumoto, I. Kojima, H. Azehara, H. Hokari, U. Akiba, M. Fujihira, *Langmuir* **1999**, *15*, 6799.

